bulletin 16

technical report

fib
CEB-FIP

Design Examples

for the 1996 FIP recommendations 'Practical design of structural concrete'

Design examples

Technical report on

Design examples for the 1996 FIP recommendations 'Practical design of structural concrete'

prepared by a working party of the

Task Group 1.1 *Design applications*

January 2002

Subject to priorities defined by the Steering Committee and the Praesidium, the results of *fib*'s work in Commissions and Task Groups are published in a continuously numbered series of technical publications called 'Bulletins'. The following categories are used:

category	minimum approval procedure required prior to publication
Technical Report	approved by a Task Group and the Chairpersons of the Commission
State-of-Art report	approved by a Commission
Manual or Guide (to good practice)	approved by the Steering Committee of *fib* or its Publication Board
Recommendation	approved by the Council of *fib*
Model Code	approved by the General Assembly of *fib*

Any publication not having met the above requirements will be clearly identified as preliminary draft.

This Bulletin N° 16 has been approved as a *fib* Technical Report in 2001 by *fib* Task Group 1.1 *Design applications* and the Chairman of Commission 1.

The report was drafted by the Working Party *Design Examples* of *fib* Task Group 1.1 *Design applications*. The Working Party had the following members:

Karl-Heinz Reineck* (Convenor, Stuttgart, Germany), João F. Almeida*(Lisbon, Portugal), Júlio Appleton* (Lisbon, Portugal), Achim Bechert (Stuttgart, Germany), Hugo Corres Peiretti* (Madrid, Spain), Thomas Friedrich (Zürich, Switzerland), Stein Atle Haugerud* (Oslo, Norway), Toshio Ichihashi (Tokyo, Japan), Milan Kalny (Prague, Czech Republic), Manfred Miehlbradt* (Lausanne, Switzerland), Santiago Pérez-Fadón* (Madrid, Spain), Jouni Rissanen* (Helsinki, Finland), Jean-Marc Voumard* (Bern, Switzerland), Bo Westerberg* (Stockholm, Sweden), Masato Yamamura (Tokyo, Japan)

* author (see list of contents)

Full affiliation details of Task Groups members may be found in the *fib* Directory.

Cover picture: Bridge of Lekeitio in Spain (see example 1)

First published 2002 by the International Federation for Structural Concrete (*fib*)
Post address: Case Postale 88, CH-1015 Lausanne, Switzerland
Street address: Federal Institute of Technology Lausanne - EPFL, Département Génie Civil
Tel (+41.21) 693 2747, Fax (+41.21) 693 5884, E-mail fib@epfl.ch, web http://fib.epfl.ch

ISSN 1562-3610
ISBN 2-88394-056-8
Printed by Sprint-Digital-Druck Stuttgart

Preface

The Task Group 1.1- *Design Applications* was established in 1998 within ***fib*** Commission 1 *Structures*. The present Technical Report summarises the work developed by the Working Party *Design Examples* of that Task Group. The Working Party started in fact as a FIP Task Group immediately after finalisation of the 1996 FIP Recommendations *Practical Design of Structural Concrete* (published by SETO in September 1999). These Recommendations are based on the CEB-FIP Model Code 1990.

The main objective of this Bulletin is to demonstrate the application of the 1996 FIP Recommendations *Practical Design of Structural Concrete*, and especially to illustrate the use of strut-and-tie models for designing discontinuity regions in concrete structures. These examples form also a continuation of the 1990 FIP *Handbook on Practical Design* that was based on the first version of the Recommendations from 1984.

Most of the examples are existing structures recently built. Although some of the presented structures can be considered quite important, the chosen examples are not intended to be exceptional. This Technical Report does not deal with the discussion of aesthetic or general conceptual aspects. The main aim is to treat particular design aspects, by selecting local regions of the presented structures that are designed and detailed following the proposed design principles and specifications.

It is hoped that this document will be of interest to those engaged in the design of structural concrete, supporting the use of more consistent design and detailing tools like strut-and-tie models.

We acknowledge the contributions of all members of the Working Party listed below, and especially the tremendous work of the authors and their co-authors in preparing these examples. The editor also wants to thank Dipl.-Ing. Duc Thanh Nguyen for his contributions to the example 1, and Ms. cand.-ing. Radoslava Guizdachka for thoroughly editing the final version of the Bulletin.

November 2001

João F. Almeida
Convenor of TG 1.1

Karl-Heinz Reineck
Convenor of WP *Design Examples*

Jean-François Klein
Chairman of Commission 1

Contents

Introduction

Karl - Heinz Reineck

1 Development of design models

The last decade brought a major breakthrough in the design methods for structural concrete. The term "structural concrete" is the unifying term for all kinds of applications of concrete and reinforcing steel in order to overcome the traditional divisions between reinforced concrete, prestressed concrete and partially prestressed concrete and even externally prestressed concrete or unreinforced concrete. These differentiations were identified as artificial, leading to confusion in codes and in teaching as well as to unnecessary restrictions in practice, as pointed out at the IABSE Colloquium „Structural Concrete" April 1991 in Stuttgart [IABSE (1991 a, b]).

The limitations of purely empirical design procedures were increasingly realised, and more and more it was accepted that clear design models should be developed. The theory of plasticity was applied for the design of members under shear and torsion, like e.g. by Thürlimann, Marti et al. (1983)], Nielsen and Braestrup (1978) and others, and this formed also a basis for developing the design concept with strut-and-tie models, which is a valuable design tool generally and especially for discontinuity regions (D-regions). These regions are up to now very poorly covered in codes although improper design and detailing of such D-regions led to many damages and even failures [IABSE (1991 a, b]). The design concept of the strut-and-tie models, as developed by Schlaich and Weischede (1982), Schlaich, Schäfer and Jennewein (1987), Schlaich (1991) and others, brought the unique chance to gain consistency in the design concept covering the D-regions with models of the same accuracy like in the B-regions for the design for flexure, shear and torsion. Furthermore, the application of strut-and-tie models emphasises the essential role of detailing in design.

This development in research was to some extent reflected in several codes like the CEB-FIP Model Codes 1978 and 1990, the Canadian Code CSA (1994) and the AASHTO (1994). Presently the design with strut-and-tie models is implemented in the new German code DIN 1045-1 (2001-07) as well as in Appendix A of the ACI 318 (2002) in the USA, and it is also to be expected in the forthcoming Eurocode 2. This triggers the hope that other codes will follow and that many code makers and engineers are not any more reluctant to accept the necessity to use clear models instead of sticking to "well known" rules.

2 The design concept of the 1996 FIP Recommendations *Practical Design of Structural Concrete*

The 1996 FIP Recommendations *Practical Design of Structural Concrete* are a revision of the edition from 1984 and were presented at the FIP Symposium in London by Miehlbradt as chairman of the Working Group [Miehlbradt / Reineck (1996)], as well as at the *fib* Symposium in Prague [Reineck (1999)].

These recommendations are based on the CEB-FIP Model Code 1990 and its design concept. However, some further developments were made, and this especially refers to the full implementation of the concept of the design with strut-and-tie models. This is already obvious from the list of contents shown in Table 1. After stating the principles and defining the material characteristics as well as the technological and durability requirements in the chapters 1 to 4, the elements of strut-and-tie models are given and defined in chapter 5. The list of contents of chapter 5 is given in Table 2 and shows that also the basic requirements for bond, anchorages and splices are defined, because these are fundamental design requirements and cannot be regarded as "detailing rules". Therefore, all requirements and principles for the design and detailing are given before the rules for the dimensioning of sections and members, which thus are based on a consistent basis.

1 Principles
2 Material characteristics
3 Prestressing
4 Technological details and durability requirements
5 Strength of ties, struts and nodes of strut-and-tie models
6 Ultimate Limit State Design
7 Serviceability Limit State
8 Structural members and structures

Table 1: List of contents of the 1996 FIP Recommendations "Practical Design of Str. Concr."

5 Strength of ties, struts and nodes of strut-and-tie models
5.1 General
5.2 Strength of steel ties
5.3 Strength of struts
5.4 Strength of concrete ties
5.5 Transfer of forces by friction across interfaces
5.6 Strength of nodes and anchorages
5.7 Reinforcement splices
5.8 Special rules for bundled bars

Table 2: Chapter 5 of the 1996 FIP Recommendations "Practical Design of Struct. Concrete"

It is noteworthy that one classical chapter in all codes does not appear in the list of contents of the FIP Recommendations, and this is the chapter „analysis". The requirements and rules for the analysis are directly given along with those for dimensioning in the chapter 6 respectively in chapter 7. This emphasises the close connection with the dimensioning, because at ULS and SLS different design procedures may be used: at ULS the theory of plasticity may be appropriate, whereas at SLS the theory of elasticity is normally used and is near to reality. By not allotting a separate chapter for the analysis it is also pointed out that the analysis should not be overemphasised as it is presently often done in practice and research.

The list of contents of chapter 6 is given in Table 3. After stating the general requirements and definitions in section 6.1, the sections 6.2 and 6.3 briefly describe the actions and action effects as well as give the requirements for the structural analysis. This is directly followed by

the sections with the dimensioning requirements, i.e. the section 6.4 "Design of B-regions" and section 6.5 "Design of D-regions". This points out that both sections are closely related and are equally important.

6 Ultimate Limit State Design
6.1 General requirements and definitions
6.2 Actions and action effects
6.3 Structural analysis
6.4 Design of B-regions
6.5 Design of D-regions
6.6 Design of slender compressed members
6.7 Design of slabs
6.8 Plate and shell elements
6.9 Fatigue

Table 3: Chapter 5 of the 1996 FIP Recommendations "Practical Design of Struct. Concrete"

6.5 Design of discontinuity regions (D-regions)
6.5.1 Requirements and general criteria for modelling
6.5.2 Statical discontinuities: beam supports and corbels
6.5.2.1 Direct supports of beams
6.5.2.2 Indirect supports
6.5.2.3 Point load near a support and corbels
6.5.3 Deep beams
6.5.4 Deviation of forces
6.5.5 Frame corners and beam-column connections
6.5.5.1 Frame corners with negative (closing) moment
6.5.5.2 Frame corners with positive (opening) moment
6.5.5.3 Beam-column connection for an external column
6.5.6 Half joints and steps in members
6.5.7 Point loads in direction of member axis and anchorage zones of prestressing reinforcements
6.5.7.1 D-regions at end-support of rectangular members
6.5.7.2 End-support of a beam with flanges
6.5.7.3 Interior anchor zones and construction joints with prestressing anchors
6.5.7.4 Deviators for external tendons

Table 4: Section 6.5 on D-regions of the 1996 FIP Recommendations

The survey of the contents of section 6.5 is given in Table 4 and demonstrates already that the treatment of D-regions plays an important role in the chapter 6 on dimensioning. This is in contrast to former and most present codes where these problems are scarcely addressed. It is also far more elaborated than the corresponding brief section 6.8 in the CEB-FIP MC 90. A few items are presently dealt with in codes as shear problems, like e.g. the case of a point load near a support, but they can only be dealt with properly by looking at the whole D-region. Even though some parts of section 6.5 may be regarded as having a textbook character, this section covers the most common problems occurring in practice and should be of great help for designers.

3 The aim and scope of this Bulletin

In point (3) of the scope of the FIP Recommendations 1996 "Practical Design of Structural Concrete" the following is stated:

> (3) The Recommendations are intended for use by practising engineers to enable them to design according to modern concepts. The rules are given in a concise form suitable for qualified engineers with adequate experience in design and detailing.

Following this statement, the primary aim of this Bulletin is to present examples where the application of the design with strut-and-tie models is demonstrated as presented in the chapter 6.5 of the FIP Recommendations 1996 "Practical Design of Structural Concrete". Whereas in previous publications mostly simple "academic" examples were selected in order to explain and demonstrate the use of strut-and-tie models, the six examples in this Bulletin are structures taken from the practice of the members of the Working Group, and they cover critical details of several bridges, of two prestressed beams and even a concrete offshore platform. This demonstrates the conviction of each designer of these examples as well as of all members of the Working Group that strut-and-tie models are a helpful tool and indispensable to solve difficult problems in practice. This should enhance the wish that for this Bulletin also applies what was stated in the foreword of the FIP Recommendations itself by the Chairman of the FIP Commission 3 on Practical Design, Prof. Júlio Appleton:

> It is the wish of (FIP) Commission 3 (*now the fib Task Group 1.1*) that this document will be of direct interest to consultants, contractors and authorities and that it will help the use of a consistent design and detailing tool like the strut-and-tie-models.

Apart form the examples, a second group of five papers are included in this Bulletin, which were called "Background papers", which aim at giving some background and explanations to the FIP Recommendations 1996. Generally, the rules of the FIP Recommendations 1996 "Practical Design of Structural Concrete" are based on the CEB-FIP Model Code 1990 (MC 90), but there are some items where new development were taken up. The justification and reason for this was already stated in the above citation of point (3) of the foreword of the FIP Recommendations, that practising engineers should be enabled to design according to modern concepts. Challenging structures and difficult design problems require the best knowledge available and force designers to solve problems even before codes may offer guidance.

In this sense the overall concept of the MC 90 was further developed to the design concept of the FIP Recommendations being fully based on the design concept of strut-and-tie models, rather than sticking to an isolated additional chapter or an appendix of the code, as it is presently done in some codes.

There are two further topics where FIP Recommendations technically differ from the rules of MC 90 and where justifications for these changes are given in background papers of this Bulletin, and this refers to the design for shear forces and to the design of columns (buckling).

The shear design of the FIP Recommendations 1996 is further explained in the background paper 10 and with the practical example of paper 11. The main reason for introducing new design rules was to comply with the main aim of the FIP Recommendations, which is to present

simple design rules for practising engineers. The treatment of prestress and of axial compressive forces in MC 90 is inconsistent and rather complicated, whereas the beneficial influence of these effects may simply taken into account by flatter angles of the inclined struts in the truss model as compared to reinforced concrete members. The shear design in the FIP Recommendations just means that the unknown angle θ of the inclined struts of the truss model is determined, and it is not a separate chapter purely to design for shear forces, but it is integrated into the design of B-regions for the combined actions of moments and shear forces. Furthermore, the shear design of the FIP Recommendations is clearly restricted to B-regions, and topics like "point load near support" or "indirect supports" are dealt with in the chapters for D-regions, where they belong to. Additionally to the presenting explanations, the background paper 10 presents comparisons with MC 90 as well as with EC 2 with respect to the required amount of transverse reinforcement and the required web width respectively the maximum allowable strength of the struts.

The column design of the FIP Recommendations 1996 is further explained in the background papers 7 and 8, which also give examples. The example 7 on column design uses and compares different methods:

- Methods based on stiffness (improved and simplified).
- Methods based on curvature (improved and simplified).
- General method.

Of these methods, the simplified "curvature method" is basically the same as the model column method in MC90 and in EC2 (ENV 1992-1-1). There is one difference in the FIP Recommendations, however: a factor is introduced to take into account creep explicitly in the value of the curvature. There is a creep factor in the design method of MC90 also, but it is not correct, since its value becomes < 1. The Eurocode EC2 (ENV) states *that* creep should be taken into account, but gives no indication of *how* to do it.

The improved "stiffness" and "curvature" methods were introduced since the simplified versions are sometimes very inaccurate (conservative).

The general method is basically a "rigorous analysis" according to MC90, but using design values of both strength and stiffness (i.e. $\gamma_c = 1{,}5$ for both f_c and E_c) throughout the analysis. (It can be mentioned that in the prEN version of EC2, final draft October 2001, the partial safety factor for E_c is set at 1,2 in connection with second order analysis.).

These explanations for the topics with changes in the FIP Recommendations 1996 "Practical Design of Structural Concrete" as compared to the CEB-FIP Model Code 1990 (MC 90), which formed the basis for it, clearly demonstrate that there was a clear need for these changes.

In the end of the Bulletin a summary and some conclusions are given.

4 References

Abbreviatons: AASHTO = American Association of State Highway and Transportation Officials
ACI = American Concrete Institute
CEB = Comité Eurointernational du Beton (until 1998)
fib = Fédération Internationale du Béton (since 1998, joint CEB and FIP)
FIP = Fédération Internationale du Précontrainte (Until 1998)
IVBH = Internationale Vereinigung für Brücken und Hochbau (IABSE)
PCI = Prestressed Concrete Institute

AASHTO (1994): AASHTO LRFD Bridge design specifications, section 5 Concrete Structures. American Association of State Highway and Transportation Officials, Washington, D.C. 2001, 1994

ACI 318 (2002): Building Code Requirements for reinforced concrete (ACI 318-89) and Commentary ACI 318 R-89, ACI, Detroit 2002

CSA (1994): Design of Concrete Structures - Structures (Design). Canadian Standards Association (CAN3-A23.3-M84), 178 Rexdale Boulevard, Rexdale (Toronto), Ontario, December 1994

CEB-FIP MC 90 (1993): Design of concrete structures. CEB-FIP-Model-Code 1990. Thomas Telford, 1993

DIN 1045-1 (2001): Tragwerke aus Beton, Stahlbeton und Spannbeton, Teil 1: Bemessung und Konstruktion. 1-148. NABau im DIN, Beuth Verl. Berlin. Juli 2001

FIP Recommendations (1996): "Practical Design of Structural Concrete". FIP-Commission 3 "Practical Design", Sept. 1996. Published by SETO (Inst. Struct. Eng.), London, Sept. 1999. (Distributed by: *fib*, Lausanne; see http://fib.epfl.ch/publications/fip/)

IABSE (1991 a): IABSE-Colloquium Stuttgart 1991: Structural Concrete. IABSE-Report V.62 (1991 a), 1-872, Zürich 1991

IABSE (1991 b): IABSE-Colloquium Stuttgart 1991: Structural Concrete - Summarizing statement.
in: - Structural Engineering International V.1 (1991), No.3, 52-54
- Concrete International 13 (1991), No.10, Oct., 74-77
- PCI-Journ. 36 (1991), Nov.-Dec., 60-63
and in German: IVBH-Kolloquium "Konstruktionsbeton" - Schlußbericht.
in: - BuStb 86 (1991), H.9, 228-230 - Bautechnik 68 (1991), H.9, 318-320
- Schweizer Ingenieur und Architekt Nr.36, 5. Sept. 1991
- Zement und Beton 1991, H.4, 25-28

Miehlbradt, M.; Reineck, K.-H. (1996): FIP Recommendations 1996: Practical Design of Structural Concrete. FIP Symposium Post-Tensioned Concrete Structures, London 25-27 Sept. 1996, p.625-634; in: Symposium Papers, Vol.2. The Concrete Society, London 1996

Nielsen, M.P.; Braestrup, M.W.; Jensen, B.C.; Bach, F. (1978): Concrete Plasticity: Beam Shear-Shear in Joints-Punching Shear. Special Publ. Danish Society for Structural Science and Engineering, Dec. 1978, 1-129

Reineck, K.-H. (1999): Towards a Modern Design Concept for Structural Concrete. Keynote Address for Session 2 "Practical Design of Structural Concrete". Appendix a - o (after p. 343) in: Proceedings, Vol. 1: "Structural Concrete - The Bridge between People", *fib* Symposium 1999 Prague, 12-15 October 1999. *fib*, Lausanne 1999

Schlaich, J.; Weischede, D. (1982): Manual for Detailing of concrete structures. CEB-Bull.150, Paris, Jan. 1982

Schlaich, J.; Schäfer, K; Jennewein, M. (1987): Toward a consistent design for structural concrete. PCI-Journ. V.32 (1987), No.3, 75-150

Schlaich, J. (1991): The need for consistent and translucent models. IABSE Rep. V.62 (1991), 169-184

Thürlimann, B.; Marti, P.; Pralong, J.; Ritz, P.; Zimmerli, B. (1983): Anwendung der Plastizitätstheorie auf Stahlbeton. Fortbildungskurs für Bauingenieure. Inst. f. Baustatik und Konstruktion, ETH Zürich, April 1983

EXAMPLE 1

Bridge of Lekeitio

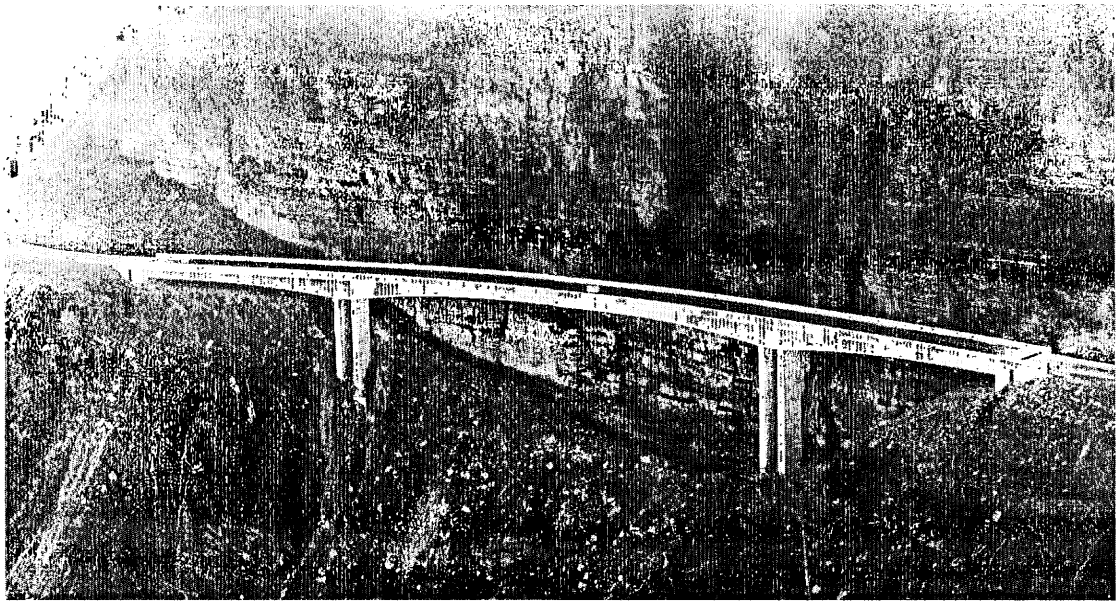

Carlos Bajo

Santiago Pérez-Fadon

Ferrovial – Agromán
Madrid, Spain

1 Description of the bridge

1.1 General description

The bridge of Lekeitio, which lies between the towns of Lekeitio and Ondarroa in Vizcaya, serves a local road which was closed in 1991 because of a landslide.

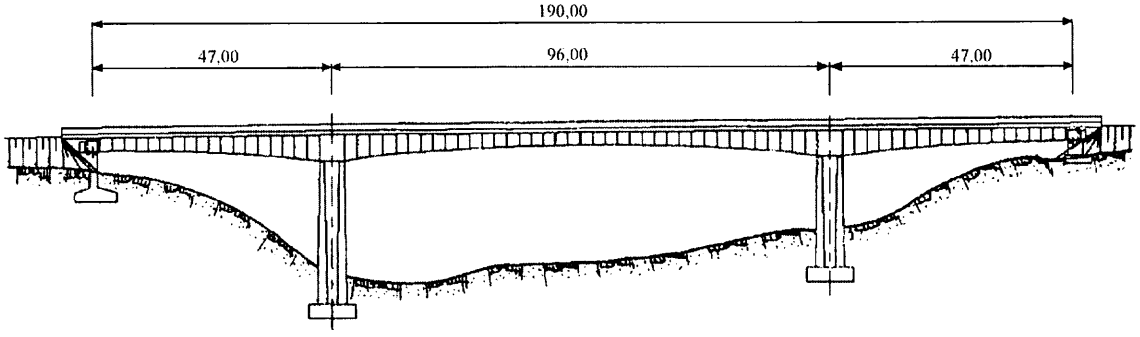

Fig. 1: Longitudinal elevation.

The bridge of prestressed concrete and has an overall length of 190 m., which is divided into two spans: the central span 96 m. and two side spans each of 47.0 m. It was constructed in cantilever with prefabricated segments and continuity exterior prestressing. The segments have a thickness of 2.40 m.

The cross-section has an overall width of 11.40 m. and is made up of a mono-cellular box with transversal cantilevers. The depth varies from 4.75 m. at the pier to 2.50 m. at the middle span.

The piers are double reinforced concrete walls, of variable thickness with a maximum height of 28.5 m. The thickness at the pier crown is 1.30 m. and this goes up to the base with a gradient of 1/200. The foundation of these piers is direct to rock by means of reinforced concrete. There are hydraulic cylinders at the crown of the piers to support the deck during construction and when this is concluded, the Freyssinet hinges are concrete filled.

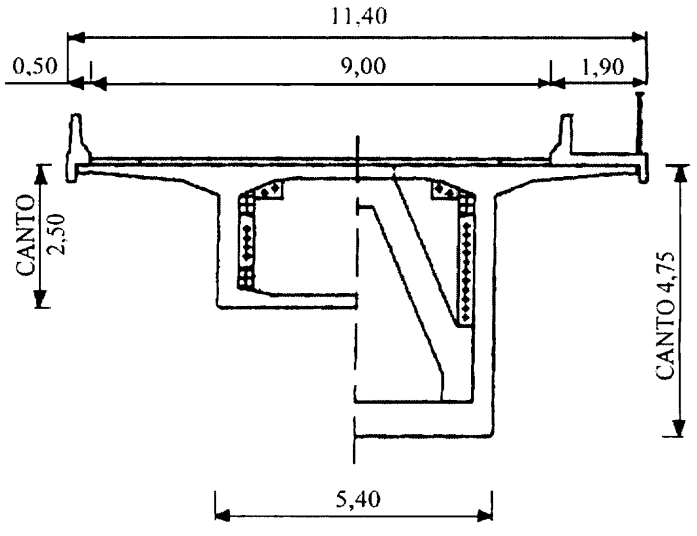

Fig. 2: Cross-section.

The abutments are also reinforced concrete and include corridors for access to inside the bridge, so that during and after construction it is accessible to perform inspection and maintenance work.

1.2 Construction process

1.2.1 Prefabrication

The Prefabrication area counts on a mould to start making the segments by the conjugated procedure, that is to say, each segment acts as mould of the rear face of the next segment. For the geometric control of the shape which each segment must have there are computer programs which control their performance.

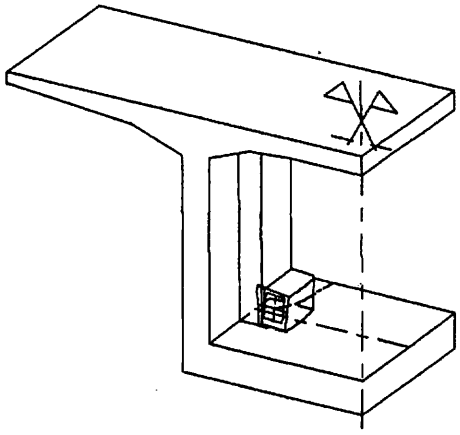

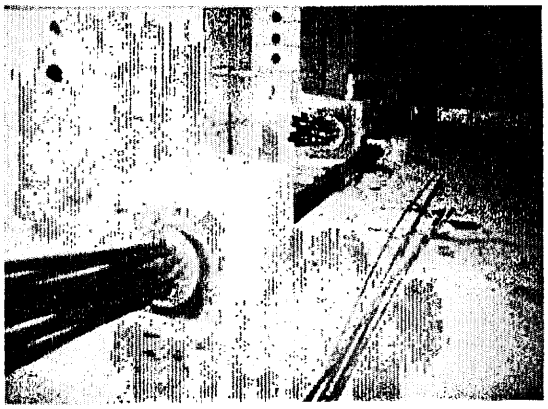

Fig. 3: Anchorage blocks.

The segments have the same cross-section as the bridge and in addition incorporate all the anchorage blocks of the isostatic prestressing, the provisional prestressing and the external prestressing. There are also deviators on the lower slab for this external prestressing.

1.2.2 Steel launching girder of segments

The launcher of segments used in the Bridge of Lekeitio is a steel trussed beam 100 m long and 2.6 m deep.

The launcher has two basic working forms: on the one hand it is capable of advancing the trussed beam, with the load hook of segments fixed on a support. And on the other hand it is capable of advancing the load hook with the trussed beam fixed on a support. It can thus carry its own supports and the different segments of the bridge, including the segment on the pier.

1.2.3 Positioning and orientation of the cantilevers

Segment 0 is positioning on the pier by means of four jacks of horizontal and vertical movement so that it can be orientated. Once two more pairs of segments are placed, the assembly is orientated by means of topographic measuring which take into account the shape of the cantilevers.

Generally speaking, the fixture by means of markings of the segment 0 and the reorientation with topography of the unit of the first five segments should be sufficient to procure closure. If closure is not achieved within acceptable limits, an orientation of the complete cantilevers in elevation, super-elevation and plant can be realized.

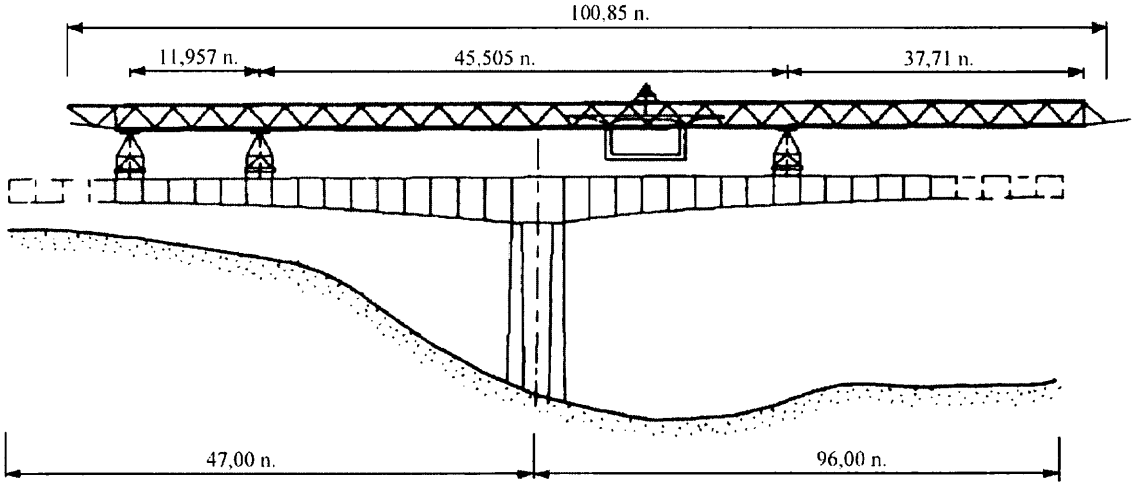

Fig. 4: Construction system.

The deck will advance in cantilevers, supported on these four jacks. The segment which is going to be placed meets the end of the cantilever, and is kept suspended from the launcher at a small distance placed flat and slightly higher than the already constructed deck, and epoxy resin is then applied. The epoxy resin is applied to the rear side of the segment which is going to be placed, and is spread by hand.

Once the resin has been applied, the segment is made to coincide with the cantilever and the Dywidag bars of the provisional prestressing are inserted. The isostatic prestressing is retarded two segments in respect of the fitting with bars. The isostatic prestressing operations are normally started in the afternoon and concluded at night.

In this interval, there are unbalances between the front arm and the rear; these unbalances cause a turning moment on the front two jacks. To have safety factor enough against overturning, fourteen Dywidag bars have been arranged tensioned at 95 T./unit on either side of the pier segment.

When the cantilever has been concluded continuity is established with the previous cantilever. This continuity is achieved with the external continuity prestressing cables. That mean that the cables are outside of the concrete cross-section. The layout of these cables is that show in the next page figure. The tendons go inside the cellular box. In plant the cables are deviated in such a way that all of them can anchored on proper blocks at the corner between down slab and web. In elevation they go parallel to the elevation of the down slab.

When there is continuity with the precedent span, the jacks are lowered and the deck is supported on the definite supports.

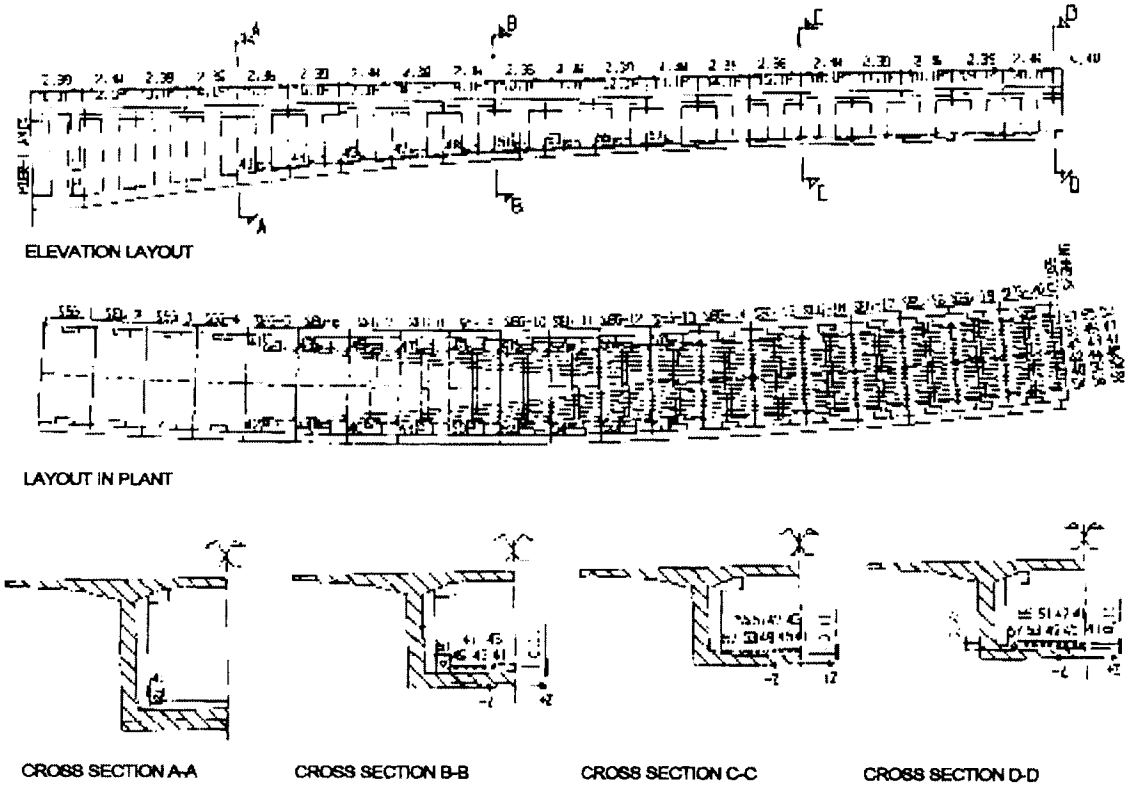

Fig. 5: External Prestressing layout.

1.3 Prestressing of external continuity

The continuity prestressing of the central span has been designed with external prestressing and is made up of 18 tendons of 15 strands of 0.6" diameter tensioned at 340 tons each. Only 6 tendons of like composition are used on the side spans.

The cables are arranged inside the box and on the lower slab. The respective deviators have been prepared on each segment. These are placed in a cross-beam which is assembled on the prefabrication area.

The deviators of the outside prestressing are made up of a cross girder placed on the lower slab in the interior of the box which contains a number of cylindrical hollows to deviate the layout on plant and elevation cables. These cross girders will be concreted in a second phase after the segments is stocked. For a correct positioning lost metal forms are prepared at the workshop which incorporate the cylindrical deviators of the cables. By means of these deviators, the cables follow a parallel layout in elevation to the lower slab without touching it and arranging the strands of each cable. The deviators moreover allow the plant layout to be adjusted, so that each cable is anchored on the respective anchorage block at the corner of the lower slab with the core.

The tendons are made up of mono-protected strands with grease and a coat of high density black polyethylene. At the deviators strands are separated by special device and grouting with epoxy resin. There is an injection on the anchorage block effected with petroliferous wax for rust protection.

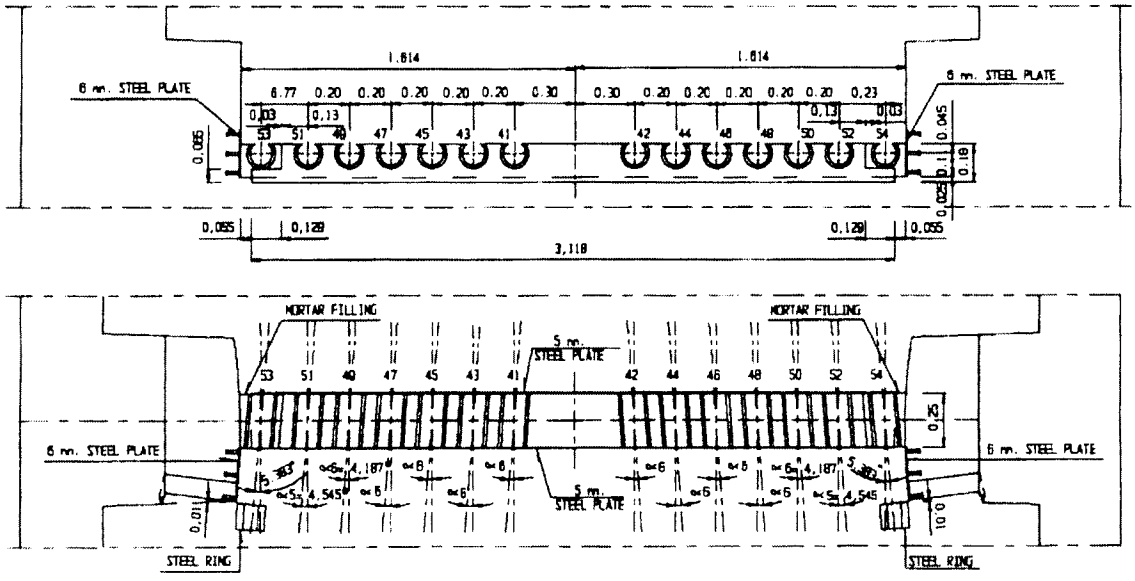

Fig. 6: Beam deviator device.

1.4 Outputs, quantities and other data

Nine men were in segments production at the precast area. These men have manufactured segments at a consistent rate of one segment per day and formwork.

Seven men were employed in placing the segments on the Bridge of Lekeitio, at an average rate of two segments per working day.

Quantities of Materials:
- Concrete 0.677 m^3/m^2.
- Internal prestressing 284.5 N/m^2.
- External prestressing 117.0 N/m^2.
- Ordinary reinforcement 1400 N/m^3.

Other data:
- Owner: Diputación de Vizcaya.
- Constructor: Ferrovial, S.A.
- Prestressing system: Tecpresa

Year of Construction: 1994

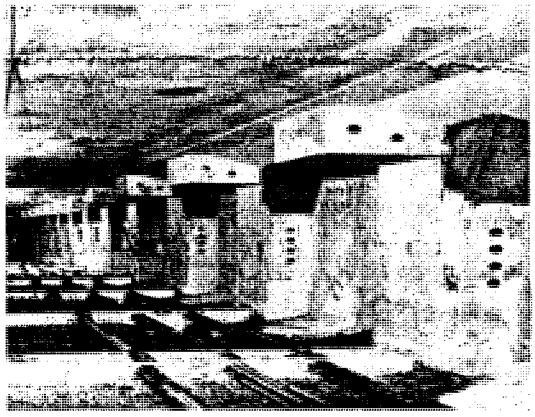

Fig. 7: External prestressing.

2 Tension stress limitation serviceability limit state

Table 1: Deck section geomechanical properties.

	Centre Span	Pier Section
Area (m^2)	6.0195	9.7498
Inertia (m^4)	5.3815	34.6784
Deck Depth (m)	2.50	4.75
Vi Distance	1.5565	2.5139
Prestressing recovering (m)	0.34	0

In segmental construction bridges it is usual to check the stress condition in S.L.S. Normally it is imposed no tension in rare combination of actiones.

The properties of the section, taken in account the concrete and the steel area in the table number 1.

The axial forces and bending moment due the different actions including isostatic and hiperstatic from internal prestressing are in table number 2. Note that prestressing figures are this of inferior characteristic (coefficient= 0.9) and after loses of forces due to steel relaxation, and concrete creep and shrinkage.

To take in account the hyperstatic bending moment from external prestressing a calculation has been made with its isostatic bending moment equal 100 mT The result of this calculation has been an hiperstatic bending moment equal to 73.91 mT.

So we assume a ratio between isostatic and hiperstatic external prestressing moment of:

$M_{hip} = -0.7391 \cdot M_{isost}$

$M_{isost} = -P_{Ext.\ Prest\infty} \cdot (Vi-r)$

$M_{hip} = 0.7391\ P_{Ext.\ Prest\infty}$

$(Vi-r) = 1.05 \cdot P_{Ext.\ Prest\infty}$

Being $P_{Ext.\ Prest\infty}$ the axial force with average figure from external prestressing.

Table 2: Internal forces at centre span after initial losses.

	N (kN)	M (kN· m)
Cantilever Prestressing (Ki =0.9)	3067.99	2548.98
Superior Continuity Prestressing(Ki=0.9)	6514.94	3483.61
Self Weight Static Changes	0	27234.30
Prestressing Static Changes	0	-29193.42
Dead Loads	0	9845.08
Live loads (4 kN/m^2)	0	12373.48
Live loads (600 kN)	0	5365.5
TOTAL	977.84	3230.36

So the total internal forces at centre span with characteristic inferior figure are:

$N = 0.9 \cdot P_{Ext.\ Prest\infty} + 9582.83$

$M = 0.9 \cdot M_{Ext.\ Prest} + 31657.53$

Taken in account that

$M_{Ext.\ Prest} = M_{isost} + M_{hyp} = - P_{Ext.\ Prest\infty} (1.5565 - 0.34) + 1.05\ P_{Ext.\ Prest\infty} = -0.1665\ P_{Ext.\ Prest\infty}$

The internal forces are:

$N = 0.9 \cdot P_{Ext.\ Prest\infty} + 9582.83$

$M = -0.1665 \cdot 0.9\ P_{Ext.\ Prest\infty} + 31657.53 = - 0.14985\ P_{Ext.\ Prest\infty} + 31657.53$

The tension at the bottom fibre will be = 0 T/m^2 so:

$$\sigma_i = 0 = \frac{N}{A} - \frac{M}{W_i} = \frac{0.9\ P_{EXT\infty} + 9582.83}{6.0195} - \frac{31657.53 - 0.14985\ P_{EXT\infty}}{3.4575}$$

$P\infty = 39220.58$ kN

If we supposed that $P_{Ext.\ Prest\infty} = 0.75 \cdot 0.85\ f_{pk}\ A_p$

$0.75 \cdot 0.85\ f_{pk} = 12.2$ T/cm^2 ; 1195.60 MPa

$$A_p = \frac{39220.58/1000}{1195.60} = 3.2804 \cdot 10^{-2} m^2 = 32804\ mm^2$$

3 Ultimate limit state of bending

In this paragraph we calculate first by a section model and second by a whole structure plastic model

3.1 Section elastic model

In this approximate model we assume that the increasing of force at the external prestressing will be 70 MPa (This is a figure from the external prestressing bibliography)

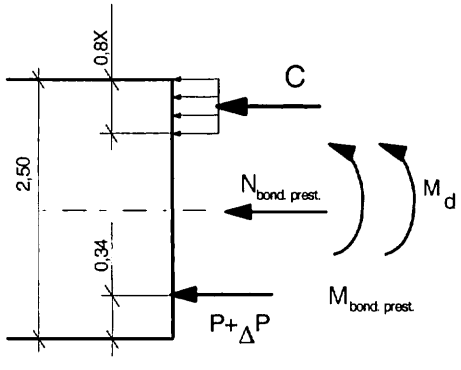

Fig. 8

The equilibrium condition are:

$C = N_{pret\ bond\ prest} + (P + \Delta P)$

$M_d + M_{bond\ prest} = C \cdot (2.16 - 0.4x) - N_{pret} (2.16 - 0.9435)$

In U.L.S. we use the average figures for prestressing internal forces:

$N_{bond\ prest} = 9582.832/0.9 = 10647.6$

$M_{bond\ prest} = 6032.59/0.9 = 6702.9$

The expression of C will be:

$$C = 0.85 \cdot \frac{35000}{1.5} \cdot 11 \cdot 0.8\, x = 174533.3\, x$$

And the expression of $M_d + M_{pret\ adh}$ will be:

$M_d+M_{bond\ prest}$ = 6702.2-29193.22+1.35(27234.2+9845.08)+1.5(12373.48+5365.5) $+M_{hip}$

$M_d+M_{bond\ prest}$ = 54175.4+1.05 (P∞+ΔP)

so the equilibrium equations will be:

174533.3 x = 10647.7 + (P∞ +ΔP)

554175.38 + 1.05 (P∞ +ΔP) = 17453.33 x (2.16 -0.4 x) - 12952.9

From were:

x = 0.3352

C = 57328.0

P +ΔP = 57328.0 - 10647.7 = 46680.3

$$A_p = \frac{46680.3/1000}{1195.60 + 70} = 0.003692\ m^2 = 36925\ mm^2$$

This area 36925 mm^2 is greater that we get in paragraph 2. for S.L.S. 32804 mm^2, which is very usual in isostatic structures with external prestressing or in hyperstatic one with elastic section model calculation.

3.2 Plastic model

In this paragraph we use a plastic model that supposed pier sections has been plastified.

3.2.1 Plastic moment at pier

Plastic moment at pier section has been calculated with a computer program:

M_u= 361361.378 kN· m

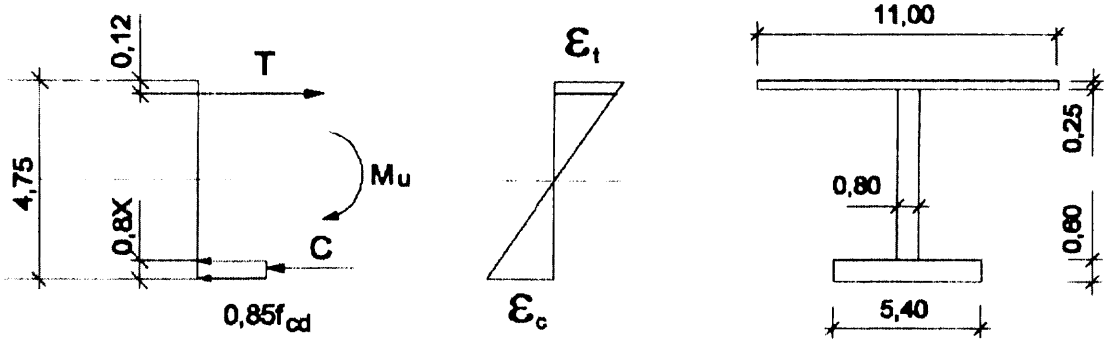

Fig. 9

3.2.2 X from axial force and bending moment at centre span

The bending moments from different actions will be:

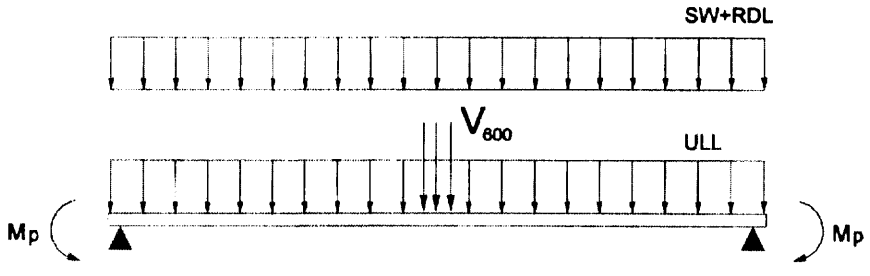

M_{cssw}= 179694.8
M_{csrdl}= 47133.1
M_{csull4}= 45679.8
M_{csV600}= 13219.2

Fig. 10

Where the meaning of the text shown in subscripts is:

cssw:	at centre of span due to self weight.
csrdl:	at centre of span due to rest of dead load.
csull400 :	at centre of span due to the uniform live load of 4kN/m2.
csV600 :	at centre of span due to a vehicle of 600 kN.

And the total bending moment at centre span will be:

M_d = 1.35 (179694.8 + 41733.1) + 1.5 (45679.8 + 13219.2) - 361361.4 =33204.8 kN· m

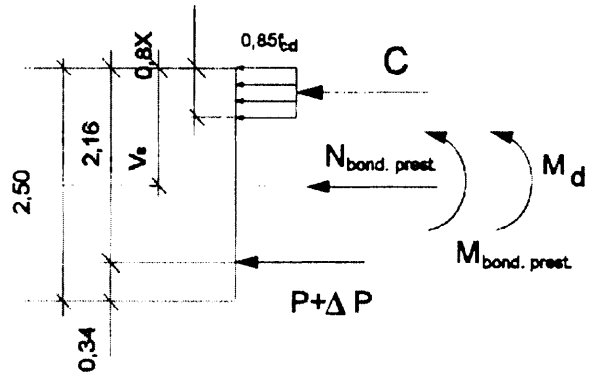

The equilibrium equations will be:

$C=N_{bond\ prest}+(P+\Delta P)$

$Md + M_{bond\ prest} = C\ (h - 0.4x) - N\ (h - Vs)$

The figures from $N_{pret\ sup}$ and $M_{pret\ sup}$ are:

$N_{pret\ sup}$= 9582.8/0.9 = 10647.6 kN

$M_{pret\ sup}$=6032.59/0.9 = 6702.9 kNm

Fig. 11

By the other hand if we assume x < 0.25 m the expression from C will be:

C= 0.85· (35000/1.5)· 11· 0.8· x=17453· x

And so the equilibrium equation will be:

174533.3 x = 10647.6 +(P_∞ + ΔP)

33204.8 + 6702.9 = 174533.3 x (2.16 - 0.4 x) - 10647.6 (2.16 - 0.9435)

from where:

x = 0.1471 m P_∞ + ΔP = 14512.8 kN C = 25160.5 kN

3.2.3 Centre span deflection calculation:

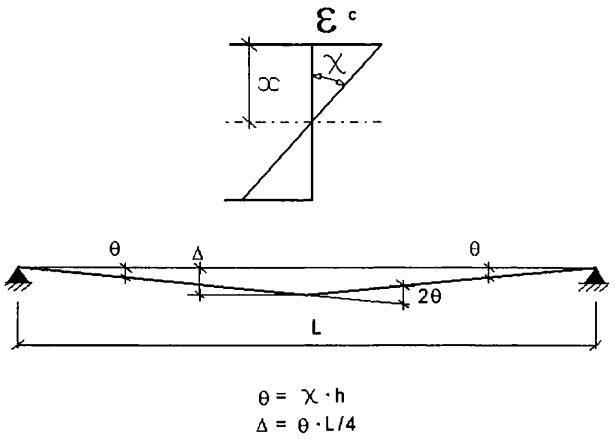

Fig. 12

First we calculate the curvature

$$\chi = \frac{\varepsilon_c}{x} = \frac{0.002}{0.1471} = 0.0135$$

Then the rotation at the pier section

$\theta = \chi \cdot h = 0.0136 \cdot 2.50 = 0.034$ *rads* And by trigonometrical calculation the deflection will be:

$$\Delta = \frac{L\theta}{4} \quad L = 96 - 3.94 = 92.06$$

$$\Delta = \frac{92.06 \cdot 0.034}{4} = 0.7824$$

3.2.4 Tendons elongation due to the deflection

As we have a deck with variable deep the calculation of the tendons elongation is not easy. So we use a simplified method that consist to use the equivalent tendon and simplified trigonometrical relationship.

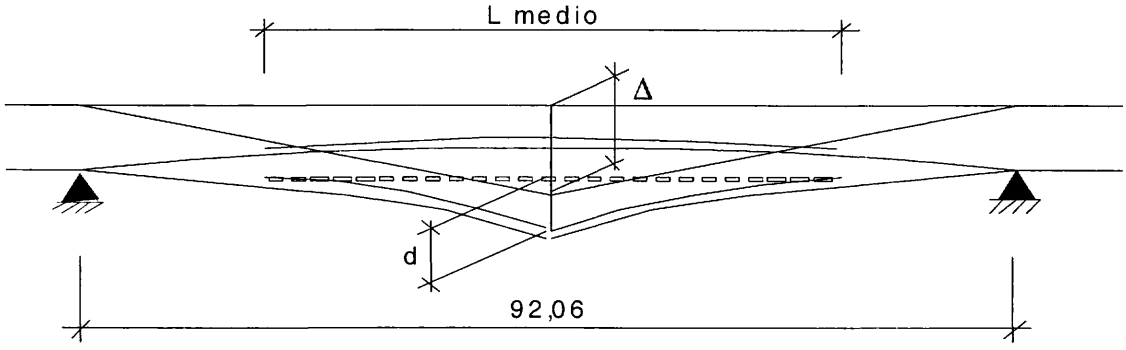

Fig. 13

L_{ave}= 55.37

d = 0.7824≅27.685/46.03=0.4706

ΔL ɜ ($\sqrt{27.685^2}$ % 0.4706^2 & 27.685) 2ɜ 0.008 m

so we get ΔL: ΔL = 0.008

3.2.5 External prestressing tension increasing

From external tendon elongation we get directly the tension increasing

$$\Delta\sigma_{pu} = E\frac{\Delta L}{L} = 1.9 \cdot 10^5 \cdot \frac{0.008}{55.37} = 27.45 \quad MPa$$

and the total tension at the ultimate limit state will be:

σ % Δσ ɜ 1195.6 % 27.45 ɜ 1223.05 MPa

By the other hand the (P + ΔP) force has been calculated in paragraph 3.2.2

(P +)P) = 14512.8 kN

So the steel area for external prestressing will be:

$$A_p = \frac{14512.8 \cdot 10^{-3}}{1223.05} = 1.1866 \cdot 10^{-2}\ cm^2 = 11872\ mm^2$$

This area is less that we get in paragraph 2 because of the plastic calculation and so is the S.L.S. which determine the steel area for external prestressing.

4 Shear force ultimate limit state

Table 3: Internal forces at joint besidepier section

Action	M (kN≡m)	V (kN)	N (kN)
Weight Load as construction	- 143799.3	12691	0
Prestressing Load × 0.9 (1)	147090.16	- 8071.3	66288.18
Dead load	-25228.14	2930.2	0
Live load (4 KN/m2)	- 30012.5	5421.4	0
Live load (600 kN)	- 8106.56	1232.84	0

In hyperstatic segmental bridges it is necessary to check the shear force U.L.S. at the joint beside de pier. Especially when this joint is open by the action of the concurrent bending moment. In this case the transmission of shear through the joint will be only for the compression zone of the webs and for the compression zone of the slabs which is near enough of the web to have the same rigidity. Table number 3 show the internal forces for this section.

So the design figures are:

M_d = 1.35(- 143799.3 - 25228.14)+147090.16+1.5(-30012.5 - 810650)=138275.5 kNm

Q_d = 1.35 (12691 + 2930.2) - 8071.3 + 1.5 (5421.36 + 1232.84) = 22998.64 kN

N_d = 66288.2 kN

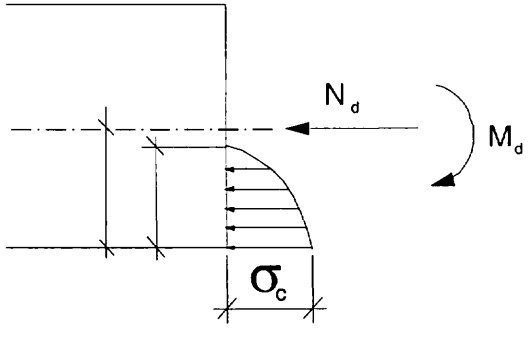

As the M_d and N_d are associated and not ultimate forces it is necessary calculate the concrete compression stresses with parabolic diagram. This has been done with a computer program and we get x:

x = 2.430 m

The ultimate shear strength is shown in Figure 14 (left) for each zone of the section according MC 90 paragraph 6.10.1

To get this figures we take in account the characteristic compression strength of the concrete see FIP Recommendations sect. 6.4.7.

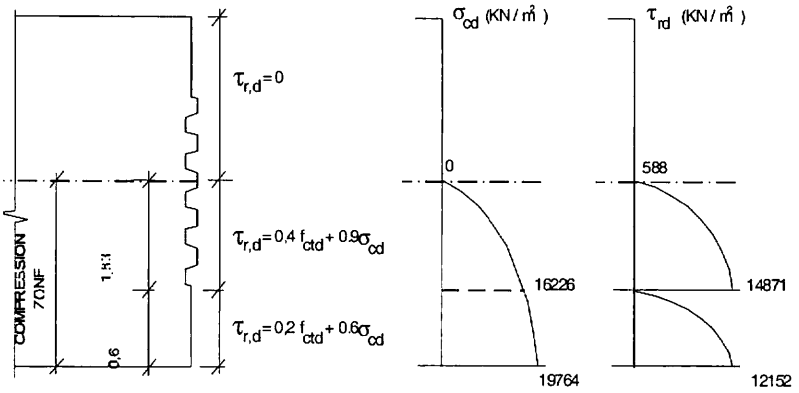

Fig. 15

$f_{ctd} = f_{ctk,min}/1.5$

$f_{ctk\ min} = 0.7\ f_{ctm} = 2.2$ MPa

$f_{ctd} = (2.2/1.5) = 1.47$ Mpa

We calculate the joint ultimate shear capacity by integration of the shear strength over the effective compression area.

The effective compression area is the compression area of the webs and the compression area of the slabs which is between the nearest face of the web and one slab depth.

So we get: T = 23949.3 kN

Design shear force is V_d = 22998.6 kN

So we find that $V_d < T$

Now we need to calculate the hanger reinforcement beside the open joint to translate the shear force to the next segment.

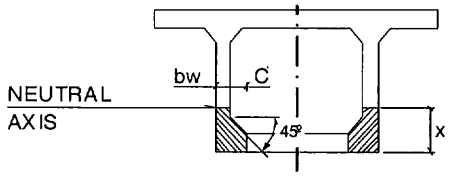

$$S_d = \frac{V_d \cdot (h-x)}{h}$$

Fig. 16

$\sigma_{xd} = 66288.2/9.75 = 6798.8$

$\cot g\ \theta = \sqrt{1+\sigma_{xd}/f_{ctk}} = 2.02$

L = x cotg θ = 2.02 2.43 0 4.92

$$S_d = \frac{V_d(h-x))}{h} = \frac{22998.6(4.75-2.43)}{4.75} = 11232.9\ kN$$

8 x 2 stirrups ∅ 14 en 5.0 m

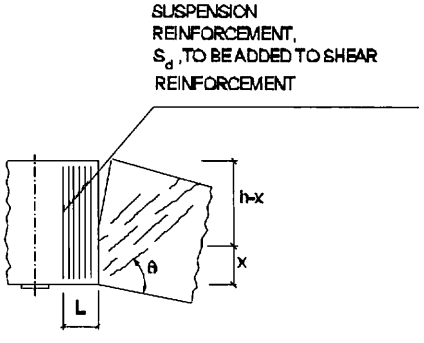

Fig. 17

5 Centre span external prestressing deviator (D region u.l.s.)

At the centre span it is necessary to design a deviator for external tendons. Otherwise due to bending deflection the lever arm of this tendons decrease. In this paragraph calculate this deviator as a D region by strut and tie model.

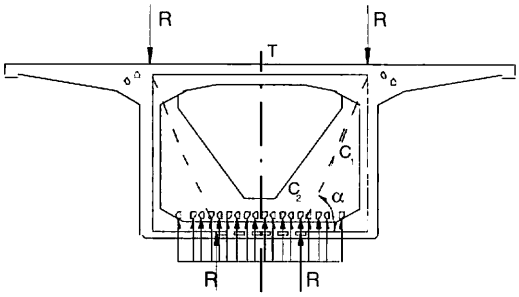

Fig. 18

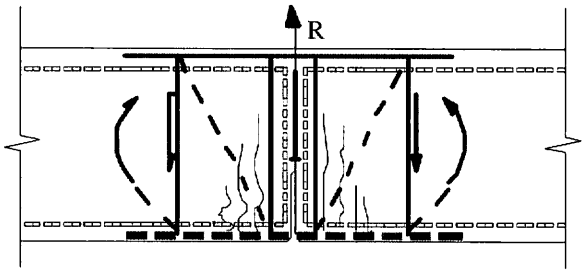

Fig. 19

To design the strut and tie model it is necessary take in account that, in bending U.L.S., the two joints beside the centre span diaphragm will be open and so the strut are going to upper corner of the cross section .

So taken from the figure the trigonometrical relationship we get:

$$\tan\alpha = \frac{2.26}{1.586} = 1.425$$

$C_1 \text{ sen } \forall = R = 31.215 \quad C_1 = 373.7 \text{ kN}$

$C_2 \cos \forall = T \qquad\qquad T = 214.7 \text{ kN}$

$C_1 \cos \forall = 21.91 = C_2$

So we need a ordinary transversal reinforcement in top slab of 3 Ø 16

6 External prestressing anchorage block

The Lekeitio bridge external prestressing anchorage blocs are isolated and situated on the corners between the bottom slab and the webs. They are submitted a very big longitudinal forces from the tendons and also transverse forces because tendons are paralell to the bottom slab but not parallel to the webs. It is necessary calculate the necessary reinforcement at U.L.S. and also check the S.L.S. crack width.

All the components of the anchorage forces (horizontal (x), longitudinal (y) and vertical (z) can be considered at the same time and we can apply the following procedure to develop strut-and-tie-models:

- Idealised that the anchorage block is supported by some supports on the web and the bottom slab. These support reactions can be found by solving a static spatial problem.

- For the anchorage block under the anchorage force and the support reactions, we can find a 3D-model within the block.

- Further, we develop 2D-models for the web and bottom slab for the spread of the reacting forces from the block to the neighbouring B-regions.

6.1 Isolating the anchorage block from the web and bottom slab

In bottom slab the anchorage block is supported statically undeterminate by the web and the bottom slab. For simplicity and based on the real spread of the anchorage force we can suppose suports as shown in Figure 20 . As result nof the combined action of P_x and P_y, (P_z=0 assumed). The components of the anchorage force are:

P=4828 kN
Py_{front}=3370 kN
Py_{rear}=1444 kN
Px=370 kN

X_2=-980 kN
X_4=-370 kN
Z_4=-1660 kN
X_6=980 kN
Y_6=-2490 kN
Y_8=-880 kN
Z_8=-1660 kN

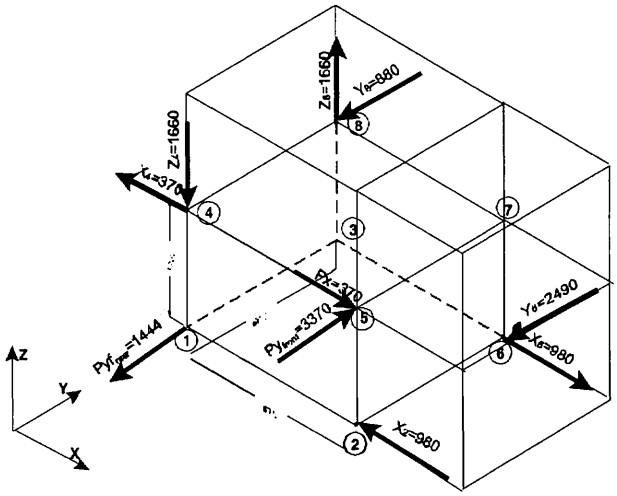

Fig. 20: Block reactions

Py_{rear} is not including in the model to avoid increasing the complexity of the equations. In fact this force is used to set the rear reinforcement of the block.

6.2 Developing a model for the block

It is clear that we need a spatial model for the anchorage block. In fact, there are many possibilities to model the block . The model we choose (Figure 21) has four vertical and horizontal ties (T_{4a}-T_{4d}) and one diagonal strut (C_3) in the rear face. This model can be explained as follows:

The force P_x is directly transferres to the support 4 by a tie. Therefore, P_x can be separately dealt with from force P_y.

Where:

$C_1=X_2/\cos((\text{atan}(0.4/0.675))=1139.1$ kN

$T_1=C_1 \cong \sin((\text{atan}(0.4/0.675))=580.7$ kN

$C_4=T_1/\sin(\text{atan}(0.4/0.6))=1047$ kN

$P_y=C_4 \cong \cos(\text{atan}(0.4/0.6))+C_3 \cong \cos(\text{atan}(0.675/0.6))$

$C_3=3761.2$ kN

$T_3=Y_8-C_3 \cong \cos(\text{atan}(0.675/0.6))=1618$ kN

$Z_4=C_1 \cong \sin(\text{atan}(0.4/0.675)+C_2 \cong \sin(\text{atan}(0.4/(0.6\text{^}2+0.675\text{^}2)\text{^}0.5))$

$C_2=2665.1$ kN

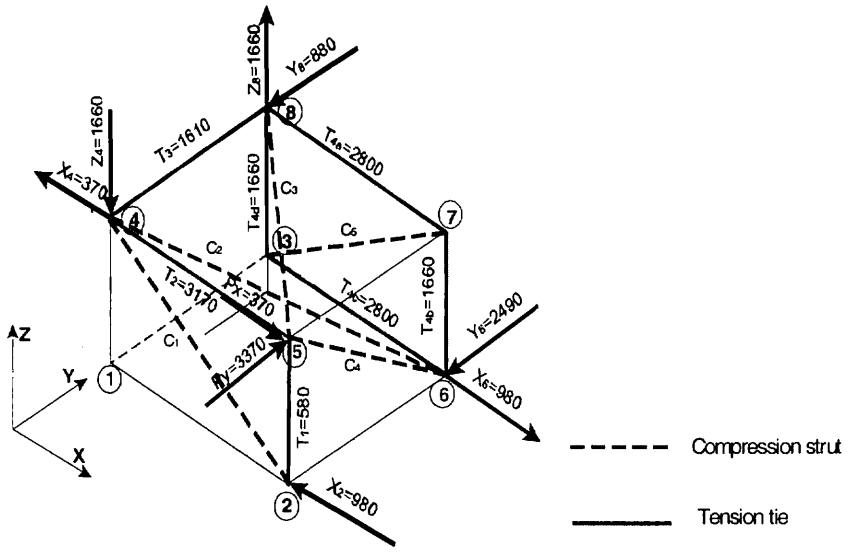

Fig. 21: Strut and tie model

$X_4=T_2-C_1\cong Cos(atan(0.4/0.675)-C_2\cong cos(atan(0.4/(0.6\text{^}2+0.675\text{^}2)\text{^}0.5))\cong cos(atan(0.6/0.675)$
$T_2=3171.2$ kN

$T_{4d}=Z_8=C_5\cong sin(atan(0.4/0.675))=T_{4b}=1660$ kN

$C_5=3256.1$ kN

$T_{4a}=T_{4c}=C_5\cong cos(atan(0.4/0.675))=2800$ kN

6.3 Spread of reactions in web and bottom slab

We need in our case a spatial model. However, for simplicity we can develope models for Px and Py separately and superpose them later.

Now, we can develop plane strut-and-tie models for each web and bottom slab. Figure 22 is a suggested model for the web and Figure 23 for the bottom slab. In this example we use average segment which has a depth of 2.918 m.

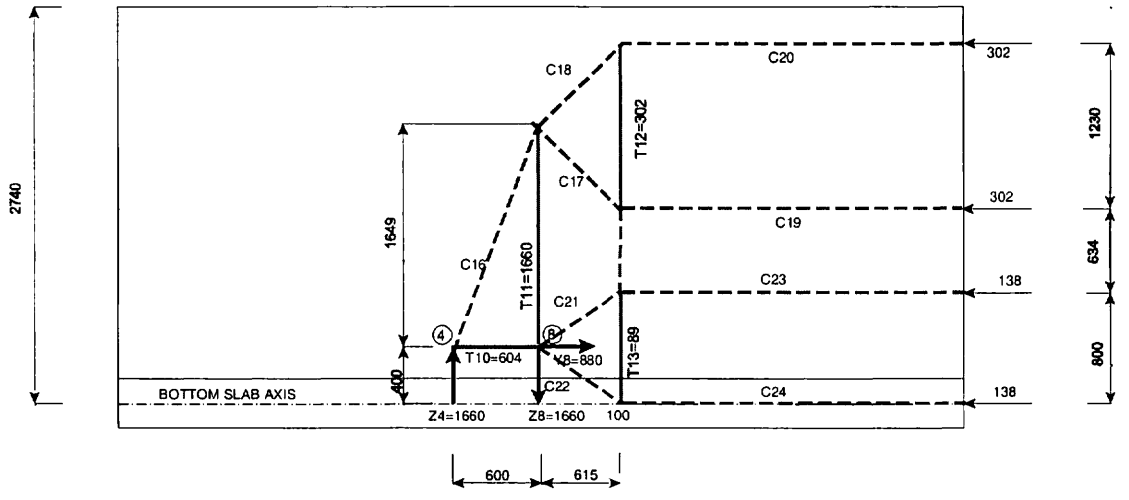

Spread of block reactions in web

Fig. 22

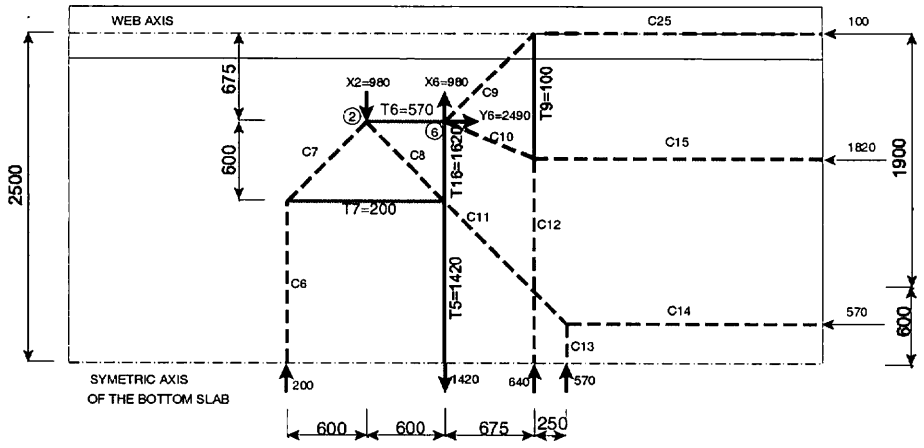

Spread of block reactions in bottom slab

Fig. 23

Where:

$\forall=70.00°$

$C_{16}=1660/\sin 70°=1766$ kN

$T_{10}=C_{16}\cong\cos 70°=604$ kN

$C_{17}=C_{18}=604/2/\cos 45°=427$ kN ; $T_{12}=C_{17}\cong\sin 45°=302$ kN

$C_{20}=C_{19}=C_{17}\cong\cos 45°=302$ kN

$C_{21}=C_{22}=276/2/\cos(\text{atan}(400/615))=164$ kN ; $T_{13}=C_{12}\cong\sin(\text{atan}(400/615))45°=89$ kN

$C_{23}=C_{24}=C_{22}\cong\cos(\text{atan}(400/615))=138$ kN

In bottom slab:

$C_{15}=1820$ kN

$C_{10}=C_{15}/\cos(\text{atan}(0.275/0.675)=1965.2$ kN

$C_9=100/\cos 45=141.4$ kN

$980=-T_{16}-C_9\cong\sin 45+C10\cong\sin(\text{atan}(0.275/0.675)=1660$; $T_{16}=1620$ kN

$2490=T_6+C_9\cong\cos 45+1820$; $T_6=570$ kN

$T_9=C_9\cong\sin 45=100$ kN

$(C_7+C_8)\cong\sin 45=980$ kN

$(C_7-C_8)\cong\cos 45+T_6=0$; $C_7=290$ kN ; $C_8=1100$ kN

$T_7=C_7\cong\cos 45=200$ kN

$C_6=C_7\cong\cos 45=200$ kN

$C_{14}=570$ kN

$C_{11}=C_{14}/\cos 45=800$ kN

$T_5=T_{16}+C_{11}\cong\sin 45-C8\cong\sin 45=1410$ kN

$C_{25}=100$ kN

Taking the tie forces, we get the tension of the ties and assign the steel to these ties in the block.

T_1 = 580.00 kN; 5Ø20
T_2 = 3170.0 kN; 24Ø20
T_3 = 1610.0 kN; 5Ø32
T_{4a} = 2800.0 kN; 20Ø20
T_{4c} = 2800.0 kN; 20Ø20
T_{4b} = 1660.0 kN; 12Ø20
T_{4d} = 1660.0 kN; 12Ø20

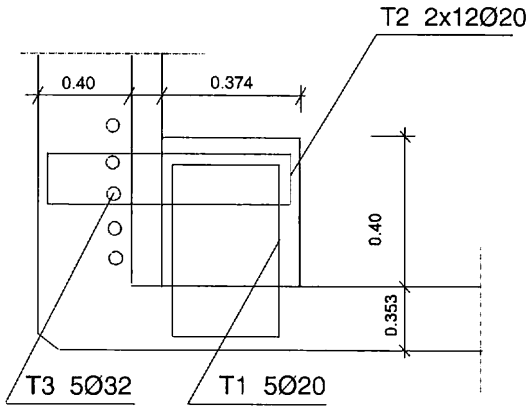

Fig. 24

6.4 Model for the spread of transversal component P_x

In addition to the longitudinal component of the anchorage force there is a transversal component as a consequence of the general layout of the cable. Taken into account the tendon layout and block geometry we get. We take the model from Recommendations paragraph 6.5.7.4. figure 6.36 which is for a deviator of external prestressing tendons.

We suppose that the model take the shear force in the web and the reaction on the bottom slab as in the elastic model. And we suppose also that the model take the web and bottom slab bending moments as in the elastic model. To calculate the web and bottom slab bending moments we use a computer program.

The model for bending is quite simple . It is a rectangular frame with the rigidity of 2,395 width (one segment) submitted a two external forces at the point of the anchorage transverse force. This frame has a bending moment distribution and we take the ratio between the moment at the corner bottom slab and the moment on the web over the transverse force point. so we get that:

M_{Me}= -106.32 kN≅m

M_s = 20.85 kN≅m

To get the figures of the reactions we assumed that the shear web and the bottom slab reaction are proportional to the distances from the transverse force point to top and bottom slab respectively.

L = 2.616; d = 0.3975

Both the reaction R and the Moment M are for 2.395 m width, so the stresses are:

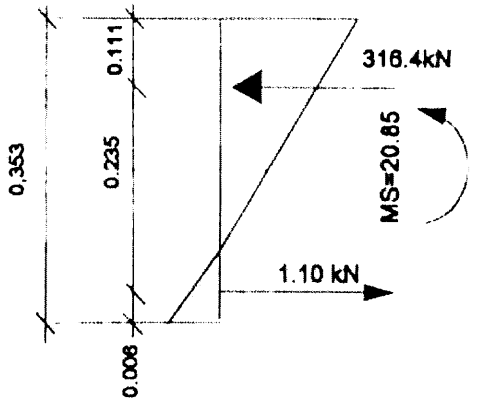

$$\sigma_t = \frac{315.35}{2.395 \cdot 0.353} + \frac{20.85 \cdot 6}{2.395 \cdot 0.353^2} = 792.2\ kN/m^2$$

$$\sigma_b = \frac{315.35}{2.395 \cdot 0.353} - \frac{20.85 \cdot 6}{2.395 \cdot 0.353^2} = -46.2\ kN/m^2$$

Fig. 25

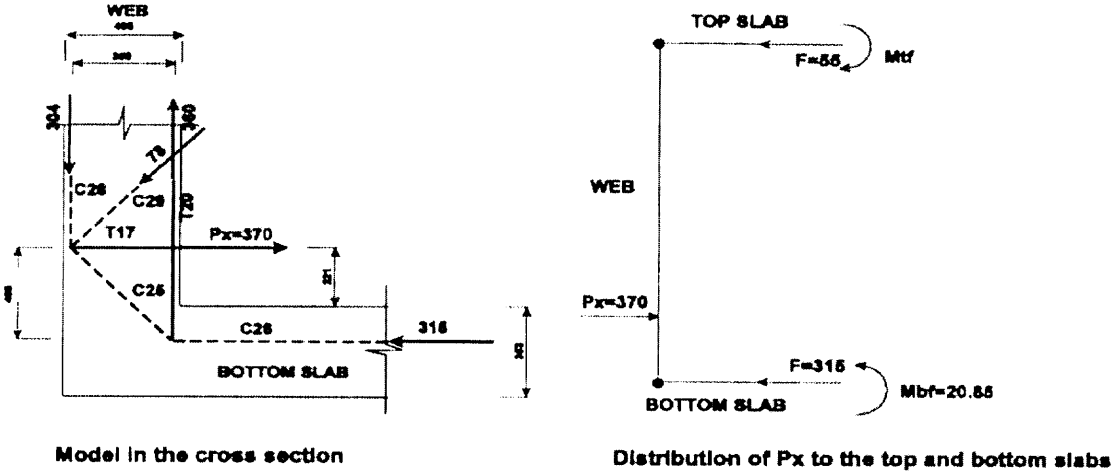

Fig. 26

Where:

C_{26}=315.0 kN

$C_{25} \cong \cos(\text{atan}(0.40/0.35)) = C_{26}$; C_{25}=478.3 kN

$T_{20} = C_{25} \cong \sin(\text{atan}(0.40/0.35)$=360.0 kN

T_{17}=370 kN

C_{29}=(370-315.0)/cos45=78.0 kN

$C_{28} = C_{25} \cong \sin(\text{atan}(0.40/0.35)) - C_{29} \cong \cos 45$=304.80 kN

Reinforcement at the wall of 4 ø 16

Block width: 0.80 m

5 c ø 12

T horizontal total = 3170 + 370 kN = 3540 kN

added 2 c ø 12

27 ø 20

14 c ø 20

7 C^{vert} ø 20

7 x 2 C^{horiz} ø 20

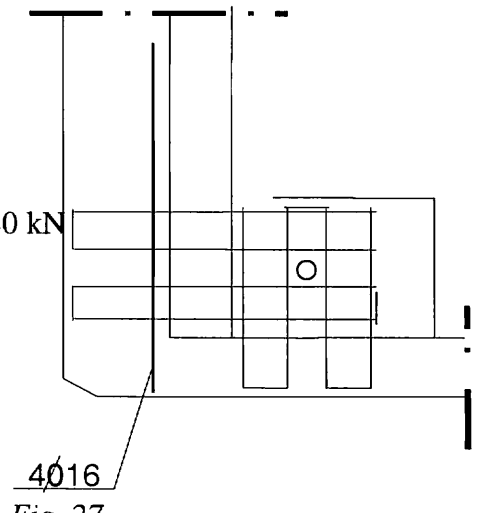

Fig. 27

6.5 Idea for a simple design

From the above models it is realised that the geometry of the anchorage block leads to complicated models, especially in the block. The idea to make the behaviour of the D-region and consequently its strut-and-tie models simpler is follows:

Geometry of the anchorage block should be chosen in such a way that the longitudinal component (Py) of the anchorage force can spread in a plane paralell to the bridge axis. That means, the block then can be idealized to behave as a deep beam and transfer the longitudinal component of the prestressing force to the web and bottom slab only in two points. Consequently the block must be bigger than in the provided design.

In Figure 28 we can see a geometry of the anchorage block. The length of the block should be so chosen that the tension force of tie T1 is not too high and we are able reinforce it well. The size of the block can only be kept small if the anchor is as near as possible to the corner of the box.

Now we can develop models for the spread of the force Py in the web and bottom slab with the same procedure in the above example.

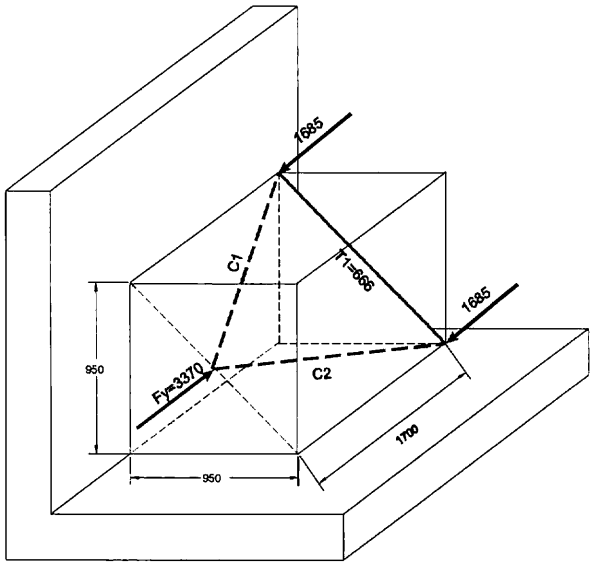

Fig. 28

6.6 Orthogonal field of tension and compression

When there is a compression field that came from two opposites concentrates forces a some distance between. The isostatic lines of compression can be represented for two opposite neck bottle shape. So between them there is a field of orthogonal tension that must be reinforced properly. Figures 29 and 30 show the model for one segment.

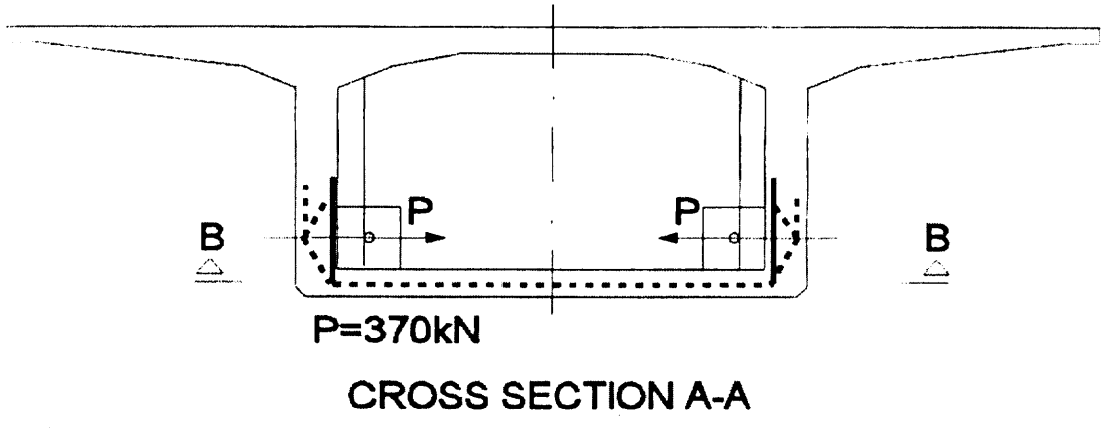

Fig. 29

Width = 1 segment = 2.39

The force that produce this field is in this case not very high but in another case could be important.

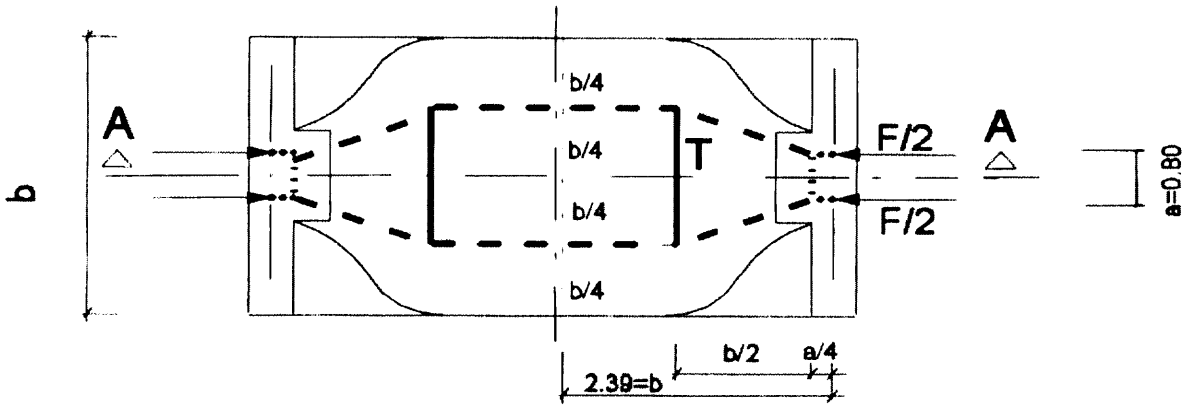

CROSS SECTION B-B

Fig. 30

The transverse force is: F = 0.85 · 370 = 314.5 kN

The geometrical relationships are: b = 2.39 L = 5.40 - 0.40 = 5.0

So: b<L/2

And the expression to use is: $T = \frac{1}{4} \cdot \left(1 - \frac{a}{b}\right) \cdot F = 52.25\ kN$; $\frac{52.25}{2.39} = 21.86\ kN/m$ 1∅ 10/m

7 Anchorage block crack control region D model for serviceability limit state

The external prestressing anchorage blocks are submitted to very high forces. So it is usual that these elements have actually cracks. So it is necessary during design to control the width of these cracks between a model. We will take 7.5.6. paragraph recommendations model. These crack control for D region model is a strut and tie model. In these case ties and struts must have areas.

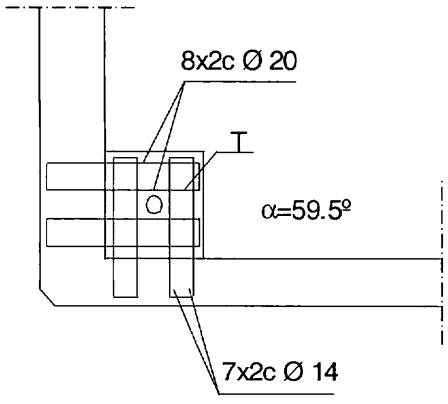

The areas of the ties are the actual areas of steel and the areas of strut are the effective areas for crack control 7.5.4. and 7.5.1 of the recommendation

In our case the tie model is coincident with the actual reinforcement. We have disposed two sets of bars, horizontal and vertical. So we assumed that the tie area is the add of the two projection from the actual reinforced an its effective areas.

Fig. 31

So we have 0.80 m of width with a: $T = 1611 \cdot 2 = 3222\ kN$

And the actual reinforcement is:

- Horizontal Stirrup : 8 x 2 Ø 20 5026 mm^2
- Vertical Stirrup : 7 x 2 Ø 14 2155 mm^2

The characteristic crack width is:

$w_k = s_r \varepsilon_{sm}$

where: s_r is the average distance between cracks

$s_r = 2\,c + \alpha_b \varnothing/\rho$ according to eq. (7.6 a) in the FIP Recomm.:

with $\alpha_b = 0.125$

$c = 40$ mm

The effective area is calculated as follows:

$$A_{cef} = (0.374\cos 59.5 + 0.4\sin 59.5)\cdot 0.8 = 0.534\cdot 0.80 = 0.427\ mm^2$$

$$A_s = 7\cdot 2\cdot 2\cdot 154\cos 59.5 + 8\cdot 2\cdot 2\cdot 314\sin 59.5 = 2188 + 8659 = 10846\ mm^2$$

$$\rho = \frac{10850}{0.427\cdot 10^6} = 0.025$$

$$\varnothing = \frac{14\cdot 2188 + 20\cdot 9659}{10846} = 18.8\ mm$$

So the average distance between cracks is:

$$s_r = 2\cdot 40 + 0.125\frac{18.8}{0.025} = 174\ mm$$

The average strain of the steel γ_{sm} is given by eq. (7.6 b) of the FIP Recomm.:

$\gamma_{sm} = \gamma_s - 0.40\,\gamma_{sr1}$

γ_{sr1} = steel strain at the crack point under the force that produce the first crack:

$$\varepsilon_{sr1} = \frac{f_{ct,\min}}{\rho\, E_s}$$

$$F_{ct,\min} = 0.7\cdot f_{ctm} = 0.7\cdot 3.2 = 2.24\ MPa$$

$$\varepsilon_{sr1} = \frac{2.24}{0.025\cdot 200\cdot 10^3} = 0.000448$$

And γ_s = Steel strain under the force T at the crack

$$\varepsilon_s = \frac{3222\cdot 10^3}{10846\cdot 200\cdot 10^3} = 0.00148$$

$$\varepsilon_{sm} = 0.00148 - 0.40\cdot 0.000448 = 0.00131$$

So we get the characteristic width that is nearly equal that the limit which is permitted

$$w_k = 174\cdot 0.00131 = 0.228\ mm \not\leq 0.20\ mm$$

EXAMPLE 2

Viaduct over the Ribeira de Grandola

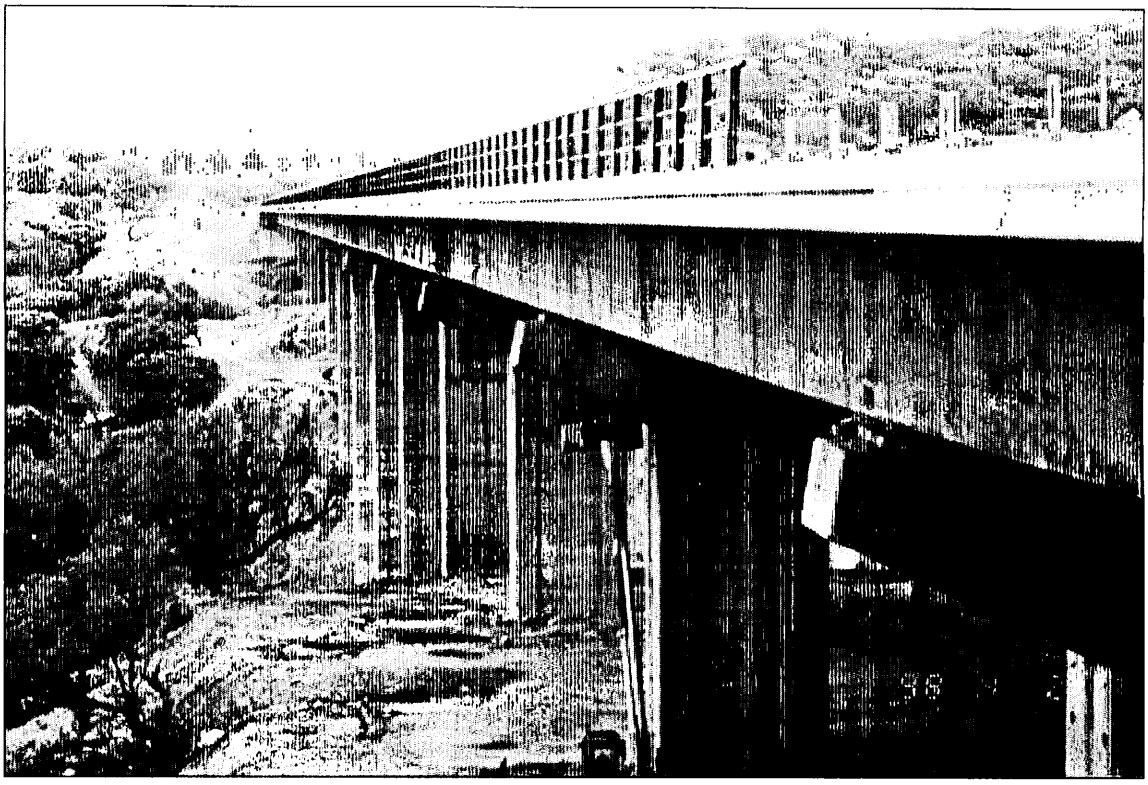

Júlio Appleton
Instituto Superior Técnico
A2P Consult
Lisbon, Portugal

João F. Almeida
Instituto Superior Técnico
JSJ Consult
Lisbon, Portugal

Miguel Sério Lourenço
JSJ Consult
Lisbon, Portugal

Summary

The Viaduct over the Ribeira de Grandola in the South Motorway A2 in Portugal was designed by A2P Consult in 1996 and its construction finished in 1998. One special aspect of this viaduct is the seismic design, which lead to the use of seismic control devices in the connection between the deck and the south abutment and to the use of fixed bearings at the six central piers.

In this example two basic and common structure elements were chosen to illustrate the Recommendations: the design of a pier column head and of a pylon cap. For the pier column head the models presented are the ones for the design for service loads and for the construction phase only with prestressing applied.

1 Description of the structure

This viaduct has a total length of 620.50 m with spans of 34.00 m + 13 x 42.50 m + 34.00 m and two twin decks of variable width from 18.85 m to 21.10 m.

Each deck is a prestressed concrete slab with two longitudinal prestressed beams, 3.20 m high.

The columns have an hollow section with external dimensions of 5.00 m x 2.20 m and 0.35 m/0.70 m thick walls. At the top a column head gives support for the deck beams.

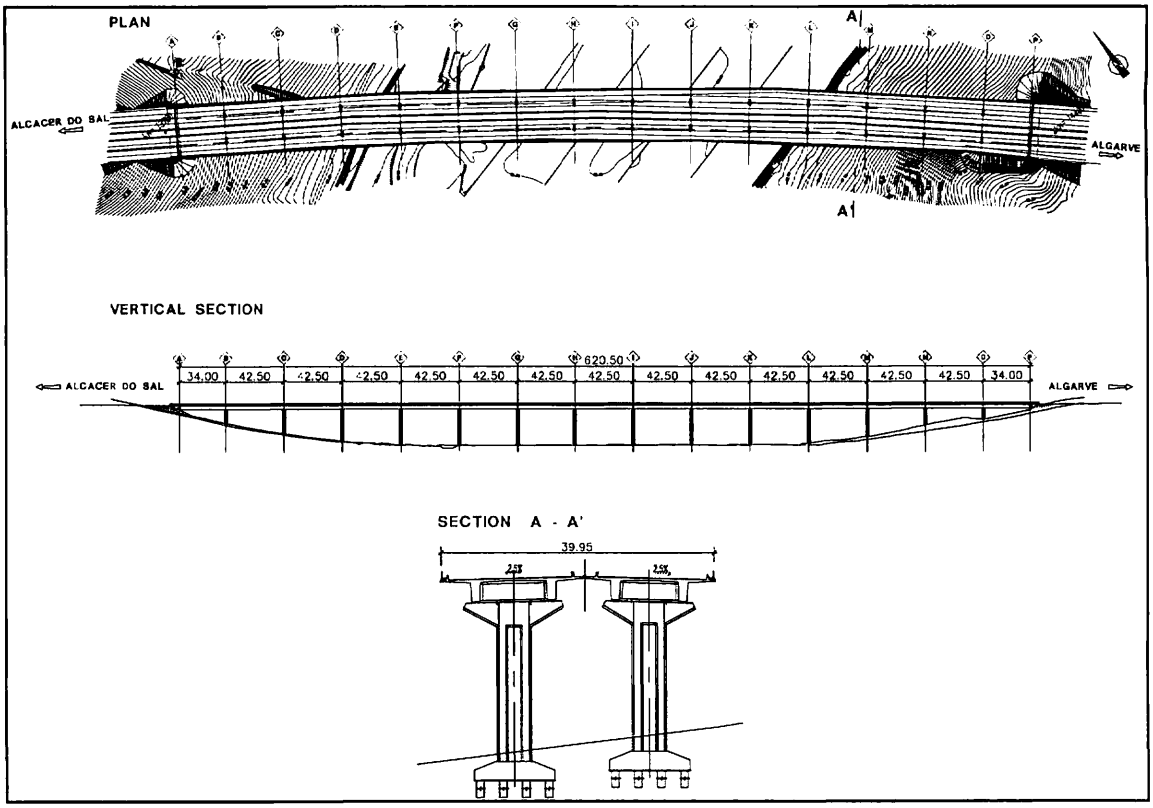

Fig. 1: Geometry of the structure

2 Column head - design for service loads

This example refers to the calculation of the column head and it is an illustration of the FIP Recommendations chapter 6.5.2.3. Corbels.

The load transferred by each beam is F = 16 095 kN and the dimensions of the column head are presented in Fig. 2.1.

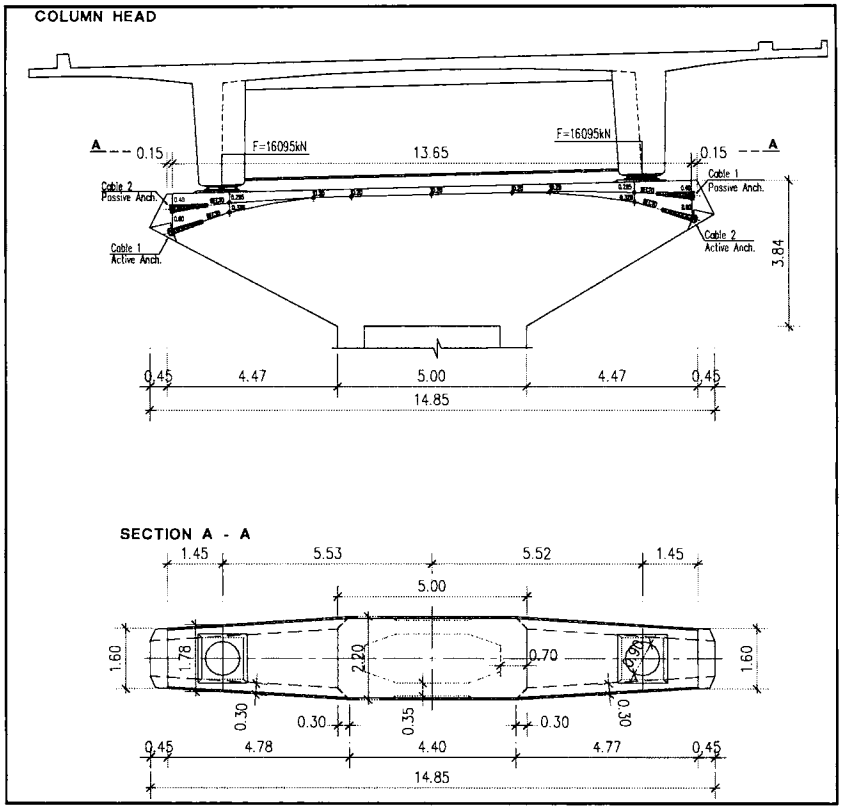

Fig. 2.1: Geometry of the corbel

2.1 Design model

Design calculations according to chapter 6.5.2.3

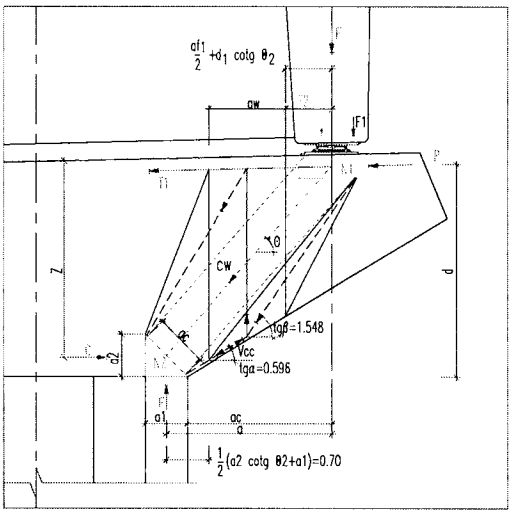

Fig. 2.2: Design model

2.2 Data

F = 16 095 kN

b = 2.20 m, d = 3.635 m, a_c = 3.025 m

f_{ck} = 30 MPa, $f_{1cd} = 0.85 \times \frac{30}{1.5} = 17$ MPa (eq. 2.1)

2.3 Design calculations

2.3.1 Geometry of the model

Step 1 $a_1 = \frac{F}{b\nu_1 f_{cd}} = \frac{16095}{2.2 \times \left(1 - \frac{30}{250}\right) \times 17 \times 10^3} = 0.489$ m

$\nu_1 = 1 - \frac{f_{ck}}{250}$

a_1 assumed as 0.70, the thickness of the column wall.

Step 2 $a_2 = d - \sqrt{d^2 - 2a.a1} = 3.635 - \sqrt{3.635^2 - 2 \times 3.27 \times 0.70} = 0.695$ m

$a = a_c + \frac{a_1}{2} = 3.025 + \frac{0.70}{2} = 3.375$ m

$z = d - \frac{a_2}{2} = 3.635 - \frac{0.695}{2} = 3.285$ m

Step 3 $\text{cotg}\,\theta = \frac{a_2}{a_1} = 0.993$ ($\theta = 45.2°$)

Since $\frac{z}{2} = 1.6425 \leq a = 3.375 \leq 2z = 6.57$ (6.5.2.3 (1))

Part of the load F shall be transferred by a beam type mechanism (F_1) and requires shear reinforcement, and the other part (F_2) is transferred by a direct inclined strut.

$\frac{F_1}{F} = \frac{\left(2\frac{a}{z} - 1\right)}{3}$; i.e. $F_1 = 0.352\,F = 5\,665$ kN

$F_2 = 10\,430$ kN

2.3.2 Transfer of load F1

Transverse reinforcement (F_1 - V_{cc}) - 6.5.2.3.(1)

To be distributed over

$$a_w = 0.85\ a - \frac{z}{4} = 2.0475\ m$$

From the figure

$$V_{cc} = \frac{F_1}{tg\beta} \cdot tg\ \alpha = \frac{5665}{1.548} \times 0.5963 = 2\ 182\ kN$$

$$\frac{F_1 - V_{cc}}{a_w} = \frac{5665 - 2182}{2.048} = 2\ 767\ kN/m \leq \frac{A_{sw}}{s} . f_{syd}$$

For $f_{syd} = 348$ MPa $\rightarrow \frac{A_{sw}}{s} \geq 48.9\ cm^2/m$ (distributed in a_w)

2.3.3 Strength of the inclined strut at load transfer F (node N1)

This check is satisfied if the width of the bearing plate a_F fulfils

$$a_F \geq \frac{x}{\sin\theta_2}\left[\frac{\nu_1}{0.6\cos\theta_2} - \cos\theta_2\right]$$

$$\cot g\ \theta_2 = \frac{a}{z} = 1.027\ ;\ x = 0.40\ m$$

$a_F \geq 0.7631$ m (bearing plate provided with 0.90 m)

2.3.4 Transfer of load F (node N1)

$T_1 = F \cot g\ \theta = 15\ 800\ kN \leq F_{spr}$

F_{spr} (6 cables of 19 strands 1.4 cm²/each, $f_{spk} = 1\ 670$ MPa) = 23 180 kN

2.3.5 Check of node N1

According to 5.6.2. - CCC Node, considering the effect of the prestressing anchorage:

$$\sigma_{c0} = \frac{F}{A_{c0}} \leq f_{2cd}\sqrt{\frac{A_{c1}}{A_{c0}}} \quad \text{(eq. 3.20)}$$

$$\leq f_{3cd} \quad \text{(eq. 5.19b)}$$

$$A_{c0} = \pi \times \frac{0.9^2}{4} = 0.636\ m^2$$

$$A_{c1} = \pi \times \frac{1.78^2}{4} = 2.49\ m^2$$

$$\sigma_{c0} = \frac{16095}{0.636} = 25\,306 \qquad \leq 1.2 \times 17 \times 10^3 \sqrt{\frac{2.49}{0.636}} = 40\,364.4 \text{ kN/m}^2$$

$$\leq 3.88 \times 17 \times 10^3 = 65\,960 \text{ kN/m}^2$$

2.3.6 Check of node N2

According to 5.6.2. - CCC Node.

$$\sigma_{c0} = \frac{F}{b \times a_1} \leq f_{1cd} \sqrt{\frac{A_{c1}}{A_{c0}}} \quad (5.20)$$

$$\sigma_{c0} = \frac{16095}{2.2 \times 0.70} = 10\,451 \text{ kN/ m}^2 \leq f_{1cd} .1 = 17\,000 \text{ kN/m}^2$$

(incorporated in Step 1 - see 2.3.1).

2.3.7 Check of inclined strut (at node N2)

According to 5.3.2.:

This verification is not required if the nodes are checked. It is presented to illustrate the recommendations:

$$\sigma_c = \frac{C_w}{x_c b} \leq \nu_1 f_{cd} \qquad \nu_1 = 0.88$$

$$\leq \nu_2 f_{cd} \qquad \nu_2 = 0.8$$

$$C_w = \frac{F}{\sin\theta} = 22\,324 \text{ kN}$$

x_c (at node N2) = 0.986

b = 2.2 m

$$\sigma_c = \frac{22324}{0.986 \times 2.2} = 10\,291.3 \leq 0.8 \times 17 \times 10^3 = 13.6 \text{ MN/m}^2$$

3 Prestressing in the column head - Model for construction phase

3.1 Introduction

Prestressing in the corbel was designed imposing no tension under rare combination of loads (P'_0 = 18183 kN). As a consequence, tension occurs, temporarily, during construction phase, at the bottom region of the corbel.

3.2 Geometry and loads

Prestressing cables are modelled by a resultant cable and the cable-layout is simplified by considering a bilinear profile. Fig. 3.1 shows the geometry of the corbel, the bending stresses at the central zone and the equivalent effects of the cable-layout considered (anchoring and deviation forces).

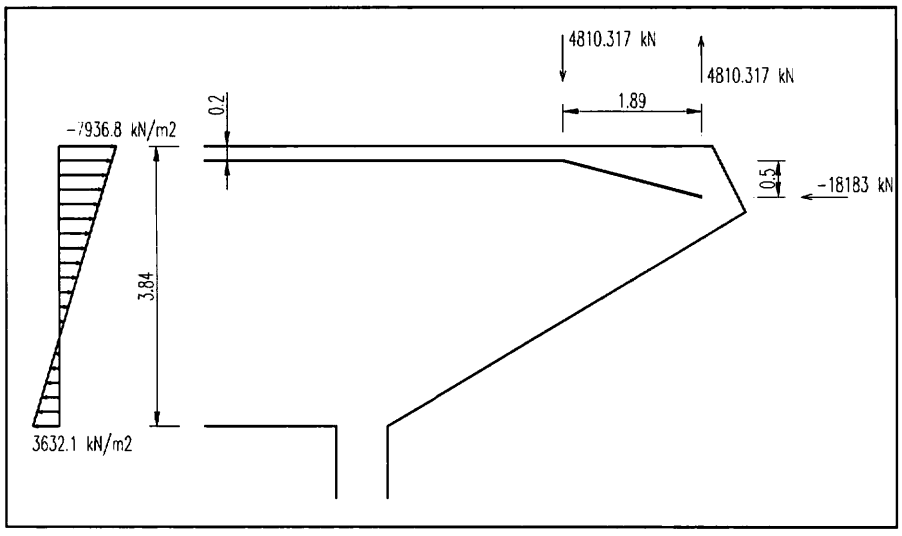

Fig. 3.1: Geometry and loads

3.3 Geometry of the model

The model presented in §6.5.7.1 should be adapted to fit with the geometry of the corbel (Fig. 3.2). The position of T_1 and C_2 is defined by the centroid of, respectively, the tension and compression zones of the stresses diagram. C_3 is related with the deviation of the tension bottom force and C_2 should split in three parts, to equilibrate the anchoring and the deviation forces. Local splitting forces near the prestressing anchor are not represented.

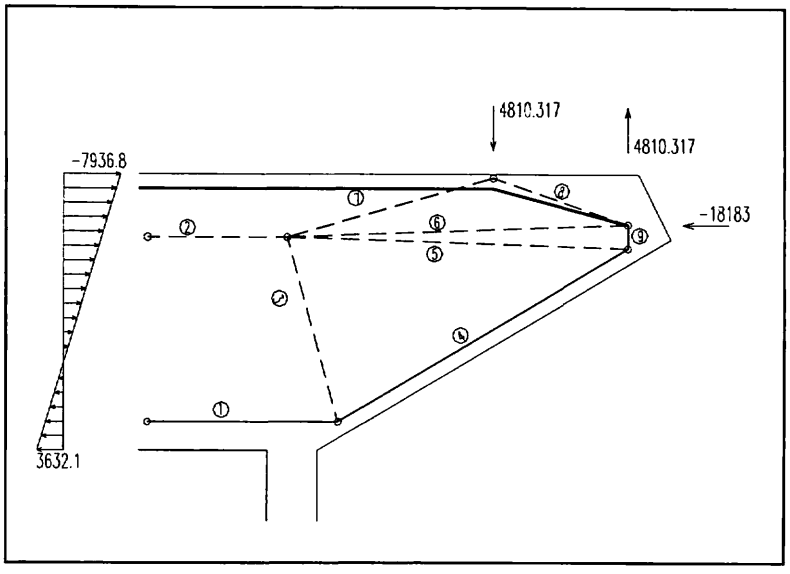

Element	Force [kN]
1	4816
2	-22999
3	-2558
4	4816
5	-4139
6	-10068
7	-8421
8	-8527
9	2600

Fig. 3.2: Geometry of the model

The inclination of C_3 is not predefined having no significant influence on the tension forces in ties T_4 and T_9. In the present case the direction of C_3 leads to similar T_1 and T_4 forces.

The model presented before can be refined following the principles of the general model proposed in §6.5.7.1. As illustrated in Fig. 3.3, the stresses compression zone should then be divided in three blocks: the first one (C_2) is equivalent to the tension force (T_1), and the remaining part, having a force resultant equivalent to the prestressing force, further sub-divided in the zones above and below the prestressing cable (C_3 and C_4).

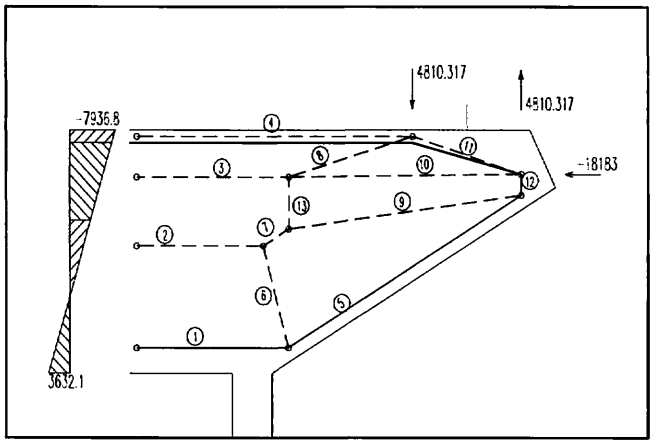

Element	Force [kN]
1	4816
2	-4816
3	-14824
4	-3359
5	4816
6	-2558
7	-4816
8	-6308
9	-4173
10	-8785
11	-9863
12	1918
13	-1918

Fig. 3.3: Refined model

The forces T5 and C7 should have the same intensity and direction in order to ensure that the vertical resultant force ("shear in the corbel") is null.

3.4 Design of steel reinforcement

T1 and T5

$A_s = 4816 \times 10^3 / 348 = 13839 \text{ mm}^2 \Rightarrow 28 \phi 25$

T12

$A_s = 1918 \times 10^3 / 348 = 5511 \text{ mm}^2 \Rightarrow 12 \phi 25$

3.5 Detailing

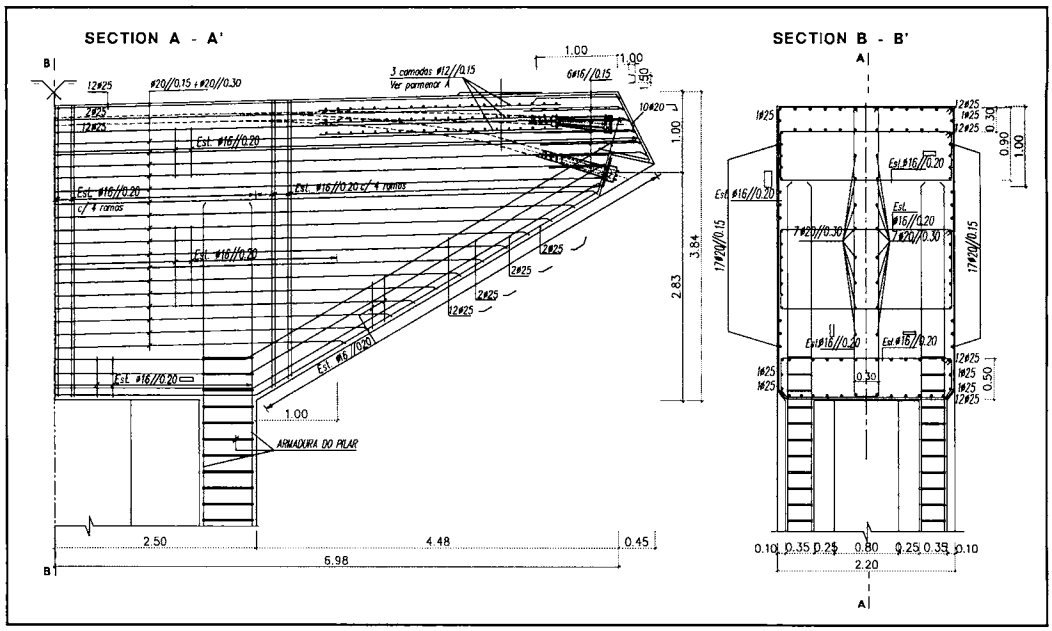

Fig. 3.4: Reinforcement layout

4 Pylon Cap Design

4.1 Geometry and Loads

The present section refers to the design of the pylon cap at the base of the columns. Figure 1 shows the geometry and the design actions (ULS) for the load case considered.

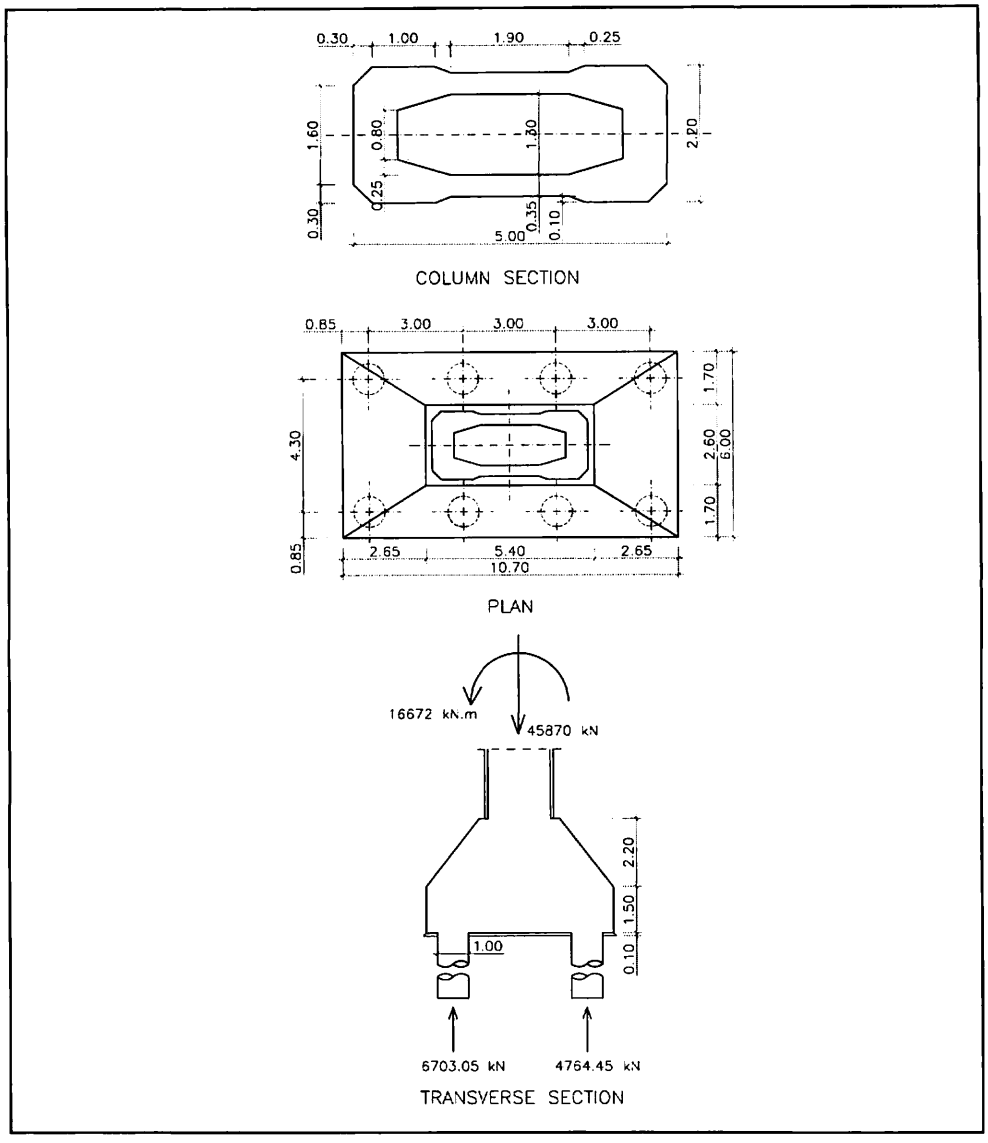

Fig.4.1: Geometry and loads

4.2 Geometry of the model

In order to simplify the model a solid column section was firstly used for the calculation of the normal stresses at the column base. Fig. 4.2 shows the geometry of the model. Taking into account the reinforcement layout, tension forces are considered along the pylons alignments. The corresponding element forces are indicated in Fig. 4.3.

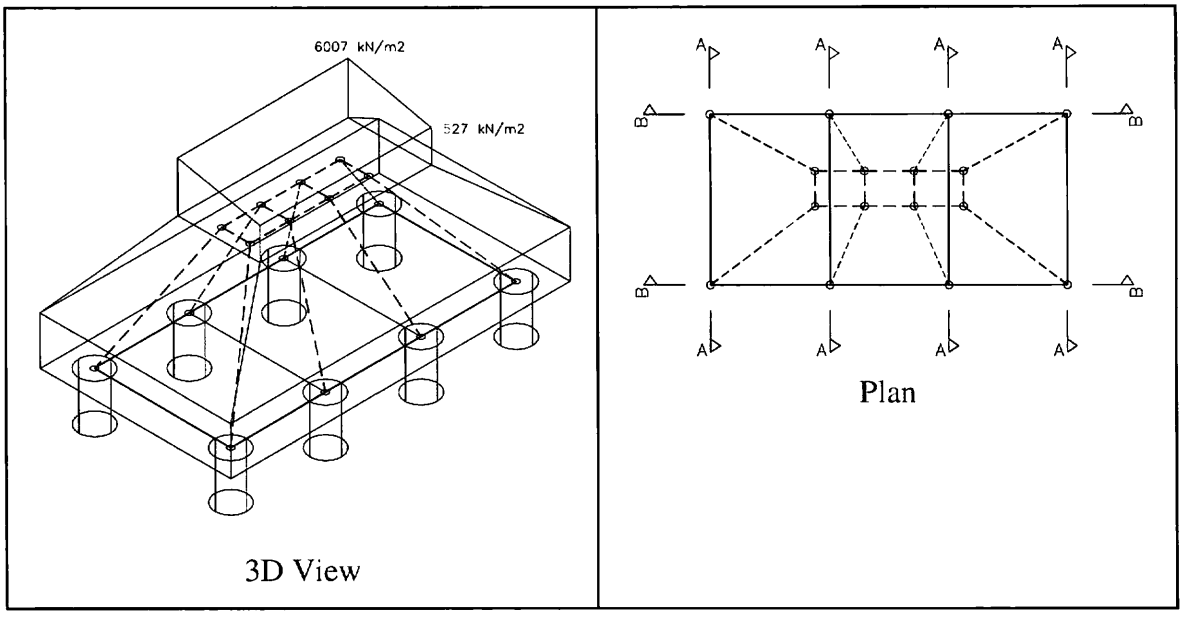

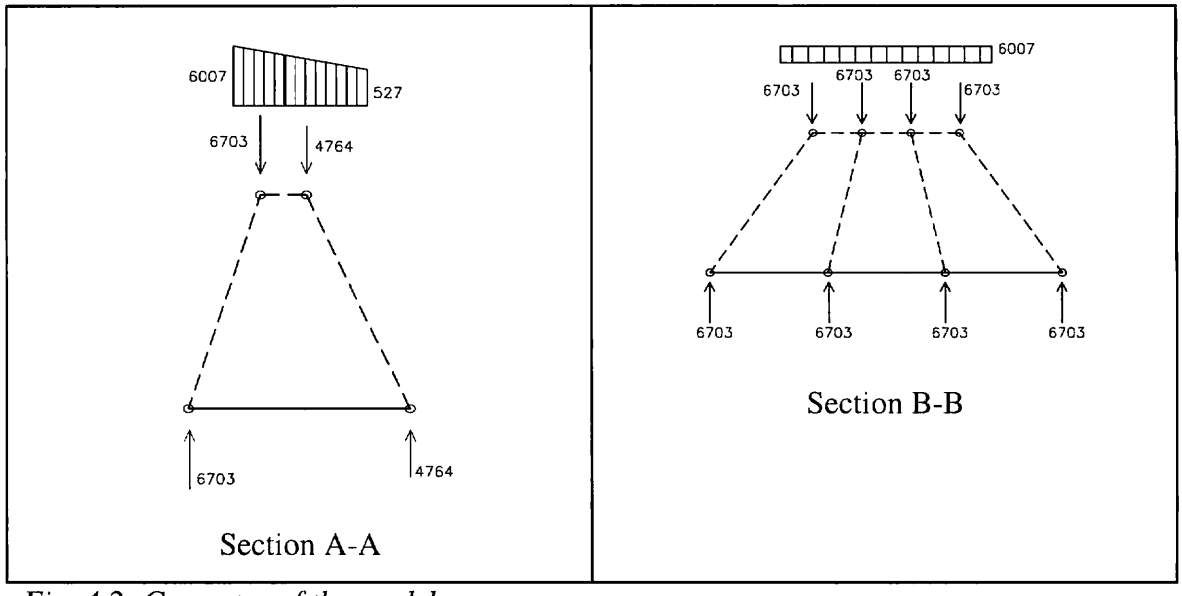

Fig. 4.2: Geometry of the model

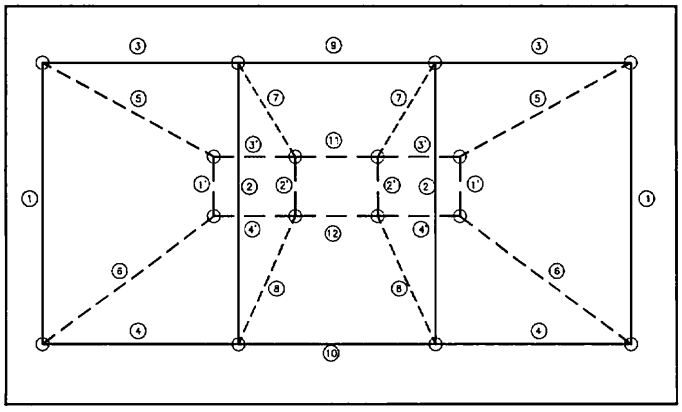

Fig. 4.3: Element forces

Element	Force [kN]
1	2917
2	2917
3	5414
4	3848
1'	-2917
2'	-2917
3'	-5414
4'	-3848
5	-9097
6	-6784
7	-7530
8	-5732
9	7219
10	5131
11	-7219
12	-5131

4.3 Steel reinforcement design

Longitudinal reinforcement

$F^{9}_{s,máx} = 7219 \times 10^3 / 348 = 20744 \text{ mm}^2 \Rightarrow 3 \times 9\ \phi\ 32$ (three layers)

Transversal reinforcement

$F^{1}_{s,máx} = 2917 \times 10^3 / 348 = 8382 \text{ mm}^2 \Rightarrow 2 \times 9\ \phi\ 25$ (two layers)

4.4 Check of node N1

$f_{1cd} = 0.85 \times f_{ck} / \gamma_c = 0.85 \times 30/1.5 = 17.0$ MPa

$f_{cd,eff} = \nu_2 \times f_{1cd} = 0.85 \times 17 = 14.5$ MPa (§5.6.4)

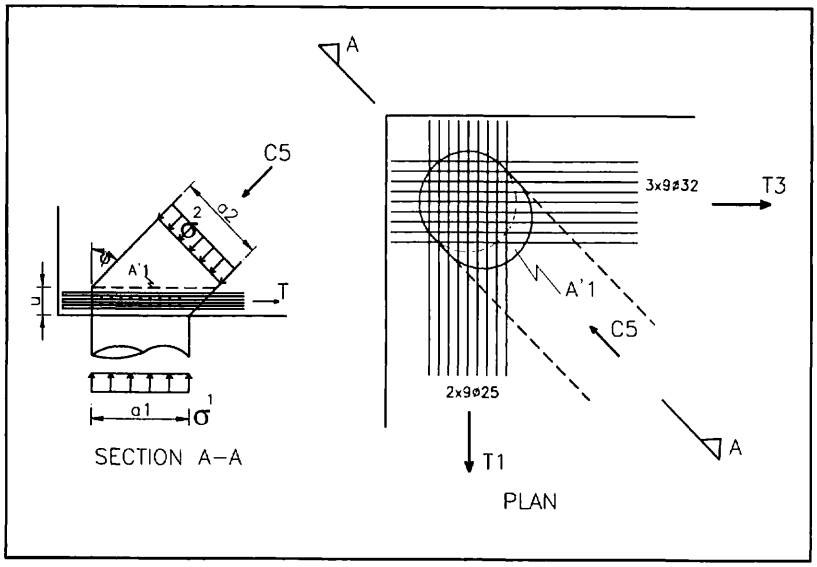

Fig. 4.4: Node N1

The equilibrium conditions lead to the equations:

$$\frac{\sigma_1}{\sigma_2} = \left(1 + \frac{4}{\pi} \times \frac{u}{a_1} \times \text{tg}\varphi\right) \times \cos^2\varphi \qquad \text{and} \qquad T = \sqrt{T_1^2 + T_3^2}$$

$a_1 = 1.0$ m

$u \approx 0.25$ m

$\varphi \approx 45^\circ$

$\sigma_1 = 8.5$ MPa

$\sigma_2 = 12.9$ MPa $< f_{cd,eff}$

Anchorage of reinforcement (§2.4.1)

$$l_b = \frac{\phi}{4} \times \frac{f_{yd}}{f_{bd}} = \frac{\phi}{4} \times \frac{348}{1.05 \times 2.9} = \begin{cases} 700\text{mm}, \phi 25 \\ 900\text{mm}, \phi 32 \end{cases}$$

$$f_{bd} = 1.05 \times f_{ctm}$$

Since horizontal tension occurs in both directions the favourable effect of the vertical transverse pressure should not be considered. On the other hand, the anchorage length of longitudinal reinforcement can be reduced ($A_{s,req}<A_{s,prov}$, §5.6.4). In fact, the steel reinforcement design was performed considering for the maximum tension force occurring at the central zone and then extended all along the longitudinal direction.

$l_b = 900$ mm

$A_{s,req} = 5414 \times 10^3 / 348 = 15557$ mm^2 (Element 3)

$A_{s,prov} = 3 \times 9 \times 804 = 21715$ mm^2

$l_{b,net} = A_{s,req} / A_{s,prov} \times l_b = 645$ mm

In both directions the tension forces can be anchored inside the node.

4.5 Transfer of the strut force C_5 across the interface (§5.5)

$$A'_1 = \frac{\pi . a_1^2}{4} + a_1 \times u \times tg\varphi = 1.035 \text{ m}^2 \text{ (see fig. 4.4)}$$

$$T = \sqrt{T_1^2 + T_3^2} = 6149.8 \text{ kN}$$

$\tau_{fd} = 0.5 f_{ctm} + 1.2 \sigma_f = 9.25$ MPa

$\sigma_f = 6703.05 \times 10^{-3} / 1.035 = 6.5$ MPa

$\tau_{sd} = T / A'_1 = 6149.8 \times 10^{-3} / 1.035 = 5.9 \text{ MPa} < \tau_{fd}$

4.6 Detailing

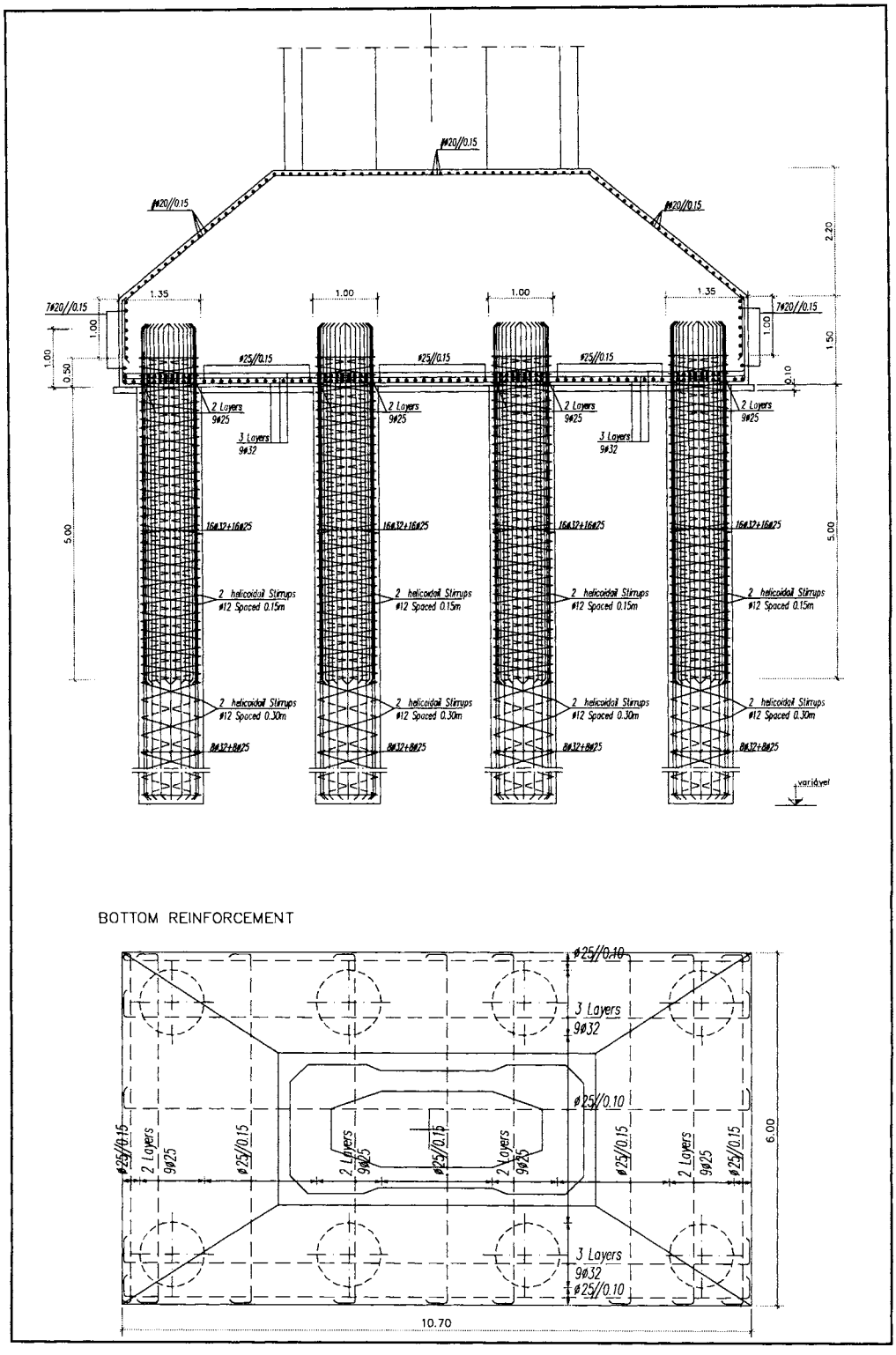

Fig. 4.5: Reinforcement layout

4.7 Final Remarks

Fig. 4.6 and 4.7 shows the model geometry and forces if normal stresses at the column base are considered assuming the box section shape. The section column geometry was considered as a box section with constant thickness walls.

The resulting model is slightly more complicated because equilibrium of transverse moments needs for struts C_{13} and C_{14}, at the bottom and top horizontal planes.

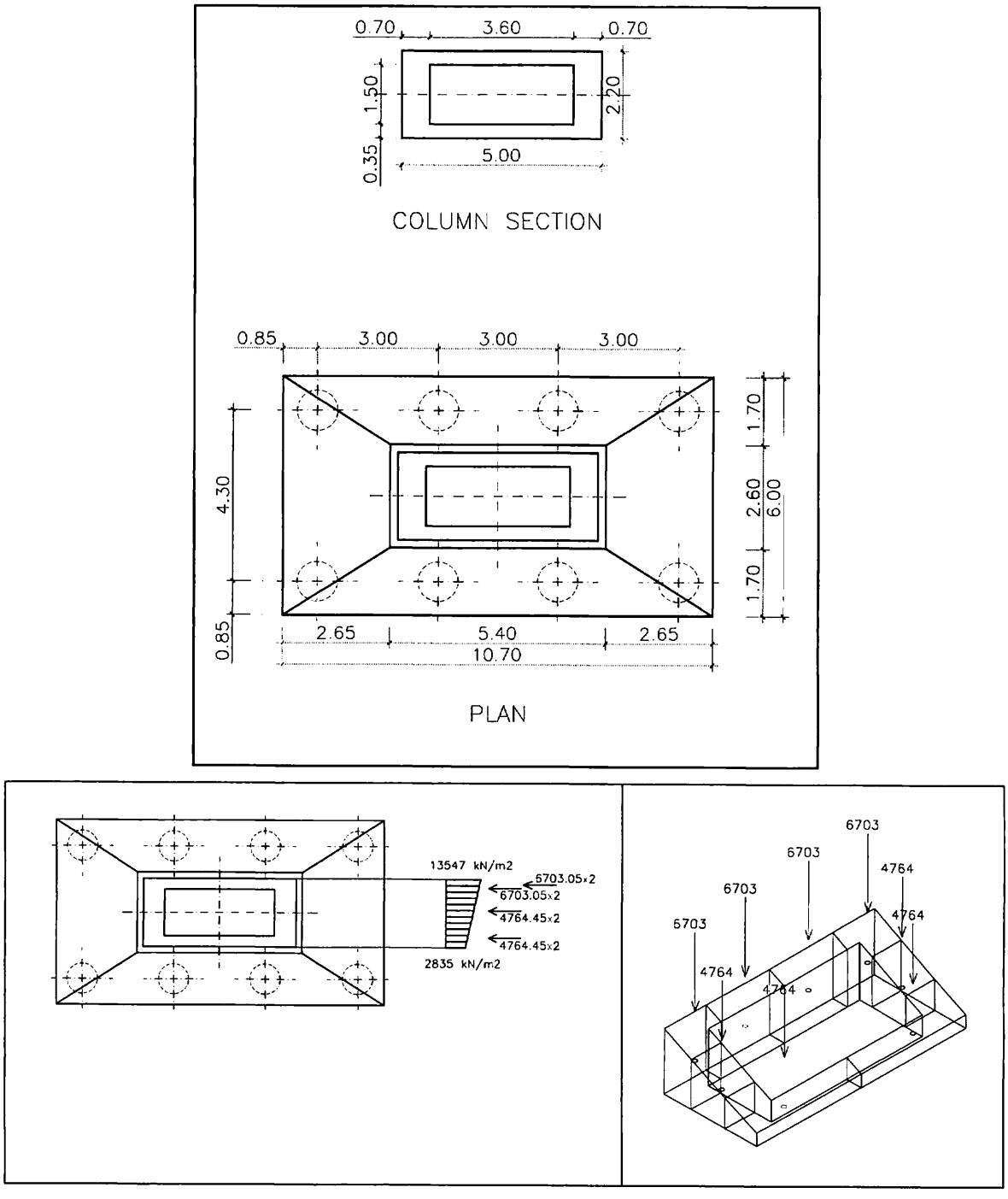

Fig. 4.6: Column box section stresses

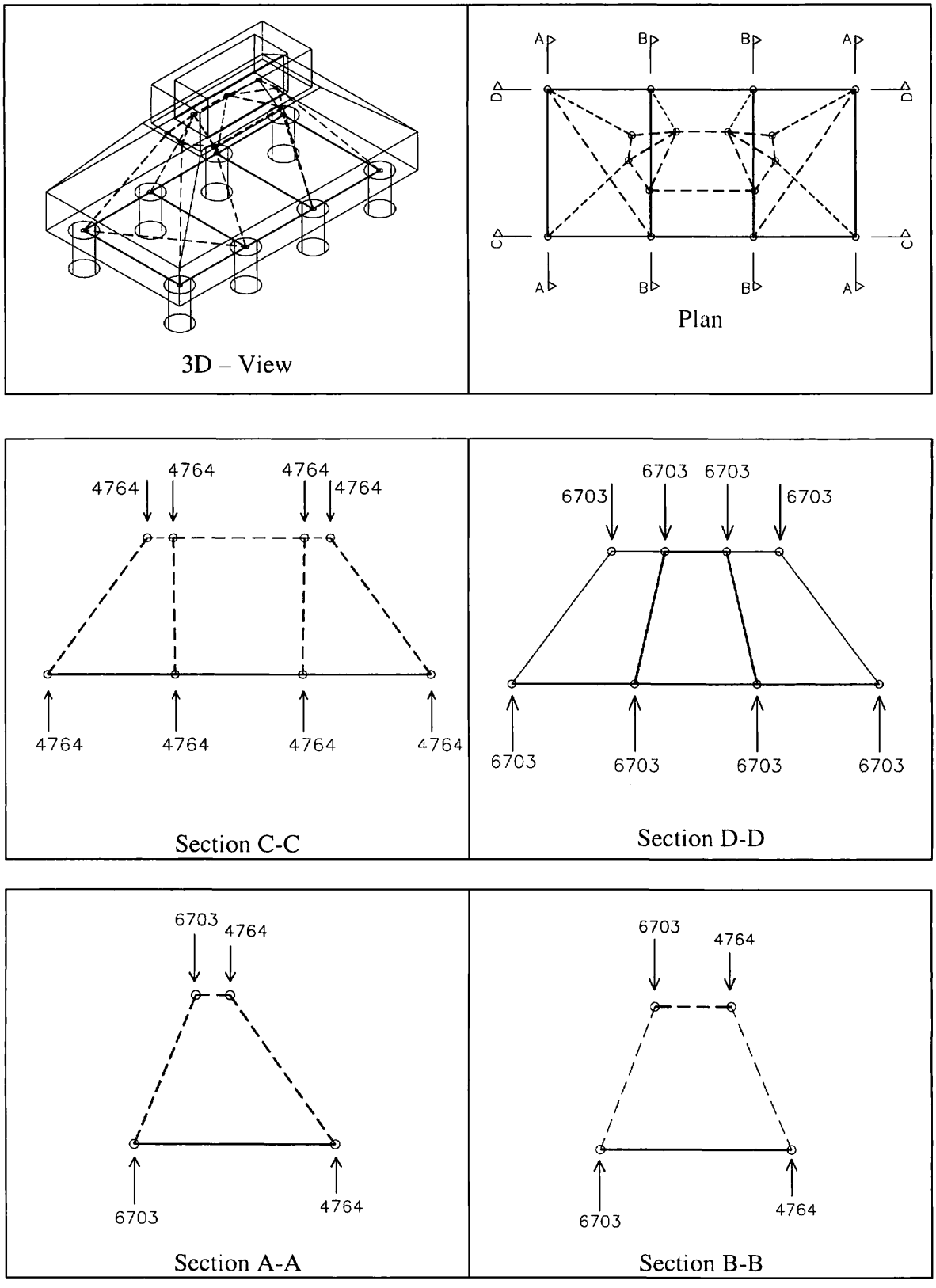

Fig. 4.7: Geometry of the model

The resulting forces are not substantially changed (T_1 and T_2 are no more equal), having no practical influence on the calculations previously presented.

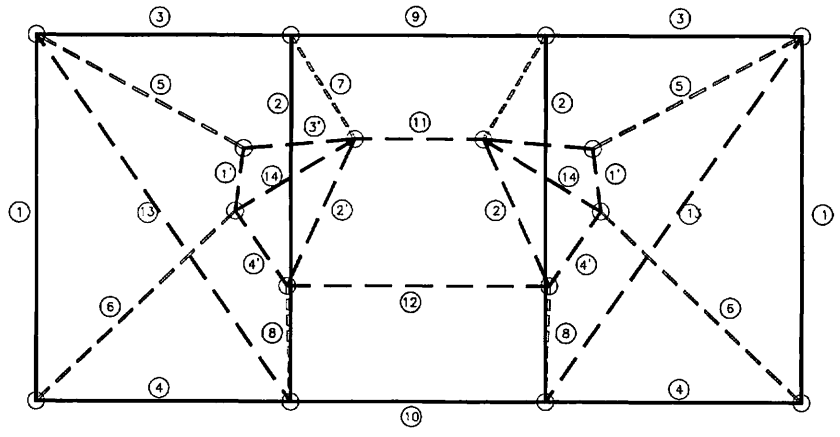

Element	Force [kN]
1	3274
2	2518
3	5412
4	3445
1'	-3241
2'	-819
3'	-5483
4'	-1520
5	-8827
6	-6729
7	-7324
8	-5164
13	-642
14	-2522
9	6950
10	3018
11	-9499
12	-469

Fig. 4.8: Element forces

EXAMPLE 3

Vallhall Monotower Platform – design of D-regions

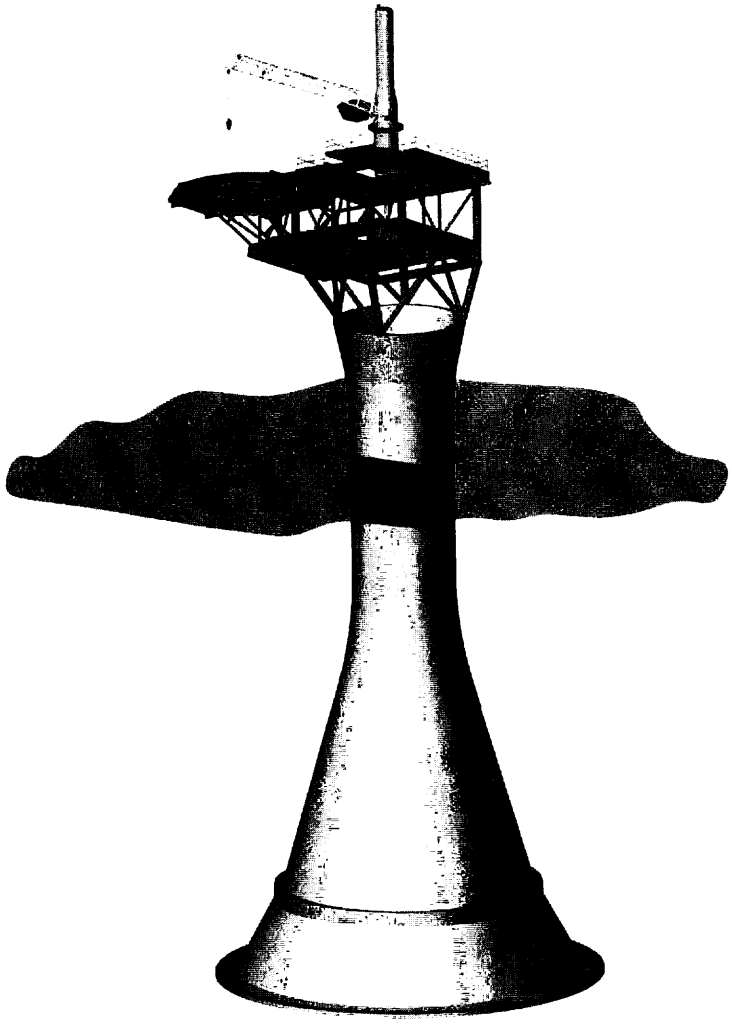

Ketil Nærum

Stein Atle Haugerud

Dr. techn. Olav Olsen a.s.
Oslo, Norway

1 General description

1.1 Description of the structure

The rotational symmetric monotower concept for Valhall consists of a deck supporting shaft and a foundation structure, which gives a simple transfer of shaft loads to the ground. The foundation structure, consisting of two conical walls on a circular base slab, is based on principles adopted from conventional onshore tower structures (fig. 1). Stiff ring beams are introduced at connection shaft/cones and inner cone/slab connection to take horizontal force components. The total height of the concrete substructure is 87.5 m. With a water depth at site of 70 m, the substructure will tower 17.5 m above the main sea level.

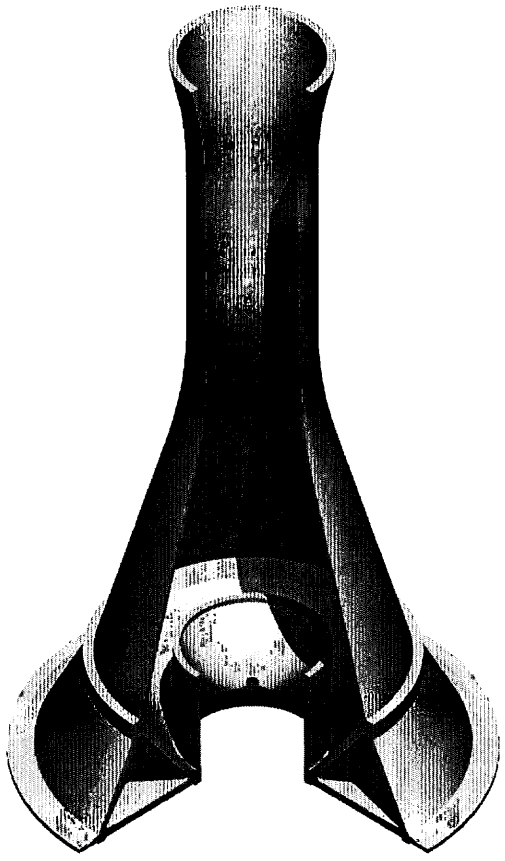

Figure 1: Valhall Monotower Platform – 270° cut-out sector.

The cone compartment (annulus) will serve as oil storage in operation. Four radial walls in the cone compartment are introduced to ensure floating stability in the construction phases only.

The shaft configuration is selected compromising the buoyancy requirements at tow to field and the wave loads during Operation. The minimum shaft diameter, $\emptyset_i$ = 13.5 m, is selected to accommodate the necessary mechanical outfitting.

The minicell with internal diameter $\emptyset_i$ = 16 m is included to provide space for predrilled wells and passive installation piles. A dome is selected to minimize weight. The dome will have penetrations for conductors and for instrumentation necessary for installation.

The entire base area will be grouted during installation at field, thus ensuring an even distribution of ground pressures into the base of the structure. The bottom slab has ribs underneath the cone walls for temporary support on the seabed at installation. Around the inner and outer periphery of the base slab, steel skirts are provided in order to prevent leakage during grouting. Outer diameter of the base slab is 54 m.

To ensure required minimum submerged weight in Operation, the shaft is ballasted with olivin reaching up to the top of the minicylinder.

A general section of the monotower structure is shown in fig. 2 together with main dimensions and key figures.

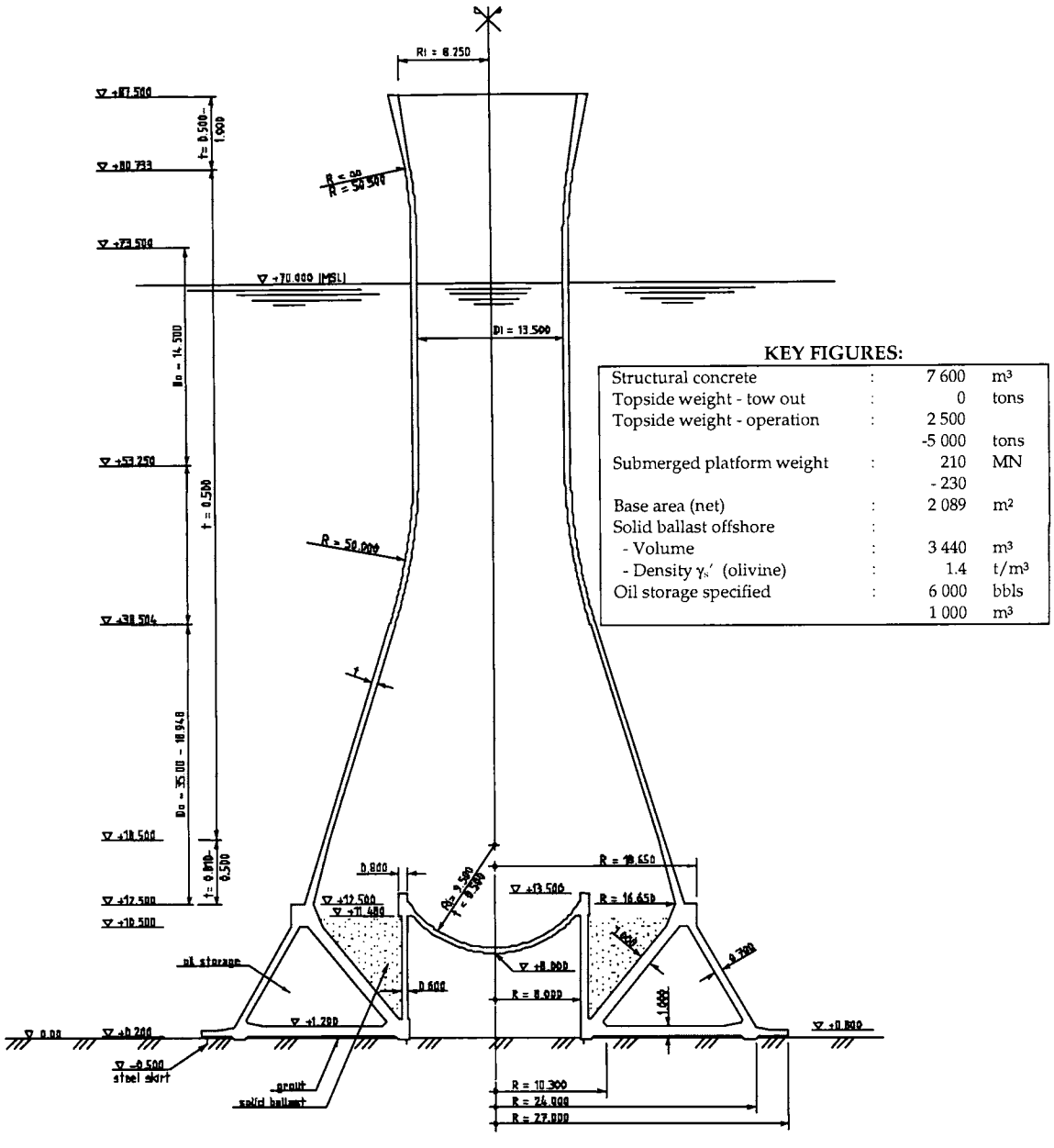

Figure 2: General section with main dimensions

1.2 Construction

The construction of the foundation and lower part of the shaft will take place in a dry dock. Subsequently, the structure is towed to a deep water site for completion (fig. 3.b). The rest of the shaft will be slipformed while the structure is lowered in the water in order to ensure adequate floating stability. Before the platform is towed to the field, mechanical outfitting and a deck module supporting frame (MSF) will be installed.

At the field, the structure will be lowered down over the predrilled wells, grouted and ballasted. Finally, the deck module will be mated onto the MSF in a lifting operation.

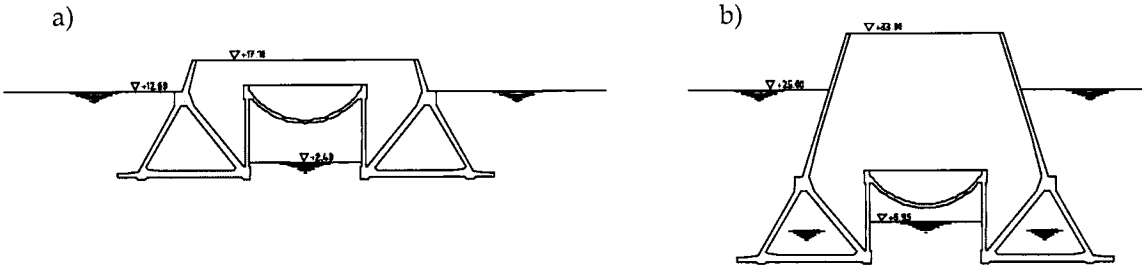

Figure 3: Construction phases - a) Out of dock and b) Filling of annulus (cone compart ments)

2 Loads and response

2.1 Typical loadings

2.1.1 Construction stages

In the construction- , transportation- and installation-phases, the governing loadings are water pressure and dead weight. For the phase "Tow out from dry dock" eccentricity between the resultants from dead weight and buoyancy will introduce hoop tensile forces due to global flexure of the structure. During slipforming of the shaft, the structure is lowered by waterfilling of the cone compartments (annulus). When the annulus is completely waterfilled, the compartments will be opened to sea. At this moment the outer cone wall and the base slab are subjected to maximum pressure differences. The shaft, minicylinder and the inner cone wall will be subjected to the highest pressure differences during the installation-phase.

2.1.2 Operation (environmental loads)

The governing loadings in the Operation phase results from the environmental loads such as waves, wind and current. In addition, the structure must resist accidental loads from ship impact and dropped objects. Minor pressure differences are set up in cone walls from ballast in lower part of the shaft and also from oil storage in the cone compartments.

The maximum environmental overturning moment at mudline is predicted to 2'527 MNm for a 100 year return period including dynamic amplification factor.

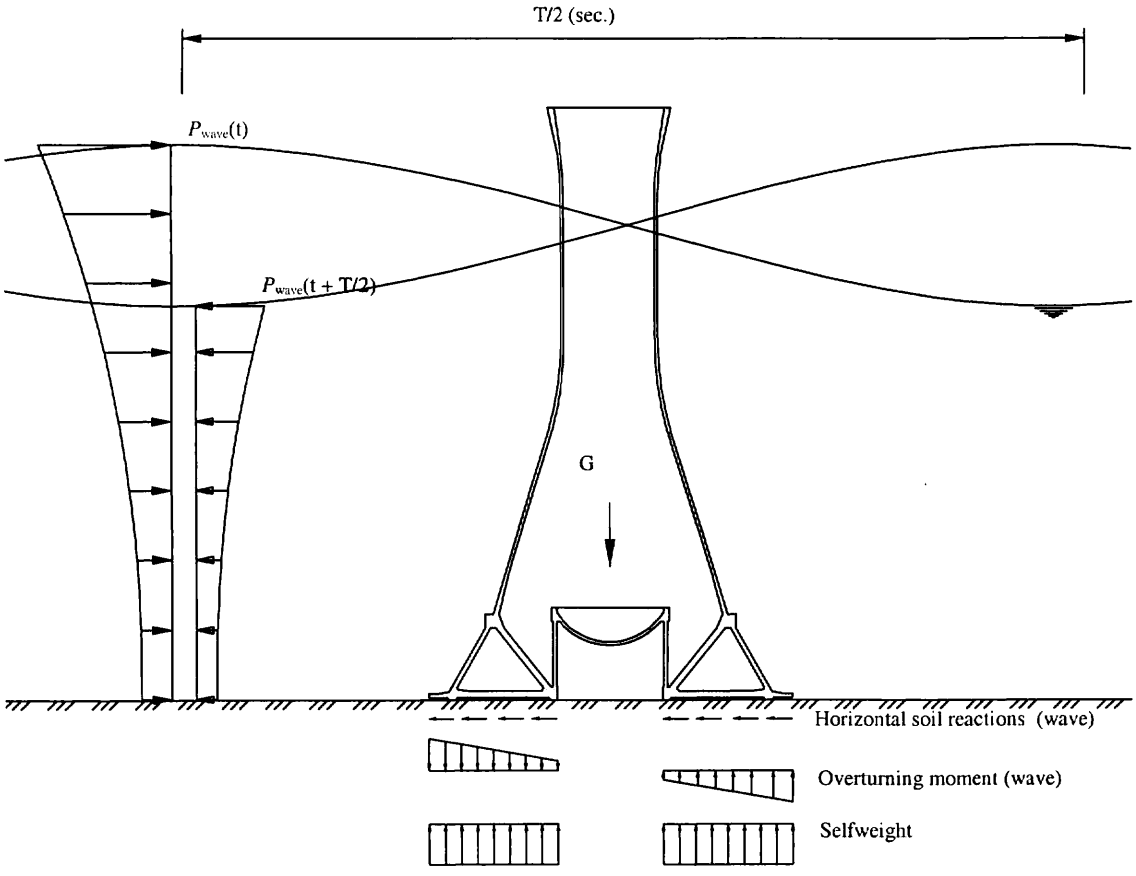

Figure 4: Governing loadings in the Operation phase.

2.2 Response predictions

2.2.1 Global FE analysis

In final design of concrete offshore platforms, several numerical analyses are performed. The response predicted from a linear global finite element analysis (GA) serves as the main basis for the structural design of the platform. The model built from higher order volume elements represent the entire structure for the actual phase of construction. Built in stresses are included by combining results from previous construction phases. Integrated stress resultants, i.e. sectional forces, from the GA are then used as input for design code check by use of post-processing program and also for the design of D-regions by strut and tie models.

Supplementary analyses for input to GA and for scaling of GA results are:

- *Dynamic analysis*: Calculation of the dynamic amplification factors and the natural period of the structure during operation.
- *Wave analysis*: Basis for design wave selection and generation of wave loading for structural analysis (GA)
- In addition, *Earthquake analysis* and *Soil-Structure-Interaction analysis* might be performed for the Operation phase.

Additional non-linear analyses are either performed for refined calculations of cut-out models from GA (e.g. design of D-regions) or on full structures of limited extension (e.g. implosion of empty shaft and ship impact).

For the conceptual study of the Valhall platform, the basis for the design is an GA analysis of a ¼ model of the platform fixed in the shaft top. The load response in lower part of the structure is simulated by putting soil reactions from dead weight and wave onto the bottom slab (fig. 4). Equilibrium is established by scaling the ground reactions to balance the results from the wave and dynamic analysis. For the design of the lower part of the structure this method gives an adequate simulation of the load response. For the design of the shaft however, the vertical tension caused by the unphysical restraint in top of shaft will require a more refined method.

2.2.2 R-plots

One barrier for a successful analysis and design of D-regions is the selection of the governing load case(s). In order to be able to evaluate and sort the vast information provided by the GA, special emphasis has been put on to systematize and ease this selection process. This resulted in the introduction of R-plots, which is simply a graphical visualization of the cross sectional response expressed by a global resultant and the associated eccentricity. The method was initially developed for the design of ring beams, but is also applicable for other structural elements subjected to high axial compression.

$$R = \sqrt{N^2 + V^2} \quad ; \quad e = \frac{M}{N}$$

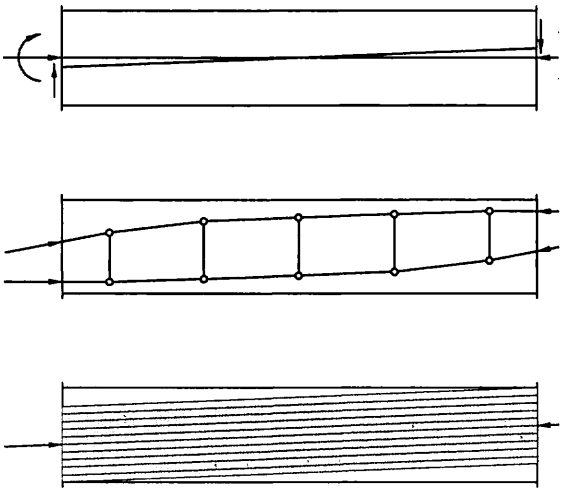

Figure 5: Structural action for a member subjected to shear and axial compression with moderate eccentricity

The procedure can be described with the aid of a structural member subjected shear, moment and axial compression subsequently increasing the eccentricity of the axial force. The structural action is described by stress fields in accordance with the theory of plasticity (rigid-plastic solution). Taking the non-linear behaviour into account, the transmission of the load will set up transverse tension in the member (fig. 5). For small eccentricities however, the transverse tension can be carried by the concrete itself or taken by the nominal stirrup reinforcement. Employing the rigid plastic solution for an unreinforced member, the maximum eccentricity is found by exploiting the compression zone simultaneous utilizing the yield strength in the compression field. Smaller eccentricities allows for direct load transmission without any reinforcement statically required.

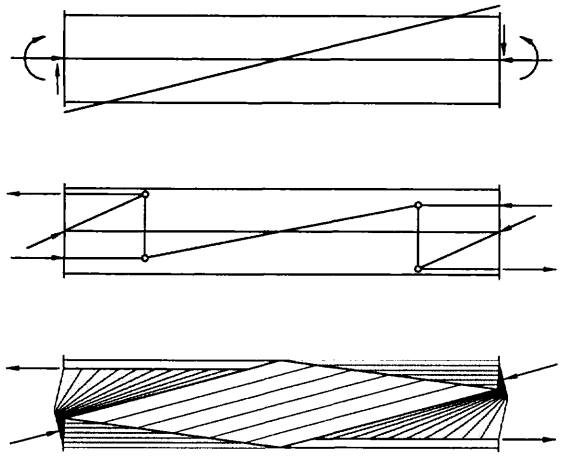

Figure 6: Structural action for a member subjected to shear and axial compression with increased eccentricity

If the eccentricity exceeds the maximum, a direct load transmission may no longer be possible. This can be seen from the structural action illustrated in fig. 6. The stress field solution discloses the need for transverse as well as longitudinal reinforcement.

As shown from the example, the need for statically reinforcement can directly be related to the eccentricity of the resultant. The procedure can be extended to capture biaxial shear and the presence of torsion.

The R-plots serve a useful aid for the investigation of D-regions. The selection of the governing load combination can be further strengthened by establishing qualitative truss models/stress fields for the different loading actions, from which the critical elements can be spotted (e.g. splitting reinforcement, anchorage details etc.).

3 Prestressing

3.1 Design for prestressing

The degree of prestress is mainly determined by the water tightness requirement. The prestressing loads are modelled as separate unit load cases in the GA. The final degree of prestress is found by scaling the prestressing loads so that the design criteria in each section is met. Although this is an complex and automated process, an adequate estimate of the required amount of prestress can be won by means of simple (long-hand) calculations.

3.1.1 Vertical tendons in shaft and outer cone

The requirements for the vertical prestress in the shaft and outer cone are:

- No tensile membrane stress is allowed to occur for a load level of 90 % of the characteristic ULS-environmental loads combined with minimum weight. No water pressure is let into cracks.
- No through cracks shall occur for the SLS environmental load. The SLS load is conservatively assumed to be 70% of the 100 year characteristic environmental loads. Water pressure in cracks is taken into account.
- In SLS the stresses in the prestressed reinforcement shall for no combination of actions exceed $0.8 f_y$, alternatively $0.8 f_{02}$.

3.1.2 Hoop tendons in ringbeam dome / minicylinder

Phase : Installation
Loads : External water pressure $\Delta h_w \cong$ - 55 m
Requirement : No tensile forces in SLS

Neglecting the ring stiffness of the cylinder wall restraining the hoop tension, an upper estimate for the hoop force in the dome can be found from:

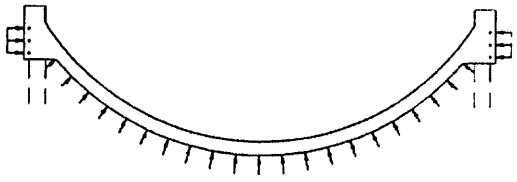

$N_{membrane,\,dome} = \Delta h_w \cdot \rho_w \cdot R_{o,dome}^2/(2 \cdot R_{m,dome}) = -55 \cdot 10.052 \cdot 10^2/(2 \cdot 9.75) = -2835$ kN/m

$N_{hoop,ringbeam} = N_{membrane,\,dome} \cdot \cos[\text{asin}(R_{m,\,ringbeam} / R_{m,dome})] \cdot R_{m,ringbeam}$

$= 2835 \cdot \cos[\text{asin}(8.4 / 9.75)] \cdot 8.4 = 12091$ kN

Prestressing: P_{eff} = 2900 kN/tendon (19 x 0.6" strands)

Required numbers of hoop tendons:

$n = N_{hoop} / P_{eff} = 12091 / 2900 = 4.2 \quad \Rightarrow$ 4 19 x 0.6"

3.1.3 Hoop tendons in minicylinder

Phase : Installation
Loads : External water pressure $\Delta h_w \cong$ - 55 m
Requirement : No tensile forces in SLS

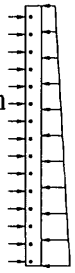

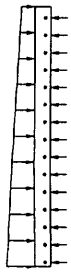

$N_{hoop} = \Delta h_w \cdot \rho_w \cdot R_{i,\,minicyl} = 55 \cdot 10.052 \cdot 8 = 4423$ kN/m

Prestressing: P_{eff} = 2900 kN/tendon (19 x 0.6" strands)

Required spacing between hoop tendons:

$c = P_{eff} / N_{hoop} = 2900 / 4423 = 0.656$ m $\Rightarrow$ 19 x 0.6" @ 650 mm

3.1.4 Vertical tendons in minicylinder

Phase : Installation
Loads : External water pressure $\Delta h_w \cong$ - 55 m
and selfweight of dome
Requirement : No tensile forces in SLS
Uplifting force on dome:

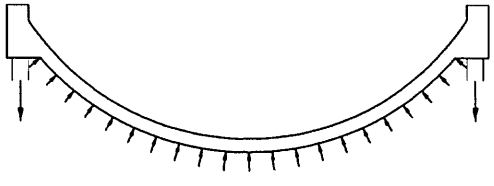

$$F_{uplift} = p \cdot A = \Delta h_w \cdot \rho_w \cdot \pi \cdot R_{i,\,minicyl}^2 = 55 \cdot 10.052 \cdot \pi \cdot 8^2 = 111.16 \text{ MN}$$

Selfweight of concrete above el. 11.48 m :

$$G_c = 217 \text{ m}^3 \cdot 2.65 \text{ } t/\text{m}^3 = 5.6 \text{ MN}$$

Required numbers of vertical tendons:

$$n = (F_{uplift} - G_c) / P_{eff} = (111.16 - 5.6) / 2.9 = 36.4 \Rightarrow 42 \text{ 19 x 0.6"} \text{ @ 1240 mm}$$

3.1.5 Vertical tendons in lower part of shaft and outer cone

Phase : Operation
Loads : Environmental loads, selfweight
Requirement : No tensile membrane stresses is allowed to occur in SLS for a load level of 90% of the characteristic ULS-environmental loads combined with minimum weight. No waterpressure is let into cracks.

Base of shaft, elevation +12.5 m:

Global overturning moment 100 years wave : $M = 2040$ MNm

Min. deck weight	:	24.5 MN
Weight of shaft	:	43.8 MN (submerged to el. 69.5 m)
Equipment and nonstructural concrete	:	16.6 MN

$$N_{prestressing} = M_{0.9} / (\pi \cdot R_m^2) - N / (2 \cdot \pi \cdot R_m)$$
$$= (0.9 \cdot 2040 \cdot 10^3) / (\pi \cdot 18.05^2) - (24.5 + 43.8 + 16.6) \cdot 10^3 / (2 \cdot \pi \cdot 18.05)$$
$$= 1794 - 749$$
$$= 1045 \text{ kN/m}$$

Required center distance:

$$c = P_{eff} / N_{prestressing} = 2900 / 1045 = 2.77 \text{ m}$$

In outer cone and base of shaft:

$$n = 2 \cdot \pi \cdot R_m / c = 2 \cdot \pi \cdot 18.05 / 2.77 = 40.9 \Rightarrow 40 \text{ 19 x 0.6"}$$

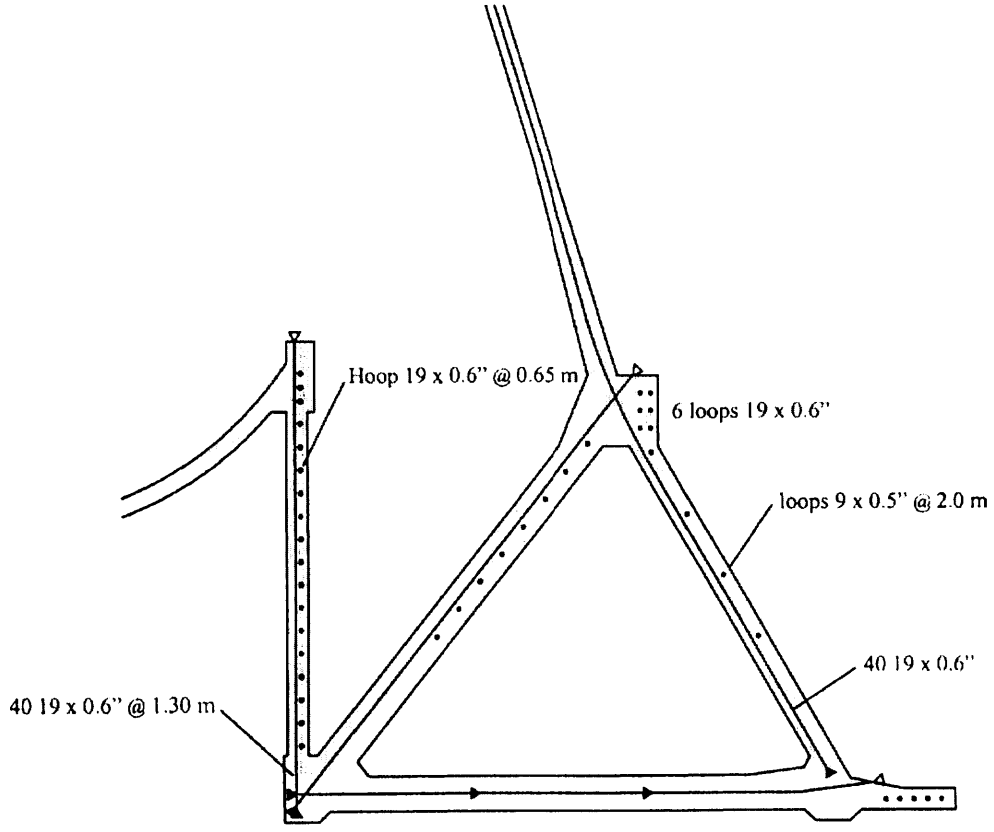

Figure 7: Prestressing configuration

4 Design of D-regions

4.1 Design aspects

In a ground based offshore structure (GBS) consisting of its typical structural parts such as skirts, lower and upper domes, cell walls and shafts the major D-regions are recognized by the structural elements junctioning these parts. Characterized as geometrical discontinuities, these typically are tricells, cell joints and ringbeams. Top of shaft is representing another important D-region due to the local introduction of the top side footing loads (ststical discontinuity). In case of the Valhall platform the identified D-region are highlighted in fig. 8. Furthermore, a platform consists of various D-regions of minor structural importance such as prestressing anchorages, secondary castings, corbels for miscellaneous items etc. These are normally designed with the aid of standard provisions or related solutions known from the literature.

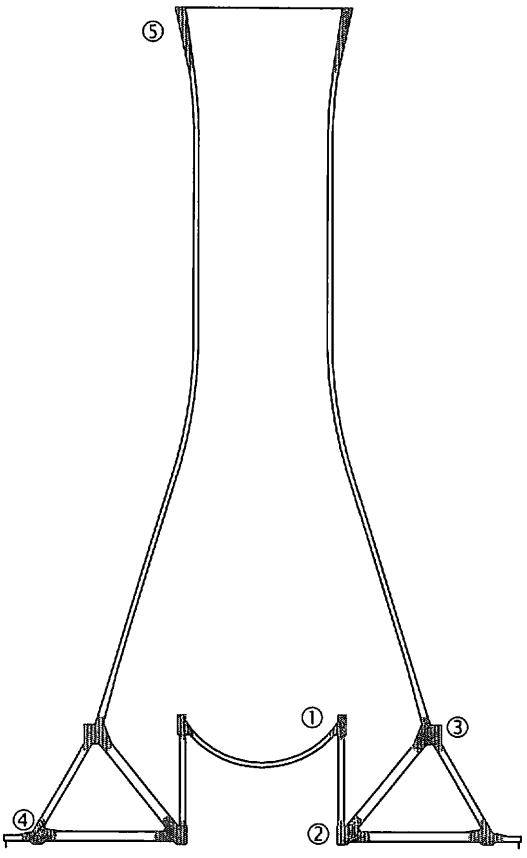

Figure 8: Identified D-regions

Statical boundary conditions for the D-regions are provided by the overall structural analysis (GA) as integrated stress resultants. These are transformed into statical equivalent truss forces, whereby the inner lever arm z normally can be adopted from the previous automatic design of the adjacent regular shell sections (B-regions). The inclination ϑ of the shear diagonal is derived from the shear design.

In most cases the D-regions to investigate have variations in loads as well as geometry. In the modelling process it may turn out to be difficult to match these complexities thoroughly. Simplifications introduced often implies the transformation of the problem into the 2-dimensional plane, where plane models are established for cut-out segments or "freebodies" with a unit depth. Such compromises are only then justified if the global structural action coincides with the truss plane and the forces acting lateral to the plane are insignificant for the internal resistance of the model.

Discrepancies between the direction of the global principal compression and the idealized truss plane are caused by the presence of in-plane shear. For the compression members the allowable concrete stresses have then to be reduced by the relation between stresses in the plane and the principal stresses out of the plane. The reduction can be calculated based on the sectional forces from the adjacent B-regions and be averaged over the D-region in question. Accordingly, the forces in the reinforcement ties are to be superimposed by the tie force required for carrying the in-plane shear. The above simplifications are rough and should be used with care when the 'out-of-plane' action is significant and governing for the ultimate resistance.

One important item highly relevant for the design of offshore structures is the implementation of water pressure in cracks. Truss models are due to their caracteristics not ideal for assessing the effect of water pressure, and so far no standard procedure or unique analytical model for addressing this effect has been developed. An approximate method commonly used is to introduce water pressure in potential cracks predicted with basis in the obtained internal stress distribution. The applied water pressure is then to be taken locally by the reinforcement. The estimation of the ultimate failure load is hence encumbered with uncertainties as it tends to be very dependent on the estimated crack pattern.

Lastly, adopting the statical boundary conditions from the GA, one will often notice that the equilibrium conditions are not always satisfied. This common problem can usually be traced back to the stress integration routine. Normally, the stress resultants are derived from integration of the stresses in the Gauss points. As the equilibrium conditions in the FE-analysis are formulated for the joints, equilibrium is not automatically warranted in the integration points. Hence, if one should eliminate this problem, the stress resultants will have to be deduced from the joint forces.

4.2 Minicell – dome connection

For the inner ringbeam the *Installation Phase* represents the governing load action. During installation the dome and minicell will be exposed to increasing water pressure difference in pace with the increasing draft. Maximum water pressure is reached at touch down prior to the shaft is waterfilled.

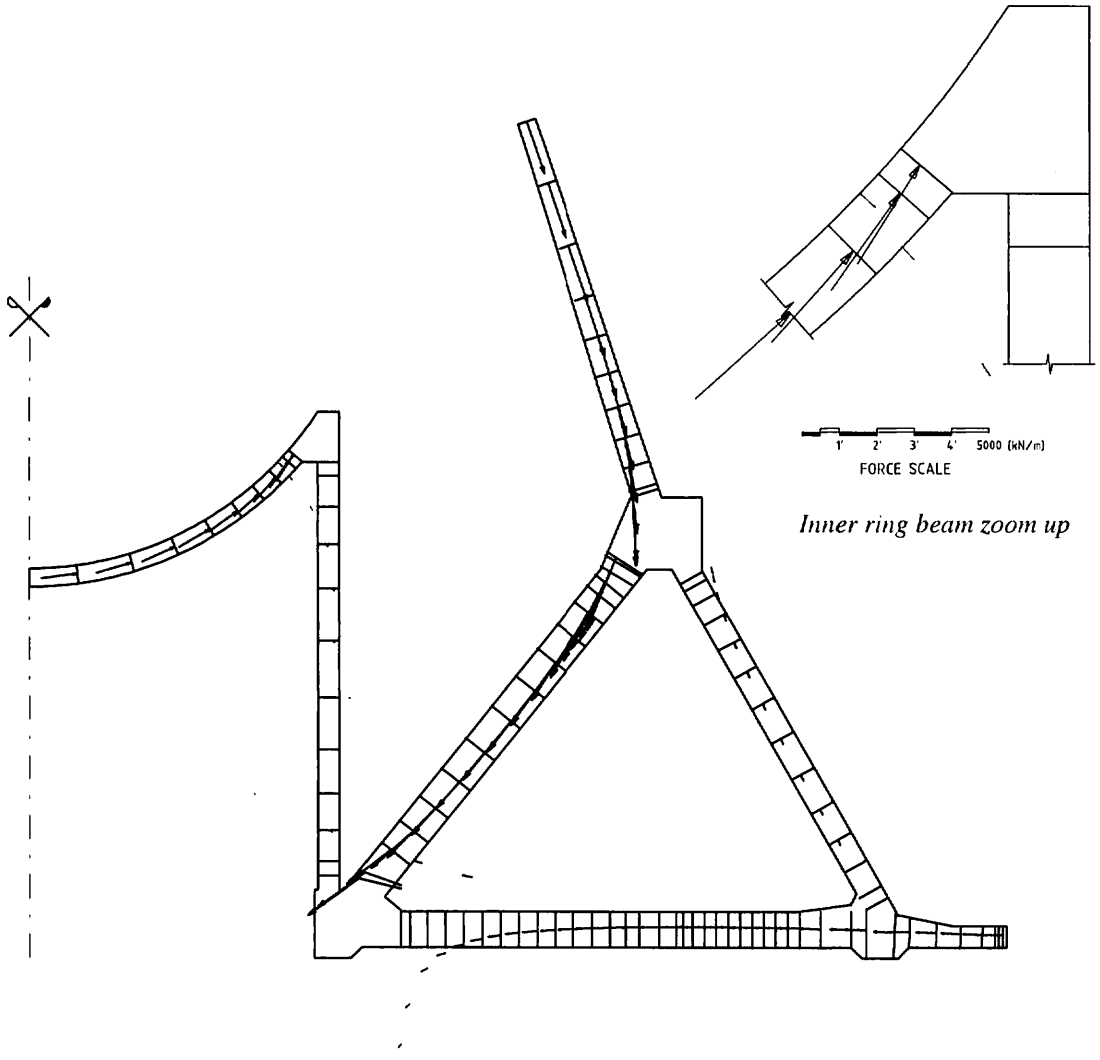

Figure 9: Response plot - installation phase (blue = compression, red = tension)

As can be seen from fig. 9 water pressure on the dome sets up a radial compression which is supported by the ringbeam. The hoop tension in the ringbeam resulting from the outward directed compression is balansed by hoop prestress (see sec. 3.1.2). The

eccentric introduction forces the ring beam to rotate, causing an opening moment in the bay between the dome and the cell wall. Analogous with a frame corner, the moment will introduce a principal splitting force in the haunch. The vertical component of the dome thrust is transferred via the ring beam and into the cylinder wall as vertical tension, for which vertical prestress is needed (sec. 3.1.4).

4.2.1 Loads

For the strut-and-tie analysis a finite beam sector with a unit arch length is considered. In case of a plane model the curvature is taken into account by scaling the forces acting on the D-region proportional to their relative radius of action:

$$\psi = R_i / R_0$$

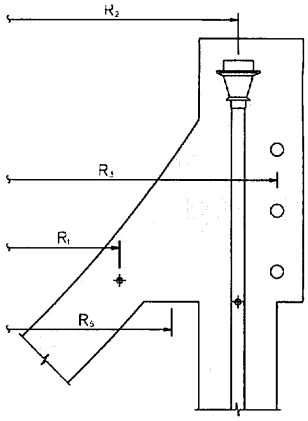

Sectional forces:

① Dome: $R_1 = 7.393$ m ⇨ $\psi = R_1 / R_0 = 0.860$

N_1	= -3097	kN/m		N_1	= -2663 kN
V_1	= 465	kN/m	⇨	V_1	= 400 kN
M_1	= 209	kNm/m		M_1	= 180 kNm

② Minicylinder: $R_2 = 8.300$ m ⇨ $\psi = R_2 / R_0 = 0.965$

N_2	= 387	kN/m		N_2	= 373 kN
V_2	= 418	kN/m	⇨	V_2	= 403 kN
M_2	= 541	kNm/m		M_2	= 522 kNm

Prestressing:

③ Hoop prestressing – radial deviation force: 3 19 × 0.6"

$R_3 = 8.600$ m ⇨ $\psi = R_3 / R_0 = 1.000$

$$\Delta F_{p,h} = \gamma_p \cdot P_{h,eff} \cdot \psi / R_3 = 0.90 \cdot (0.95 \cdot 3 \cdot 2\,900) \cdot 1.0 / 8.60 = 865 \text{ kN}$$

④ Vertical prestressing minicylinder: 40 19×0.6" @ 1.304 m

$R_4 = 8.300$ m ⇨ $\psi = R_4 / R_0 = 0.965$

$$F_{p,v} = \gamma_p \cdot P_{eff} \cdot \psi / s = 1.0 \cdot 2\,900 \cdot 0.965 / 1.304 = 2146 \text{ kN}$$

External water pressure:

⑤ Water pressure in haunch: $\Delta h_w = 58.52$ m

$$R_5 = 7.791 \text{ m} \quad \Rightarrow \quad \psi = R_5/R_0 = 0.906$$

$$\begin{aligned} F_w &= \gamma_w \cdot \rho_w \cdot b_{haunch} \cdot \Delta h_w \cdot \psi \\ &= 1.2 \cdot 10.052 \cdot 0.418 \cdot 58.52 \cdot 0.906 \\ &= 267 \text{ kN} \end{aligned}$$

Selfweight:

⑥ Selfweight of ring beam: $A_c = 1.442$ m

$$R_6 = 8.058 \text{ m} \quad \Rightarrow \quad \psi = R_6/R_0 = 0.937$$

$$\begin{aligned} G_c &= \gamma_g \cdot \rho_c \cdot A_c \cdot \psi \\ &= 1.2 \cdot 25.5 \cdot 1.442 \cdot 0.937 \\ &= 41 \text{ kN} \end{aligned}$$

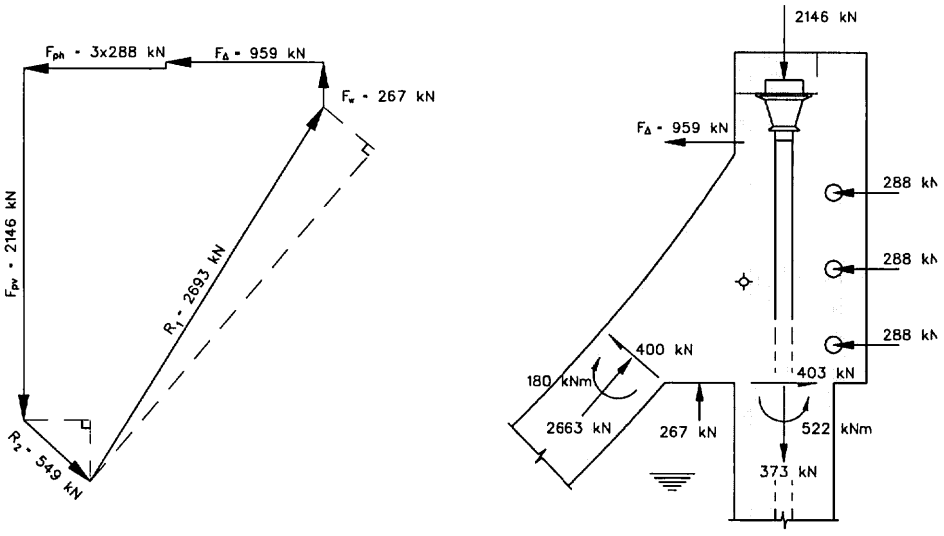

Figure 10: Acting loads and corresponding force diagram

Force equilibrium of the D-region is established with the introduction of the radial force F_Δ (see fig. 10). The force is partly associated with the curvature of the ring beam, where the inward radial deviation results from a net hoop tension. The 'eccentricity' expressing the rotation of the ring beam, is found from moment equilibrium:

$$\begin{aligned} \Sigma M^{①} &= 180 + 2146 \cdot 0.907 - 864 \cdot 0.535 + 373 \cdot 0.907 - 403 \cdot 0.163 - 267 \cdot 0.399 - 522 \\ &= 1308 \text{ kNm} \\ a &= \Sigma M^{①} / F_\Delta = 1308 / 959 = 1.364 \text{ m} \end{aligned}$$

Relating F_Δ to the idealized ring beam geometry in the GA (hatched contour, fig. 11), the eccentricity becomes:

$$e = 1.364 + 0.163 - 1.397 / 2 = 0.829 \text{ m}$$

And hence the corresponding moment:

$$M_\Delta = F_\Delta \cdot e = 959 \cdot 0.829 = 795 \text{ kNm}$$

A further simplification is introduced by applying the deviation force F_Δ as descrete forces distributed over the hight of the ring beam as shown in fig. 11.

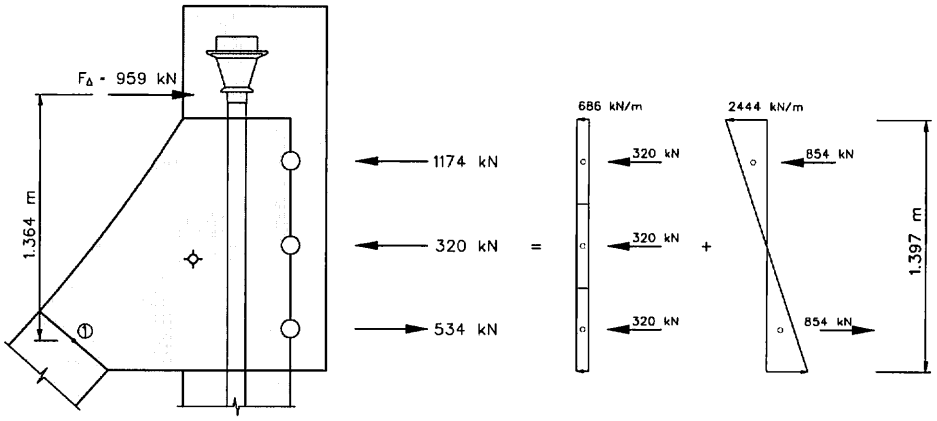

Figure 11: Distribution of the hoop deviation force F_Δ

4.2.2 Strut-and-tie analysis

Justified by the global rotational symmetry a plane strut-and-tie model is established for the ringbeam (an idealization which to some degree is disturbed by the singularity and hence the out-of-plane spreading of the vertical prestressing).

The small eccentricity of the compression force in the dome allows for a direct load transmission without any reinforcement statically required ($e_① = 209 / 3097 = 0.067$ m < $h/6$). For the cylinder wall the response is transformed into statical equivalent truss forces, whereby the inner leverarm z is adopted from the adjacent B-region design. Due to the prevailing axial tension, the inclination ϑ of the diagonal stress fields is chosen to 45°. The inclination ϑ' of the fan shaped stress field then equals 56.2°.

Chord forces:

$$F_t = M_1 / z + N_1 (z - z_s) / z + V_1 \cot \vartheta' (z - z_v) / z$$
$$= 522 / 0.426 + 373 (0.426 - 0.213) / 0.426 + 403 \cdot \cot 56.2° (0.426 - 0.254) / 0.426$$
$$= 1520 \text{ kN}$$

$$F_c = M_1 / z - N_1 z_s / z - V_1 \cot \vartheta' z_v / z$$
$$= 522 / 0.426 - 373 \cdot 0.213 / 0.426 - 403 \cdot \cot 56.2° \cdot 0.254 / 0.426$$
$$= 880 \text{ kN}$$

$$D_c = V_1 / \sin \vartheta' = 403 / \sin 56.2° = 484 \text{ kN}$$

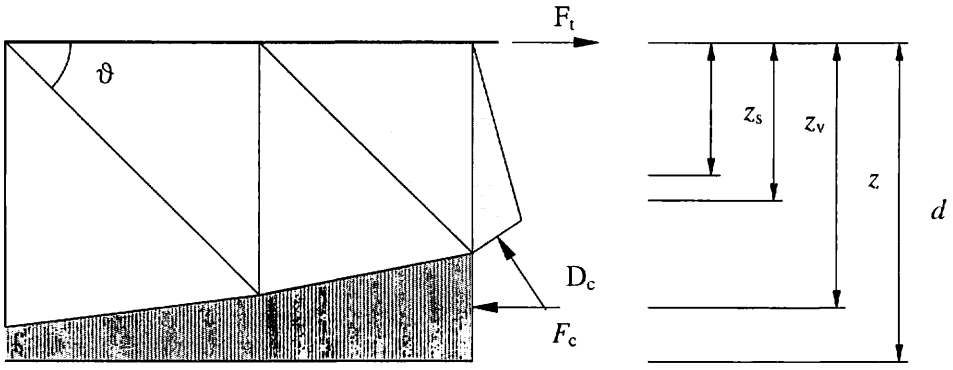

Figur 12: Equivalent truss forces - top of minicylinder wall

The obtained strut-and-tie model is shown in fig. 13, the associated stress fields in fig. 14. The internal force distribution is characterized by the deviation of the incoming compression strut from the dome into a compression 'arc'. The deviation is achieved, concentrated, by the reinforcement ties (splitting reinforcement and the vertical bars from the cylinder wall) and more uniformly by the vertical prestress. The ultimate load resistance of the region will primarely depend on the anchorage of the reinforcement ties.

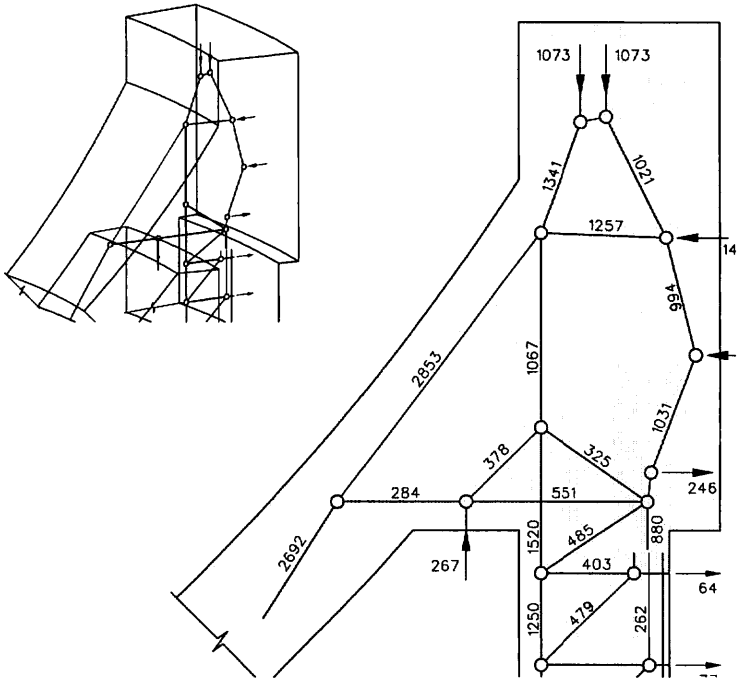

Figur 13: Inner ringbeam – stress field resultants

4.2.3 Concrete capacity check

The stress field, disclosing a moderate stress level varying from 5.1 to 9.4 MPa, is constructed by exploiting the available concrete area. The effective crushing strength for the struts taking the hoop tension into consideration is given by:

$$f_{1cd} = \alpha f_{ck} / \gamma_c = 0.85 \cdot 60 / 1.5 = 34.0 \text{ MPa} \quad ; \text{Grade C60}$$

$$f_{cd,eff} = \nu_2 \cdot f_{1cd} = 0.80 \cdot 34.0 = 27.2 \text{ MPa}$$

A specific check of the compression stress in the nodes is considered redundant as T-headed bars preferably will be used for the anchorage of the reinfocement ties (fig. 15).

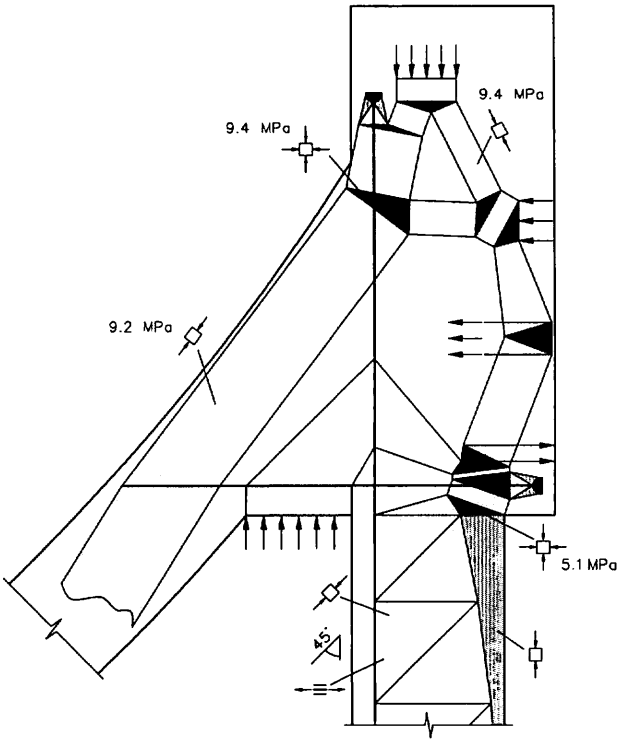

Figur 14: Inner ringbeam – stress field

4.2.3 Reinforcement capacity check

Splitting reinforcement:

req. $a_s = F_s / f_{yd} = 551 \cdot 10^3 / (500 / 1.15) = 1267 \text{ mm}^2/\text{m}$ (see sec. 4.2.4)

Vertical reinforcement:

req. $a_s = F_s / f_{yd} = 1520 \cdot 10^3 / (500 / 1.15) = 3496 \text{ mm}^2/\text{m}$;overruled by the SLS crack width criteria

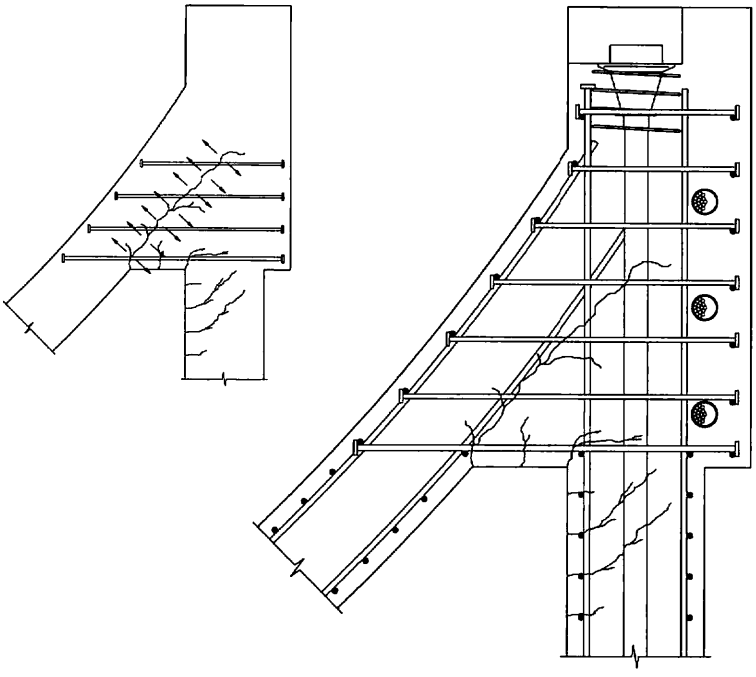

Figur 15: Principal reinforcement layout and potential crack pattern

4.2.4 Water pressure in cracks

Cracking in the bay is likely to generate an increase of the tensile force in the splitting reinforcement due to the ingress of water. The crack is conservatively assumed to develop up to the compression 'arc'. The additional force due to water pressure is calculated as:

$$F_{sw} \approx p_w \cdot h_w \cdot a / z = 1.2\,(70.0 - 11.48) \cdot 10.052 \cdot 1.10 / 1.065 = 729 \text{ kN/m}$$

Hence,

$$\text{req. } a_s = (F_s + F_{sw}) / f_{yd} = (551 + 729) \cdot 10^3 / (500 / 1.15) = 2944 \text{ mm}^2\text{/m}$$

$$\Rightarrow 1.2\ \text{Ø}\ 25\ @\ 200 \text{ mm}$$

In addition the splitting reinforcement will have to comply with the general crack width criteria under service conditions (SLS). For simplicity, the crack control is here performed on basis of the same force distribution as obtained for the ULS (fig. 13).

Crack width control:

$$w_k = s_r \cdot \varepsilon_{sm}$$

$$s_r = 2c + \alpha_b \cdot \text{Ø} / \rho$$

where:

c = 50 mm

α_b = 0.125

$$\begin{aligned} \varnothing &= 25 \text{ mm} \\ \rho &= A_s / A_{c,eff} \\ A_{c,eff} &= (6.5\,\varnothing + c)\, s = (6.5 \cdot 25 + 50) \cdot 1000 = 212\,500 \text{ mm}^2 \end{aligned}$$

Assume 2 Ø 25 @ 200 mm:

$$\rho = 5 \cdot 2 \cdot 491 / 212\,500 = 0.023$$

$$s_r = 2 \cdot 50 + 0.125 \cdot 25 / 0.023 = 236 \text{ mm}$$

Average steel strain:

$$\varepsilon_{sm} = \varepsilon_s - 0.4\, \varepsilon_{sr1}$$

$$\varepsilon_s \approx \frac{F_s + F_{sw}}{\gamma_g E_s A_s} = \frac{(551+729)\cdot 10^3}{1.2 \cdot 200000 \cdot 4910} = 1.086 \cdot 10^{-3}$$

$$f_{ct,\min} = f_{ctko,\min}\left(\frac{f_{ck}}{f_{cko}}\right)^{2/3} = 0.95\left(\frac{60}{10}\right)^{2/3} = 3.13\,MPa$$

$$\varepsilon_{sr1} = \frac{f_{ct,\min}}{\rho \cdot E_s} = \frac{3.13}{0.023 \cdot 200000} = 0.68 \cdot 10^{-3}$$

$$\varepsilon_{sm} = 1.086 \cdot 10^{-3} - 0.4 \cdot 0.68 \cdot 10^{-3} = 0.814 \cdot 10^{-3}$$

Characteristic crack width:

$$w_k = 236 \cdot 0.814 \cdot 10^{-3} = 0.192 \text{ mm} < \lim w_k = 0.20 \text{ mm}$$

$$\Rightarrow 2\,\varnothing\,25 \text{ @ } 200 \text{ mm OK!}$$

Note also that due to the presence of inclined shear cracks in the cylinder wall, the water pressure is here acting as suspended load (see fig. 13).

EXAMPLE 4

Precast pretensioned beam in composite action with in situ concrete

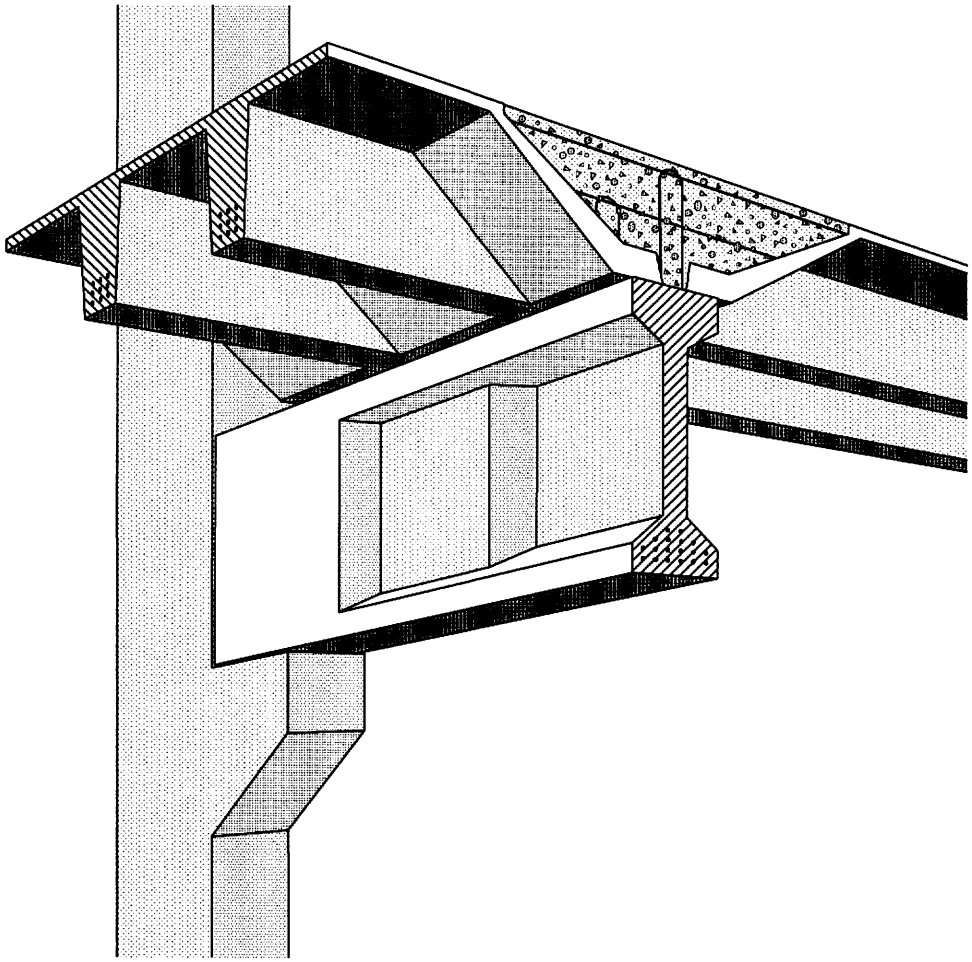

Bo Westerberg

Tyrens Byggkonsult AB
Stockholm, Sweden

1 Introduction

The example is a precast, prestensioned beam in composite action with in situ concrete.

The beam is part of a floor in a tennis hall, built in Stockholm a few years ago. The example has been used also for comparisons with Eurocodes 1 and 2. Therefore, this FIP calculation can be compared to calculations with both Swedish code and Eurocodes.

The floor structure is characterized by large spans, 18 m both for the beam and for the precast, pretensioned double-T slabs carried by the beam. Another characteristic feature is the composite action between the 1,5 m deep beam and in situ concrete, adding another 0,64 m to the depth. See front page and figures 1 and 2.

Two stages have to be considered:

1. the construction stage with the full weight of the slabs and the in situ concrete but without composite action
2. the finished building with additional imposed load and with composite action.

2. Summary of results

The object has been primarily to compare the *design* models, and therefore the same loads have been used in the FIP calculation as in the EC1 calculation.The main results are summarized in table 1, including those according to Swedish code and EC 1 and 2.

Table 1: Summary of main results.

		Sweden	EC1/EC2	FIP
Concrete grade	Precast element	C50	C60	C60
	In situ concrete	C25	C25	C25
Design load in ULS, kN/m	Construction stage	144	175	175
	Finished building	194	230	230
Required area of prestr. st., mm^2		2860	3170	3850 (3170)
Total shear reinforcement, mm^2		6900	8200	9900
Total joint reinforcement, mm^2		17600	26900	21400

The high area of prestressing steel is obtained with simplified models in FIP Recommendations. The same value as in the EC2 calculation can be obtained, if one uses a "realistic" stress block for the concrete and a stress-strain diagram for the prestressing steel with an ascending branch up to the design value of the ultimate strength. See clause 8.1.

Apart from this the result of the FIP calculation is rather close to that according to Eurocodes. A somewhat higher area of shear reinforcement is obtained with the FIP

model compared to the "standard method" in EC2. This is because the standard method gives a higher "concrete contribution" in uncracked regions, and because EC2 gives somewhat less minimum reinforcement. A lower amount of joint shear reinforcement according to FIP is due to a somewhat higher shear friction coefficient.

The Swedish calculation is more favourable in all respects, which is due to partial safety factors, design criteria and design models.

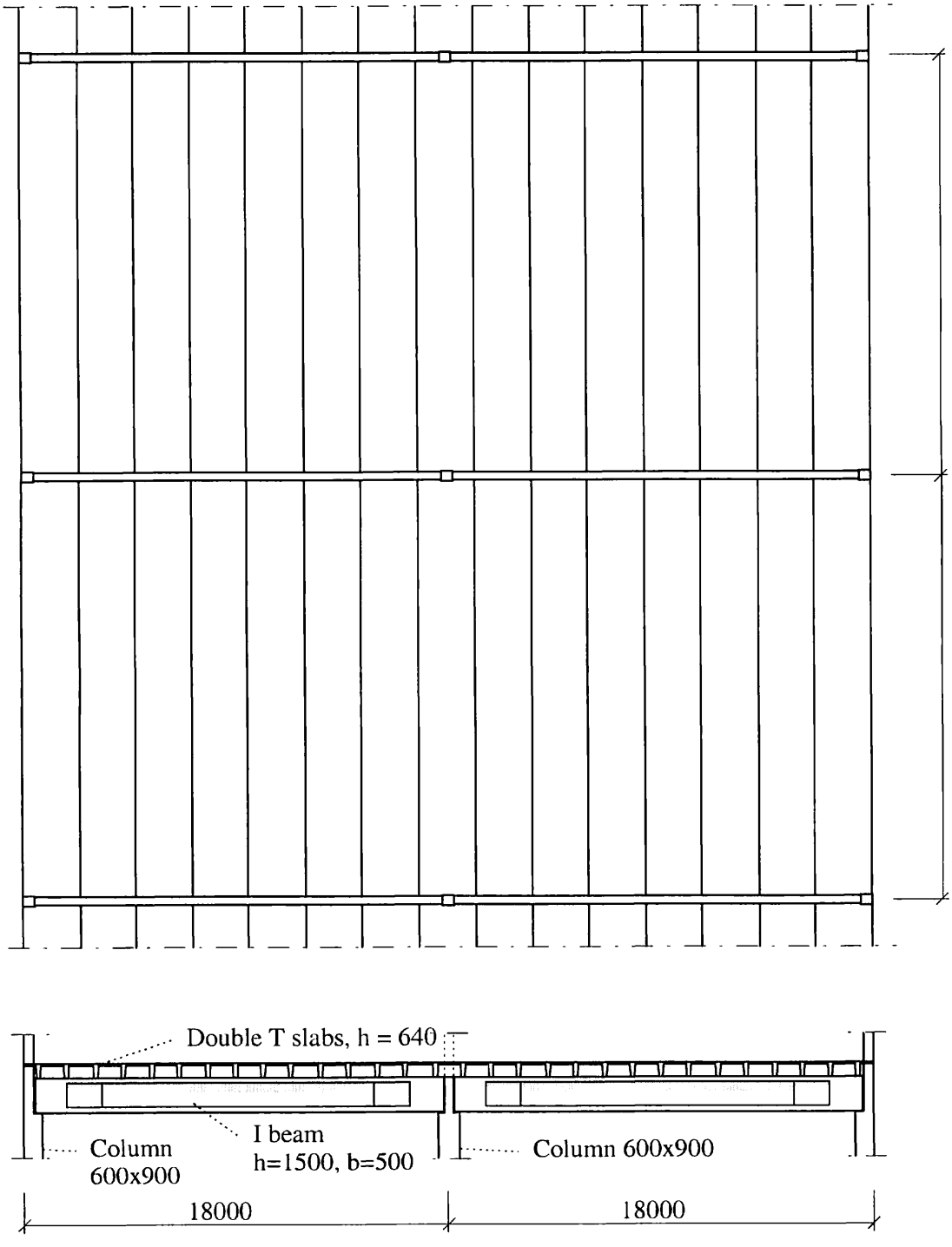

Figure 1: Outline of floor structure

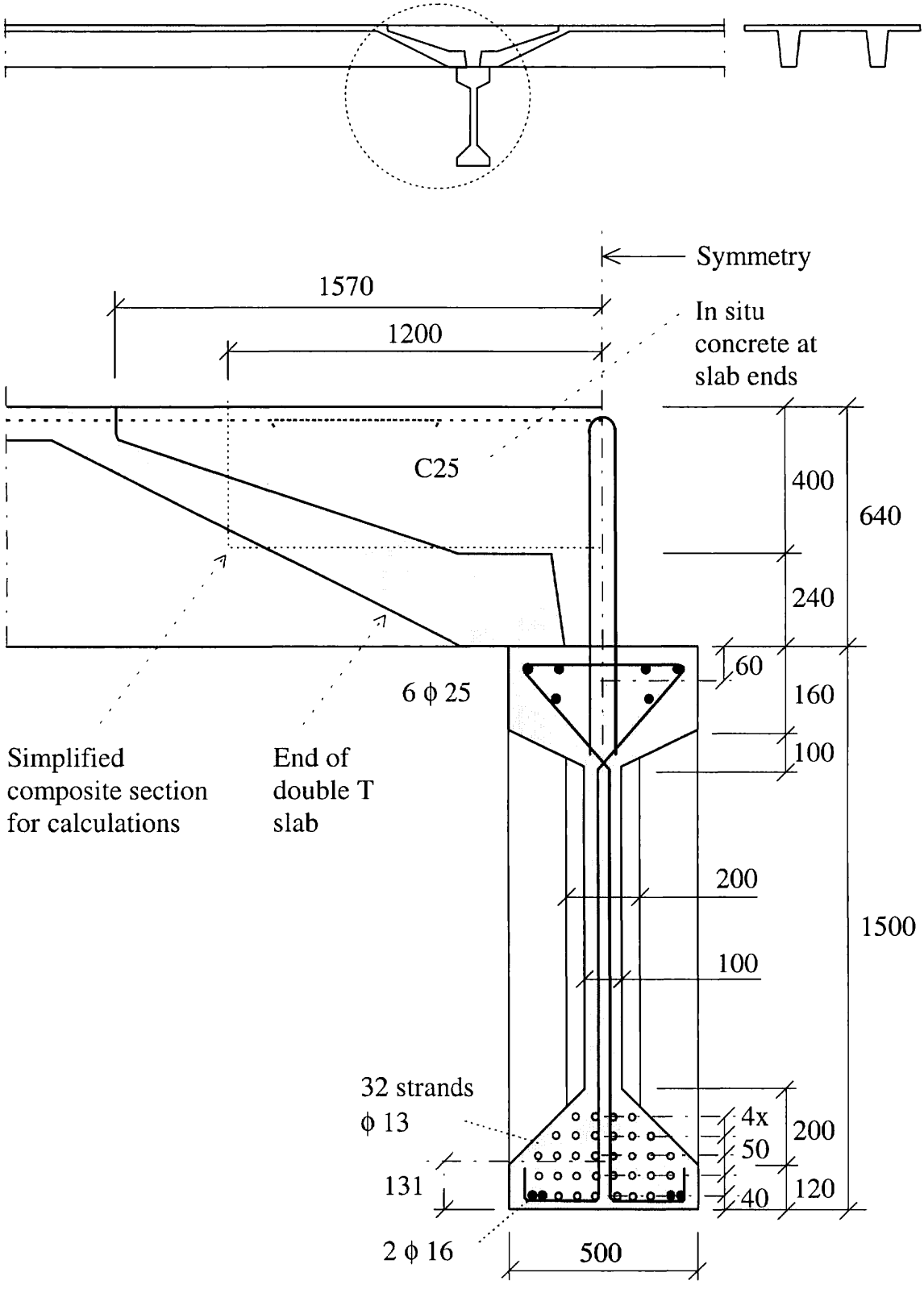

Figure 2: Cross section of beam including adjacent slabs and in situ concrete (shown only on one side).

3 Material values

In the original structure, designed according to the Swedish code, concrete grades C50 in the beam and C25 in the situ concrete were used. In this calculation, like in the one according to EC2, it is necessary to use a higher concrete grade with regard to the compressive stress from prestressing; C60 is chosen. Prestressing strands with f_{yk}/f_{ptk} = 1680/1860 MPa. Ordinary reinforcement with f_{yk} = 500. Design values according to 2.1.2:

$f_{cd} = 60/1,5 = 40,0$ MPa (beam)
$f_{cd} = 25/1,5 = 16,7$ MPa (in situ concrete)
$f_{yd} = 500/1,15 = 435$ MPa (ordinary reinforcement)
$f_{yd} = 1680/1,15 = 1461$ MPa (prestressing steel)
$f_{ud} = 1860/1,15 = 1617$ MPa (prestressing steel)

4 Loads

4.1 General

The aim of this example is to demonstrate the use of design rules in FIP Recommendations, and to compare with other codes, with which calculations were already made. These are the Swedish code (BBK 94) and Eurocodes 1 and 2 respectively (ENV 1991-1and 2 and ENV 1992-1-1 and 1-3). The same load values as in the Eurocode calculation will be used. For comparison, a calculation of loads according to FIP Recommendations is shown in Appendix.

4.2 Imposed load

According to EC1 part 2-1 table 6.1 the structure belongs to category C4, which gives the characteristic load value 5,0 kN/m^2. Table 9.3, gives the following ψ-values for catergory C:

$\psi_0 = \psi_1 = 0,7$, $\psi_2 = 0,6$.

Reduction factor depending on loaded area according to EC1part 2-1:

$\alpha_A = (5/7)\cdot\psi_0 + A_0/A = (5/7)\cdot 0,7 + 10/(2\cdot 18\cdot 18) = 0,515$

The characteristic load on the beam is then $q_k = 18\cdot 5,0\cdot 0,515 =$ <u>46,4 kN/m</u>

4.3 Permanent load

According to EC1, selfweight of reinforced concrete is taken as 25 kN/m^3.

Flooring	g_1	=	3,6	kN/m
In situ concrete	g_2	=	4,6	«
TT-slabs	g_3	=	91,4	«
In situ concrete at slab ends (cf fig 2)	g_4	=	25,9	«
Beam, middle part (web thickness 0,1 m)	g_5	=	8,0	«
Total permanent load	g	=	133,5	«

Within 0 - 1,2 from the ends, web thickness is 0,5 m and the selfweight increases by 10,7 kN/m. Within 1,2 - 3,6 m web thickness is 0,2 m and selfweight increases by 2,4 kN/m.

4.4 Design values of load

4.4.1 Serviceability limit state

During construction:

$q_d = 133,5 - 3,6 = 129,9$ kN/m (add 10,7 and 2,4 kN/m respecitively at ends)

Finished building, quasi-permanent load:

$q_d = 133,5 + 0,6 \cdot 46,4 = 161,3$ kN/m - « -

Finished building, frequent load:

$q_d = 133,5 + 0,7 \cdot 46,4 = 166,0$ kN/m - « -

4.4.2 Ultimate limit state

For load combinations in ULS EC1 gives two basic relations, (9.10a) and (9.10b). In (9.10b) the factor ξ has been given the value 0,89, a value given in the Swedish NAD to EC1.

During construction:

$q_{Sd} = 1,35 \cdot 129,9 = 175,4$ kN/m - « -

Finished building:

Load combination 1, EC1 part 1 (9.10a):

$q_{Sd} = 1,35 \cdot 133,5 + 1,5 \cdot 0,7 \cdot 46,4 = 228,9$ kN/m - « -

Load combination 2, EC1 part 1 (9.10b):

$q_{Sd} = 0,89 \cdot 1,35 \cdot 133,5 + 1,5 \cdot 46,4 = \underline{230,0 \text{ kN/m}}$ - « -

5 Calculation of load effects

5.1 Serviceability limit state

During storage:

$M = 8,0 \cdot 17,2^2/8 + 2,4 \cdot 2,4 \cdot 2,4 + 10,7 \cdot 1,2 \cdot 0,6 = 295,8 + 21,5 = \underline{317 \text{ kNm}}$

During construction:

$M = 129,9 \cdot 16,9^2/8 + 21,5 = \underline{4638 \text{ kNm}}$

In finished building, permanent load only (for calculation of prestress losses)

$M = 4638 + 3,6 \cdot 16,9^2/8 = \underline{4767 \text{ kNm}}$

Finished building, quasi-permanent load

$M = 161,3 \cdot 16,9^2/8 + 21,5 = \underline{5780 \text{ kNm}}$

Finished building, frequent load

$M = 166,0 \cdot 16,9^2/8 + 21,5 = \underline{5948 \text{ kNm}}$

5.2 Ultimate limit state

During construction:

$V_{Sd} = 175{,}4 \cdot 16{,}9/2 + 1{,}35 \cdot (2{,}4 \cdot 2{,}4 + 10{,}7 \cdot 1{,}2) = \underline{1507 \text{ kN}}$

$M_{Sd} = 175{,}4 \cdot 16{,}9^2/8 + 1{,}35 \cdot 21{,}5 = \underline{6291 \text{ kNm}}$

In finished building:

$V_{Sd} = 230{,}0 \cdot 16{,}9/2 + 0{,}89 \cdot 1{,}35 \cdot 18{,}6 = \underline{1966 \text{ kN}}$

$M_{Sd} = 230{,}0 \cdot 16{,}9^2/8 + 0{,}89 \cdot 1{,}35 \cdot 21{,}5 = \underline{8237 \text{ kNm}}$

Table 1: Summary of action effects

(kN, m)	Serviceability limit state		Ultimate limit state	
	$M_{quasi\text{-}permanent}$	$M_{frequent}$	V_{Sd}	M_{Sd}
During construction	4638		1507	6291
Finished building	5780	5948	1966	8237

6 Preliminary estimation of prestressing steel

ULS during construction:

$M_{Sd} = 6291$ kNm (table 1)

$z \approx 1{,}3$ m (=1,5 - 0,1 - 0,1)

$A_s = M_{Sd}/zf_{st} = 6291 \cdot 10^3/1{,}3/1461 = 3312 \text{ mm}^2$ $\underline{32 \text{ strands } \phi \text{ 13 à 100 mm}^2}$

(4 ϕ 16 in bottom flange can also be utilised, which will give suffucient tensile force)

ULS in finished building:

$M_{Sd} = 8237$ kNm (table 1)

$z \approx 1{,}3 + 0{,}64 = 1{,}94$ m

$A_s = M_{Sd}/zf_{st} = 8237 \cdot 10^3/1{,}94/1461 = 2906 \text{ mm}^2$ (not governing)

Section data are given in table 2 below, calculated for 32 strands and $E_c = 39$ GPa.

Table 2: Summary of cross section data for uncracked section, web thickness 0,1 m.

		Beam only	Beam + in situ conc.
Area	m^2	0,351	1,151
C.g. distance from bottom	m	0,740	1,574
Eccentricity of prestressing force	m	0,585	1,419
Moment of inertia	m^4	0,111	0,473
Moment of area w.r.t. top of in situ concrete	m^3		0,836
Moment of area w.r.t. top of beam	m^3	0,146	-6,360
Moment of area w.r.t. c.g. of strands	m^3	0,190	0,333
Moment of area w.r.t. bottom of beam	m^3	0,150	0,300

7 Serviceability limit state

7.1 Stresses

7.1.1 Initial prestress

$\sigma_{p0} \leq 0{,}75 \cdot f_{ptk} = 1395$ MPa (clause 3.2.1 in FIP Recommendations)

In this case 32 strands are required in ULS compared to 30 according to the Swedish calculation. In order to have the same total prestressing *force* as in the Swedish calculation, the prestress is proportioned with regard to the number of strands:

$\sigma_{pi} = 1395 \cdot 30/32 = \underline{1310 \text{ MPa}}$

Even with this reduced prestress the compressive stresses in the concrete become high, and non-linear creep has to be considered. See the following subclause.

7.1.2 Stresses at release of prestress

Transmission length according to equation (2.13) in FIP Recommendations:

$l_b = \alpha_1 \cdot \alpha_2 \cdot \alpha_3 \cdot \phi \cdot \sigma_{pi} / (4 \cdot f_{bpd}(t))$

where α_1 = 1,0 (gradual relase is assumed)
α_2 = 1,0 (verification in ULS)
α_2 = 0,5 (verification at release)
α_3 = 0,5 (strands)
ϕ = 13 mm
σ_{pi} = 1310 MPa
f_{bpd} = 1,9 MPa, assuming concrete strength corresponding to C40 at release

$l_{bpt} = 1{,}0 \cdot 1{,}0 \cdot 0{,}5 \cdot 13 \cdot 1310 / (4 \cdot 1{,}9) = 1120$ mmin ULS

$l_{bpt} = 1{,}0 \cdot 0{,}5 \cdot 0{,}5 \cdot 13 \cdot 1310 / (4 \cdot 1{,}8) = 591$ mm at release of prestress

The selfweight of the beam is

$g = 7{,}7 \cdot 17{,}2 + 2 \cdot (10{,}3 \cdot 1{,}35 + 2{,}3 \cdot 2{,}4) = 171{,}3$ kN

Moment of selfweight at the end of the transmission length:

$M_1 = (171{,}3/2) \cdot 0{,}59 - (7{,}7 + 10{,}3) \cdot 0{,}59^2/2 = 47$ kNm

Compressive stress at the bottom of the beam due to prestressing force and self-weight, with cross sectional data for web thickness 0,5 m and with reinforcement included ($A = 0{,}779$ m^2, $W_{bottom} = 0{,}204$ m^3, $W_{top} = 0{,}203$ m^3, $e = 0{,}593$ m):

$P_0 = 1310 \cdot 3200 \cdot 10^{-6} = \underline{4{,}19 \text{ MN}}$

$$\sigma = -\frac{P_0}{A} - \frac{P_0 \cdot e - M}{W_{bottom}} = -\frac{4{,}19}{0{,}779} - \frac{4{,}19 \cdot 0{,}593 - 0{,}047}{0{,}204} = -17{,}3 \text{ MPa}$$

Stress at a distance 1,35 + 2,4 m from the end (where the web thickness is 0,1 m), with cross sectional data according to table 2:

$$M_2 = 85{,}6 \cdot 3{,}75 - 7{,}7 \cdot 3{,}75^2/2 - 10{,}3 \cdot 1{,}35 \cdot (2{,}4 + 1{,}35/2) - 2{,}3 \cdot 2{,}4^2/2 = 217 \text{ kNm}$$

$$\sigma = -\frac{4{,}19}{0{,}351} - \frac{4{,}18 \cdot 0{,}585 - 0{,}217}{0{,}150} = \underline{-26{,}8 \text{ MPa}}$$

The FIP Recommendations give no definit limit for the concrete stress at release. It has been assumed above that the concrete strength has attained the equivalence of C40 at release. Then the above stress is 67 % of $f_{ck}(t)$. According to 7.4.3 non-linear creep should be considered if the compressive stress exceeds 45 % of $f_{cm}(t)$, but no model for this is given. However, a model in MC90 can be used (a similar model exists in ENV 1992-1-3):

$f_{cm}(t) = f_{ck}(t) + 8 = 48$ MPa

$k_\sigma = \sigma_c / f_{cm}(t) = 26{,}8/48 = 0{,}56$

$\varphi_{0,k} = \varphi_0 \cdot \exp[1{,}5(k_\sigma - 0{,}4)] = 1{,}27 \cdot \varphi_0$ (MC90, 2.1.6.4.3 (d))

Thus, the creep coefficient should be increased by 27 % during storage. φ_0 is the creep coefficient for linear creep, i.e. for stresses below the limit. At later stages the stress will fall below the limit due to increased external load, decrease of prestress and increased concrete strength.

7.1.3 Time dependent prestress losses and stresses at different stages

Creep coefficient and shrinkage are taken from clause 2.1.5 in FIP Recommendations. Release of prestress is assumed to take place after 2 days, loading during construction after 28 days and loading in the finished building after 90 days. The equivalent thickness 2A/u is 300 mm. Outdoor conditions are assumed during storage and construction, indoor conditions in the finished building. This gives the following final values of creep and shrinkage after interpolation in table 2.2 and 2.3:

During storage $\varphi = 2{,}97$ $\varepsilon_{cs} = 0{,}26$ °/oo

During construction $\varphi = 1{,}70$ $\varepsilon_{cs} = 0{,}26$ °/oo

In the finished building $\varphi = 1{,}87$ $\varepsilon_{cs} = 0{,}46$ °/oo

Relaxation is assumed to be totally 6 % (low relaxation steel, initial stress $< 0{,}7 \cdot f_{ptk}$). During storage and construction, ¼ of the final values are assumed to be reached in each period; thus 1/2 remains in the finished building. During storage the creep coefficient is multiplied by 1,27 with regard to the high compressive stress at release of prestress, see the preceding clause. The following values of creep, shrinkage and relaxation are then obtained for the different periods:

Storage	$\varphi = 1{,}27 \cdot 2{,}97/4 = 0{,}94$	$\varepsilon_{cs} = 0{,}26/4 = 0{,}07$ °/oo	$\chi = 6/4 = 1{,}5$ %
Construction	$\varphi = 1{,}70/4 = 0{,}43$	$\varepsilon_{cs} = 0{,}26/4 = 0{,}07$ °/oo	$\chi = 6/4 = 1{,}5$ %
Finished building	$\varphi = 1{,}87/2 = 0{,}94$	$\varepsilon_{cs} = 0{,}46/2 = 0{,}13$ °/oo	$\chi = 6/2 = 3{,}0$ %

Prestress losses are calculated according to equation (3.2) in FIP Recommendations (some symbols are simplified):

$$\Delta\sigma_p = \frac{E_p\varepsilon_{cs} + \varphi \cdot \alpha \cdot (\sigma_{cg} + \sigma_{cp0}) + 0{,}8 \cdot \Delta\sigma_{pr}}{1 + \alpha \cdot (1 + 0{,}8 \cdot \varphi) \cdot A_p \cdot C}$$

where E_p = 200 GPa
ε_{cs} = shrinkage (to be inserted with negative sign)
α = E_s/E_c = 200/39 = 5,13
φ = creep coefficient
σ_{cg} = concrete stress at level of prestressing steel due to permanent actions
σ_{cp0} = concrete stress at level of prestr. steel due to prestressing alone
$\Delta\sigma_{pr}$ = relaxation loss (to be inserted with negative sign)
χ = relaxation
C = $1/A_c + y_p^2/I_c$
A_c = area of cross section
y_p = eccentricity of prestressing force
I_c = moment of inertia
A_p = area of prestressing steel

Calculated losses are summarized in table 3. Calculation details are not shown.

Table 3: Prestress losses. 0 means beginning and 1 means end of the respective stage.

		During storage		During construction		Finished building		
						Quasi-permanent load		Frequent load
		0	1	0	1	0	1	
Prestressing force	kN	4190	3810		3740		3660	
Prestress	MPa	1310	1189		1169		1145	
Prestress loss	«	121		20		24		
Moment, external load	kNm	317		4638		5780		5948
- permanent load only*)	«	«		«		4767		
Top of in situ concrete	MPa	-	-	-	-	-2,7	-3,1	-3,5
Bottom of in situ concr.	«	-	-	-	-	2,0	2,1	2,4
Top of beam	«	2,7	2,2	-27,4	-27,4	-25,4	-25,3	-25,0
Level of strands	«	-23,2	-20,9	1,9	2,3	14,2	15,5	17,3
- permanent load only*)	«			«		3,6		
Bottom of beam	«	-26,2	-23,6	5,2	5,7	18,7	20,2	22,1

*) In the calculation of the effect of creep on the time-dependent losses, the concrete stress under prestressing force and *permanent load only* is used. Quasi-permanent load and permanent load is the same during storage and construction, whereas quasi-permanent load in the finished building also includes a part of the imposed load; σ_{cp} then has two different values.

The highest compressive stress under quasi-permanent load is 25,4 MPa, which is below the limiting value according to 7.4.3: $0{,}45 \cdot f_{ck} = 27{,}0$ MPa for C60.

The beam is cracked in the finished building. Stresses in table 3 are calculated for an average depth of the cracked zone = 0,6 m (≈ average for quasi-permanent and frequent load). The high tensile stresses in table 3 are ficitious values corresponding to the theoretical strain in the cracked section. These values have no physical meaning, but can be used in the calculation of crack width. Cross sectional data for this case are summarized in table 4.

Table 4: Cross sectional data for cracked cross section

Depth of cracked zone	0,60
Area	1,007
Center of gravity level	1,772
Moment of inertia	0,155
Eccentricity of prestressing force	1,617
Moment of area w.r.t. top of in situ concrete	0,421
Moment of area w.r.t. top of beam	-0,571
Moment of area w.r.t. bottom of beam	0,088

7.1.4 Control of crack width

FIP Recommendations, like EC2, has a requirement on crack width for prestressed concrete, even for indoor conditions. The maximum crack width under frequent load is 0,2 mm according to table 4.10. Crack widths are calculated according to equation (7.5):

$w_k = 1{,}7 \cdot s_r \cdot \varepsilon_{sm}$

$s_r = 2 \cdot c + \alpha_b \cdot \phi / \rho$

c = concrete cover = 33 mm at bottom

$\alpha_b = 0{,}19$ for good bond conditions

$\phi = 13$ mm

$\rho = A_s / A_{c,eff}$

A_s = area of bonded reinforcement (ordinary reinforcement in bottom can be included)

$A_{c,eff}$ = effective concrete area according to figure 7.6, in this case = 120000 mm^2

$\rho = (4 \cdot 201 + 32 \cdot 100) / 120000 = 0{,}0334$

$s_r = 2 \cdot 33 + 0{,}19 \cdot 13 / 0{,}0334 = 140$ mm

$\varepsilon_{sm} = \varepsilon_s - 0{,}4 \cdot \varepsilon_{sr1}$

ε_s = strain in reinforcement in a crack

$\varepsilon_{sr1} = f_{ct,min} / \rho E_s = 3{,}2 / (0{,}0334 \cdot 200) = 0{,}48$ ‰

The strain in the reinforcement should be measured from zero strain in the concrete, i.e. the prestrain should not be included. It can be calculated as the (fictitious) concrete strain at the level of reinforcement, in this case the bottom layer; see comments after

table 3. Creep of concrete under under quasi-permanent load should be considered, whereby an effective creep ratio can be used:

$\varphi_{ef} = \varphi \cdot \sigma_{quasi\text{-}permanent} / \sigma_{frequent}$

where $\varphi = 0{,}94$ (see page 6)

$\sigma_{quasi\text{-}permanent} = (14{,}2 + 15{,}5)/2 = 14{,}9$ MPa (mean stress under quasi-perm. load)

$\sigma_{frequent} = 17{,}3$ MPa

$\varphi_{ef} = 0{,}94 \cdot 14{,}9/17{,}3 = 0{,}81$

The crack width at the level of the bottom reinforcement layer can now be calculated, with values taken from table 3:

$\sigma_c = 17{,}3 + (22{,}1 - 17{,}3) \cdot (155 - 40)/155 = 20{,}9$ MPa (at level of bottom layer)

$\varepsilon_s = (1 + \varphi_{ef}) \cdot \sigma_c / E_c = (1 + 0{,}81) \cdot 20{,}9/39 = 0{,}97$ ‰

$\varepsilon_{sm} = 0{,}97 - 0{,}4 \cdot 0{,}48 = 0{,}77$ ‰

$w_k = 1{,}7 \cdot 140 \cdot 0{,}77 \cdot 10^{-3} = \underline{0{,}18 \text{ mm}}$

The crack width requirement is fullfilled.

Note. The calculated crack width according to EC2 is 0,19 mm.

7.2 Deformations

According to 7.6.2 (2) deformations need normally not be checked for simply supported beams, if the span-depth ratio is less than 25. For the beam in the example the span-depth ratio is clearly below this limit: l/h = 16,9/1,5 = 11 during construction and 16,9/2,14 = 8 in the finished building.

The deformation of the beam due to prestress and moment during storage and construction may be of practical interest, however. Thus, the situation at the end of the construction period will be studied here. The deflection can be calculated in the following way, if constant stiffness is assumed along the beam:

$$y = \frac{1}{r_M} \cdot \frac{l^2}{9{,}6} - \frac{1}{r_P} \cdot \frac{l^2}{8}$$

where $1/r_M$ = M/EI = curvature due to external moment

$1/r_P$ = Pe/EI = curvature due to prestress

During storage:

P = 3,81 MN, e = 0,585, M = 0,317 MNm

$EI = I \cdot E_c/(1+\varphi) = 0{,}111 \cdot 39000/(1+0{,}94) = 2230$ MNm^2

$1/r_P = 3{,}81 \cdot 0{,}585/2230 = 1{,}00 \cdot 10^3$ m^{-1}

$1/r_M = 0{,}317/2230 = 0{,}14 \cdot 10^3$ m^{-1}

Construction stage:

In this case no composite action is assumed, since this is the case when the dead load

of the floor is applied. To assume this for the whole period is a simplification, since composite action will affect part of the creep deformation.

$P = 3{,}74$ MN, $e = 0{,}585$, $M = 4{,}64$ MNm

$EI = I \cdot E_c/(1+\varphi) = 0{,}111 \cdot 39000/(1+0{,}43) = 3030$ MNm^2

$1/r_P = 3{,}74 \cdot 0{,}585/3030 = 0{,}72 \cdot 10^3$ m^{-1}

$1/r_M = 4{,}64/3030 = 1{,}53 \cdot 10^3$ m^{-1}

Total: $1/r_P = 1{,}00 + 0{,}72 = 1{,}72 \cdot 10^3$ m^{-1}

$1/r_M = 0{,}14 + 1{,}53 = 1{,}67 \cdot 10^3$ m^{-1}

$$y = 1{,}67 \cdot \frac{18^2}{9{,}6} - 1{,}72 \cdot \frac{18^2}{8} = \underline{-13 \text{ mm}}$$

Thus, after construction the beam will have an upward deflection of 13 mm, which is very little compared to the span (span/1400).

8 Design in ultimate limit state

8.1 Bending moment

The prestressing reinforcement assumed so far is 32 strands (3200 mm^2) and the concrete grade is C25 in the in-situ concrete, C60 in the beam. At first a stress-strain diagram of the prestressing steel according to figure 2.9 is used together with a rectangular stress block in the concrete, FIP Recommendations 5.3.2. All the ordinary reinforcement is included, see figure 2. The effective compressive strengths for in-situ concrete (compression zone in finished building) and precast concrete (construction stage) are:

$f_{cd,eff} = \nu_1 \cdot f_{1cd}$

Finished building:	Construction stage:
$\nu_1 = 1 - f_{ck}/250 = 1 - 25/250 = 0{,}90$	$1 - 60/250 = 0{,}76$
$f_{1cd} = 0{,}85 \cdot f_{cd} = 0{,}85 \cdot 16{,}7 = 14{,}2$ MPa	$0{,}85 \cdot 40 = 34$ MPa
$f_{cd,eff} = 0{,}90 \cdot 14{,}2 = \underline{12{,}8 \text{ MPa}}$	$0{,}76 \cdot 34 = \underline{25{,}8 \text{ MPa}}$

This gives the following design values of the bending moment capacity:

$M_{Rd} = \underline{5902 \text{ kNm}}$ in construction stage

$M_{Rd} = \underline{9723 \text{ kNm}}$ in finished building

Design moments are $M_{Sd} = \underline{6291}$ and $\underline{8237 \text{kNm}}$ respectively (table 1). Thus the estimated reinforcement 32 strands is not sufficient in the construction stage with the models used. In order to obtain the required moment capacity with the simplified models, it would be necessary to increase the area of prestressing steel to

$A_s = \underline{3850 \text{ mm}^2}$

According to EC2, on the other hand, the same concrete grades and the originally assumed reinforcement area (3200 mm^2) give the following moment capacities:

M_{Rd} = 6429 and 10714 kNm respectively.

There are two reasons for the FIP calculation to give lower moment capacities:

1. The strength in the compression zone is reduced by the factor ν_1 if a rectangular stress block is used. There is no such reduction in EC2; instead a reduction 0,8 of the depth of the compression zone is used. In this example the stress in the rectangular stress block has a significant influence, particularly in the construction stage.

2. The simplified stress-strain diagram for the prestressing steel according to figure 2.9 has a horizontal upper branch, whereas the simplified diagram in EC2 has an inclined upper branch. The ascending branch has a significant influence in this example, particularly in the finished building.

Thus, the simple models in FIP Recommendations may give quite conservative results. In order to obtain a sufficient moment capacity in this case, one has to use a more "realistic" stress block, e.g the bilinear one according to figure 2.2, and a more realistic stress-strain curve for the prestressing steel, including an inclined upper branch based on the design value of the ultimate strength. In that case, the result will be very close to the one according to EC2. Key parameters according to the different calculation alternatives are compared in tables 5 and 6.

Table 5: Comparison between key parameters in different moment capacity calculations.

In all cases the prestressing reinforcement is 32 strands = 3200 mm^2. Construction stage.

	Calculation alternative		
	FIP		EC2
	Simplified	More realistic	
Compressive stress (rect. block)	25,8	34,0	34,0
Depth of compression zone x	0,63	0,40	0,40
Internal lever arm z	1,18	1,25	1,25
Stress in prestressing steel σ_s	1456	1490	1494
Ultimate moment capacity M_{Rd}	5902	6417	6429

Table 6: Comparison between key parameters in different moment capacity calculations.

In all cases the prestressing reinforcement is 32 strands = 3200 mm^2. Finished building.

	Calculation alternative		
	FIP		EC2
	Simplified	More realistic	
Compressive stress	12,8	14,2	14,2
Depth of compression zone x	0,15	0,19	0,19
Internal lever arm z	1,94	1,94	1,94
Stress in prestressing steel σ_s	1456	1617	1617
Ultimate moment capacity M_{Rd}	9723	10706	10714

8.2 Transverse shear

Shear design according to 6.4.3.2 in FIP Recommendations is summarized with certain key parameters in tables 7 and 8. Required and chosen reinforcement is shown in figure 4. The details of one calculation for the construction stage are shown below.

Geometrical parameters:	$b_w = 0{,}1$ m; d = 1,39 m; $z \approx 0{,}9d = 1{,}25$ m, x = 3,6 m (dist. fr. supp.)
Design shear force:	$V_{Sd} = 851$ kN
Prestress:	P = 3,74 MN; $\sigma_{cpm} = P/A = 3{,}74 / 0{,}353 = 10{,}6$ MPa
Crack angle:	$\cot \beta_r = 1{,}20 - 0{,}2\, \sigma_{xd} / f_{ctm} = 1{,}20 + 0{,}2 \cdot 10{,}6 / 4{,}60 = 1{,}66$
Friction in cracks:	$V_{fd} = 0{,}10(1-\cot \beta_r/4) b_w z f_{cwd} = 0{,}10 \cdot (1-1{,}66/4) \cdot 0{,}1 \cdot 1{,}25 \cdot 20{,}4 = 149$ kN
Shear reinforcement:	$V_{swd} = V_{Sd} - V_{fd} = 851 - 149 = 702$ kN
	$A_{sw}/s = V_{swd} / (f_{ywd}\, z \cot \beta_r) = 702 / (435 \cdot 1{,}25 \cdot 1{,}56) = 0{,}778$ mm²/mm
	$A_{sw,min}/s = 0{,}2\, b_w\, f_{ctm} / f_{yk} = 0{,}2 \cdot 100 \cdot 4{,}60 / 500 = 0{,}184$ mm²/mm
Upper limit:	$\cot \theta = \cot \beta_r / (1 - V_{fd}/V_{Sd,web}) = 1{,}66 / (1 - 149 / 851) = 2{,}01$
	$V_{Rd,max} = b_w\, z\, f_{cwd} \sin\theta \cos\theta = 100 \cdot 1{,}25 \cdot 20{,}4 \cdot 0{,}44 \cdot 0{,}90 = 1010$ kN

Table 7: Summary of shear design, construction stage. d = 1,39 m, z = 1,25 m. The first value of x (2,17 m) is d·cot(βcr).

x	m	2,17	3,6		6,66	7,60
V_{Sd}	kN	1106	851		314	149
b_w	m	0,2	0,2	0,1	0,1	0,1
A	m^2	0,449	0,449	0,353	0,353	0,353
σ_{cpm}	MPa	8,33	8,33	10,6	10,6	10,6
$\cot(\beta_{cr})$		1,562	1,562	1,661	1,661	1,661
V_f	kN	310	298	149	149	149
V_{sw}	kN	796	553	702	166	0
A_{sw}/s - req	mm²/mm	**0,938**	**0,613**	**0,778**	0,184	0
A_{sw}/s - min	mm²/mm	0,368	0,368	0,184	**0,184**	**0,184**

Table 8: Summary of shear design, finished building. d = 2,03 m, z = 1,94 m. The first value of x (2,69 m) is d·cot(βcr).

x	m	2,69	3,6		6,40	7,31
V_{Sd}	kN	1327	1116		472	262
b_w	m	0,2	0,2	0,1	0,1	0,1
A	m^2	1,246	1,246	1,151	1,151	1,151
σ_{cpm}	MPa	2,94	2,94	3,18	3,18	3,18
$\cot(\beta_{cr})$		1,328	1,328	1,338	1,338	1,338
V_f	kN	529	529	263	263	263
V_{sw}	kN	799	587	852	208	0
$V_{Rd,max}$	kN	2976	2710	1704	1177	-
A_{sw}/s - req	mm²/mm	**0,713**	**0,524**	**0,755**	0,184	0,000
A_{sw}/s - min	mm²/mm	0,368	0,368	0,184	**0,184**	**0,184**

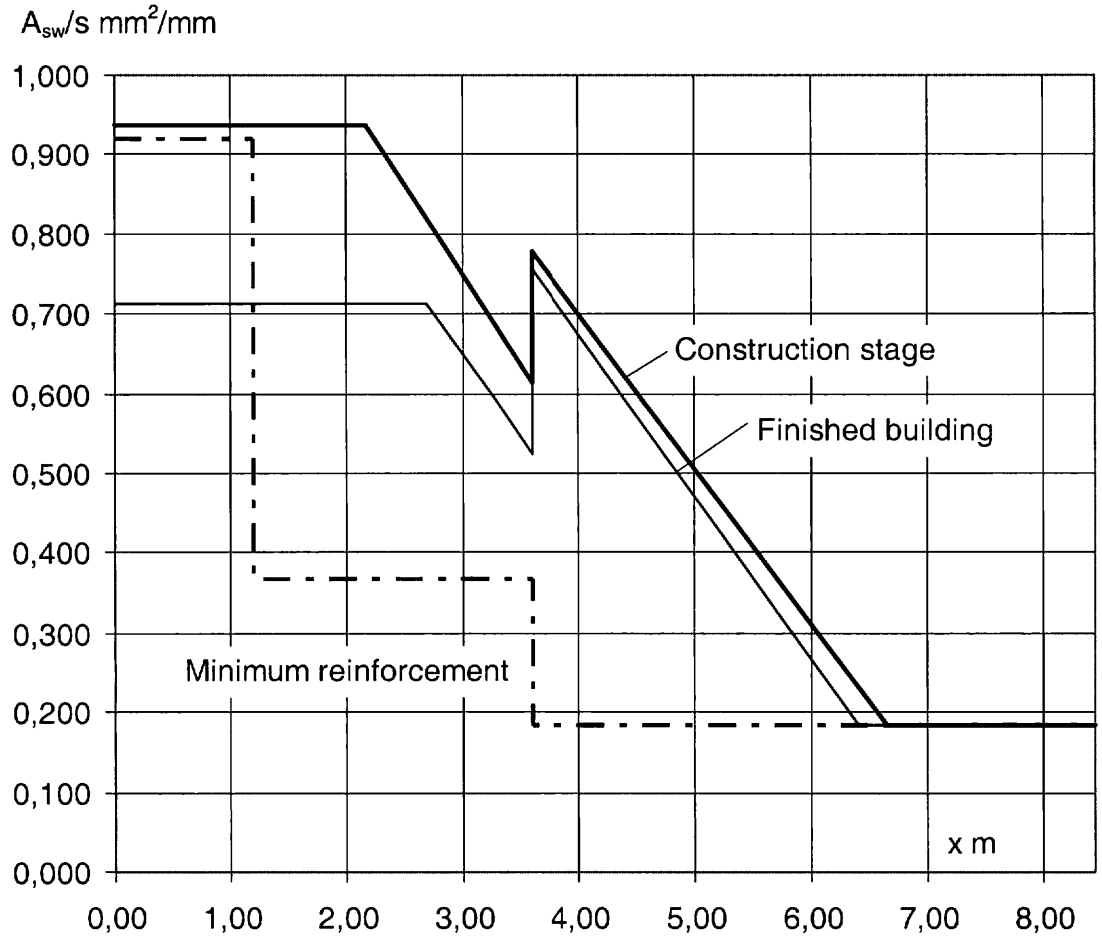

Figure 4: Required shear reinforcement. The increased minimum reinforcement for x < 3,6 m is due to the increased web thickness (b_w = 0,2 and 0,5 m respectively).

No difference has been made here between areas with and without flexural cracks. In this example, rather long parts of the beam near the supports are uncracked due to the high prestress (e.g. 3,5 m in the construction stage). The shear reinforcement in this area could be reduced, but there is no rule for this in FIP Recommendations. For the "standard method" in EC2, a higher concrete contribution is given for uncracked parts (part 1-3, resistance to diagonal cracking, see V'_{Rd} in 8.4 below). This is one reason why EC2 gives less total shear reinforcement in this example (see chapter 2).

8.3 Longitudinal shear (joint between element and in-situ concrete)

Joint reinforcement is designed according to 6.4.7. The width of the joint between precast element and in situ concrete is 200 mm, see figure 2. The shear stress in the joint is:

$$\tau_{fSd} = V_{Sd}/zb_f \approx V_{Sd}/(0{,}9db_f)$$

The maximum value at the beam end is:

$$\tau_{fSd} = 1{,}966/(0{,}9 \cdot 2{,}03 \cdot 0{,}2) = 5{,}38 \text{ Mpa}$$

The upper surface of the beam is assumed to be "rough" according to table 5.1. This gives $\beta = 0{,}4$ and $\mu = 0{,}9$ in equation (6.29). Furthermore $\sigma_{cd} \approx 0$, $\alpha_j = 90°$ and

$f_{ctd} = f_{ctk,0.05}/\gamma_c = 0{,}21 \cdot f_{ck}^{2/3}/1{,}7 = 1{,}06$ MPa

for in situ concrete C25. The required reinforcement is then

$\rho = (\tau_{fSd} - \beta \cdot f_{ctd}) / \mu \cdot f_{yd} = (5{,}38 - 0{,}4 \cdot 1{,}06) / (0{,}9 \cdot 435) = 0{,}0127$

$A_s = b_f \cdot \rho = 200 \cdot 0{,}0127 = \underline{2{,}54 \text{ mm}^2/\text{mm}}$

The minimum area is

$\rho_{min} = \beta \cdot f_{ctd} / \mu \cdot \sin\alpha_j \cdot f_{yd} = 0{,}4 \cdot 1{,}06 / 0{,}9 \cdot 1{,}0 \cdot 435 = 0{,}0011$

$A_{s,min} = 200 \cdot 0{,}0011 = 0{,}22 \text{ mm}^2/\text{mm}$

The upper limit of the resistance according to equation (6.30) is

$0{,}25 \cdot f_{1cd} = 0{,}25 \cdot 14{,}2 = 3{,}55 \text{ MPa} < \tau_{fSd}$

Thus the simple criterion is not fulfilled. A check according to 6.4.3.4 is done.

$\tau_{fRd,max} = V_{Rd,max}/b_w z = f_{cwd} \cdot \sin\theta \cdot \cos\theta$

Here θ should be the angle according to figure 6.10. The reinforcement ratio with 2 x ϕ 16 s 200 is $\rho = 2 \cdot 201/200/200 = 0{,}0101$.

$\theta = \arctan(F_s/V_f) = \arctan(\rho f_{yd}/\tau_{fSd}) = \arctan(0{,}0101 \cdot 435/5{,}38) = 39{,}2°$

$f_{cwd} = \nu_2 f_{1cd} = 0{,}80 \cdot 14{,}2 = 11{,}4$ MPa with ν_2 according to 6.4.3.1 (1)

$\tau_{fRd,max} = 11{,}4 \cdot \sin(39{,}2) \cdot \cos(39{,}2) = 5{,}6 \text{ MPa} > \tau_{fSd}$ OK

Figure 5 shows the required joint reinforcement and one example of reinforcement that will cover the necessary total amount with a reasonable distribution.

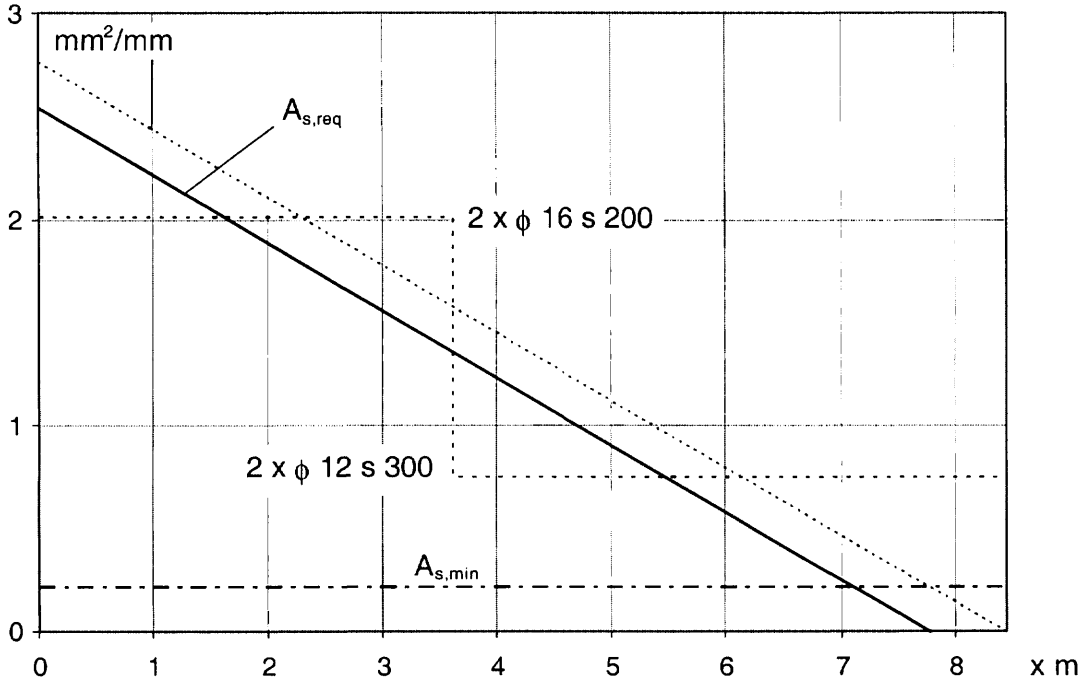

Figure 5: Shear reinforcement in joint

8.4 Anchorage of reinforcement

There are no bending cracks within a distance of about 3 m from the support. A diagonal crack could theoretically form close to the support, depending on the principal tensile stress. There is no criterion for a direct check of this stress in FIP Recommendations. There is one in EC2 part 1-3, however. A check according to this criterion will be shown below for the finished building. The capacity with regard to diagonal tension is defined as

$$V_{Rd1}^{I} = \frac{I \cdot b_w}{S} \cdot \sqrt{f_{ctd}^{\,2} + \alpha \cdot \sigma_{cpm} \cdot f_{ctd}}$$

where I = moment of inertia = 0,724 m^4 at the end of the beam

b_w = web thickness = 0,5 m

S = moment of area on either side of CG = 0,457 m^3 in this case

$f_{ctd} = f_{ctk}/\gamma_c = 0{,}7 \cdot 4{,}6/1{,}7 = 1{,}89$ MPa

$\sigma_{cpm} = P/A = 3{,}66/1{,}58 = 2{,}32$ MPa

$\alpha = x/l_{bpt} \leq 1$

l_{bpt} = transmission length value for ULS = 1,12 m (7.1.2)

x = distance from face of support to centroidal axis = 1,35 m $\Rightarrow \alpha = 1$

It can be discussed if the lower tensile strength for the in-situ concrete should also be considered. However, it seems reasonable to use only the strength of the precast concrete, since the crack will hardly start to form in the in situ concrete. With the above values the following capacity is obtained:

$$V_{Rd1}^{I} = \frac{0{,}724 \cdot 0{,}5}{0{,}457} \cdot \sqrt{1{,}89^2 + 1 \cdot 2{,}32 \cdot 1{,}89} = 2{,}23 \text{ MN} > V_{Sd,max} \text{ (1,966 MN)}$$

Thus, the capacity can be considered to be sufficient with regard to diagonal tension. This means that it should ***not be necessary to check the anchorage according to 6.5.2.1*** (It can be mentioned that the same capacity calculated according to EC2 part 1-3 would be 2,66 MN, due to a lower partial safety factor for the tensile strength, $\gamma_c = 1{,}5$.)

However, since there is no "diagonal tension criterion" in FIP Recommendations, and ***in order to demonstrate the calculation***, an anchorage check according to 6.5.2.1 will be shown, despite the fact that it is not necessary in this case. The calculation is done "backwards", to verify that a certain anchorage reinforcement is sufficient.

It is assumed that the strands have an anchorage length of 150 mm outside the center of the support, see figure 6 This is within the transmission length, and therefore the stress that can be anchored in this length is, cf section 7.1.2 above:

$\sigma_{pd} = \sigma_{p0} \cdot 150/l_{bpt} = 1310 \cdot 150/1120 = 175$ MPa

$F_1 = A_p \sigma_{pd} = 3200 \cdot 175 \cdot 10^{-3} = 560$ kN

At the botton of the cross section there are 4 ϕ 16, which will normally be welded to a support plate at the bottom of the beam. These bars will then be end anchored for a force

$F_2 = 4 \cdot 201 \cdot 435 \cdot 10^{-3} = 350$ kN

Thus the total anchored force is

$F_s = F_1 + F_2 = 910$ kN

The maximum shear force in the finished building is

$V_{Sd} = 1966$ kN

This shear force and the tensile force F_s correspond to a strut inclination of, cf 6.5.2.1 and figure 6.11:

$\cot\theta_A = F_s/V_{Sd} = 910/1966 = 0{,}46$

The corresponding strut inclination in the truss will be, cf equation (6.32):

$\cot\theta = (\cot\theta_A - 0{,}5a_l/z) / (d_l/z + 0{,}5)$

Here $z = 1{,}94$ m (see table 6), $a_l \approx 0{,}1$ m, $d_l = 0{,}13$ m (figure 2), which gives

$\cot\theta = (0{,}46 - 0{,}5 \cdot 0{,}1/1{,}94) / (0{,}13/1{,}94 + 0{,}5) = 0{,}77$

The amount of stirrups necessary for this follows from equation (6.11b):

$A_{sw}/s = V_{Sd} / (\cot\theta \cdot f_{ywd} \cdot z) = 1966 / (0{,}77 \cdot 435 \cdot 1{,}94) = 3{,}03$ mm^2/mm

This is quite a heavy shear reinforcement, e.g. 4 x ϕ 10 s 100. An alternative solution is to add a couple of loops in the end of the beam, see figure 6. With 4 ϕ 20 an additional 556 kN is taken, and the total anchored force is

$F_s = 560 + 350 + 550 = 1460$ kN

$\cot\theta_A = F_s/V_{Sd} = 1460/1966 = 0{,}74$

$\cot\theta = (0{,}74 - 0{,}5 \cdot 0{,}1/1{,}94) / (0{,}13/1{,}94 + 0{,}5) = 1{,}26$

$A_{sw}/s = V_{Sd} / (\cot\theta \cdot f_{ywd} \cdot z) = 1966 / (1{,}26 \cdot 435 \cdot 1{,}94) = 1{,}84$ mm^2/mm

Either stirrups 2 x ϕ 10 s 85 or 4 x ϕ 10 s 170 over a distance $z \cdot \cot\theta = 1{,}24$ m from the support is needed in this case. (The joint reinforcement connecting the precast beam with the in situ concrete, cf figure 2 and clause 8.3, is 2,54 mm^2/mm which also covers the need with regard to the anchorage.)[1]

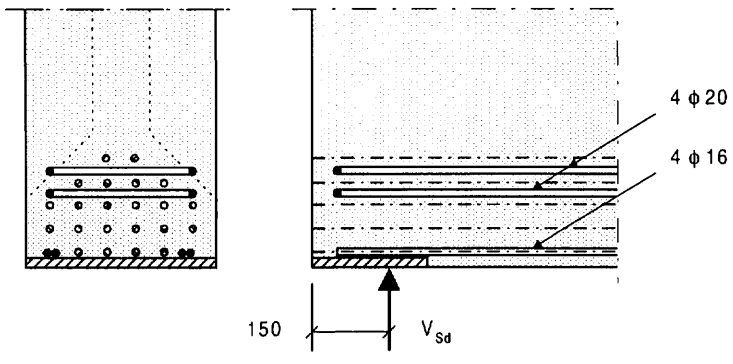

Figure 6: Extra reinforcement 4 ∅ 20 for anchoring the tensile force. This reinforcement would have been needed according to 6.5.2.1, ***unless*** *it had been shown that neither flexural cracks nor diagonal tension cracks will occur near the support.*

[1] Extra shear reinforcement for the anchorage is not included in the total area given in table 1. The reason is that this is not necessary, and that it was not included in the comparison between EC1/EC2 and the Swedish code.

8.5 Spalling reinforcement in beam end

8.5.1 Simple check

According to equation (6.37) local transverse stresses (splitting) can be assumed to be taken by the concrete if the following simplified conditions are fulfilled:

$c/\phi > 2,5$ and $c_{eff}/\phi > 2,25$

c = concrete cover = 40 - 13/2 = 33,5 mm; $c/\phi = 2,6$ OK

$c_{eff} = [2 \cdot c + 1,5 \cdot (n-1) \cdot s_n] / 2n$

s_n = clear distance = 50 - 13 = 37 mm, n = 32

$c_{eff} = [2 \cdot 33,5 + 1,5 \cdot (32-1) \cdot 37] / 2 \cdot 32 = 28$ mm; $c_{eff}/\phi = 2,15 < 2,25$

The simplified condition is not fulfilled. Therefore, transverse forces are calculated.

8.5.2 Transverse forces

FIP Recommendations figure 6.28 gives a model for calculating the transverse force T_1 ("splitting" force). The following value of the force can be derived from this model, with $d_1 = 131$ mm and $a = 2 \cdot (131 - 40) = 182$ mm:

$$T_1 = (P/4) \cdot (1 - a/2d_1) = (4,19/4) \cdot (1 - 182/2 \cdot 131) = 0,32 \text{ MN} \Rightarrow A_s = 735 \text{ mm}^2$$

According to figure 6.28 the vertical force T_2 ("spalling" force) at the end of the beam can be assumed equal to the horizontal force T_3, which in turn is equal to the sum of the tensile stresses in the upper part of the beam. The maximum tensile stress is, cf 7.1.2:

$$\sigma_t = -\frac{P_0}{A} + \frac{P_0 \cdot e - M}{W_{top}} = -\frac{4,19}{0,779} + \frac{4,19 \cdot 0,593 - 0,047}{0,203} = 6,63 \text{ MPa}$$

In the same section, the stress at the bottom is, cf 7.1.2, $\sigma_b = -17,3$ MPa

The depth of the tensile zone is thus

$x = h \cdot \sigma_t / (\sigma_t - \sigma_b) = 1,5 \cdot 6,6 / (6,6 + 17,3) = 0,41$ m

The stress exceeds the tensile strength of the concrete. However, it can be used as a basis for calculation of the tensile force. Of course, this force has to be taken by reinforcement also in the horizontal direction. The tensile force is

$T_2 = T_3 = \sigma_t \cdot b \cdot x/2 = 6,63 \cdot 0,5 \cdot 0,41/2 = 0,69$ MN

$A_s = T_2/f_{yd} = \underline{1580 \text{ mm}^2}$

This reinforcement could be partly concentrated to the end and partly dispersed along the transmission length, e.g.

2 ϕ 20 + 4 x 2 ϕ12

The 2 ϕ 20 could be welded to the plate in figure 3 and bent horizontally at the top of the section, figure 7:

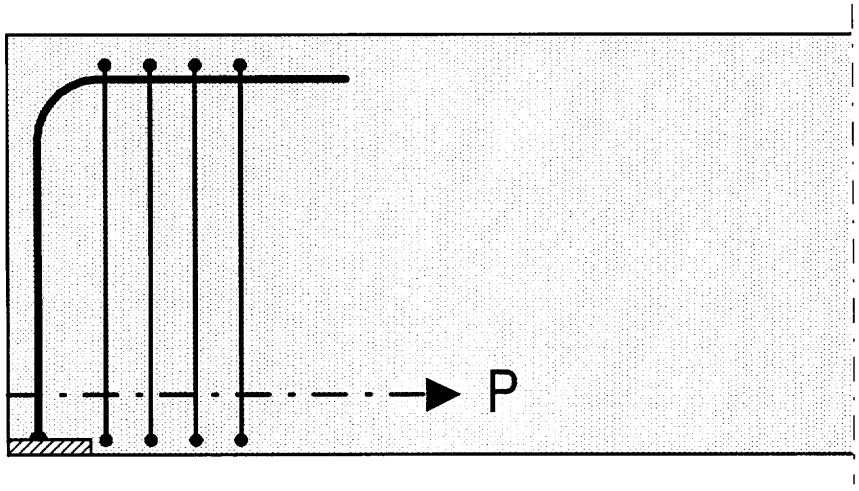

Figure 7: Example of spalling reinforcement. (No other reinforcement is shown.)

APPENDIX. Load values according to FIP Recommendations

Imposed load

The real structure is part of a tennis hall. The nearest category in FIP Recommendations, table A1, Appendix 1, is *dance halls*, with characteristic load 5,0 kN/m^2 m.

Clauses 6.2.2 and 7.2.2 give the following ψ-values for *offices*, which seems to be the nearest category here:

$\psi_0 = \psi_1 = 0{,}6$, $\psi_2 = 0{,}3$.

FIP gives no reduction of the load intensity with regard to the loaded area. Without this, the characteristic load on the beam would be

$q_k = 18 \cdot 5{,}0 = 90$ kN/m

Permanent load

Selfweight of reinforced concrete is assumed to be 25 kN/m^3. Then the permanent load will be the same as according to EC1.

Load values

Serviceability limit state

During construction:

$q_d = 133{,}5 - 3{,}6 = 129{,}9$ kN/m same according to EC1

Finished building, quasi-permanent load:

$q_d = 133{,}5 + 0{,}3 \cdot 90 = 160{,}5$ kN/m 161 according to EC1

Finished building, frequent load:

$q_d = 133{,}5 + 0{,}6 \cdot 90 = \underline{187{,}5}$ kN/m <u>166</u> according to EC1

Ultimate limit state

During construction:

$q_{Sd} = 1{,}35 \cdot 129{,}9 = 175{,}4$ kN/m same according to EC1

Finished building, clause 6.2.2:

$q_{Sd} = 1{,}35 \cdot 133{,}5 + 1{,}5 \cdot 90 = \underline{315 \text{ kN/m}}$ $\underline{230}$ according to EC1

There are two reasons for the FIP load in ULS of finished building to be 37 % higher:

- no reduction of intensity of imposed load with regard to area is given (EC1: $\alpha_A = 0{,}515$)
- no reduction of permanent load combined with variable load (EC1: $\xi = 0{,}89$ used here)

As regards the reduction of imposed load for large areas, FIP gives no specific rule but refers to other codes, e.g. Eurocode 1. It is obvious that such a reduction is important, and justified, since such high load intensities as 5,0 kN/m^2 are very unlikely to occur all over large areas like, in this case, 650 m^2.

EXAMPLE 5

Design of the D-region of a precast post-tensioned I-beam

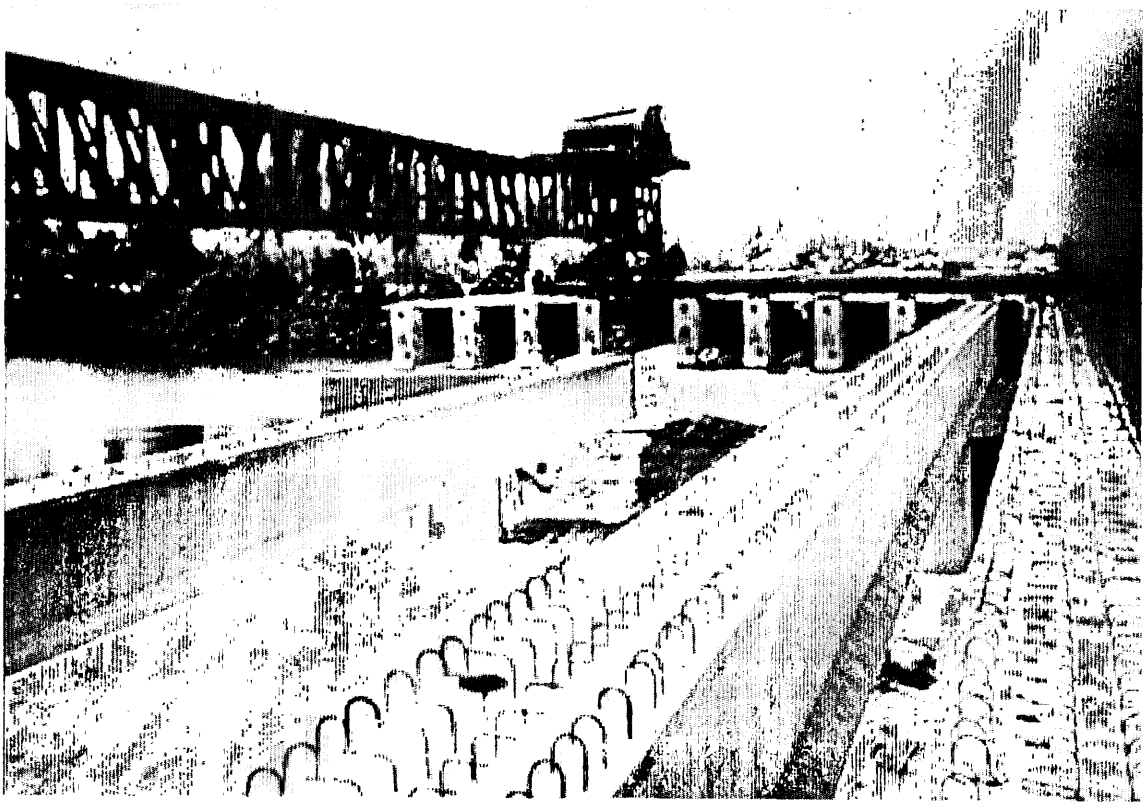

Jean Marc Voumard
VSL
Lyssach, Switzerland

Summary

1 General

For the Sungai Terengganu Bridge in Malaysia, on the east coast of Malayan peninsula, an alternative design with 520 modified I-beams replaced the originally designed I-beams and eliminated the deck slab formvork. The area of the river mouth is generally shallow, traversed by a series of islands and crossed by a line of bridges. This consists of the North Bridge I, the Toll Plaza on the small island of Pulau Besar, the North Bridge 2, the Pulau Duyong Interchange with the Interchange Bridge and the South Bridge. The latter is subdivided into the South Channel Approach Bridges 1 and 2 and the Main Spans. In the above sequence the bridges have the following lengths (and spans): 240 m (6x40m);320 m (8x40m); 40 m; 1.195 m (11x40-40.15-39.85-3x65-39.85-40.15-10x40m). Each bridge comprises a north-bound and a south-bound half, each 12.65 m wide (in the standard section). Typical spans were 40 m with a cross section consisting of six girders spaced at 2.1 m, placed by a specific launching girder allowing transverse movement. The continuity is done with longitudinal reinforcement in the composite deck slab. The end block design for the typical post tensioned T girder will be investigated in this example.

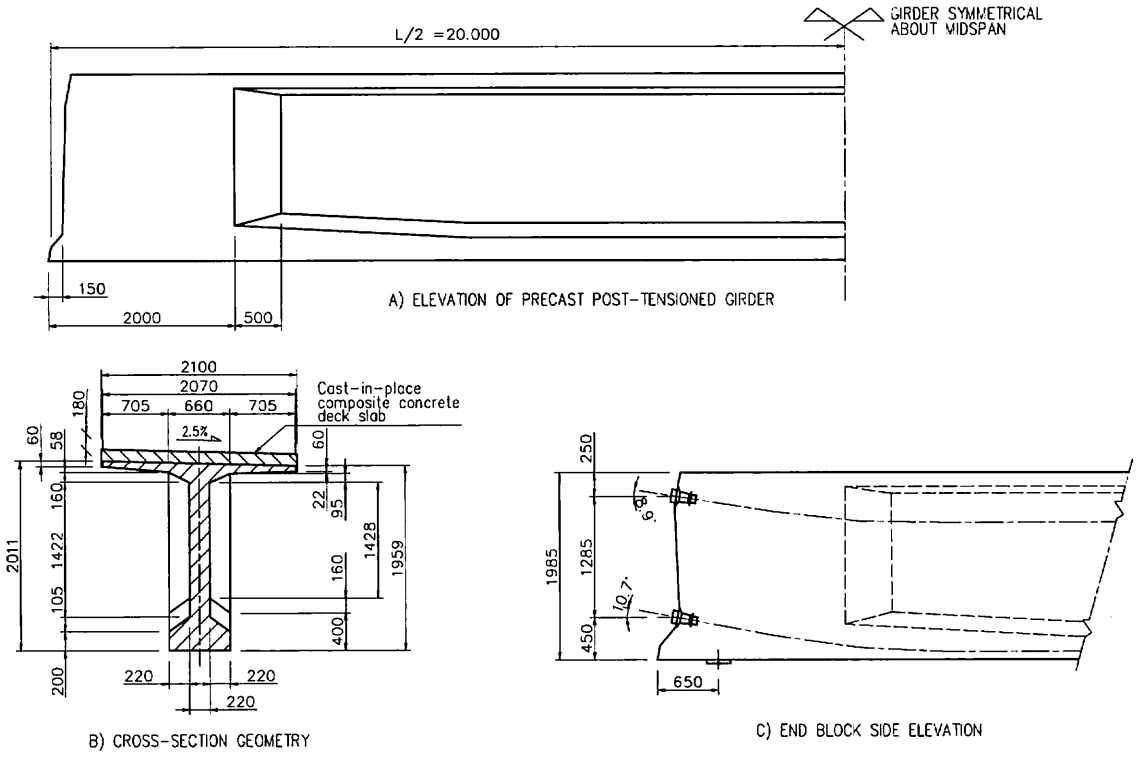

Figure 1: Illustration of the geometry of the girder and the overall tendon profile

2 Local zone design

The local zone is the region immediately surrounding each anchorage device. It may be taken as a cylinder or a prism with transverse dimensions equal to the size of the bearing plate plus the side or edge cover.

In general, for the design of the local zone, the priority should be given to the standard data sheets available in the technical approval (documents) of the post tensioning systems.

The simplified models given in this example are similar to those used as a basis for the calculation of the standard data sheets, however, they may differ slightly because the data sheets are based on experimental results and more comprehensive analysis.

As in this case, the dimensions of the end block do not allow the use of the standard elements, some adaptations have been necessary, based on the simplified models.

2.1 Check of the minimum local zone

The local zone may be assumed to be a cube with side dimensions of b determined by :

$$0.85 \cdot f_{ci}\,(b^2 - \pi \frac{d_d^{\,2}}{4}) = 1.1 P_n \qquad \text{or}$$

$$b = \sqrt{\frac{1.1 P_n}{0.85 \cdot f_{ci}} + \pi \frac{d_d^{\,2}}{4}}$$

f_{ci} = min required concrete cylinder strength at stressing
d_d = external duct diameter
P_n = specified tensile strength of the cable
f_{ci} = 45 N/mm²
(C50 is required in this area with f_{ck}=50N/mm²)
d_d = 87 mm (for the VSL unit 5-19)
P_n =19· 1860· 100· 10^{-3} = 3534 kN

$$b = \sqrt{\frac{1.1 \cdot 3534 \cdot 10^3}{0.85 \cdot 45} + \frac{\pi \cdot 87^2}{4}} = 328 \text{ mm} < 660/2 = 330 \text{ mm}$$

2.2 Check of the confinement reinforcement

For practical design, the confinement reinforcement can be determined with the following equation :

$(0.85 f_{ci} + 4\, f_l) \cdot A_{cc} = 1.1\, P_n$

f_{ci} = min required concrete cylinder strength at stressing
f_l = force acting on the confinement reinforcement
A_{cc} = area of concrete core encompassed by the confining transverse reinforcement

$$f_l = \frac{2 \cdot A_{sw} \cdot \sigma_s}{d_c \cdot s}$$

A_{sw} = cross sectional area of the reinforcement used to form the confinement [mm²]
σ_s = stress corresponding to a steel strain of 1‰ or 200 N/mm²
d_c = inside diameter of the reinforcement used to form the confinement (p.ex.spiral) [mm]

s = pitch [mm]

$$f_l = \frac{2 \cdot 200 \cdot 200}{288 \cdot 50} = 5.55 \text{N/mm}^2$$

A_{sw} = 200 mm² for 16 mm - rebar

σ_s = 200 N/mm²

d_c = 320-2· 16 = 288 mm

s = 320/6 = 53 mm, say 50 mm

$$(0.85 \cdot 45 + 4 \cdot 5.55) \cdot 6.51 \cdot 10^4 \cdot 10^{-3} = 3935 \text{ kN} > 1.1 \cdot 3534$$

$$A_{cc} = \pi \frac{(320 - 32)^2}{4} = 6.51 \cdot 10^4 \text{ mm}^2$$

Note that the spiral diameter given in the standard data sheets for stressing at f_{ci} = 22.4 N/mm² is 365 mm and the minimal spacing of anchorages is 385 mm

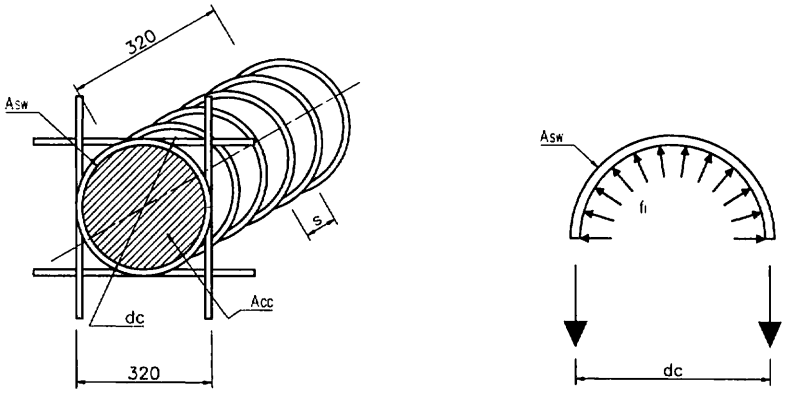

3 Design of D-region

The D-region is the region in front of the anchor which extends along the tendon axis for about a distance equal to the overall depth of the member. In accordance with the St Venant's principle, the length l of the dispersion zone or D-region is approximately equal to the height h of the member.

When detailing the end block, all forces acting on the concrete must be considered.

3.1 In vertical direction

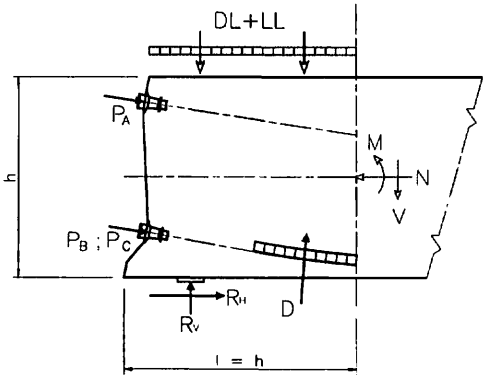

Note :
In N, M, V the effect of P_A, P_B and P_C is included

Figure 2: Loads in D-region

The height of the centroidal axis of the cross section varies from the end block to the typical cross section producing an additional deviation force which is small and has been neglected.

The tendons introduce point loads P_A, P_B, $_C$ into the concrete at their respective anchorages. In addition, due to changes in the tendon direction with respect to the centroidal axis of the concrete section, deviation forces are imposed in the concrete.

The stress resultants N, M and V in the section at the end of the D-region can be determined from equilibrium.

In a variety of load cases, 4 cases of interest for the design of the end block were adopted :

a) load case 1 : after final tensioning of first tendon
b) load case 2 : after first stage post tensioning
c) load case 3 : during erection
d) load case 4 : ultimate loads acting on the composite cross section

The general approach to the analysis is to use a truss model to deal with the primary forces as well as with the secondary spalling forces (see section 6.5.7 in the FIP recommendations). The deviation of the force is assumed to take place on a distance ½ l from ¼ l to ¾ l. As the vertical forces are taken into account, the equilibrium is done at ¾ l in the D-region.

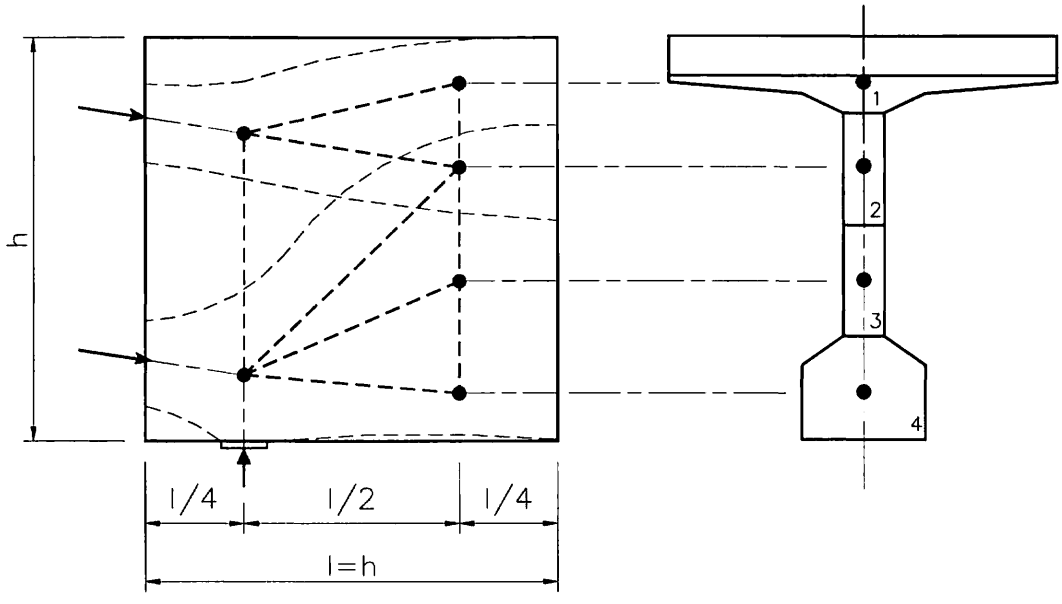

Figure 3: Model representing the flow of forces

The following loading cases shows some possibilities to determine the forces.

a) graphically
b) calculated at each node (Σ H=0, Σ V=0)
c) and d) with help of a computer calculation

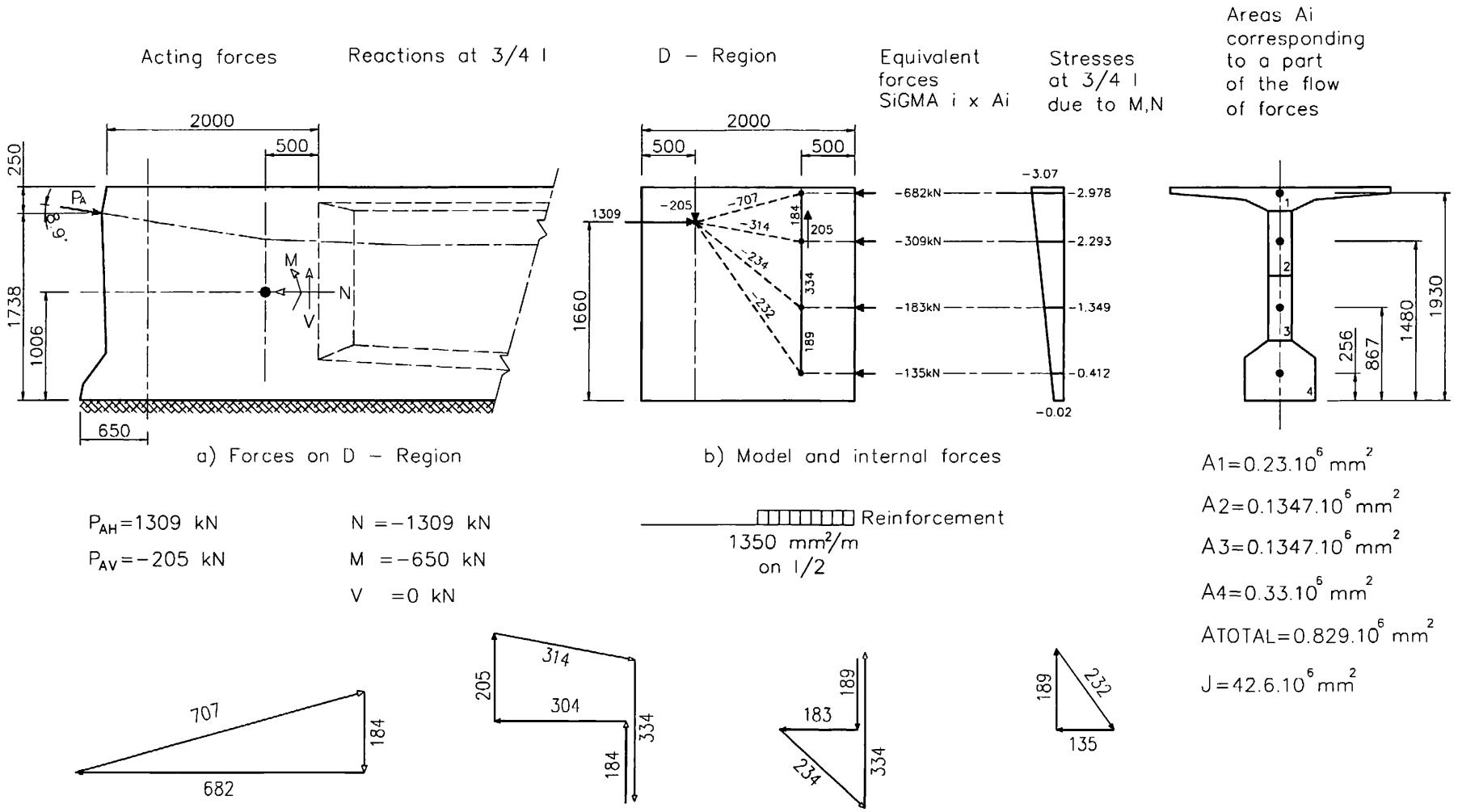

Figure 4: Strut and tie model for a) load case 1, after initial tensioning of first tendon

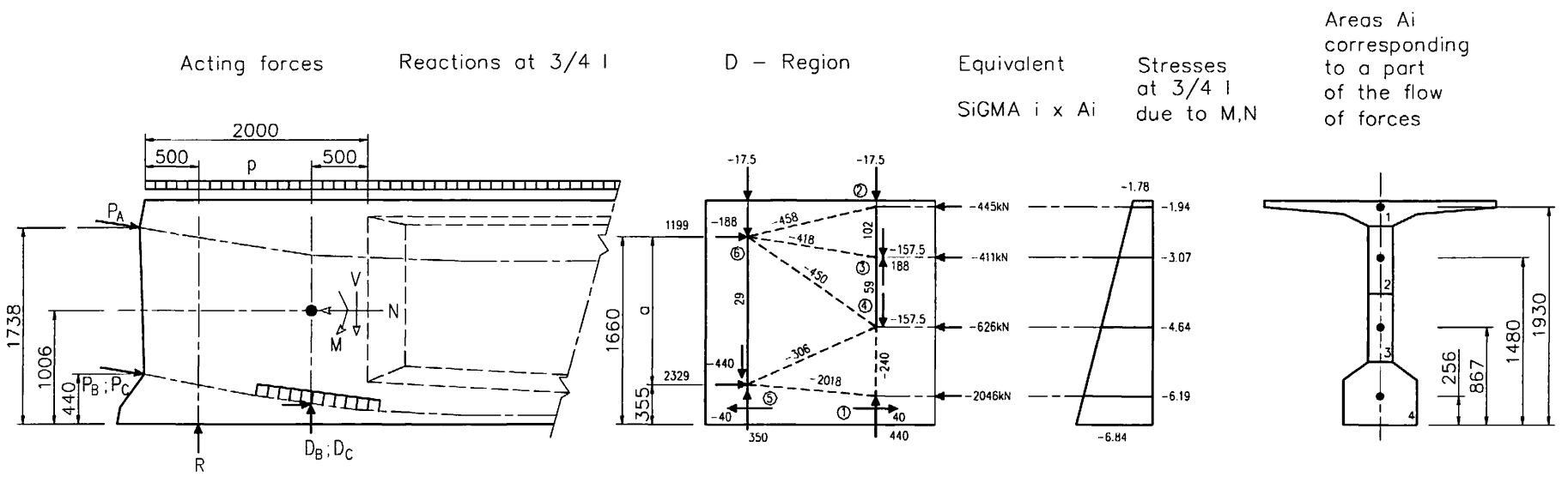

P_{AH} = 1199 kN
P_{AV} = −188 kN
$P_{B,CH}$ = 2329 kN
$P_{B,CV}$ = −440 kN
R_H = −40 kN
R_V = 350 kN
$D_{B,CH}$ = 40 kN
$D_{B,CV}$ = 440 kN
p = −17.5 kN/m

N = −3528 kN
M = −1027 kN
V = −315 kN

$A_1 = 0.23.10^6$ mm²
$A_2 = 0.1347.10^6$ mm²
$A_3 = 0.1347.10^6$ mm²
$A_4 = 0.33.10^6$ mm²
$A_{TOTAL} = 0.829.10^6$ mm²
$J = 42.6.10^6$ mm²

Figure 5: Strut and tie model for b) load case 2, after first stage post tensioning

Node ①

$$tg\alpha = \frac{0.355 - 0.256}{1.0} = 0.099 \qquad \alpha = 5.65°$$

$$\sin\alpha = 0.0985 \qquad \cos\alpha = 0.9951$$

$\Sigma H = 0$	$-2046+H \cdot 0.9951 = 0$	H = 2018 kN
$\Sigma V = 0$	$440 - 2018 \cdot 0.0985 + V = 0$	V = -240 kN

Node ②

$$tg\alpha = \frac{1.93 - 1.66}{1.0} = 0.27 \qquad \alpha = 15.109°$$

$$\sin\alpha = 0.26066 \qquad \cos\alpha = 0.9654$$

$\Sigma H = 0$	$-445+H \cdot 0.9654 = 0$	H = 460 kN
$\Sigma V = 0$	$-17.5 + 460 \cdot 0.26066 + V = 0$	V = -102 kN

Node ③

$$tg\alpha = \frac{1.66 - 1.48}{1.0} = 0.18 \qquad \alpha = 10.204°$$

$$\sin\alpha = 0.1772 \qquad \cos\alpha = 0.9842$$

$\Sigma H = 0$	$-411+H \cdot 0{,}9842 = 0$	H = 418 kN
$\Sigma V = 0$	$102 + 188 - 157.5 - 418 \cdot 0.1772 + V = 0$	V = -59 kN

Node ④

$$tg\alpha = \frac{1.66 - 0.867}{1.0} = 0.793 \qquad \alpha = 38.41°$$

$$\sin\alpha = 0.6213 \qquad \cos\alpha = 0.7836$$

$$tg\beta = \frac{0.867 - 0.355}{1.0} = 0.512 \qquad \beta = 27.11°$$

$$\sin\beta = 0.4557 \qquad \cos\beta = 0.890$$

$\Sigma H = 0$	$-626+A\cos\alpha \cdot B\cos\beta = 0$	
$\Sigma V = 0$	$240 - 157.5 + 59 - A\sin\alpha + B\sin\beta = 0$	
	$-626 + 0.7835 \cdot A + 0.89B = 0$	
	$141.5 - 0.6213 \cdot A + 0.455B = 0$ x 1.26	
B = 448/1.463		B = 306 kN
A = 353/0.7836		A = 450 kN

Node ⑤

$\Sigma V = 0$	$350 - 440 - 306 \cdot 0.4557 + 2018 \cdot 0.0985 + V = 0$	V = -30 kN

Calculation of the forces for load case 2 using equilibrium at each node

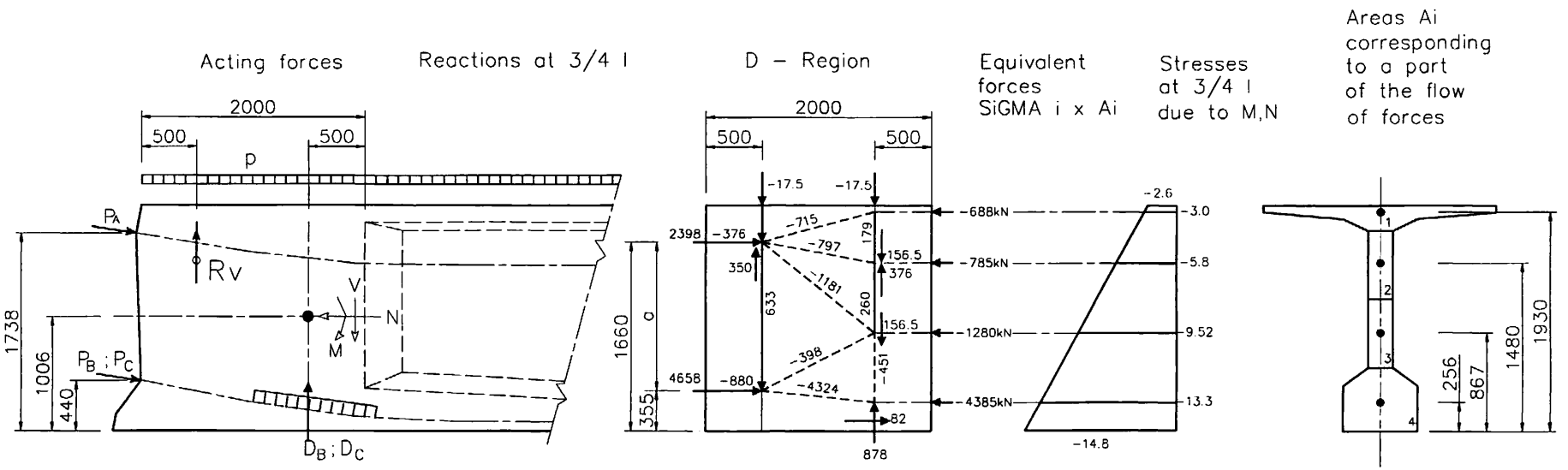

Figure 6: Strut and tie model for c) load case 3, during erection

S T A T I K - 3 V.2.24 Page 19
VSL (SCHWEIZ) AG 29.06.99
- 14:07

Scale 1 : 23.8

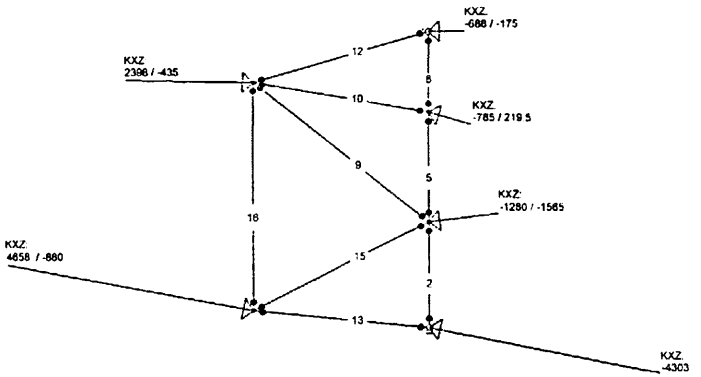

All the loads acting on the free body must be in equilibrium.
All the support reactions are near to zero.

Calculation of forces for load case 3 with a static program (STATIC 3 of CUBUS)

S T A T I K - 3 V.2.24 Page 19
VSL (SCHWEIZ) AG 29.06.99
14:14

Scale 1 : 8.5
Int. Force, Loadcase 1, Subsys. "ALL"
- Structure: Elmnts.
- Normal ForceN , Scale 5.00E-05
  min: -4.32E+03 max: 6.33E+02 [kN]
- Text Normal ForceN [kN]

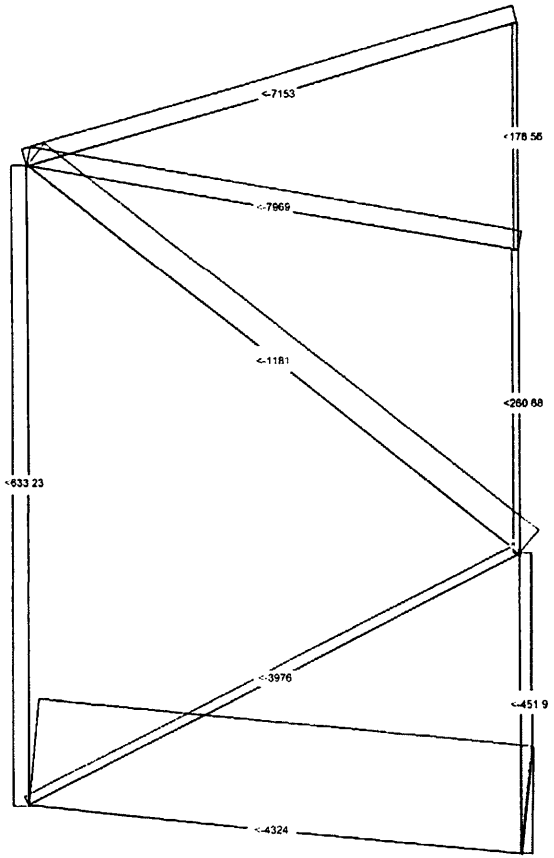

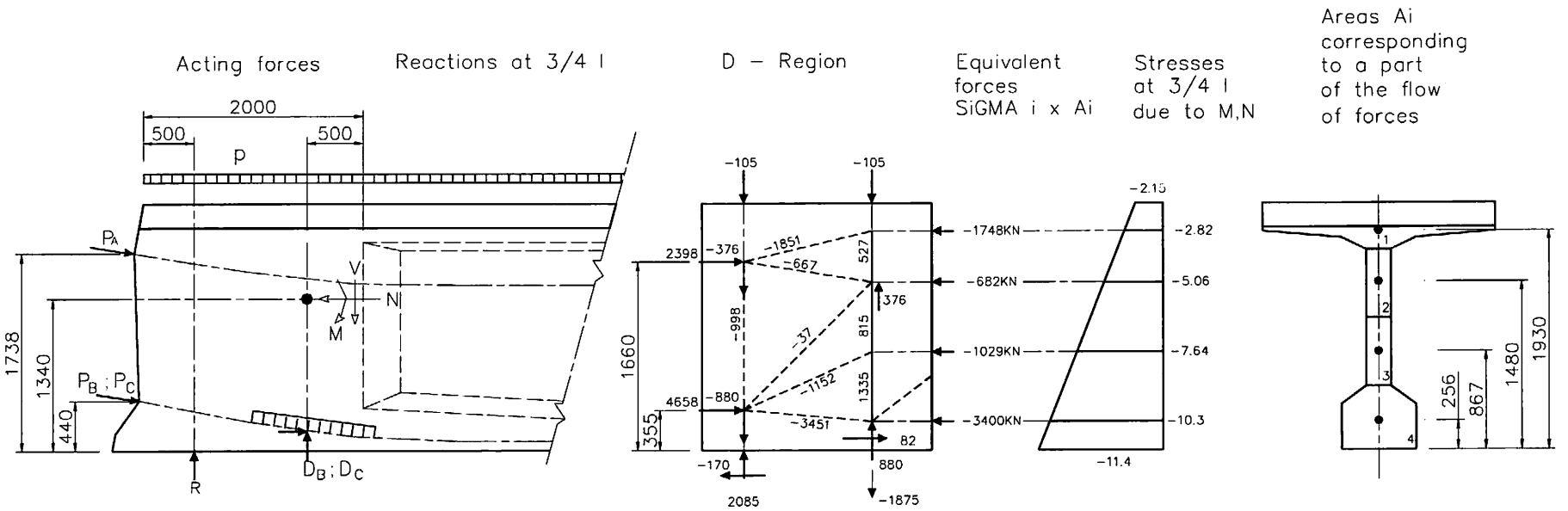

P_{AH} = 2398 kN
P_{AV} = −376 kN
$P_{B,CH}$ = 4658 kN
$P_{B,CV}$ = −880 kN
R_H = −170 kN
R_V = 2085 kN
$D_{B,CH}$ = 82 kN
$D_{B,CV}$ = 878 kN
p = −105 kN/M

N = −6969 kN
M = −2959 kN
V = −1872 kN

Reinforcement
2100 mm²/m
on l/2

Shear reinforcement
1900 mm²/m
on l

$$As = \frac{1335.10^3}{(410/1.15) \times 1940} = 1900 \text{ mm}^2/\text{m}$$

$A1 = 0.62.10^6$ mm²
$A2 = 0.1347.10^6$ mm²
$A3 = 0.1347.10^6$ mm²
$A4 = 0.33.10^6$ mm²
$ATOTAL = 1.23.10^6$ mm²
$J = 73.3.10^6$ mm²

Figure 7: Strut and tie model for d) load case 4, ultimate loads acting on the composite cross section

3.2 In transverse direction

3.2.1 In web

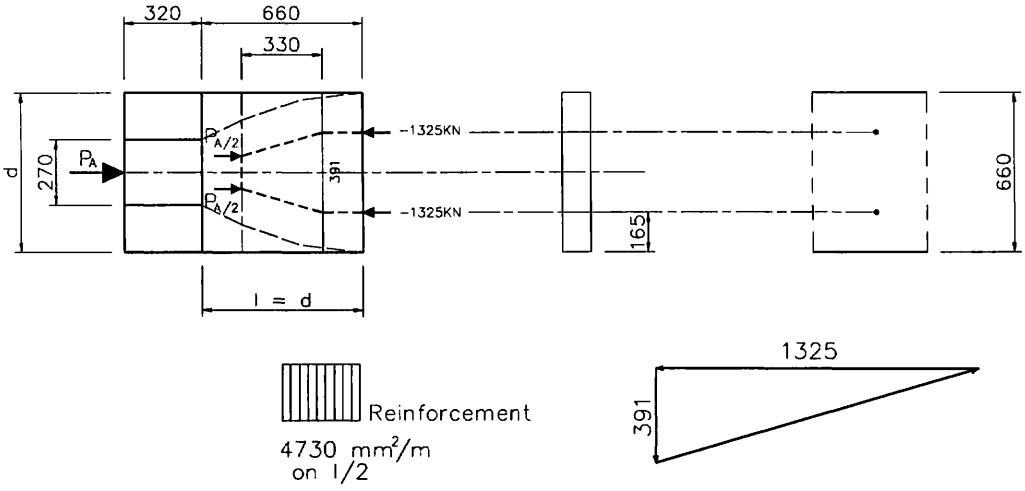

$P_A = 2650$ kN

$$F_{transverse} = \frac{262.5-165}{330} \times 1325 = 391 \text{ kN}$$

Figure 8: Transverse reinforcement requirements in the girder web

3.2.2 In girder flange

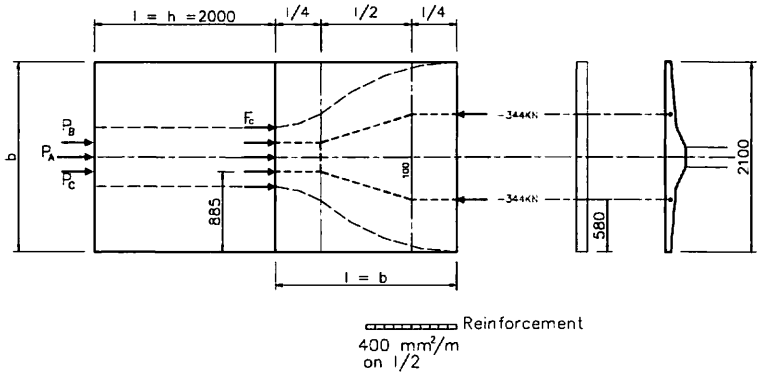

Forces acting from the web in the girder flange

Case ① F_C=682 kN

② F_C=445 kN

③ F_C=688 kN (decisive)

④ F_C is acting the composite section

$$F_{transverse} = \frac{885-580}{1050} \times 344 = 100 \text{ kN}$$

Figure 9: Transverse reinforcement requirement in the girder flange

4 Sketch of end block reinforcement

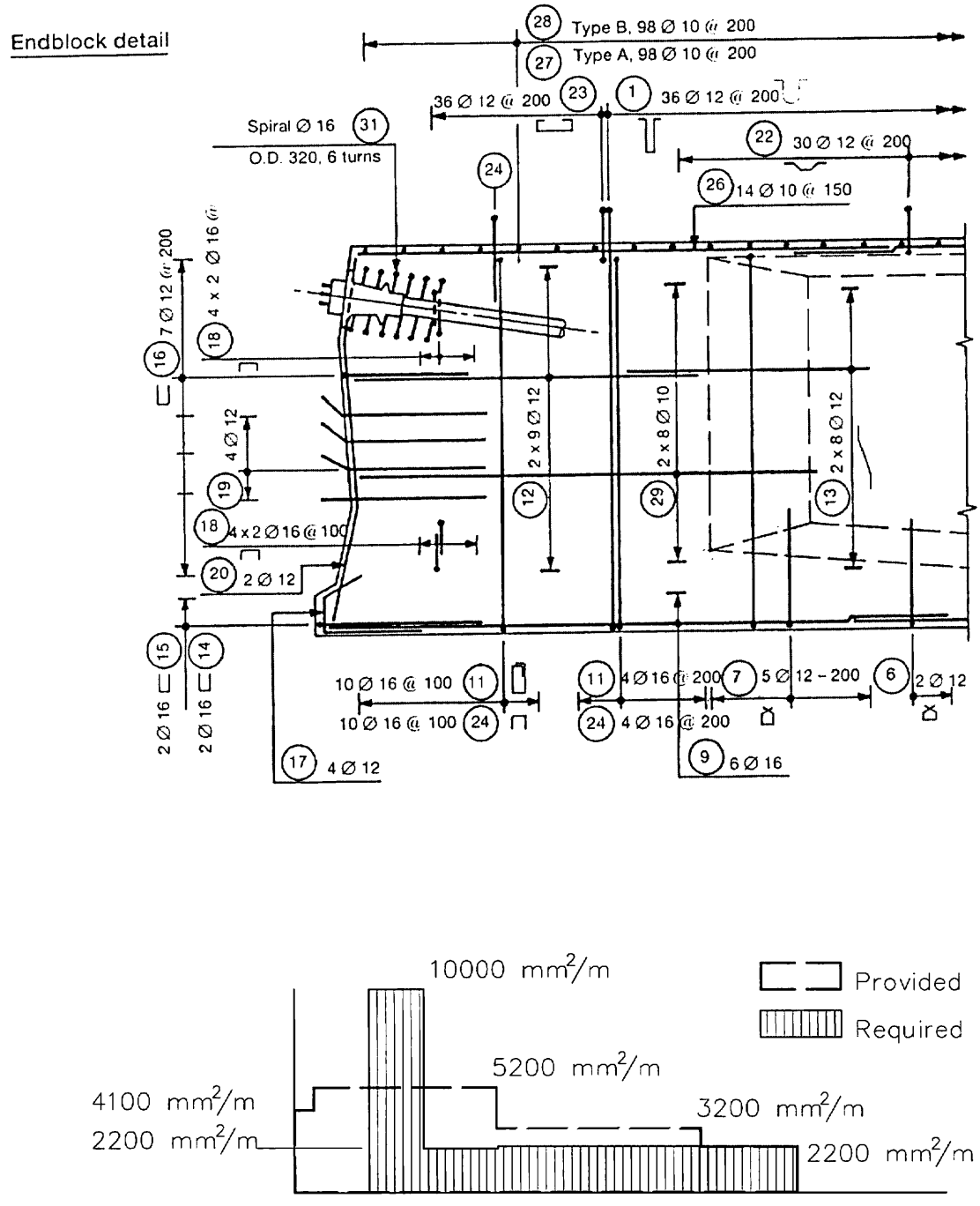

Figure 10: Comparison of the reinforcement actually used and the requirements for the load cases 1 to 4

EXAMPLE 6

Slender piers design according to FIP Recommendations 1996 and comparison with non-linear analysis
- Viaduct over the Alberche River

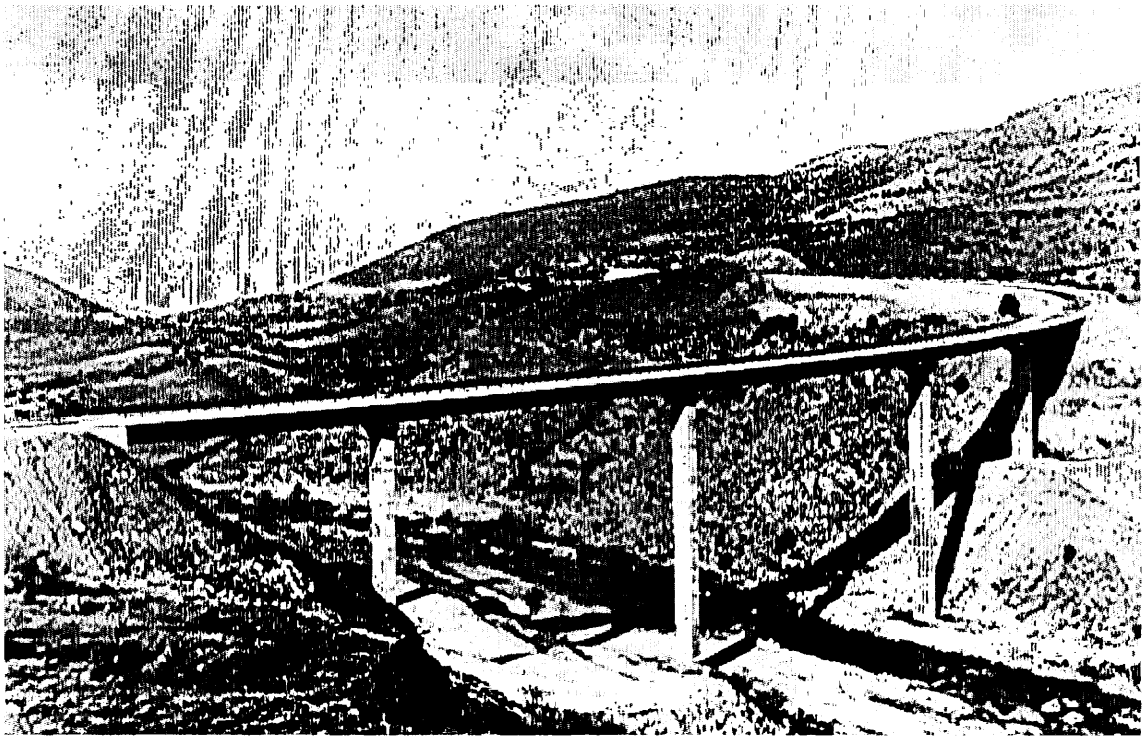

Álvaro Ruiz Herranz
Hugo Corres Peiretti
Alejandro Pérez Caldentey
Dpto. Mecánica de Medios Continuos y T[a] de Estructuras
Universidad Politécnica de Madrid
Madrid, Spain

1 Introduction

In this paper the design of the supports of the Viaduct over the Alberche river is undertaken, using the method proposed by the FIP Recommendations 1996 (FIP 96) [1].

The solution, thus obtained, is then compared with two non-linear analysis, taking into account non-linear material behaviour, as well as non-linearity due to changes in geometry, with different degrees of simplification.

In a first non-linear analysis, the supports are considered as cantilevers in the transversal direction and as simply supported at one end and embedded in the other end in the longitudinal direction. Transversal loads transmitted to the supports by the deck are obtained considering a linear behaviour of the structure. Wind loads acting directly on the columns are also considered. In the longitudinal direction a displacement of 100 mm is imposed on the top of the column to take into account a displacement-limiting device installed at the abutments (the maximum displacement allowed is 100 mm).

In a second non-linear analysis, the whole structure is modelled. In this case, a linear behaviour of the deck has been assumed, while geometric and material non-linearities are considered in the behaviour of the supports.

Finally, the same columns have been designed according to the procedures proposed by Eurocode 2 (EC2)[2] and Model Code 90 (MC90)[3].

2 Description of the structure and loads considered

The Viaduct over the Alberche River is a five span composite structure. The length of the spans are 38.00, 56.00, 66.00, 52.00 and 34.00 m with a total length of 246 m (figure 1). The layout in plan is complex, beginning with a straight line, followed by a transition curve and ending in a circle with a radius of 350 m. The cross-section is composed of two double T steel beams with a height of 2.30 m connected to a reinforced concrete slab of variable depth from 0.15 to 0.30 m (figure 2).

The four columns have a hollow rectangular cross section of exterior dimensions 4.00x1.80 m^2 and a wall depth of 0.30 m. The columns are ended at the top by a composite steel-concrete structure designed to extend the width of the columns in order to support the deck. The two central columns, P2 and P3 (figure 4) have a height of 40.92 and 44.05 m, respectively. The two exterior columns, P1 and P4, are 23.04 and 22.58 m high.

The deck is fixed in the longitudinal direction to piers P2 and P3, and supported on neoprene bearings at piers P1 and P4 as well as at the abutments.

At the abutments, a special system is installed in order to limit the maximum longitudinal displacement of the deck (and therefore that of the more slender columns as well) to 100 mm (figure 5).

The material properties of the piers, as well as the partial safety factors, are given in table 1.

Table 1: Pier material properties and partial safety factors.

Material	f_{ck}, f_{yk} [MPa]	E_c, E_s [MPa]	γ
Concrete C250	25.0	30000	1.50
Reinforcing Steel S500	500.0	200000	1.15

For the design, the loads and load combinations required by the Spanish Standard of Loads on Road Bridges IAP [4] have been considered. In table 2, a brief summary is presented.

Table 2: Loads considered.

Loads	
- Permanents (G)	
Deck self-weight	95.0 KN/m
Pavement, sidewalks and safety barriers	45.0 KN/m
Pier self weight	25.0 KN/m
- Free shrinkage of deck slab (G*)	- 260 με
- Variable actions	
Traffic	
Vertical	
uniform load	4.0 KN/m^2
concentrated load	600.0 KN
Horizontal	
braking	2.5 KN/m
centrifugal force	1.2 KN/m
Other external loads	
Longitudinal or transversal wind	±2.0 KN/m^2
Temperature on deck	
concrete	± 17.3°
steel	± 35.0°

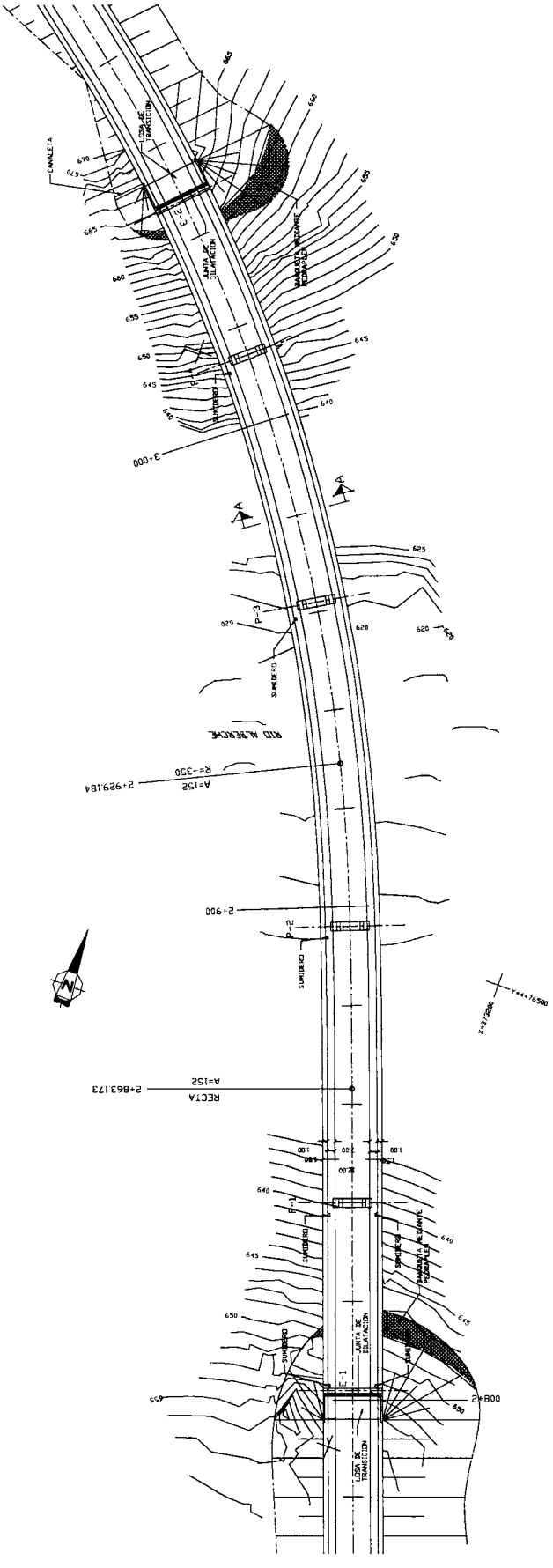

Figure 1: Plan view of the structure.

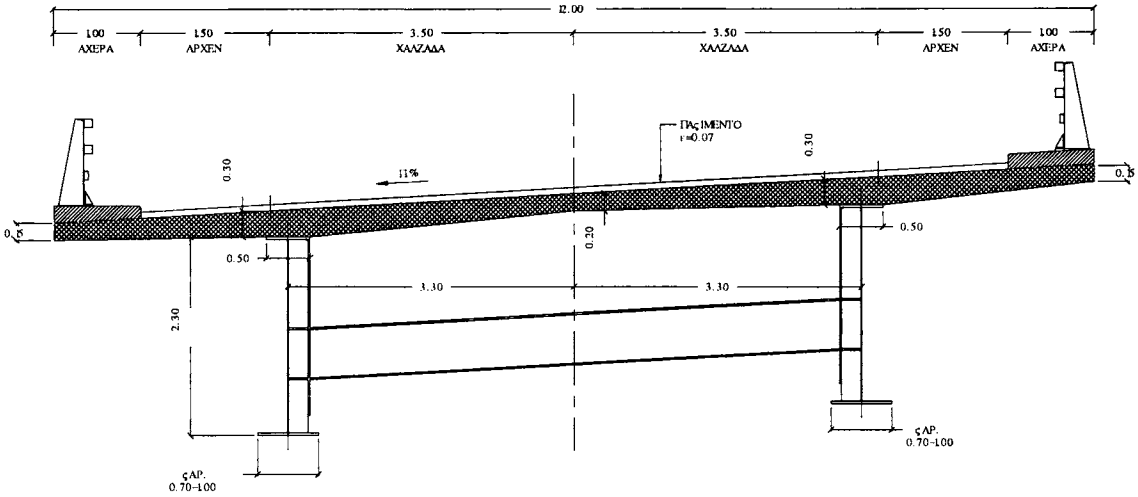

Figure 2: Deck cross-section

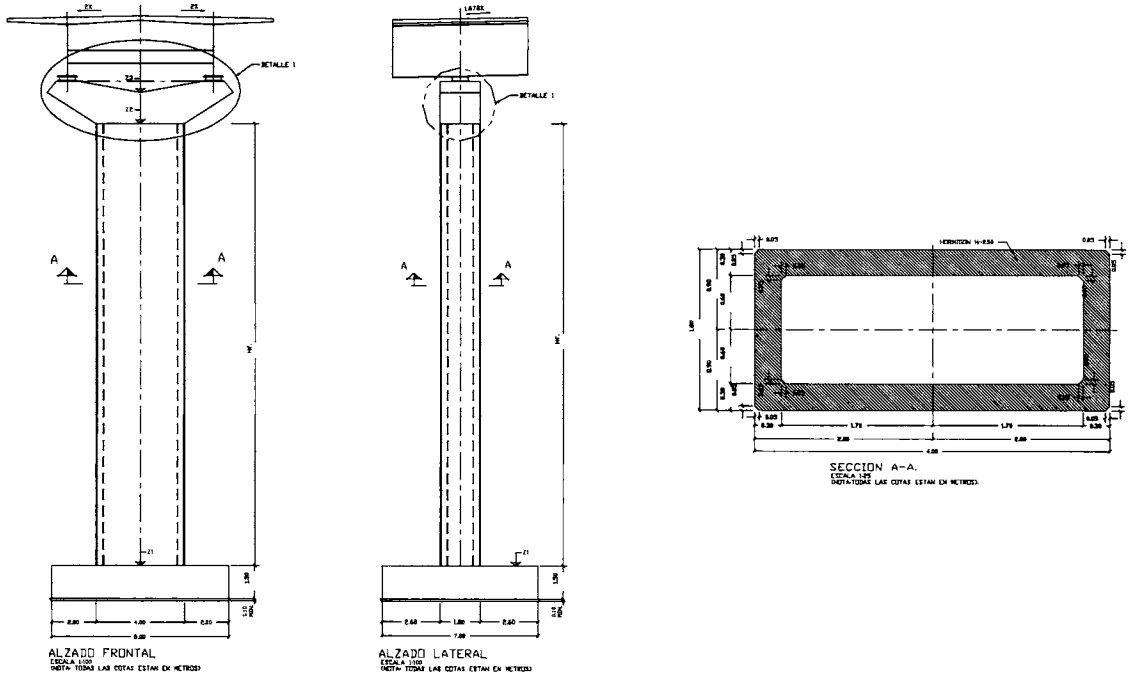

Figure 3: Piers P1 and P4. Elevation and cross-section

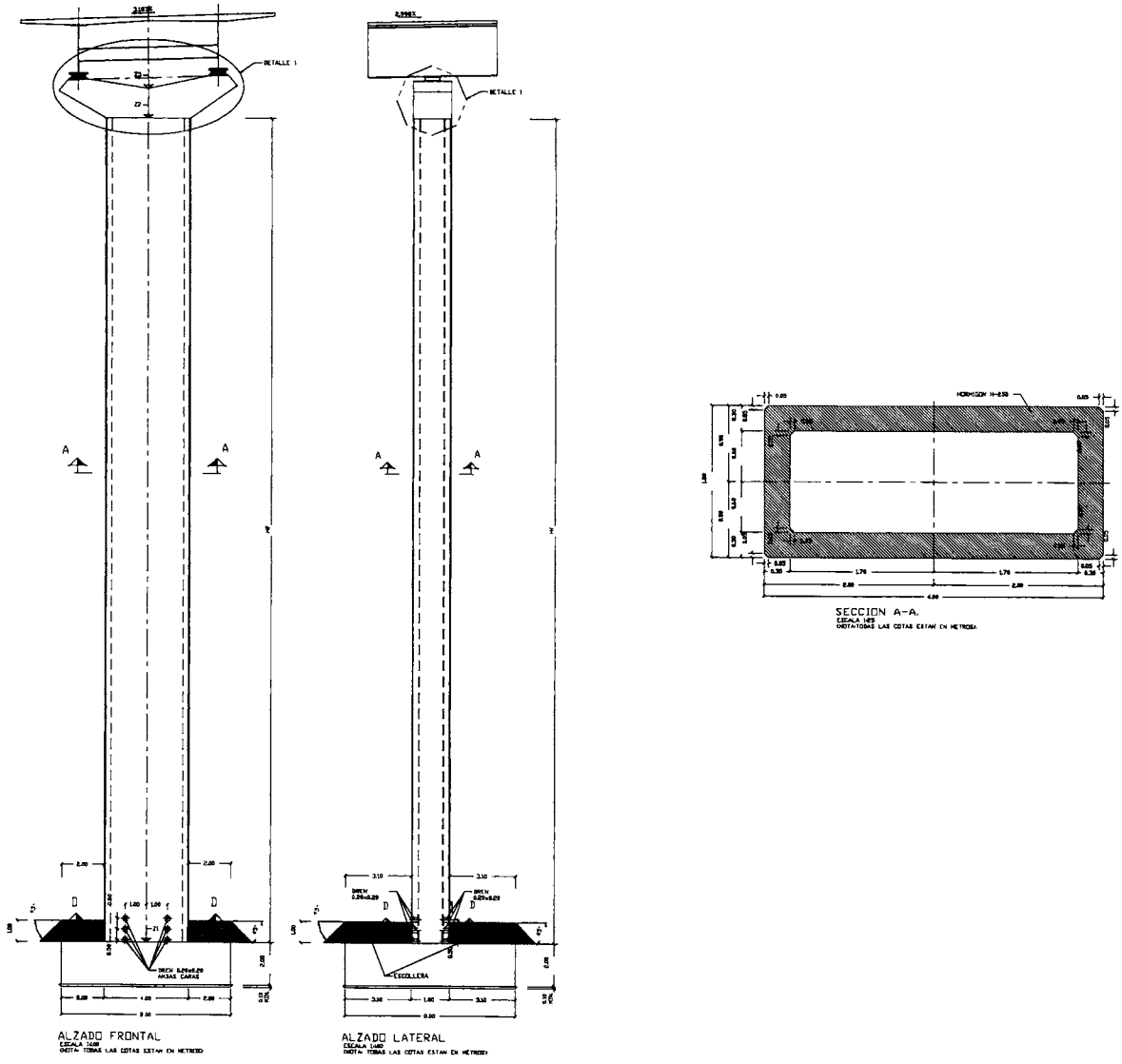

Figure 4: Piers P2 and P3. Elevation and cross-section

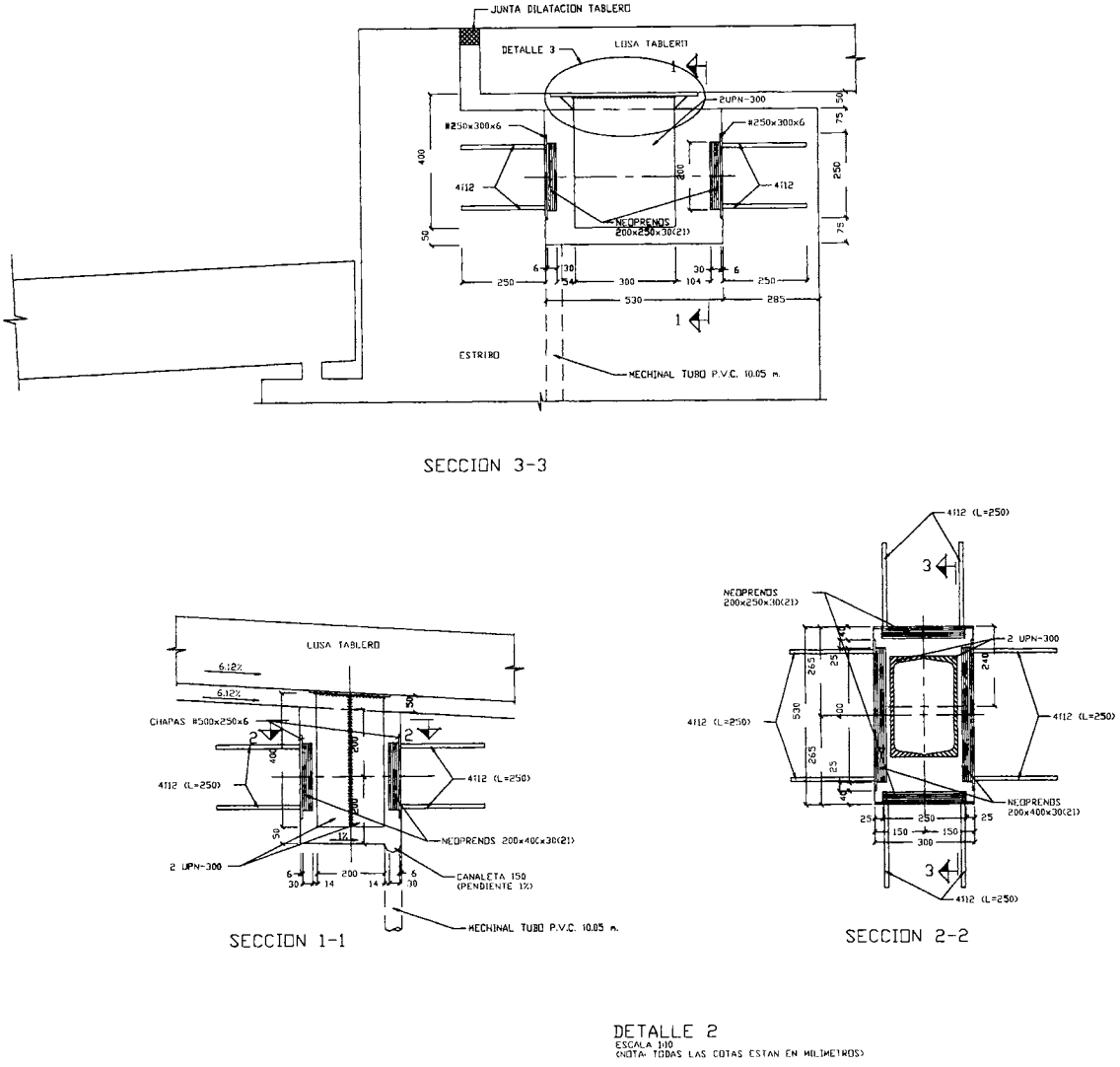

Figure 5: Detail of displacement-limiting system.

The load partial safety factors and the load combinations considered are described in tables 3 and 4.

Table 3: Load partial safety factors

Load	Favourable effect	Unfavourable effect
Permanent	$\gamma_G=\gamma_{G^*}=1.00$	$\gamma_G=\gamma_{G^*}=1.35$
Variable	$\gamma_Q=0$	$\gamma_Q=1.50$

Table 4: Load combinations considered

Combination	Description and combination factors
I	Permanent load, traffic load on half of deck width and transversal wind $1.35\ (G+G^*) + 1.50 \cdot Q_{\text{traffic load on half of deck width}} + 0.45 \cdot Q_{\text{transversal wind}}$
II	Permanent load and transversal wind $1.35\ (G+G^*) + 1.50 \cdot Q_{\text{transversal wind}}$
III	Permanent load, traffic load on full deck width and transversal wind $1.35\ (G+G^*) + 1.50 \cdot Q_{\text{traffic load on full deck}} + 0.45 \cdot Q_{\text{longitudinal wind}}$
IV	Permanent load, traffic load on half of deck width and longitudinal wind $1.35\ (G+G^*) + 1.50 \cdot Q_{\text{traffic load on half of deck width}} + 0.45 \cdot Q_{\text{longitudinal wind}}$
V	Permanent load and longitudinal wind $1.35\ (G+G^*) + 1.50 \cdot Q_{\text{longitudinal wind}}$

3 Design according to FIP Recommendations 1996

FIP 96 establish a simplified procedure for slender supports subject to non-skew bending, which allows the design of reinforcement by adding an additional eccentricity e_2, obtained in a simplified manner, which takes into account second order effects. For skew bending, the use of a simplified interaction diagram is proposed:

$$\left(\frac{M_{sd,x}}{M_{Rd,x}}\right)+\left(\frac{M_{sd,y}}{M_{Rd,y}}\right)\leq 1$$

where:

$M_{sd,x}$ Design bending moment in the x direction, including second order effects
$M_{sd,y}$ Design bending moment in the y direction, including second order effects
$M_{Rd,x}$ Ultimate bending moment in the x direction resisted by the cross section, for the given normal force, N_{sd}.
$M_{Rd,y}$ Ultimate bending moment in the y direction resisted by the cross section, for the given normal force, N_{sd}.

To determine $M_{sd,x}$ and $M_{sd,y}$ the procedure established in paragraph 6.6.6 of FIP 96 is used. In each direction:

$$M_{sd} = M^0_{sd} + M_2$$
$$M_2 = N_{sd} \cdot e_2$$
$$e_2 = (1/r) \cdot l^2_0/10$$

where:

M_{sd}^0 First order design bending moment
M_2 Bending moment due to second order effects
e_2 Second order eccentricity
l_0 Equivalent support length (buckling length)
$1/r$ Reference curvature
defined according to FIP 96.

In the case of bridge piers, the worst design combinations usually involve skew bending. The value of l_0 depends on the type of connection between pier and deck, as well as on the boundary conditions of the structure as a whole, making it difficult to determine this parameter. Furthermore l_0, usually, has a different value in the longitudinal and in the transversal direction. Finally, the forces transmitted to the piers by the deck are a function of the general behaviour of the structure, and, in particular, of the stiffness of the piers.

For this example, the first order forces have been determined assuming a linear behaviour of the structure, using the non-cracked stiffness for both deck and piers and modelling the connections between deck and piers in a realistic way, taking into account the different characteristics of the bearing supports. In tables 5 and 6 the first order forces for each combination group are shown for piers P1 and P4, and piers P2 and P3, respectively. For each group of piers, the worst combination considering each two piers is shown in each case.

Table 5: First order forces. Piers P1 and P4.

Load combination	N_{sd} [KN]	$M_{sd,transversal}^0$ [mKN]	$M_{sd,longitudinal}^0$ [mKN]
I	14900	11300	1100
II	13250	13500	2150
III	16700	1950	3800
IV	14900	7450	3400
V	12900	200	6100

Table 6: First order forces. Piers P2 and P3.

Load combination	N_{sd} [KN]	$M_{sd,transversal}^{0}$ [mKN]	$M_{sd,longitudinal}^{0}$ [mKN]
I	20900	19950	700
II	17700	40950	1250
III	23150	6100	2950
IV	20900	8200	2800
V	17650	750	5000

In the transversal direction, for the determination of the second order forces, the piers are considered as cantilevers and, therefore, $l_0=2\cdot l$. In this way, any contribution of the deck to the transversal stability of the piers is neglected.

In the longitudinal direction, in order to take into account that the longitudinal displacement has been limited to 100 mm, e_2 has been taken as 100 mm for both groups of piers, P1-P4 and P2-P3. Besides, the favourable effect of the bending moment, due to the horizontal reaction at the displacement-limiting system, is neglected.

In tables 7 and 8, the resulting design forces for the embedded section of the pier are shown. Since the reinforcement is constant along the full length of the piers, the embedding is the critical section.

Table 7: Design forces, including second order effects. Piers P1 and P4.

Load combination	N_{sd} [KN]	$M_{sd,transversal}$ [mKN]	$M_{sd,longitudinal}$ [mKN]
I	14900	14035	2595
II	13250	15925	3470
III	16700	5045	5460
IV	14900	10160	4890
V	12900	2540	7390

In order to determine the required reinforcement, an iterative procedure is necessary. A certain amount of reinforcement is firstly proposed. For this amount, M_{Rd} and M_{sd} are determined for each direction and the condition established by the proposed interaction diagram is checked. The procedure is repeated until the interaction condition is strictly fulfilled.

Table 8: Design forces, including second order effects. Piers P2 and P3.

Load combination	N_{sd} [KN]	$M_{sd,transversal}$ [mKN]	$M_{sd,longitudinal}$ [mKN]
I	20900	30400	2780
II	17700	51685	3025
III	23150	16830	5255
IV	20900	18650	4890
V	17650	10480	6760

Table 9: Interaction diagram. Piers P1 and P4.

Load combination	N_{sd} [KN]	$M_{Rd,transversal}$ [mKN]	$M_{Rd,longitudinal}$ [mKN]	$\left(\frac{M_{sd,t}}{M_{Rd,t}}+\frac{M_{sd,l}}{M_{Rd,l}}\right)$
I	14900	30000	15210	0.64
II	13250	28870	14160	0.80
III	16700	30920	16240	0.50
IV	14900	30000	15210	0.66
V	12900	28595	13935	0.62

Tables 9 and 10 give the values of M_{Rd} (in each direction) and of $(M_{sdx}/M_{Rdx}+M_{sdy}/M_{Rdy})$ for each group of piers, for the different combinations and for the proposed reinforcement. For piers P1 and P4 the proposed reinforcement A_s = 12480 mm^2 (ω=0.11) is the minimum reinforcement required by the Spanish reinforced concrete Standard [5]. For piers P2 and P3, the proposed reinforcement is A_s = 65663 mm^2 (ω=0.56), results from combination II, as can be seen in table 10.

Table 10: Interaction diagram. Piers P2 and P3.

Load combination	N_{sd} [KN]	$M_{Rd,transversal}$ [mKN]	$M_{Rd,longitudinal}$ [mKN]	$\left(\frac{M_{sd,t}}{M_{Rd,t}}+\frac{M_{sd,l}}{M_{Rd,l}}\right)$
I	20900	57260	31210	0.77
II	17700	57435	31090	0.99
III	23150	56780	30655	0.46
IV	20900	57260	31210	0.48
V	17650	57435	31085	0.40

4 Design according to EC2 and CEB-FIP Model Code 90

EC2 and MC90 establish, for the design of slender columns subject to compression and non-skew bending, similar criteria between them. These criteria are also similar to the one proposed by FIP 96.

For skew bending, an independent check for each plane of bending is allowed, only if there is a predominant eccentricity, as shown in figure 6.

This type of proposal is clearly insufficient for the design of bridge columns since, in many cases, the design combinations involve skew bending without a predominant eccentricity and, therefore do not fulfill the above condition.

In this example, however, load combination number II, which governs the design of piers P2 and P3, is a combination with a predominant eccentricity in the transversal direction, and fulfills the condition established by both EC2 and MC90. Table 11 shows the amount of reinforcement obtained with EC2 and MC90. These are compared to the amount of reinforcement determined in paragraph 3[1].

[1] For the design according EC2 and MC90, the piers are supported as explained in paragraph 3. In the transversal direction, the piers are considered as cantilevers and the second order eccentricity in the longitudinal direction has been taken as 100 mm.

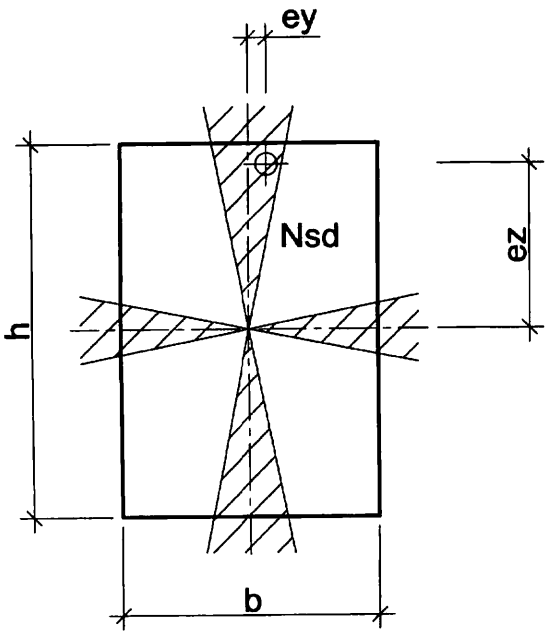

$$\frac{e_z / h}{e_y / b} \le \frac{1}{4} \quad \acute{o} \quad \frac{e_y / b}{e_z / h} \le \frac{1}{4} \qquad (MC90)$$

$$\frac{e_z / h}{e_y / b} \le \frac{1}{5} \quad \acute{o} \quad \frac{e_y / b}{e_z / h} \le \frac{1}{5} \qquad (EC2)$$

Figure 6: Condition which must be fulfilled in order to be allowed to check each bending plane separately.

Table 11: Design of piers P2 and P3 according to FIP Recommendations 1996, EC2 and CEB-FIP Model Code 90.

	A_s [mm^2]	ω
Eurocode 2	64171	0.55
CEB-FIP Model Code 90	69965	0.60
FIP Recommendations 1996	65663	0.56

In this case, where the criteria of EC2 and MC90 is of application, similar results are obtained.

5 Non-linear check

In order to check the reinforcement obtained using FIP 96, a non-linear computation was undertaken.

For this check a finite element program was used taking into account both the mechanical non-linearity, due to the non-linear behaviour of the materials, as well as the geometrical non-linearity, due to the effect of the displacements on the forces.

The non-linear behaviour of concrete was modelled using the parabola-rectangle diagram shown in figure 7, with a maximum stress of f_{cd}. It is well known that this diagram was developed in order to determine the ultimate limit state due to normal forces and that it underestimates the stiffness of the cross-section for the lower range of stresses.

However, taking f_{cd} as maximum stress, instead of $0.85 \cdot f_{cd}$ (see figure 7), it has been shown [6] that, for the ultimate limit state of instability, the parabola-rectangle diagram leads to adequate results, similar to those obtained with more precise diagrams, such as that also shown in figure 7, proposed in the paragraph 2.1.4.4.1 of MC90 .

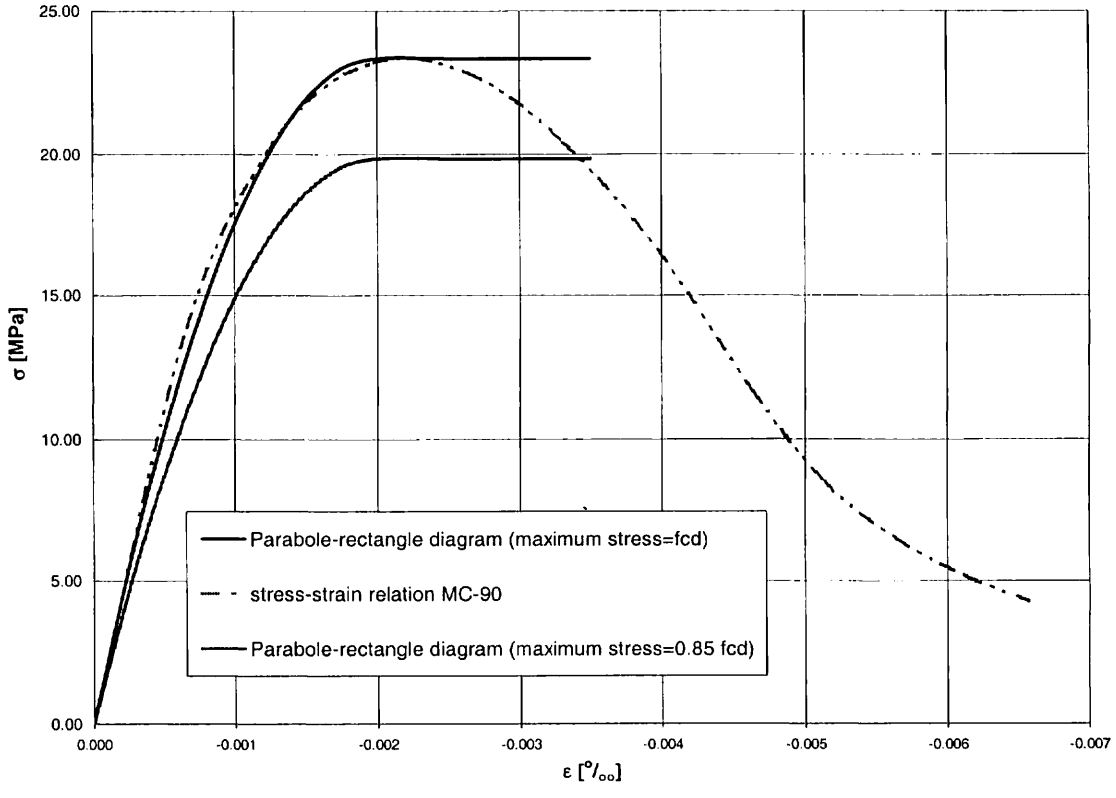

Figure 7: Constitutive relations of concrete

Tension stiffening is neglected. For steel, a bilinear diagram has been used, considering a maximum stress equal f_{yd}.

In all cases, load combination II, which governs the design of the slender columns, was checked. A first analysis is undertaken with the same loads used to determine the amount of reinforcement. Then, the wind load is increased until the collapse of the structure comes about.

Two different structural systems were studied. The results of table 12 correspond to the analysis of the pier alone, supported in the same manner as considered for the design of the reinforcement, as explained in paragraph 3. In this case, the vertical and the transversal horizontal loads are determined through linear analysis using the non-cracked stiffness of deck and piers. In the longitudinal direction, an imposed displacement of 100 mm is considered, in order to take into account the limit to the displacement allowed by the structural system (see figure 8).

The results show that the system is stable under combination II, and reaches a collapse only after the wind load has been increased by a factor of 1.20.

Table 12: Analysis of the ultimate bearing capacity of an isolated column. Piers P2 and P3.

	N_{sd} [KN]	$M_{sd,transversal}$ [mKN]	$M_{sd,longitudinal}$ [mKN]
First order design bending moments	17700	40950	1250
Ultimate Load Capacity β=1.20	17700	62280	1535

Finally, a non-linear analysis considering the whole system (see figure 9) was undertaken. The results of this analysis are shown in table 13. In this case, a linear behaviour of the deck was assumed, while both the mechanical and the geometrical non-linearities were considered in the piers. Other results [6] show that the non-linear behaviour of the deck is of little importance in the results of this type of structural analysis.

Table 13: Analysis of the ultimate bearing capacity of the structure. Piers P2 and P3.

	N_{sd} [KN]	$M_{sd,transversal}$ [mKN]	$M_{sd,longitudinal}$ [mKN]
First order bending moments	17700	40950	1250
Ultimate Load Capacity β=1.80	17700	60815	1345

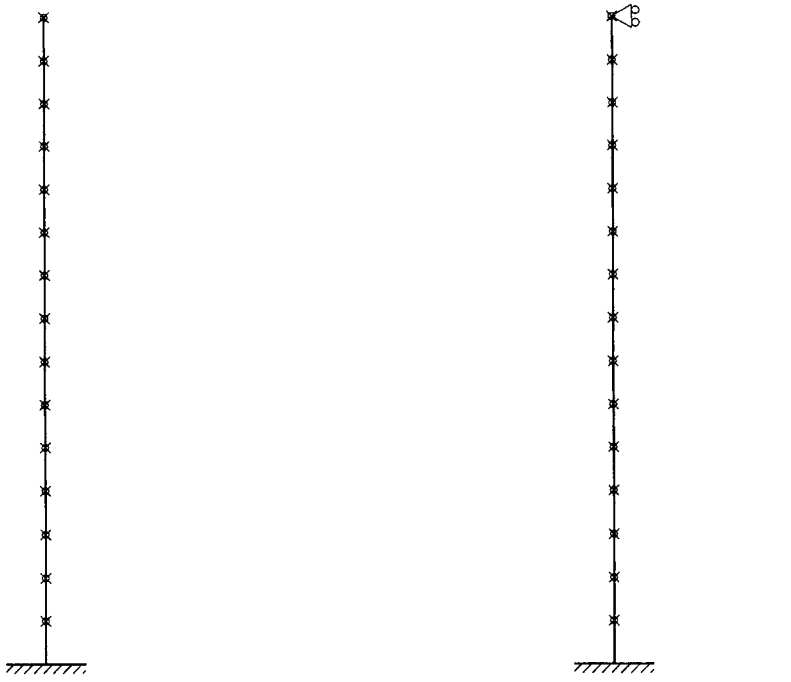

Figure 8: Structural Model. Non-linear analysis of the isolated column.

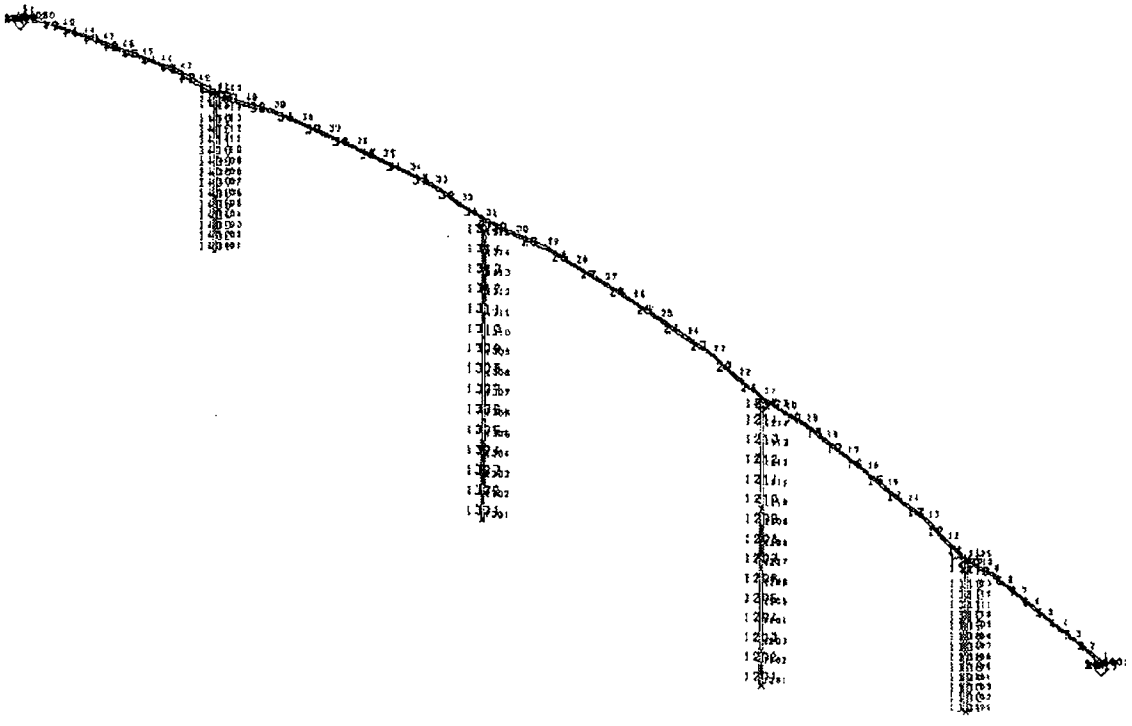

Figure 9: Structural model. Non-linear analysis of the whole structure.

As in the previous analysis, the structures is first checked for the initial loads of Combination II, which proves stable. Then, the wind load is increased until the collapse of the structure is attained. Table 13 shows that the wind load has to be multiplied by 1.80 before the structure collapses.

6 Conclusion

The method proposed by FIP 96 allows the study of slender bridge columns, subject to skew bending. This method has been applied to a real structure having very slender piers. In this case, it has been shown that this method leads to results which are both reasonable and on the safe side, according to the more precise non-linear checks carried out.

7 References

[1] FIP Recommendations 1996 'Practical design of structural concrete'. SETO for FIP (International Federation for Prestressing), London, September 1999

[2] Eurocode 2 (1989). Eurocode 2, Design of concrete structures. European Committee for Standardisation, 1989.

[3] CEB-FIP Model Code (1990). CEB-FIP Model Code for concrete structures, Euro-International Committe for Concrete, Bulletin n° 213/214, Lausanne, May 1993.

[4] Spanish Code of Loads on Road Bridges (1995). IAP Instrucción sobre Acciones a considerar en el Proyecto de Puentes de Carretera. Ministerio de Fomento. Dirección General de Carreteras. Madrid, April 1997.

[5] Spanish Reinforced Concrete Code (1991). EH-91 Instrucción para el Proyecto y la Ejecución de Obras de Hormigón en masa o armado. Comisión Permanente del Hormigón. Ministerio de Obras Públicas, Transportes y Medio Ambiente. Madrid, 1992.

[6] Working Group 'Design Examples' of FIP Commision 3. Meeting in Madrid, on 24th and 25th October 1997.

Background paper 7

Slender column with uniaxial bending

Part 1: Example

Part 2: Background to design methods for slender compression members

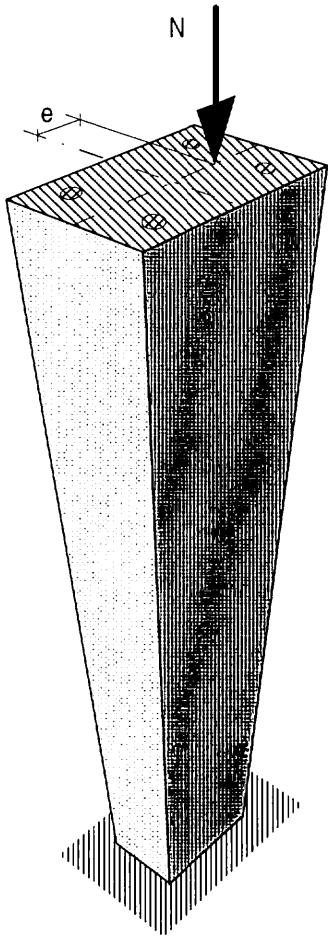

Bo Westerberg
Tyrens Byggkonsult AB
Stockholm, Sweden

Part 1: Example

1 Basic assumptions

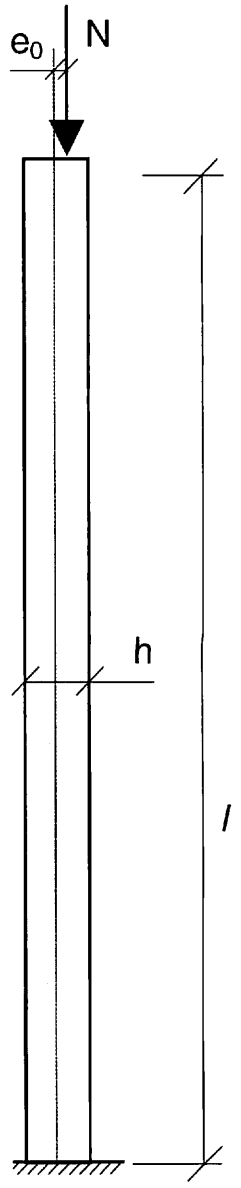

Figure 1: Geometry and loads

1.1 Geometry

Cantilever column with rectangular cross section, figure 1

l = **6,0 m**, b x h = **0,4 x 0,6 m**

Slenderness: $l_0/h = 2 \cdot 6{,}0 / 0{,}6 = 20 \Rightarrow \lambda = l_0 / i = 20 \cdot \sqrt{12} = \mathbf{69{,}3}$

1st order eccentricity: e_0 = 120 mm = **0,12 m** (incl. all imperfections)

1.2 Loads

Ultimate limit state (ULS):

Axial load: N_{Sd} = **1600 kN** (design value for one load combination)

First order moment: $M_{0Sd} = 1600 \cdot 0{,}12 =$ **192 kNm**

Serviceability limit state (SLS) (quasi-permanent load):

Axial load: N_{qp} = **800 kN**, first order moment: M_{0qp} = **96 kNm**

1.3 Material parameters

Concrete grade C35:

f_{ck} = 35 MPa, $f_{1cd} = 0{,}85 \cdot f_{ck} / 1{,}5 =$ **19,8 Mpa**

Note. All calculations in this example will be based on the uniaxial concrete compressive strength f_{1cd} according to equation 2.1 in FIP Recommendations

E_{cm} = **35 GPa**, $E_{cd} = 35 / 1{,}5 =$ **23,3 GPa**

$f_{ctk,min} = 0{,}7 \cdot 3{,}2 =$ **2,2 MPa**

Reinforcement:

f_{yk} = 500 MPa, $f_{yd} = 500/1{,}15 =$ **435 MPa**

$E_{sd} = E_{sk} =$ **200 GPa**

1.4 Creep

Basic creep ratio: φ = 2,0 is assumed

Effective creep ratio: $\varphi_{ef} = \varphi \cdot M_{0qp} / M_{0Sd} = 2 \cdot 96/192 =$ **1,0**[1]

[1]The effective creep ratio φ_{ef} is based on first order moments throughout this example. It *can* also be based on total moments including second order moments. This is less conservative, but would require iterations, since second order moments depend on creep. Such iterations will not be made here.

2 Resistance of cross section in ULS

For simplicity, the edge distance of the reinforcement is assumed to be t = 60 mm regardless of the area of the reinforcement, see figure 2. (In a real case, the edge distance used would depend on the diameter, number and placing of bars.)

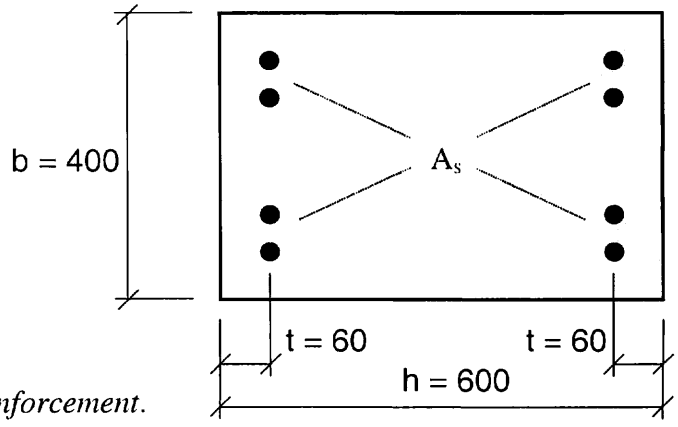

Figure 2: Cross section and reinforcement.

The resistance of the cross section to bending moment and axial force in ULS is shown in figure 3 for different values of the mechanical reinforcement ratio $\omega = A_s \cdot f_{yd}/bhf_{1cd}$. The moment capacity for axial force N_{Sd} = 1600 kN is plotted separately against the reinforcement ratio in figure 4. The relationship is practically linear, therefore a linear function has been given.

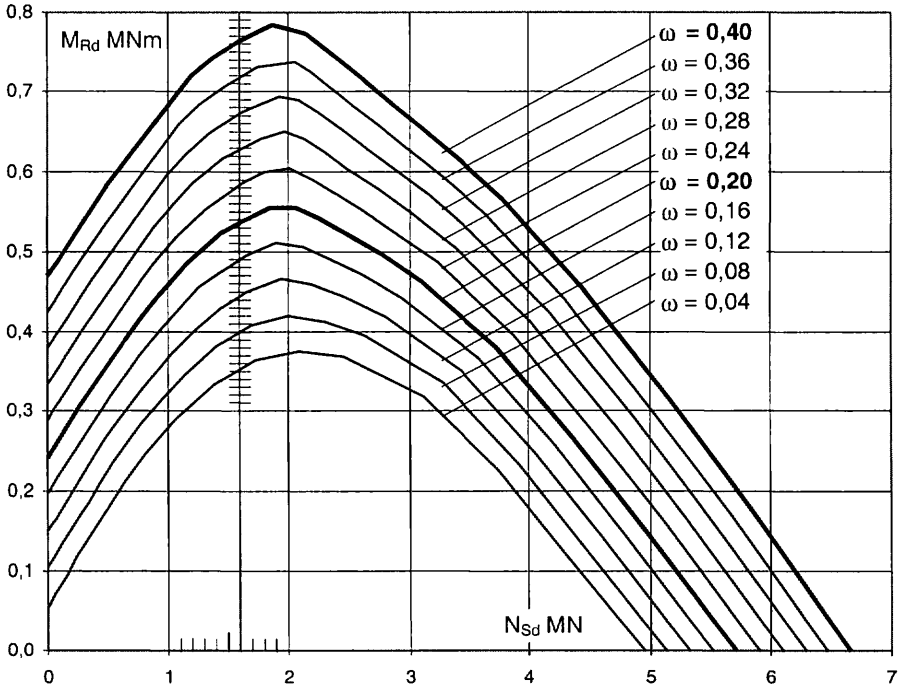

Figure 3: Interaction curves for cross section according to fig 2-2 with f_{1cd} = 19,8 MPa and f_{yd} = 435 MPa. All curves are based on t/h = 0,1, cf. figure 2

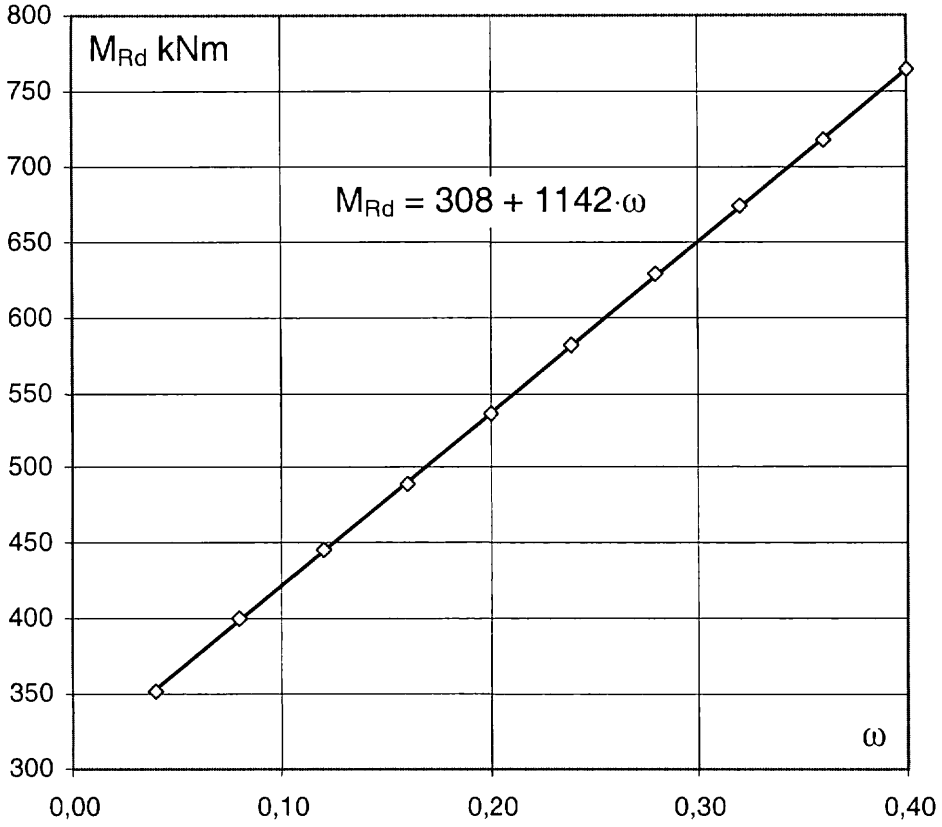

Figure 4: Moment capacity in ULS for N_{Sd} = 1600 kN as a function of ω.

3 Calculation methods for ULS

The following methods will be used and compared:

1. Method based on linear analysis with reduced stiffness (6.6.5)
2. Method based on curvature (6.6.6)
3. General method (6.6.1 (6))

3.1 Method based on stiffness and linear analysis

3.1.1 With stiffness according to 6.6.5 (6):

$EI = \alpha_\varphi \cdot \alpha_e \cdot E_c I_c + E_s I_s$

$E_c I_c = 23300 \cdot 0{,}4 \cdot 0{,}6^3/12 = 168$ MNm^2

$E_s I_s = 200000 \cdot A_s \cdot (0{,}6/2 - 0{,}06)^2 = 11520 \cdot A_s$ MNm^2 (with A_s in m^2)

If expressed in terms of the mechanical reinforcement ratio ω:

$A_s = \omega \cdot bhf_{1cd}/f_{yd} = \omega \cdot 0{,}4 \cdot 0{,}6 \cdot 19{,}8/435 = \omega \cdot 0{,}0109$

$E_s I_s = 11520 \cdot \omega \cdot 0{,}0109 = \omega \cdot 126$

The relative axial force is $\nu = N_{Sd}/(bdf_{1cd}) = 1{,}6/(0{,}4 \cdot 0{,}6 \cdot 19{,}8) = 0{,}336$

The calculation is shown in detail for an assumed value of $\omega = 0{,}1$:

$\alpha_\varphi = 1 - 0{,}8\varphi_{ef} \cdot (1 - \lambda/200) \cdot \omega^{0{,}25} = 1 - 0{,}8 \cdot 1{,}0 \cdot (1 - 69{,}3/200) \cdot 0{,}1^{0{,}25} = 0{,}706$

$\alpha_e = 0{,}08 \cdot \nu \cdot f_{1cd}{}^{0.6} \cdot e^{\lambda/100 - 2\omega} = 0{,}08 \cdot 0{,}336 \cdot 19{,}8^{0{,}6} \cdot e^{69{,}3/100 - 2 \cdot 0{,}1} = 0{,}264$

$EI = 0{,}706 \cdot 0{,}264 \cdot 168 + 126 \cdot 0{,}1 = 44{,}0\ \text{MNm}^2$

The critical load corresponding to this stiffness is

$N_{cr} = \pi^2 EI/l^2 = \pi^2 \cdot 44{,}0/12^2 = 3{,}01\ \text{MN}$

The design moment is calculated by means of the magnification factor, see Appendix, A.2.4:

$M_{Sd} = M_{0Sd} \cdot [1 + \beta / (N_{cr}/N_d - 1)]$

In this case the first order moment is constant. Then the following value of β should be used:

$\beta = \pi^2/8 = 1{,}234$

$M_{Sd} = 192 \cdot [1 + 1{,}234 / (3{,}01/1{,}6 - 1)] = \underline{460\ \text{kNm}}$

The moment capacity for $\omega = 0{,}1$ is, cf. figure 4:

$M_{Rd} = 308 + 1142 \cdot 0{,}1 = 422\ \text{kNm} < M_{Sd}$

Thus, the reinforcement ratio has to be somewhat increased. By iteration the reinforcement that gives $M_{Sd} = M_{Rd} = 450$ kNm is found to be

$\omega = \underline{0{,}124} \Rightarrow A_s = \omega \cdot bdf_{1cd}/f_{yd} = \underline{1357\ \text{mm}^2}$

3.1.2 Comparison with simplified stiffness method according to 6.6.5 (4)

Bending stiffness:

$EI = \alpha_\varphi \cdot \alpha_e \cdot E_c I_c + E_s I_s$ where $\alpha_e = 0{,}2$, $\alpha_\varphi = 1/(1+\varphi_{ef})$

Calculation is shown for $\omega = 0{,}2$:

$EI = 0{,}2 \cdot 168 / (1 + 1{,}0) + 126 \cdot 0{,}2 = 42{,}0\ \text{MNm}^2$

$N_{cr} = \pi^2 EI/l^2 = \pi^2 \cdot 42{,}0/12^2 = 2{,}88\ \text{MN}$

$M_{Sd} = 192 \cdot [1 + 1{,}234 / (2{,}88/1{,}6 - 1)] = \underline{488\ \text{kNm}} < M_{Rd} = 536$

The reinforcement can be reduced to the following amount, giving $M_{Sd} = M_{Rd} = 520$ kNm: $\omega = \underline{0{,}186} \Rightarrow A_s = \omega \cdot bdf_{cc}/f_{st} = \underline{2032\ \text{mm}^2}$

Thus, in this example the stiffness method with simple coefficients requires 50 % more reinforcement.

3.2 Method based on curvature

3.2.1 Curvature method according to 6.6.6 (7)

Estimated curvature:

$1/r = \alpha_\varphi \cdot \alpha_r \cdot 1/r_0$

$1/r_0 = 2 \cdot \varepsilon_{yd} / z_s$

$\varepsilon_{yd} = f_{yd}/E_{sd} = 435/200000 = 0{,}00217$

$z_s = 600 - 2 \cdot 60 = 480$ mm

$1/r_0 = 2 \cdot 0{,}00218/0{,}480 = 0{,}00906\ m^{-1}$

$\alpha_\varphi = 1 + (20/\lambda) \cdot \varphi_{ef} = 1 + (20/69{,}3) \cdot 1{,}0 = 1{,}289$

In order to calculate α_r the reinforcement ratio must be known. $\omega = 0{,}1$ is used in a first attempt:

$\nu_u = 1 + \omega = 1{,}1$

$\alpha_r = 2(1 - \nu/\nu_u) \cdot e^{-(1-\omega) \cdot \lambda/100} = 2 \cdot (1 - 0{,}336/1{,}1) \cdot e^{-(1-0{,}1) \cdot 0{,}693} = 0{,}744$

$1/r = 1{,}289 \cdot 0{,}745 \cdot 0{,}00906 = 0{,}00869\ m^{-1}$

Second order deflection and design moment:

$e_2 = (1/r) \cdot l^2/c$

With a constant first order moment c = 8 should be used, cf. 2.3.1.

$e_2 = 0{,}00869 \cdot 12^2/8 = 0{,}156$ m

$M_2 = N_{Sd} \cdot e_2 = 1600 \cdot 0{,}156 = 250$ kNm

The design moment is

$M_{Sd} = M_{0Sd} + M_2 = 192 + 250 = \underline{442\ kNm}$

This is more than the moment capacity $M_{Sd} = 422$ kNm for $\omega = 0{,}1$. The reinforcement must be increased to the following value, giving $M_{Sd} = M_{Rd} = 449$ kNm:

$\omega = \underline{0{,}123} \Rightarrow A_s = \omega \cdot bdf_{cc}/f_{st} = \underline{1348\ mm^2}$

3.2.2 Comparison with simplified curvature method according to 6.3.3.2 e)

Calculation is shown for $\omega = 0{,}2$:

$\alpha_\varphi = 1 + \varphi_{ef}/4 = 1 + 1{,}0/4 = 1{,}25$

$\alpha_r = (\nu_u - \nu) / (\nu_u - 0{,}4) = (1{,}2 - 0{,}336) / (1{,}2 - 0{,}4) = 1{,}08 \leq \underline{1{,}0}$

$1/r = \alpha_\varphi \cdot \alpha_r \cdot 1/r_0 = 1{,}25 \cdot 1{,}0 \cdot 0{,}00906 = 0{,}0113\ m^{-1}$

$e_2 = 0{,}0113 \cdot 12^2/8 = 0{,}204$ m

$M_2 = N \cdot e_2 = 1600 \cdot 0{,}204 = 326$ kNm

$M_{Sd} = M_0 + M_2 = 192 + 326 = \underline{518\ kNm} < M_{Rd} = 536$. The reinforcement can be reduced:

$M_{Sd} = M_{Rd} = 518$ kNm for $\omega = \underline{0{,}184} \Rightarrow A_s = \omega \cdot bdf_{cc}/f_{st} = \underline{2010\ mm^2}$

Thus, the simplified curvature method in this case gives 49 % more reinforcement than the improved version.

3.3 Comparison with general method

Calculations with the general method are based on a stress strain curve for the concrete according to 2.1.3.1 (2), i.e. MC90 2.1.4.4.1. All strain values are multiplied by 1 + φ_{ef} to take into account creep, see 6.6.1 (6). The curvature is determined for agreement with the axial force and the moment in 13 points along the column, and the deflection is calculated by numerical integration of the curvature, assuming linear variation between the points. The load capacity is found by varying the maximum curvature as an independent variable. The calculations are very extensive and can not be presented in detail.

The load capacity with a constant first order moment corresponding to $e_0 = 0{,}12$ m is calculated for different reinforcement ratios. The reinforcement ratio which gives a capacity equal to the actual load 1,6 MN is found to be

$$\omega = 0{,}124 \Rightarrow A_s = \omega \cdot b d f_{1cd}/f_{st} = \underline{1354 \text{ mm}^2}$$

The required reinforcement ratio for N = 1,6 MN according to the different methods is summarized in table 2-1.

Table 2-1: Summary of results.

Method	Required reinforcement area, mm^2	
General method:	**1354**	**(100 %)**
Stiffness method in 6.6.5 (6) (improved)	1357	(+ 0 %)
in 6.6.5 (3) (simplified)	2032	(+50 %)
Curvature method in 6.6.6 (7) (improved)	1348	(- 0 %)
in 6.6.6 (6) (simplified)	2010	(+48 %)

The improved stiffness and curvature methods give results very close to the general method in this example. (The agreement is almost "too good"; one should not always expect such close agreement.)

The simplified versions of these methods, based on BBK 94 and EC2/MC0 respectively, give rather conservative results. They may be even more conservative in many cases, particularly for higher slenderness and/or smaller eccentricity.

See Part 2 for the background to the methods, references etc.

4 Concrete stress in SLS

The concrete stress under long-term load may have to be limited in order to avoid excessive creep deformations. A stress limit with regard to linear creep is given in 7.4.3 (2):

$$|\sigma_c| \le 0{,}45 \cdot f_{cm} = 0{,}45 \cdot (f_{ck} + 8) = 0{,}45 \cdot (35 + 8) = 19{,}4 \text{ MPa}$$

Cracking is considered if the stress exceeds the value according to 7.4.2 and 2.1.4 (4):

$$\sigma_c \le f_{ctk,0.05} \cdot (1 - \nu_t \cdot c_t/h) / (1 - c_t/h)$$

This stress limit will always be greater than $f_{ctk,0.05}$ in the case of a compressive axial force. Thus, if $\sigma_c \le f_{ctk,0.05} = 0{,}7 \cdot 3{,}2 = \underline{2{,}2 \text{ MPa}}$ no further check is necessary.

First the bending stiffness for *uncracked section* is calculated. The reinforcement is included and the modular ratio is based on the full creep coefficient $\varphi = 2$:

$\alpha = E_s/E_{ef} = (1 + \varphi) \cdot E_s/E_c = (1 + 2) \cdot 200 / 35 = 17{,}1$

$A_s = 6873 \text{ mm}^2$ (the area required in ULS according to general method)

$A = A_c + (\alpha - 1) \cdot A_s = 0{,}4 \cdot 0{,}6 + (17{,}1 - 1) \cdot 1354 \cdot 10^{-6} = 0{,}262 \text{ m}^2$

$I = I_c + (\alpha - 1) \cdot I_s = 0{,}4 \cdot 0{,}6^3/12 + (17{,}1 - 1) \cdot 1354 \cdot 10^{-6} \cdot (0{,}3 - 0{,}06)^2 = 0{,}00846 \text{ m}^4$

$EI = E_c \cdot I = 35000 \cdot 0{,}00846 = 296 \text{ MNm}^2$

The moment including second order is calculated in the same way as in ULS:

$N_{cr} = EI \cdot (\pi/l)^2 = 20{,}3 \text{ MN}$

$M = M_0[1 + 1{,}234/(N_{cr}/N - 1)] = 0{,}096 \cdot [1 + 1{,}234/(20{,}3/0{,}8 - 1)] = 0{,}101 \text{ MNm}$

$$\sigma_c = -\frac{N}{A} \pm \frac{M \cdot h/2}{I} = -\frac{0{,}8}{0{,}262} \pm \frac{0{,}101 \cdot 0{,}6/2}{0{,}00846} = \underline{-6{,}6} \text{ and } \underline{+0{,}5} \text{ MPa respectively}$$

The tensile stress is less than $f_{ctk,0.05}$. Thus, the cross section *is* uncracked and the compressive stress is far below the limiting value.

(If no tensile strength is considered, i.e. the cross section is assumed to be cracked, then the compressive stress becomes higher; however, still far below the limit. The calculation then involves an iteration, since the stiffness will depend on the stress distribution.)

Part 2: Background to design methods for slender compression members

1 General

The so called stiffness and curvature methods in FIP Recommendations (FIPR) are explained in detail in a report [1], which was prepared as a background document for both FIPR and HPC Design Handbook [2], where the same methods are included. This Appendix gives a shortened description of their background.

2 Calculation methods in FIP Recommendations

Three methods for the design/analysis with regard to second order effects are given in FIPR:

1. General method based on non-linar analysis (6.6.1 (6))
2. Simplified method based on linear analysis and reduced stiffness (6.6.5)
3. Simplified method based on estimation of curvature (6.6.6)

2.1 General method

The general method is an application of non-linear analysis, and it is described in detail in [3]. Extensive comparisons with tests were presented in [3], showing that the method is a reliable tool for predicting the behaviour of slender columns. Comparisons within the recently finished national Swedish research project *High Performance Concrete* indicate that this is true also for high strength concrete [4].

For non-linear analysis as a design tool, the safety format has been the subject of various proposals e.g. in connection with EC2 and MC90[2], see e.g. [5]. In the author's opinion, the only reasonable safety format, at least for second order analysis, is to use *design values of material parameters* for the limit state in question [6]. The correct design value of the load bearing capacity is then obtained as a direct result of the analysis, and no further factors are required. This format is in line with the general concept of partial safety factors, and has been taken for granted in FIPR 6.6.1 (6) (in other words, it is not explicitly mentioned). There appears to be no reason to use a different safety format only because the analysis is "non-linear".

The general method can be used for direct design applications, but its main application is probably to serve as a basis for simplified methods. The "stiffness" and "curvature methods" given in FIPR have been calibrated in this way.

[2] Eurocode 2 and CEB/FIP Model Code 90 respectively

2.2 Creep

The effective creep ratio φ_{ef} defined in 6.6.3 is inspired by BBK 94[3], although with a slightly different definition. Thus, φ_{ef} is here based on *bending moments*; the deflection is connected to the curvature, which is primarily influenced by bending moment. (In BBK 94 φ_{ef} is based on the concrete *compressive stress*, which may give an undue influence of the axial force on the curvature.)

In the general method, creep can be taken into account by multiplying all strains in the concrete stress strain diagram by $(1 + \varphi_{ef})$. In the simplified methods, φ_{ef} is explicitly included in the expressions for stiffness and curvature respectively.

2.3 Background to simplified methods

Methods based on stiffness or curvature exist in various simple forms in codes and handbooks, e.g. in BBK 94 and EC2/MC90 respectively. These methods are often very conservative, and the aim here has been to improve them in order to avoid unnecessary over-dimensioning.

The capacity of slender members can be illustrated in a diagram like Figure A-1, showing relationships between axial force and bending moment.

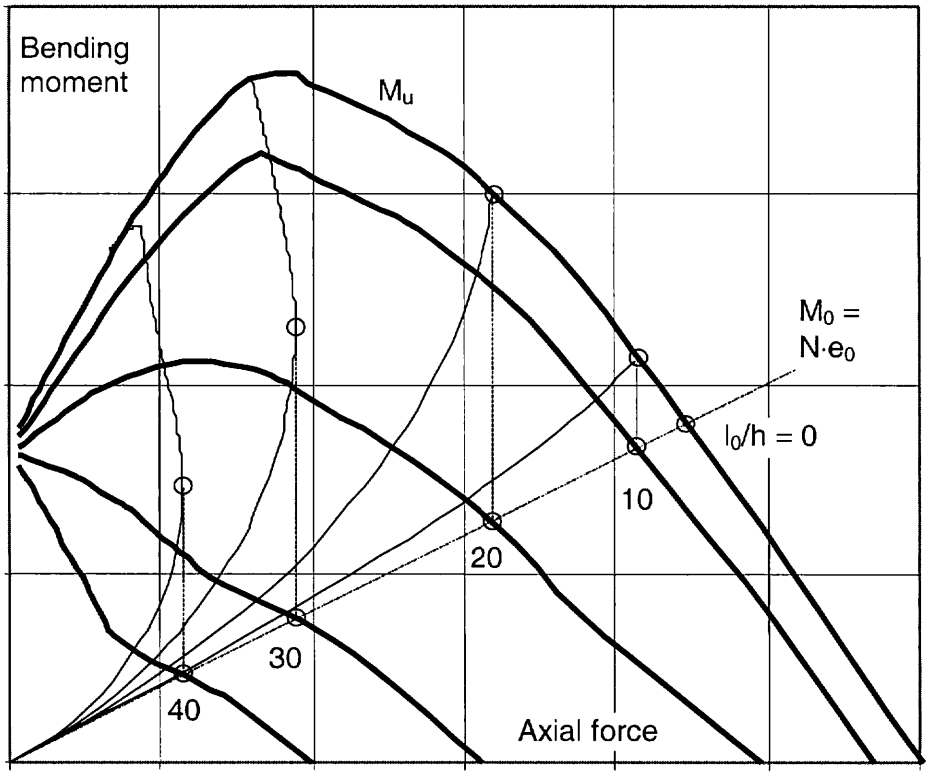

Figure A-1: Interaction curves for different slenderness ratios and a given mechanical reinforcement ratio. The curves are based on calculations with the general method

[3] The Swedish code for concrete structures

For slenderness $l_0/h = 0$, the interaction curve represents the *ultimate capacity of the cross section*. For slenderness > 0 the interaction curves represent the *maximum combination of axial force and first order moment.*

Note. The slenderness is here expressed as l_0/h for rectangular section. In the methods presented below, which are not restricted to rectangular sections, it will be expressed as l_0/i.

The thinner curves in figure A-1 show the total bending moment for an increasing axial force with a given first order eccentricity e_0. For slenderness = 0 this relationship is simply a straight line corresponding to the first order moment. For slenderness > 0 the relationship is non-linear, due to the additional second order moment caused by deflection.

For low and moderate slenderness ratios, the capacity of the member is limited by the *capacity of the cross section*, as for l_0/h = 10 and 20 in figure A-1. For higher slenderness ratios the maximum capacity of the *member* may be reached before the capacity of the cross section, as for l_0/h = 30 and 40 in figure A-1. This can be defined as a *stability failure.*

The interaction curves for different slenderness ratios are obtained by plotting the maximum axial force on the straight line for the first order moment, for different eccentricities.

The difference between total and first order moments (represented by vertical lines o-----o) is equal to the *second order moment.* For low and moderate slenderness, this second order moment is also equal to the difference between ultimate moment and first order moment:

$$M_2 = M_u - M_0 \qquad \text{(A-1)}$$

where:

M_u is the *ultimate moment capacity* of the cross section for a certain axial force N

M_0 is the *maximum first order moment* for same N and a certain slenderness

For higher slenderness ratios, l_0/h = 30 and 40 in figure A-1, the second order moment is less than M_2 according to equation (A-1), and then M_2 does not represent the "true" second order moment. However, it can be used for design purposes as a *nominal* second order moment, if it is defined to give a correct end result, when the cross section is designed for a design moment:

$$M_{Sd} = M_0 + M_2 \qquad \text{(A-2)}$$

The links between general and simplified methods are further explained below.

2.4 Stiffness method

In this method (FIPR 6.6.5) the nominal second order moment is determined by linear analysis. The design moment can then be expressed by means of a magnification factor:

$$M_{Sd} = M_0 \cdot \left(1 + \frac{\beta}{N_{cr} / N_{Sd} - 1} \right) \qquad \text{(A-3)}$$

where M_0 = first order moment
β = factor depending on the first order moment distribution, see below
N_{Sd} = design value of axial force
N_{cr} = nominal buckling load (l_0 = buckling length, EI = stiffness):

$$N_{cr} = \pi^2 EI / l_0^2 \qquad \text{(A-4)}$$

N_{cr} is a parameter, or symbol, in the above formulation of the design moment, based on a reduced stiffness influenced by cracking, creep and non-linear material behaviour. Thus, it is not a "true" buckling load, for which the stiffness should not be reduced by cracking and creep.

The factor β is defined as follows:

$$\beta = \pi^2 / c_0 \qquad \text{(A-5)}$$

where c_0 depends on the first order moment distribution, e.g. c_0 = 8 for constant moment, c_0 = 9,6 for parabolic distribution, c_0 = 12 for triangular distribution etc.

The expression for N_{cr} is inserted in expression (A-3), and the design moment is replaced by the cross section capacity M_u, to which it should be compared. The stiffness EI that would give the correct end result can then be found, if the correct values of M_u and M_0 are known:

$$EI = N \cdot \frac{l_0^2}{\pi^2} \cdot \left(1 + \frac{\beta}{M_u / M_0 - 1} \right) \qquad \text{(A-6)}$$

For design purposes a simple expression for the stiffness is needed. The following format has been chosen here:

$$EI = \alpha_\varphi \cdot \alpha_e \cdot E_c I_c + E_s I_s \qquad \text{(A-7)}$$

in which the coefficients α_φ and α_e can be calibrated for agreement with the "correct" value according to equation (A-6). See clause A.3.1.

2.5 Curvature method

In this method (FIPR 6.6.6) the nominal second order moment is estimated by means of a deflection or second order eccentricity e_2:

$$M_2 = N \cdot e_2 \qquad \text{(A-8)}$$

The second order eccentricity can be expressed in terms of a curvature 1/r and the buckling length l_0:

$$e_2 = \frac{1}{r} \cdot \frac{l_0^2}{c} \qquad \text{(A-9)}$$

By combining expressions (A-8) and (A-9), and assuming that correct values of M_u and M_0 are known, the proper value of the curvature can be found:

$$\frac{1}{r} = \frac{M_u - M_0}{N \cdot l_0^2 / c} \qquad \text{(A-10)}$$

In these expressions c (β in FIPR) depends on the curvature distribution. It is similar to c_0 in A.2.4, but c refers to the *total* curvature or moment whereas c_0 refers to the *first order* moment only. Examples: c = 8 if 1/r is constant, $c = \pi^2 \approx 10$ if 1/r is sinusoidal. See 6.6.6 (4).

Note. By substituting 1/r by M/EI, the link to the stiffness method can be found. Equation (A-3) can then be derived from (A-8) and (A-9), if 1/r is subdivided into parts corresponding to the first and second order moments M_0 and M_2, often having different distributions.
For design purposes the following simple format for estimating 1/r has been chosen:

$$\frac{1}{r} = \alpha_\varphi \cdot \alpha_r \cdot \frac{1}{r_0} \qquad \text{(A-11)}$$

where:

$$\frac{1}{r_0} = 2 \cdot \frac{\varepsilon_{yd}}{z_s}$$

$\varepsilon_{yd} = f_{yd} / E_s$

$z_s = 2 \cdot i_s$

i_s = the radius of gyration of the reinforcement area

The coefficients α_φ and α_r can be calibrated for agreement with the "correct" value according to equation (A-10). See clause A.3.2.

3 Calibration of simplified methods

3.1 Stiffness method

3.1.1 Stiffness factors

The formulation of stiffness in equation (A-7), with correction factors for the concrete term but not on the reinforcement term, has been taken from Swedish code BBK 94. Of course, other formulations are possible, for instance with a correction factor also on the reinforcement term. However, this would be more complicated and it is found that a function like equation (A-7) works quite well.

The simple factors in 6.6.5 (3)-(5) are taken from BBK 94. Improved values of α_φ and a_e in equation (A-7) can be derived from

$$\alpha_\varphi \cdot \alpha_e = (EI - E_s I_s) / E_c I_c \qquad \text{(A-12)}$$

where EI is obtained from equation (A-6) on the basis of calculations with the general method. a_e is first determined from calculations with $\varphi_{ef} = 0$, since α_φ should be = 1,0 in this case. Figure A-2 shows one example of a_e as a function of the relative axial force

$$\nu = N/A_c f_{1cd} \qquad \text{(A-13)}$$

for different values of the slenderness ratio l_e/h. The curves in figure A-2 are based on $f_{1cd} = 38{,}9$ (K100 ≈ C80), $f_{yd} = 362$ MPa, $\omega = A_s f_{st}/A_c f_{cc} = 0{,}2$ and $\varphi_{ef} = 0$. Design values are based on Swedish partial safety factors; see A.4.

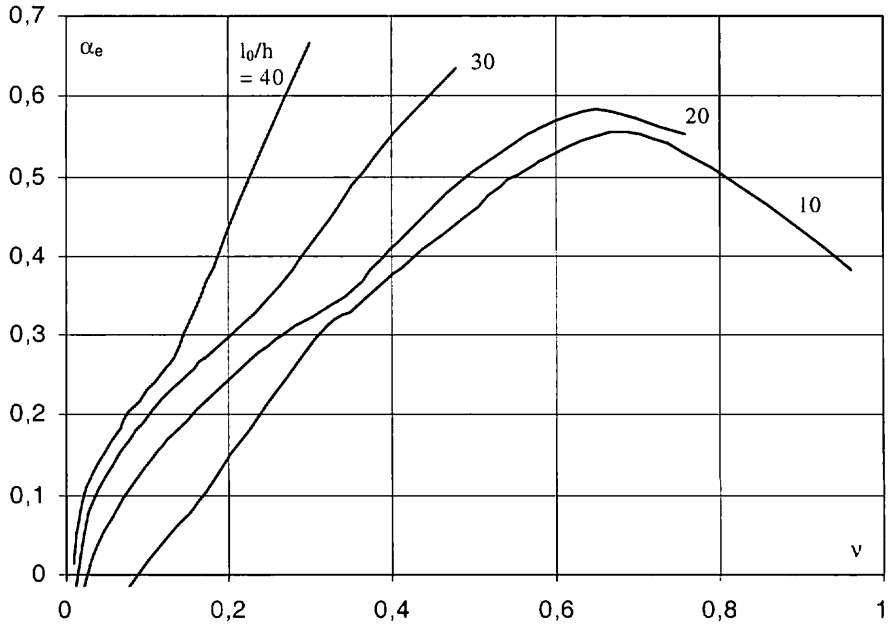

Figure A-2: Example of factor α_e in the stiffness derived "backwards" from calculations with the general method.

After testing different types of functions, the following expression for α_e has been found to give good agreement with the general method, also for other values of reinforcement ratio and concrete grade than those represented in figure A-2:

$$\alpha_e = 0{,}07 \cdot \nu \cdot f_{cc}^{0{,}6} \cdot e^{\lambda/100 \, - \, 2 \cdot \omega} \leq \nu_u - \nu \qquad \text{(A-14)}$$

where:

$\nu_u = N_u/A_c f_{cc} = (A_c f_{cc} + A_s f_{st})/A_c f_{cc} = 1 + \omega$

$\lambda = l_0/i$, slenderness ratio (= $\sqrt{12} \cdot l_0 / h$ for rectangular cross section)

Equation (A-14) is based on Swedish material parameters, see A.4. With material parameters according to EC2/MC90/FIPR, the constant **0,08** instead of 0,07 will give better agreement.

3.1.2 Comparison with general method

Interaction curves based on the reduced stiffness can be calculated, with the first order moment derived from equation (A-3):

$$M_0 = \frac{M_u}{1+\beta/(N_{cr}/N-1)} = \frac{M_u}{1+\dfrac{\beta}{\pi^2 EI/l_0^2 N-1}} \qquad \text{(A-15)}$$

where EI is the stiffness according to equation (A-11). Figure A-3 shows such interaction curves in comparison with curves according to the general method. Figure A-3 also includes curves where the reduced stiffness is calculated in the simpler way according to 6.6.5 (3) in FIPR.

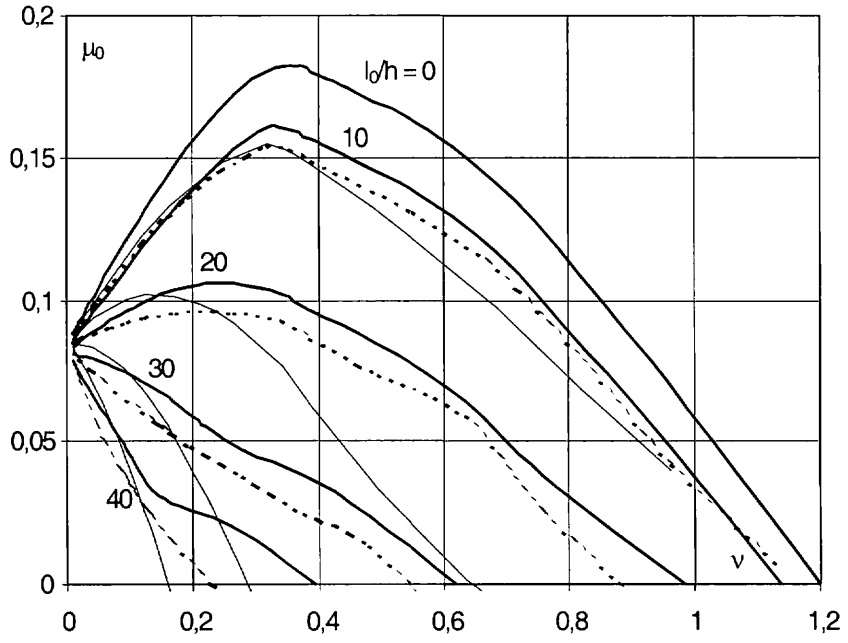

Figure A-3: Interaction curves for φ_{ef} = 0 calculated on the basis of a reduced stiffness (- - -) in comparison with curves according to the general method (——). For comparison, curves based on simplified stiffness factors according to FIPR 6.6.5 (3) are also included (—· —). Both N and M are expressed in relative terms: $\nu = N/(bhf1cd)$ and $\mu = M/(bh^2 f1cd)$.

Figure A-3 shows that the "improved" stiffness method gives results in good agreement with the general method. With the simple coefficients according to FIPR 6.6.5 (3), the result is very much on the safe side in many cases, particularly for moderate to high slenderness ratios in combination with a small eccentricity. For more extensive comparisons, see [1].

3.1.3 Taking into account creep

The next step is to find an expression for α_φ to take into account creep. Figure A-4 shows interaction curves for the same basic parameters as in figure A-3, except that they are based on an effective creep ratio $\varphi_{ef} = 2$. Figure A-5 shows the product of factors α_φ and α_e, cf equation (A-12), based on figure A-4.

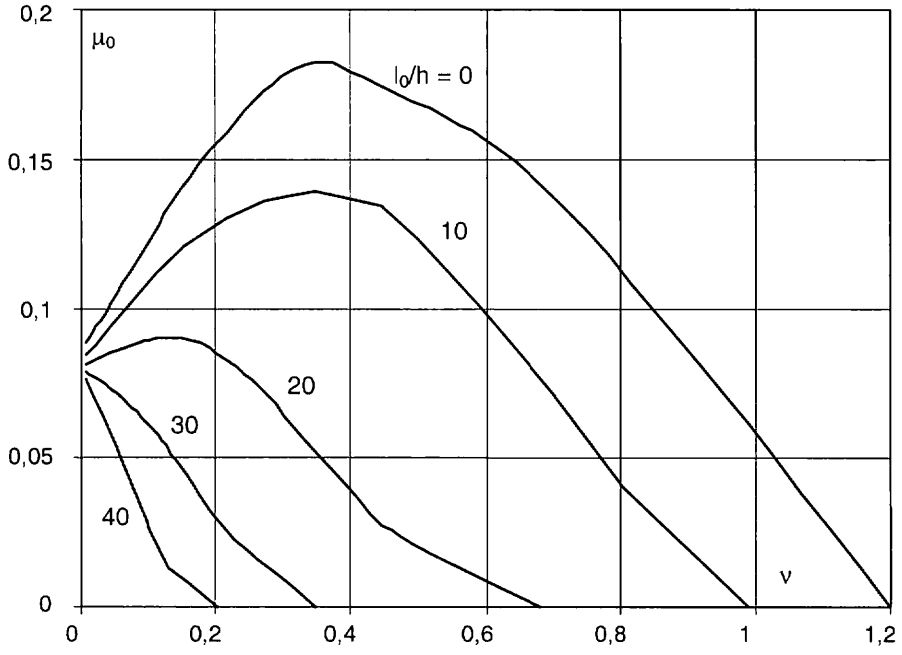

Figure A-4: Interaction curves for $\varphi_{ef} = 2$. ν and μ are relative axial force and moment resp.

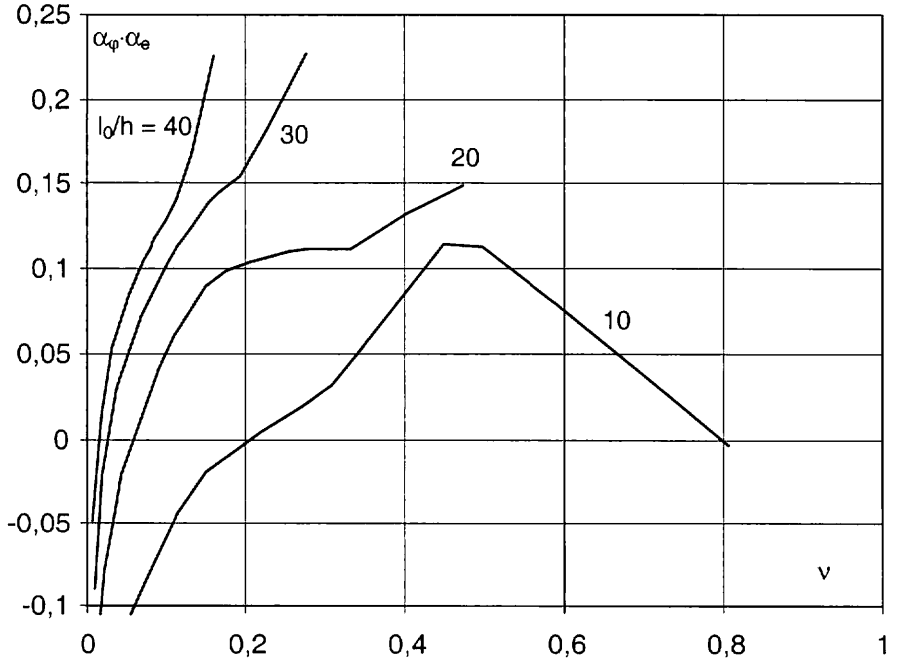

Figure A-5: Correction factors for stiffness based on interaction curves for $\varphi_{ef} = 2$.

Division of $\alpha_\varphi \cdot \alpha_e$ according to figure A-5 by α_e according to equation (A-14) provides the basis for factor α_φ. The following expression has been found to give acceptable results:

$$\alpha_\varphi = 1 - 0{,}8 \cdot \varphi_{ef} \cdot (1 - \lambda/200) \cdot \omega^{0{,}25} \qquad \text{(A-16)}$$

Figure A-6 shows the same comparison as figure A-3 but for $\varphi_{ef} = 2{,}0$. It should be kept in mind that this value of φ_{ef} is comparatively high; in many practical cases it is lower.

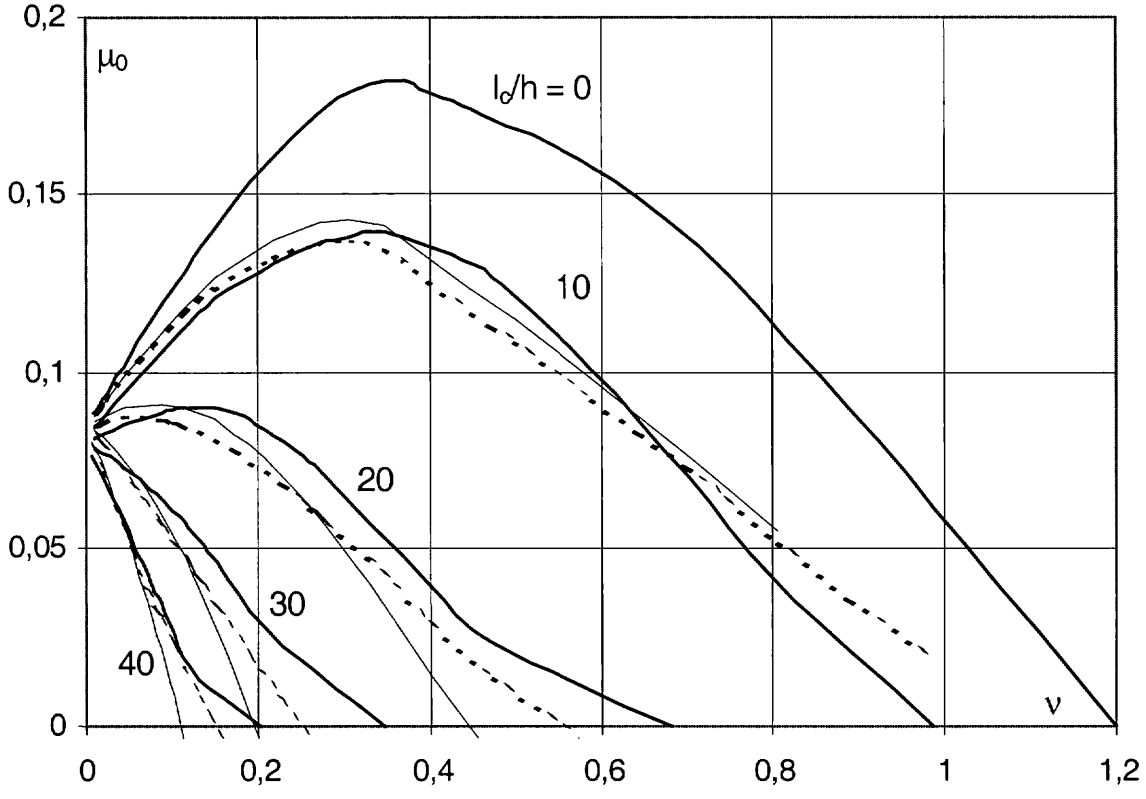

Figure A-6: Interaction curves for $\varphi_{ef} = 2{,}0$ calculated on the basis of a reduced stiffness (- -) in comparison with curves according to the general method (——). For comparison, curves based on stiffness factors according to FIPR 6.6.5 (3) are also included (— - —).

The agreement between the stiffness method and the general method is good. With this high effective creep ratio also the simplified coefficients according to 6.6.5 (3) give quite a good agreement. It could then be argued that it is not worth while to use the more complicated coefficients according to equations (A-14) and (A-16). However, this conclusion should not be drawn from just one example. Considering a wide range of values of slenderness, reinforcement ratio, concrete grade and creep coefficient, the improved coefficients generally give a much better agreement than the simple ones. See [1] for extensive comparisons between general and simplified methods.

3.2 Curvature method

Combining equations (A-10) and (A-11), the correction factors for curvature can be derived in the following way:

$$\alpha_\varphi \cdot \alpha_r = \frac{M_u - M_0}{N \cdot \frac{1}{r_0} \cdot \frac{l_c^2}{c}} \qquad \text{(A-17)}$$

The first step is to determine α_r based on calculations with $\varphi_{ef} = 0$, for which $\alpha_\varphi = 1{,}0$. Figure A-7 shows α_r as a function of relative axial force ν for different slenderness ratios, based on the interaction curves in figure A-1.

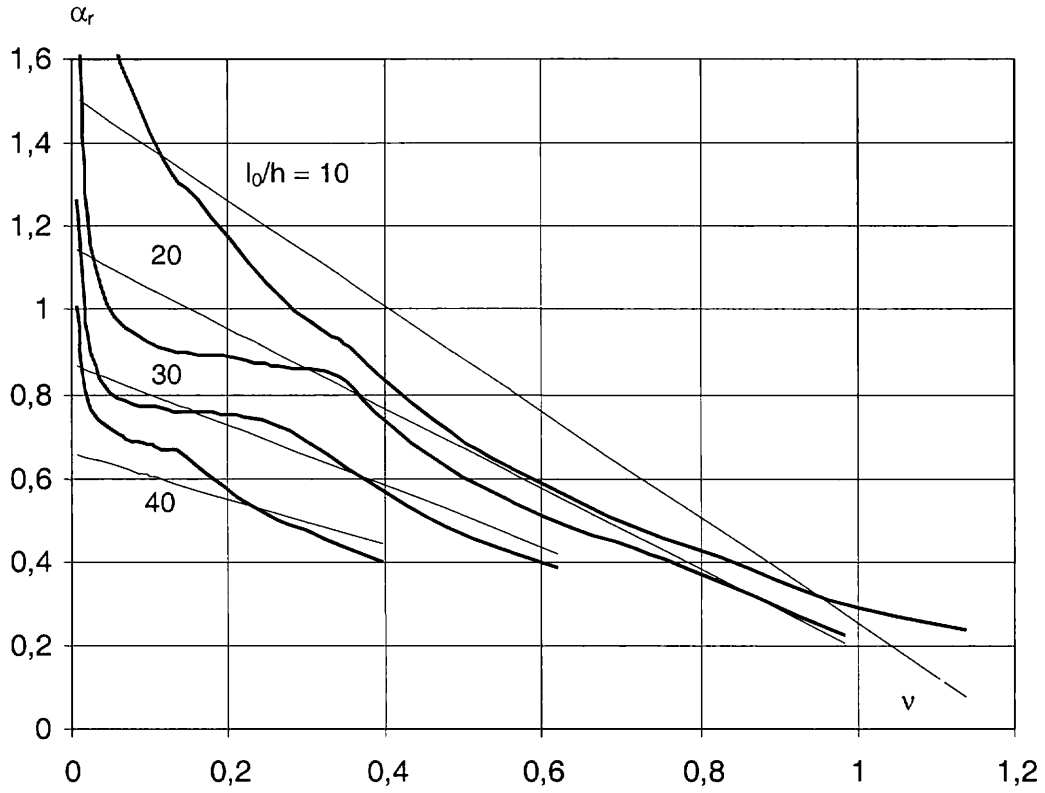

Figure A-7: Coefficient α_r derived from interaction curves for $\varphi_{ef} = 0$ according to figure A-1 (—). The dashed lines (- - -) are calculated according to equation (20).

The following expression has been found to be a good approximation of α_r, see figure A-7, also for other values of reinforcement ratio and concrete grade than those represented in the figure ($\omega = 0{,}2$ and concrete K100 $\approx$ C80):

$$\alpha_r = 2 \cdot (1 - \nu/\nu_u) \cdot e^{-(1 - \omega) \cdot \lambda/100} \qquad \text{(A-18)}$$

Interaction curves for $\varphi_{ef} = 0$ based on a curvature according to equations (A-11) and (A-18) are shown in figure A-8, together with curves according to the general method. The figure also includes curves with α_r according to 6.6.6 (6) in FIPR.

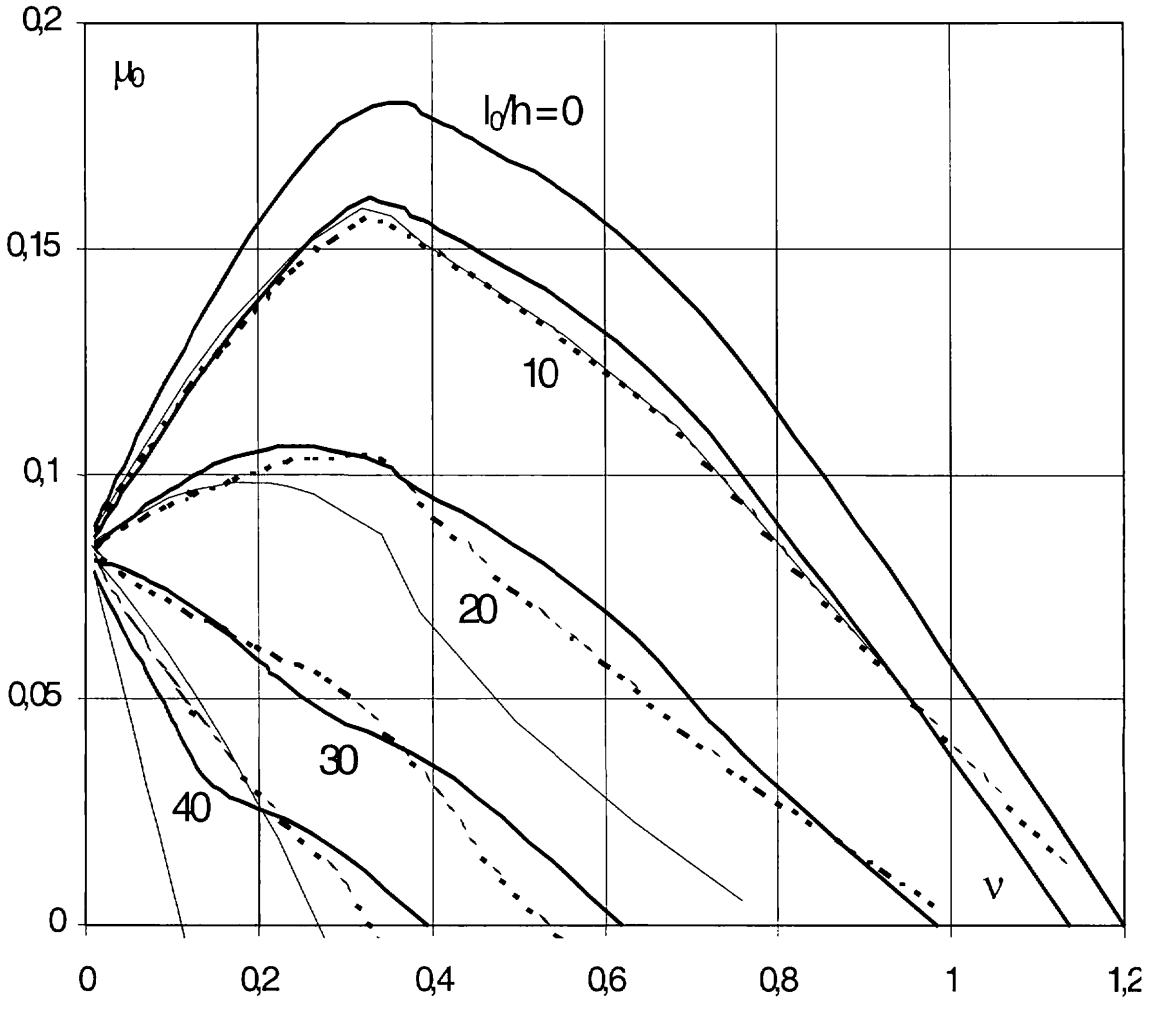

Figure A-8: Interaction curves for φ_{ef} = 0 calculated on the basis of an estimated curvature (- - -) in comparison with curves according to the general method (——). For comparison, curves based on simplified curvature factors according to FIPR 6.6.6 (5) are also included (— - —).

The "improved" curvature method gives results in good agreement with the general method, in most cases a bit on the safe side, in some cases slightly on the unsafe side, however within acceptable limits. With the simple coefficients according to FIPR 6.6.6 (5) the result is extremely conservative for high slenderness ratios, particularly in combination with a moderate to small eccentricity.

3.2.1 Taking into account creep

The next step is to find an expression for the coefficient α_φ to take into account creep. Figure A-9 shows the "correct" product of correction factors α_φ and α_r, cf equation (A-17), as a function of ν, based on figure A-4, i.e φ_{ef} = 2,0.

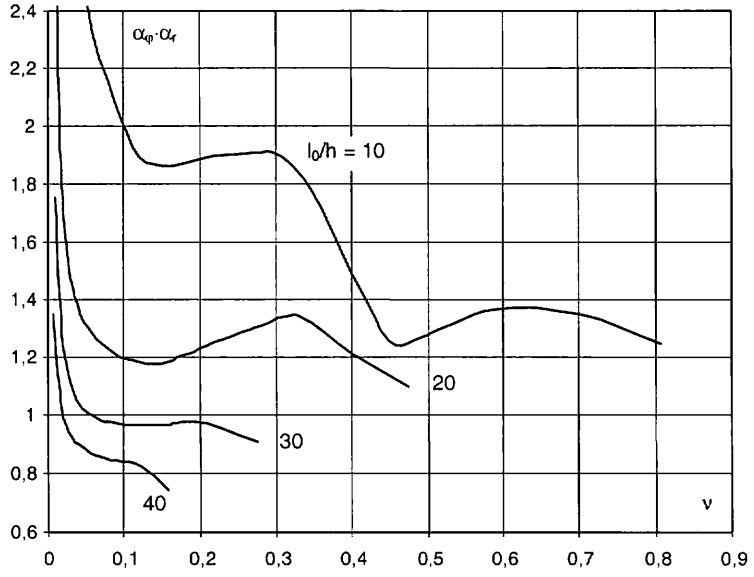

Figure A-9: Correction factors for curvature based on interaction curves for φ_{ef} = 2.

By dividing $\alpha_\varphi \cdot \alpha_r$ according to figure A-9 by α_r according to equation (A-18), values of α_φ can be found. After studying different values of reinforcement ratio and concrete grade, the following simple expression has been found to give acceptable results:

$$\alpha_\varphi = 1 + (20/\lambda) \cdot \varphi_{ef} \qquad \text{(A-19)}$$

Figure A-10 shows the same comparison as figure A-8 but with φ_{ef} = 2,0.

Figures A-9 and A-10 indicate that better agreement could have been obtained by making α_φ depending also on ν. However, such high values of φ_{ef} as 2,0 are rare in practical cases, and therefore equation (A-19) will give satisfactory agreement in most cases. See [1] for extensive comparisons.

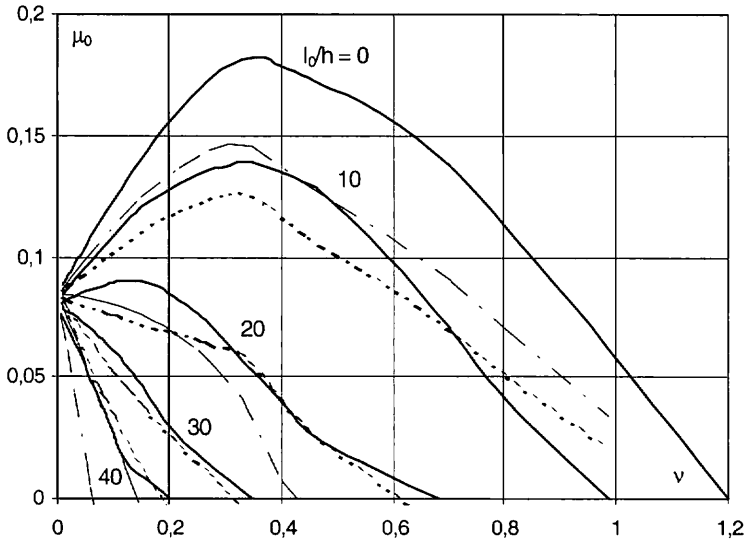

Figure A-10: Interaction curves for φ_{ef} = 2,0 calculated on the basis of curvature (- - -) in comparison with curves according to the general method (——). For comparison, curves based on simplified factors α_r and α_φ according to 6.6.6 (6) are also included (— · —).

4 Calibration calculations

In the calibration of the simplified methods along the principles described above, comparisons with the general method have been made for more than 3000 combinations of different concrete grades (C30 - C100), reinforcement ratios (ω = 0,1 - 0,4), slenderness ratios (l_0/i = 0 - 140, first order eccentricities (0 - ∞) or moments, creep coefficients (φ_{ef} = 0 - 2), cross sections (symmetric rectangular and circular) and first order moment distributions (constant and triangular). For further details, see [1].

Material parameters have mostly been according to the Swedish code and HPC Design Handbook, but parameters according to EC2, MC90 and FIPR have also been considered. The material factors are summarized below:

Factor	Parameter	Swedish code + HPC Handbook	EC2, MC90 and FIPR
γ_c	Concrete strength	$1{,}5 \cdot \gamma_n$	1,5
	Concrete modulus	$1{,}2 \cdot \gamma_n$	1,5
γ_s	Steel strength	$1{,}15 \cdot \gamma_n$	1,15
	Steel modulus	$1{,}05 \cdot \gamma_n$	1,0

γ_n is an additional factor used in Sweden, with values from 1,0 to 1,2 depending on the so called safety class. Since it is applied to all material parameters it does not affect the *relationship* between factors, and therefore it does not affect the calibration.

In EC2, MC90 and FIPR the concrete modulus has a higher factor, whereas the steel modulus has a lower factor, compared to the Swedish values. Despite this, it is found that the same stiffness and curvature coefficients can be used as those calibrated against calculations with Swedish safety factors, with one small exception: as mentioned before the agreement with the general method can be further improved by a slight adjustment of the expression for α_e in the stiffness method, changing the constant to 0,08 instead of 0,07.

In conclusion, the main restriction for the stiffness and curvature methods is that the cross section and reinforcement should be *symmetric*. Thus, different types of cross sections can be treated as long as this condition is fulfilled. Furthermore, the calibrations cover a wide range of concrete strengths, reinforment ratios, slenderness ratios, creep coefficients, first order eccentricities and moment distributions.

5 References

[1] Westerberg B: *Design Methods for Slender Concrete Columns*. Tyréns Technical Report 1997:1.

[2] *High Performance Concrete Structures - Design Handbook*. A handbook based on the national Swedish research project High Performance Concrete. A preliminary version was issued in October 1998. The final version will be published in the beginning of 1999.

[3] Westerberg B: Beräkning av slanka betongpelare med datamaskin *(Computerized Calculation of Slender Concrete Columns)*. Nordisk Betong 1:1971.

[4] Claeson, C: *Structural Behaviour of Reinforced High-strength Concrete Columns*. Chalmers University of Technology. Division of Concrete Structures. Publication 98:1. Göteborg 1998.

[5] CEB/FIP Bulletin 239, *Non-linear Analysis*. May 1997.

[6] Westerberg B: *Safety Format for Non-Linear Analysis*. Discussion paper in connection with the conversion of Eurocode 2 into an EN. Stockholm June 1998.

Background paper 8

Slender column with biaxial bending

Part 1: Example

Part 2: Background to design methods for biaxial bending

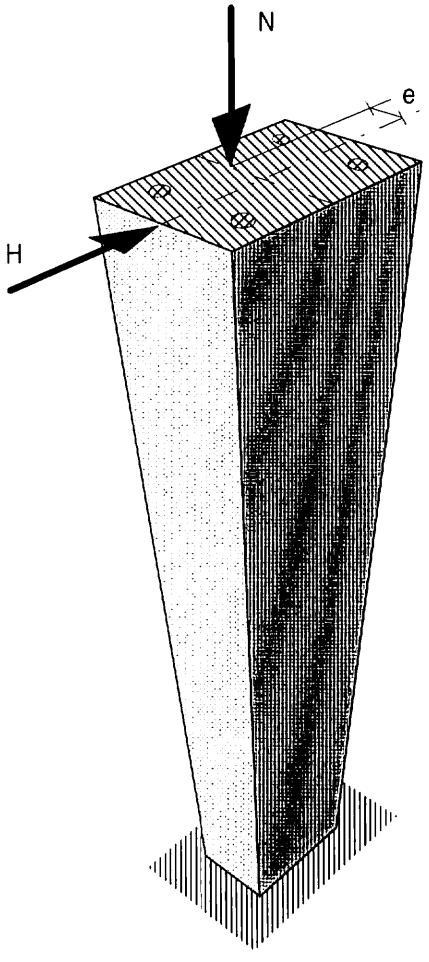

Bo Westerberg
Tyrens Byggkonsult AB
Stockholm, Sweden

Part 1: Example

1 Basic assumptions

1.1 Geometry

The example deals with a cantilever column with rectangular cross section and loading according to figure 1.

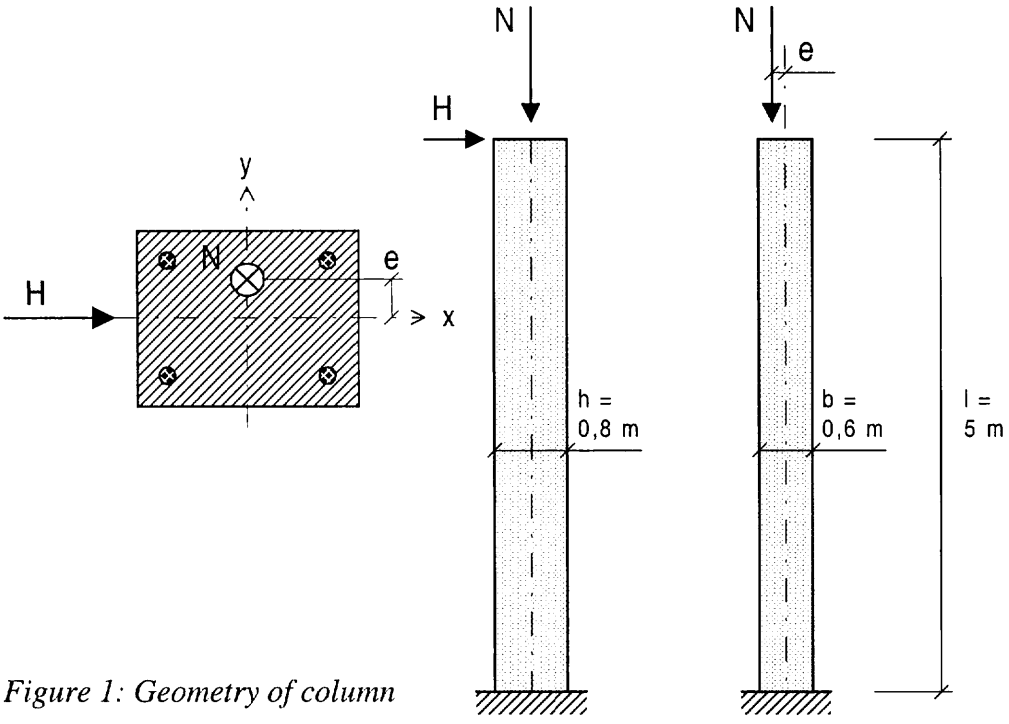

Figure 1: Geometry of column

1.2 Load values

ULS:

N_{Sd} = **2000 kN**, H_{Sd} = **150 kN**, e = **0,15 m**

$M_{0Sd,x} = H_{Sd} \cdot l = 100 \cdot 5 =$ **750 kNm**

$M_{0Sd,y} = N_{Sd} \cdot e = 2000 \cdot 0{,}15 =$ **300 kNm**

SLS (quasi-permanent):

N_{qp} = **1500 kN**, H_{qp} = **30 kN**, e = **0,15 m**

$M_{0qp,x} = H_{qp} \cdot l = 30 \cdot 5 =$ **150 kNm**

$M_{0qp,y} = N_{qp} \cdot e = 1500 \cdot 0{,}15 =$ **225 kNm**

Note. The example is schematic and primarily intended to show the application of design methods. Therefore, the effects of imperfections are assumed to be included in H and e respectively, and values of imperfections are not shown explicitly.

1.3 Material parameters

Concrete grade C35:

f_{ck} = 35 MPa, f_{1cd} = 0,85·35 / 1,5 = **19,8 MPa**

E_{cm} = **35 GPa**, E_{cd} = 35 / 1,5 = **23,3 GPa**

$f_{ctk,min}$ = 0,7·3,2 = **2,2 MPa**

Reinforcement:

f_{yk} = 500 MPa, f_{yd} = 500 / 1,15 = **435 MPa**

1.4 Creep

The basic creep ratio is assumed to be $\varphi = 3$. The effective creep ratio is calculated on the basis of first order moments, and will in this case be different for the x- and y-directions:

$\varphi_{ef,x} = (M_{0qx} / M_{0Sd,x})\cdot\varphi = (150 / 750)\cdot 3 = \mathbf{0,6}$

$\varphi_{ef,y} = (M_{0qy} / M_{0Sd,y})\cdot\varphi = (225 / 300)\cdot 3 = \mathbf{2,25}$

2 Resistance of cross section in ULS

Without going into the detailing of reinforcement, it is assumed that it is concentrated to the corners with a relative edge distance $t_x/h = t_y/b = 0,1$, regardless of the reinforcement area. The resistance of the cross section to axial force and bending moment can then be shown in one and the same interaction diagram, with relative parameters

$\nu = N / A_c f_{1cd}$ and $\mu = M / (hA_c f_{1cd})$ (for M_y use b instead of h)

See figure 2. The amount of reinforcement is expressed as a mechanical reinforcement ratio: $\omega = A_s f_{yd} / (A_c f_{1cd})$

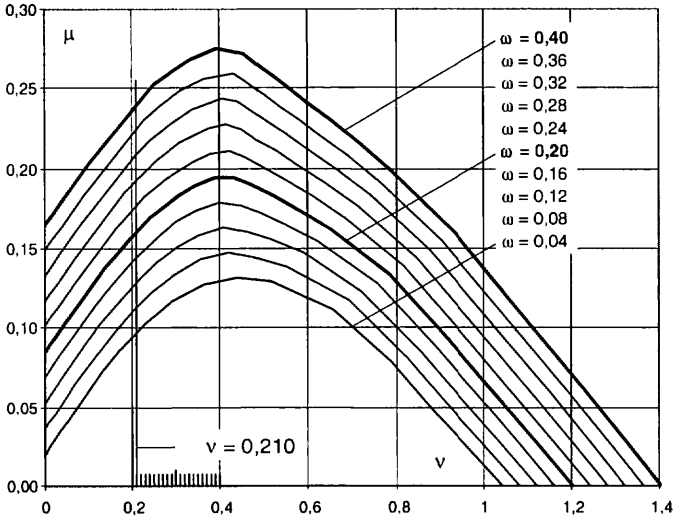

Figure 2: Resistance of cross section to axial force and bending moment, expressed in relative terms $\nu = N / (A_c f_{1cd})$ and $\mu = M / (hA_c f_{1cd})$.

The relative axial force is

$$\nu_{Sd} = N_{Sd} / (A_c f_{1cd}) = 2{,}0 / (0{,}48 \cdot 19{,}8) = 0{,}210$$

For this relative axial force the bending moment resistance can be expressed as a linear function of ω, cf figure 2:

$$\mu_{Rd} = 0{,}0815 + 0{,}3959 \cdot \omega$$

Now the full moment capacities M_{Rdx} and M_{Rdy} can be expressed:

$$M_{Rdx} = \mu_{Rd,x} \cdot h \cdot A_c \cdot f_{1cd} = \mu_{Rd,x} \cdot 0{,}8 \cdot 0{,}48 \cdot 19{,}8 \cdot 10^3 \text{ (kNm)} = \mu_{Rd,x} \cdot 7603 = 621 + 3015 \cdot \omega$$

$$M_{Rdy} = \mu_{Rd,y} \cdot b \cdot A_c \cdot f_{1cd} = \mu_{Rd,x} \cdot 0{,}6 \cdot 0{,}48 \cdot 19{,}8 \cdot 10^3 \text{ (kNm)} = \mu_{Rd,x} \cdot 5702 = 466 + 2261 \cdot \omega$$

3 Design in ULS

3.1 General

Design will be based on the interaction model in FIP Recommendations 6.6.7. Exponents *a* and *b* in equation (6.54) will be assumed to have the same value, $a = b = n$. In a first step $n = 1$ will be assumed, which is a simplification on the safe side. In the next step refined values of n according to Appendix will be used.

3.2 Interaction method with simple exponent n = 1

The practical design procedure according to clause A.3 in Appendix is followed here.

1. Calculate first order moments $M_{0Sd,x}$ and $M_{Sd,y}$ in the respective direction

$$M_{0Sd,x} = H_{Sd} \cdot l = 150 \cdot 5 = \mathbf{750\ kNm}$$

$$M_{0Sd,y} = N_{Sd} \cdot e = 2000 \cdot 0{,}15 = \mathbf{300\ kNm}$$

2. Calculate design moments M_{Sdx} and M_{Sd}, including nominal second order moments

For this the "stiffness method" according to 6.6.5 will be chosen. The design moment can then be determined by means of a magnification factor (see e.g. Appendix to column example 1):

$$M_{Sd} = M_{0Sd} \cdot [1 + \beta / (N_{cr}/N_{Sd} - 1)]$$

The mechanical reinforcement ratio is first estimated at $\omega = 0{,}2$.

x-direction:

Stiffness parameters:

$$E_c I_c = 23300 \cdot 0{,}6 \cdot 0{,}8^3 / 12 = 597 \text{ MNm}^2$$

$$E_s I_s = E_s \cdot A_s \cdot (h/2\text{-}t)^2 = E_s \cdot \omega \cdot (A_c f_{1cd}/f_{yd}) \cdot (h/2\text{-}t)^2$$
$$= 200000 \cdot \omega \cdot (0{,}48 \cdot 19{,}8/435) \cdot (0{,}8/2\text{-}0{,}08)^2$$

$E_sI_s = 448 \cdot \omega$

$\lambda = l_0/i = (l_0 / h) \cdot \sqrt{12} = (2{\cdot}5 / 0{,}8) \cdot \sqrt{12} = 43{,}3$

$\alpha_\varphi = 1 - 0{,}8 \cdot \varphi_{eff} \cdot (1 - \lambda/200) \cdot \omega^{0{,}25} = 1 - 0{,}8 \cdot 0{,}6 \cdot (1 - 43{,}3/200) \cdot 0{,}2^{0{,}25} = 0{,}749$

$\alpha_e = 0{,}08 \cdot \nu \cdot {f_{1cd}}^{0{,}6} \cdot e^{\lambda/100 - 2 \cdot \omega} = 0{,}08 \cdot 0{,}210 \cdot 19{,}8^{0{,}6} \cdot e^{43{,}3/100 - 2 \cdot 0{,}2} = 0{,}1043$

$EI = \alpha_\varphi \cdot \alpha_e \cdot E_cI_c + E_sI_s = 0{,}749 \cdot 0{,}1043 \cdot 597 + 0{,}2 \cdot 448 = 46{,}6 + 89{,}6 = 136 \text{ MNm}^2$

$N_{cr,x} = \pi^2 EI / {l_0}^2 = \pi^2 \cdot 136 / 10^2 = 13{,}4 \text{ MN}$

In this direction the first order moment has a triangular distribution. Then $\beta_x = \pi^2/12 = 0{,}822$.

$M_{Sd,x} = M_{0Sd,x} \cdot [1 + \beta_x / (N_{cr,x}/N_{Sd} - 1)] = 750 \cdot [1 + 0{,}822 / (13{,}4/2{,}0 - 1)] = \underline{858 \text{ kNm}}$

y-direction:

$E_cI_c = 23300 \cdot 0{,}8 \cdot 0{,}6^3 / 12 = 336 \text{ MNm}^2$

$E_sI_s = E_s \cdot A_s \cdot (h/2\text{-}t)^2 = 200000 \cdot \omega \cdot (0{,}48 \cdot 19{,}8/435) \cdot (0{,}6/2\text{-}0{,}06)^2 = 252 \cdot \omega$

$\lambda = l_0/i = (l_0 / b) \cdot \sqrt{12} = (2{\cdot}5 / 0{,}6) \cdot \sqrt{12} = 57{,}7$

$\alpha_\varphi = 1 - 0{,}8 \cdot \varphi_{eff} \cdot (1 - \lambda/200) \cdot \omega^{0{,}25} = 1 - 0{,}8 \cdot 2{,}25 \cdot (1 - 57{,}7/200) \cdot 0{,}2^{0{,}25} = 0{,}144$

$\alpha_e = 0{,}08 \cdot \nu \cdot {f_{1cd}}^{0{,}6} \cdot e^{\lambda/100 - 2 \cdot \omega} = 0{,}08 \cdot 0{,}210 \cdot 19{,}8^{0{,}6} \cdot e^{57{,}7/100 - 2 \cdot 0{,}2} = 0{,}1205$

$EI = \alpha_\varphi \cdot \alpha_e \cdot E_cI_c + E_sI_s = 0{,}144 \cdot 0{,}1205 \cdot 336 + 0{,}2 \cdot 252 = 5{,}8 + 50{,}4 = 56{,}3 \text{ MNm}^2$

$N_{cr,y} = \pi^2 EI / {l_0}^2 = \pi^2 \cdot 56{,}3 / 10^2 = 5{,}55 \text{ MN}$

In this direction the first order moment is constant. This gives $\beta_y = \pi^2/8 = 1{,}234$.

$M_{Sd,y} = M_{0Sd,y} \cdot [1 + \beta_x / (N_{cr,x}/N_{Sd} - 1)] = 300 \cdot [1 + 1{,}234 / (5{,}55/2{,}0 - 1)] = \underline{508 \text{ kNm}}$

3. Calculate magnified design moments M_{Sdx}/u and M_{Sdy}/v

Here u and v should satisfy the condition $u^n + v^n \leq 1$. In this case $n = 1$, thus $u + v \leq 1$.

In order to obtain the optimum result, where the moment capacities are fully utilized in both directions, u and v can be determined through a parameter m according to the Appendix. In a case like this, where the reinforcement is assumed to be concentrated to the corners with equal relative edge distances, the optimum result is then obtained directly.

$m = (M_{Sd,y}/M_{Sd,x}) \cdot (h/b) = (508/858) \cdot (0{,}8/0{,}6) = 0{,}790$

$u = (1 + m^n)^{-1/n} = (1 + 0{,}790^1)^{-1/1} = 0{,}559$

$v = m \cdot u = 0{,}441$ (check: $u + v = 1$)

$M_{Sd,x}/u = 858/0{,}559 = 1535 \text{ kNm}$

$M_{Sd,y}/v = 508/0{,}441 = 1152 \text{ kNm}$

4. Check moment resistances

The magnified design moments should be compared to the moment capacities for the assumed reinforcement ratio $\omega = 0{,}2$:

$M_{Rdx} = 621 + 3015 \cdot \omega = 1224$ kNm < 1535

$M_{Rdy} = 466 + 2261 \cdot \omega = 918$ kNm < 1152

Thus, reinforcement has to be increased. This requires an iteration. The next value of ω can be obtained in the following way:

$\omega_x = (1535 - 621) / 3015 = 0{,}303$

$\omega_y = (1152 - 466) / 2261 = 0{,}303$

Note. Due to the "optimum choice"of u and v we obtain the same result for both directions.

5. Repeat calculation from step 2 with new value of ω

After a few iterations the following end result is obtained:

$\omega = 0{,}271$	$A_s = \omega \cdot A_c \cdot f_{1cd} / f_{yd} = \underline{5920\ mm^2}$	
$M_{Sdx} = 839$ kNm	$M_{Sdy} = 448$ kNm	$m = 0{,}712$
$u = 0{,}584$	$v = 0{,}416$	
$M_{Sdx}/u = 1436$ kNm	$M_{Sdy}/v = 1077$ kNm	
$M_{Rdx} = 1438$ kNm	$M_{Rdy} = 1078$ kNm	

3.3 Interaction method with refined exponent

The exponent in the interaction formula are now determined according to the Appendix. The method in Appendix assumes one and the same value n for the two exponenets in 6.6.7:

$n = 1 + (0{,}5 - \alpha\rho) \cdot (1 + 0{,}006 \cdot \lambda) \geq 1{,}1$

where $\alpha = E_s / E_{ef}$, $E_{ef} = E_{cd} / (1+\varphi_{ef})$ and $\rho = A_s / A_c$

The calculation will be shown in detail for the reinforcement that gives the correct end result; previous steps are not shown. The required reinforcement is found to be

$\omega = \underline{0{,}21}$; $\rho = \omega \cdot f_{1cd} / f_{yd} = \underline{0{,}0096}$; $A_s = \rho \cdot A_c = \underline{4590\ mm^2}$

The calculation steps according to the Appendix are shown below.

2. Calculate design moments M_{Sdx} and M_{Sdy}, including nominal second order moments

x-direction:

$\alpha_\varphi = 1 - 0{,}8 \cdot \varphi_{eff} \cdot (1 - \lambda/200) \cdot \omega^{0{,}25} = 1 - 0{,}8 \cdot 0{,}6 \cdot (1 - 43{,}3/200) \cdot 0{,}21^{0{,}25} = 0{,}745$

$\alpha_e = 0{,}08 \cdot \nu \cdot f_{1cd}{}^{0{,}6} \cdot e^{\lambda/100 \cdot 2 \cdot \omega} = 0{,}08 \cdot 0{,}210 \cdot 19{,}8^{0{,}6} \cdot e^{43{,}3/100 \cdot 2 \cdot 0{,}21} = 0{,}1022$

$EI = \alpha_\varphi \cdot \alpha_e \cdot E_c I_c + E_s I_s = 0{,}745 \cdot 0{,}1022 \cdot 597 + 0{,}21 \cdot 448 = 45{,}5 + 94{,}6 = 140\ MNm^2$

$N_{cr,x} = \pi^2 EI / l_0^2 = \pi^2 \cdot 140 / 10^2 = 13{,}8\ MN$

$M_{Sd,x} = M_{0Sd,x} \cdot [1 + \beta_x / (N_{cr,x}/N_{Sd} - 1)] = 750 \cdot [1 + 0{,}822 / (13{,}8/2{,}0 - 1)] = \underline{855\ kNm}$

y-direction:

$\alpha_\varphi = 1 - 0{,}8 \cdot \varphi_{eff} \cdot (1 - \lambda/200) \cdot \omega^{0{,}25} = 1 - 0{,}8 \cdot 2{,}25 \cdot (1 - 57{,}7/200) \cdot 0{,}21^{0{,}25} = 0{,}133$

$\alpha_e = 0{,}08 \cdot \nu \cdot f_{1cd}{}^{0{,}6} \cdot e^{\lambda/100 \cdot 2 \cdot \omega} = 0{,}08 \cdot 0{,}210 \cdot 19{,}8^{0{,}6} \cdot e^{57{,}7/100 \cdot 2 \cdot 0{,}21} = 0{,}1181$

$EI = \alpha_\varphi \cdot \alpha_e \cdot E_c I_c + E_s I_s = 0{,}133 \cdot 0{,}1181 \cdot 336 + 0{,}21 \cdot 252 = 5{,}3 + 53{,}0 = 58{,}3\ MNm^2$

$N_{cr,y} = \pi^2 EI / l_0^2 = \pi^2 \cdot 58{,}3 / 10^2 = 5{,}75\ MN$

$M_{Sd,y} = M_{0Sd,y} \cdot [1 + \beta_x / (N_{cr,x}/N_{Sd} - 1)] = 300 \cdot [1 + 1{,}234 / (5{,}75/2{,}0 - 1)] = \underline{497\ kNm}$

3. Calculate magnified design moments M_{Sdx} / u and M_{Sdy} / v

Parameters u and v should satisfy $u^n + v^n \leq 1$. Exponent n is first calculated for each direction:

$n_x = 1 + [0{,}5 - (1 + 0{,}6) \cdot (200/23{,}3) \cdot 0{,}00963] \cdot (1 + 0{,}006 \cdot 43{,}3) = 1{,}46$

$n_y = 1 + [0{,}5 - (1 + 2{,}0) \cdot (200/23{,}3) \cdot 0{,}00963] \cdot (1 + 0{,}006 \cdot 57{,}7) = 1{,}31$

Either the lowest value is chosen, which is on the safe side, or a mean value:

$n = (n_x n_y)^{1/2} = \underline{1{,}39}$

Parameter m for optimum result:

$m = (M_{Sd,y}/M_{Sd,x}) \cdot (h/b) = (497/855) \cdot (0{,}8/0{,}6) = 0{,}776$

$u = (1 + m^n)^{-1/n} = (1 + 0{,}776^{1{,}39})^{-1/1{,}39} = 0{,}681$

$v = m \cdot u = 0{,}529$

$(u^n + v^n = 0{,}681^{1{,}39} + 0{,}529^{1{,}39} = 1{,}00)$

$M_{Sd,x}/u = 855/0{,}681 = \underline{1255\ kNm}$

$M_{Sd,y}/v = 497/0{,}529 = \underline{941\ kNm}$

4. Check moment resistances for $\omega = 0{,}21$

The magnified design moments are compared to the moment capacities for $\omega = 0{,}21$:

$M_{Rdx} = 621 + 3015 \cdot \omega = \underline{1254\ kNm} \approx M_{Sdx}$ / u OK

$M_{Rdy} = 466 + 2261 \cdot \omega = \underline{940\ kNm} \approx M_{Sdy}$ / v OK

No further calculation is necessary.

4. Comments

The calculation with the refined interaction exponent (in this case $n = 1{,}38$) gives $A_s = 4590\ mm^2$, whereas the simple exponent $n = 1$ gives $A_s = 5920\ mm^2$, about 30 % more. The difference is not dramatic in this example. However, under other circumstances the refined exponent n may have higher values, in which case the difference increases. This would be the case with lower load values and/or higher slenderness ratios. The physical background to this is explained in the Appendix.

If the reinforcement had not been concentrated to the corners with equal relative edge distances, then the optimum result result would not have been obtained directly. The parameter m can always be used for a first estimate of the magnification factors u and v, but corrections may have to be made in order to fully utilize the moment resistances in both directions, if considered worthwhile. It should be noted that any combination of u and v that fulfils the condition $u^n + v^n \leq 1$ is permissible, even if it might not be the optimum.

Part 2: Background to design methods for biaxial bending

This is a translation and adaptation of [1].

1 General

An accurate calculation of a slender column for bending in two principal directions is very complicated. It is complicated even for uniaxial bending, but in this case a further complicationis that bending in the two directions mutually affects the stiffness - and thus second order moments - as well as the ultimate moment capacity in the other direction.

Extensive non-linear biaxial calculations were made by the author in the mid 70's[1]. The calculations were based on the following assumptions:

- linear strain distribution
- the effect of torsion is negligible
- a curved stress-strain curve with a descending branch for the concrete
- elasto-plastic stress-strain diagram for the reinforcement
- the tensile strength of concrete is neglected
- rectangular cross section with the reinforcement concentrated to the corners

The corresponding method for uniaxial bending has been described in [2]. See also [3] about the so called "general method". Given the assumptions above, extending this method to biaxial bending is basically a mathematical problem. Therefore, reference [2] and [3] should suffice.

Figure 1 shows one example of results from the non-linear calculations, the load capacity as a function of the first order eccentricities in the respective direction for a certain value of slenderness, reinforcement ratio and creep (the latter is taken into account by means of different values for the concrete strain at maximum stress). In the calculations these parameters were varied within a wide range. Figure 1 is only one example of how to present the results; another possibility would be interaction curves for moment and axial force.

The amount of parameters involved (type of cross section, width to depth ratio, concrete strength, reinforcement strength, reinforcement ratio, creep coefficient, slenderness ratio, distribution of first order moment, boundary conditions etc) excludes the possibility of presenting a complete set of diagrams - this is not practicable even for slender columns in uniaxial bending.

The alternative is to use the non-linear calculations as a basis for a simplified procedure, in which the design can be brought back to current methods for uniaxial bending in each direction. In the following an interaction procedure is presented, which

[1] These calculations were never published, but they were later used as a basis for the method included in [1].

takes into account the non-linear nature of the problem in an empirical way, based on the above mentioned calculations.

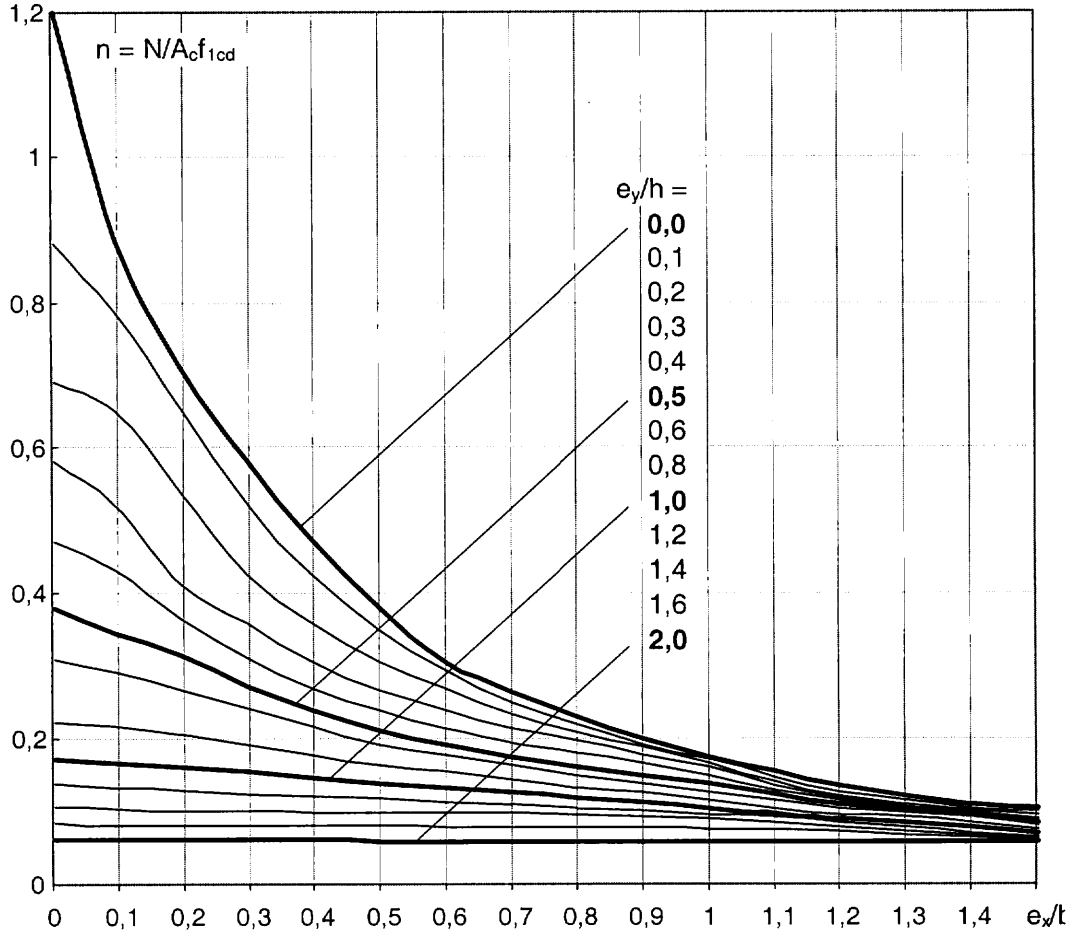

Figure 1 Example of diagram over the load capacity as a function of the first order eccentricities in the respective direction. l_0/h = 10, b/h = 1,0, ω = 0,3.

2 Basic principles

The design method is based on checking the combined effect of bending in the two principal directions by means of an interaction formula. It is also based on the use of some practical design method for uniaxial bending, in which the stability check is transferred to an ultimate moment check, including a nominal second order moment (see the Appendix in example 1).

The following condition should be fulfilled in the design (FIP Recommendations 6.6.7 indicates the possibility of having two different exponents, but here one and the same exponent n will be used for both directions):

$$\left(\frac{M_{Sdx}}{M_{Rdx}}\right)^n + \left(\frac{M_{Sdy}}{M_{Rdy}}\right)^n \leq 1 \qquad (1)$$

where M_{Sdx} = design moment in x-direction, including nominal 2nd order moment

M_{Rdx} = uniaxial moment capacity in x-direction

M_{Sdy} = design moment in y-direction, including nominal 2nd order moment

M_{Rdy} = uniaxial moment capacity in y-direction

The exponent *n* accounts for the influence of bending in one direction on the capacity and stiffness for bending in the other direction. For a high reinforcement ratio combined with a small slenderness, the non-linear properties of concrete and reinforcement will come into play, in which case bending in the two directions will have a strong mutual influence on each other. Then the exponent should have a low value. For a low reinforcement ratio combined with a high slenderness, on the other hand, the strains will mainly stay in the elastic range, in which case this influence is less. Then the exponent should have a high value.

These circumstances are taken into account in the following empirical expression for *n*, based on comparisons with non-linear calculations according to the general method:

$$n = 1 + (0{,}5 - \alpha\rho)\cdot(1 + 0{,}006\cdot\lambda) \geq 1{,}1 \qquad (2)$$

where λ = l_0/i = slenderness ratio

l_0 = buckling length in the respective direction

i = radius of gyration in the respective direction

α = $E_{sd}\cdot(1 + \varphi_{ef}) / E_{cd}$

E_{sd} = design value of steel modulus

E_{cd} = design value of concrete modulus

φ_{ef} = effective creep ratio for the respective direction

ρ = A_s/A_c

A_s = total area of reinforcement

A_c = area of concrete cross section

Normally there will be different values of λ and φ_{ef} in the two principal directions. Then one can either conservatively choose the lower of the two *n*-values, or a mean value

$$n = (n_x n_y)^{1/2} \qquad (3)$$

3 Practical design procedure

The following procedure is suitable in practical design, either to determine the necessary reinforcement for a given cross section, or to check the capacity for a given reinforcement.

1. *Calculate first order moments M_{0x} and M_{0y} in the respective direction*

2. *Calculate design moments M_{Sdx} and M_{Sdy}, including nominal second order moments*

   This can be done according to some current method, eg. the "curvature method" or the "stiffness method" in the FIP Recommendations. Like in the design for uniaxial bending with these methods, a first estimate of the reinforcement has to be made.

Other methods can be used, if based on nominal design moments compatible with the ultimate section capacity.

3. *Calculate magnified design moments M_{Sdx}/u and M_{Sdy}/v*

   The "magnification factors" u and v should satisfy the following condition, corresponding to equation (1):

   $$u^n + v^n \leq 1 \qquad (4)$$

   with n according to eq. (3). When reinforcement is not known, n = 1,5 can be used on trial.

   In principle, the choice of u and v is arbitrary within the limits of eq. (4), but the following choice is optimal under certain conditions (see comments under *4.* below):

   $$u = (1 + m^n)^{-1/n} \qquad (5)$$

   $$v = m \cdot u \qquad (6)$$

   where $m = (M_{Sdy} / M_{Sdx}) \cdot (h / b)$
   h = is the cross section dimension in direction x
   b = is the cross section dimension in direction y

4. *Check the uniaxial moment resistances M_{Rdx} and M_{Rdy} against moments M_{Sdx}/u and M_{Sdy}/v, separately for each direction. If necessary, change the reinforcement*

   If *u* and *v* have been determined according to eq. (5)-(6), and if the reinforcement is concentrated to the corners with about the same relative edge distance, then only one direction has to considered here, since the parameter *m* is based on the condition that the magnified moments should require the same amount of reinforcement for each direction.

   For other conditions of cross section, this way to determine *u* and *v* may not lead directly to the optimum result. Then, either the reinforcement is determined for each direction and the highest amount is chosen, which is conservative, or a few iteration steps are made with different sets of *u* and *v* values in order to optimize the result.

5. *Repeat the calculation from step 2*

   The new reinforcement obtained in step 4 may change 2nd order moments and exponent *n*, which may necessitate further iteration.

4 References

[1] Westerberg B. *Design of concrete columns with regard to biaxial bending.* (In Swedish). Clause 6.3:47 in Betonghandbok - Konstruktion (Concrete handbook - Design). 1990

[2 Westerberg B. *Computerized calculation of slender concrete columns.* (In Swedish). Nordisk Betong nr 4, 1971.

[3] Westerberg B. *Design Methods for Slender Concrete Columns.* Background to design methods given in HPC Design Handbook and FIP Recommendations. Tyréns Technical Report 1997:1.

Background paper 9

Interface between old and new concrete

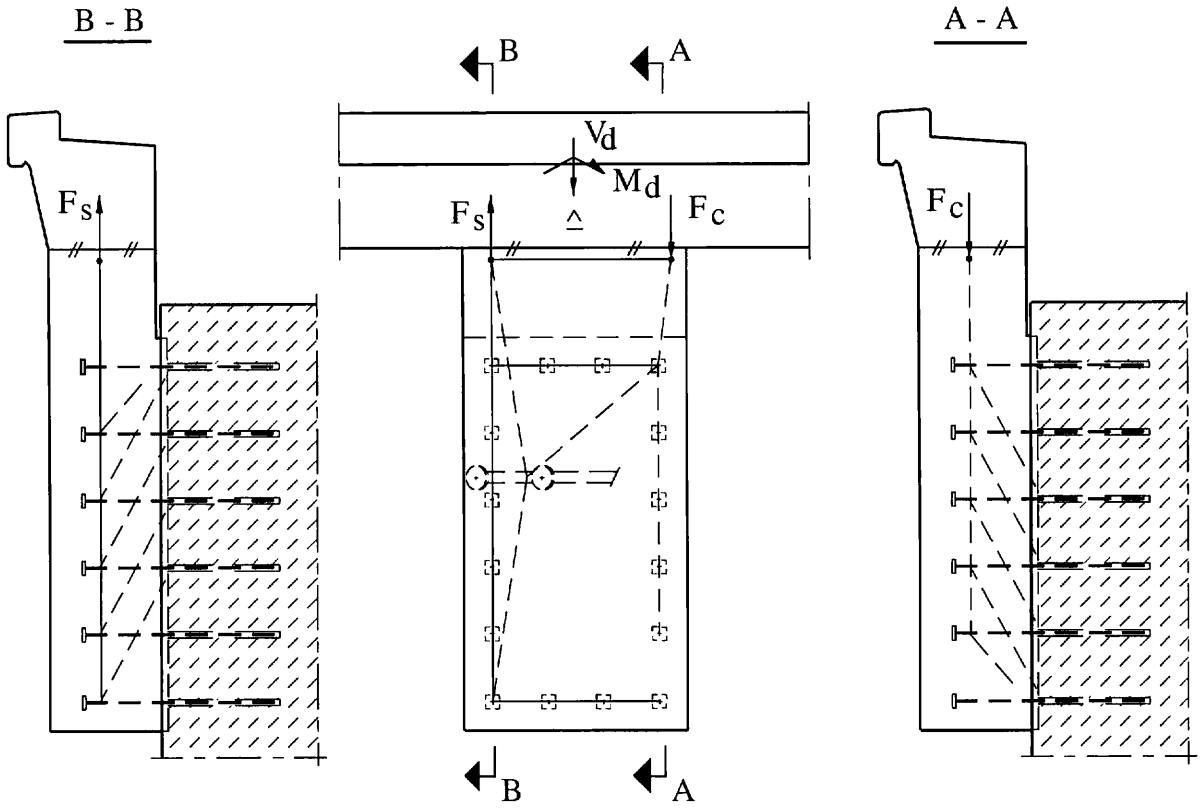

Jouni Rissanen

Pontek Oy, Consulting Engineers
Espoo, Finland

Summary

In this example transfer of loads from an enlargement structure of a small archbridge across the construction (shear) joint to an old structure is studied. A strut and tie model is developed to illustrate the path of forces and to dimension the reinforcement of a new structure.

1 Introduction

In conjuction with making a main road broader a small arch bridge was enlarged.

The bridge is located in southern Finland. (Fig. 1)

The bridge is a reinforced concrete arch bridge. Its' horizontal clearance is 3.00 m and the effective width of the deck is 8.00 m. The skewness of the bridge is 30□.

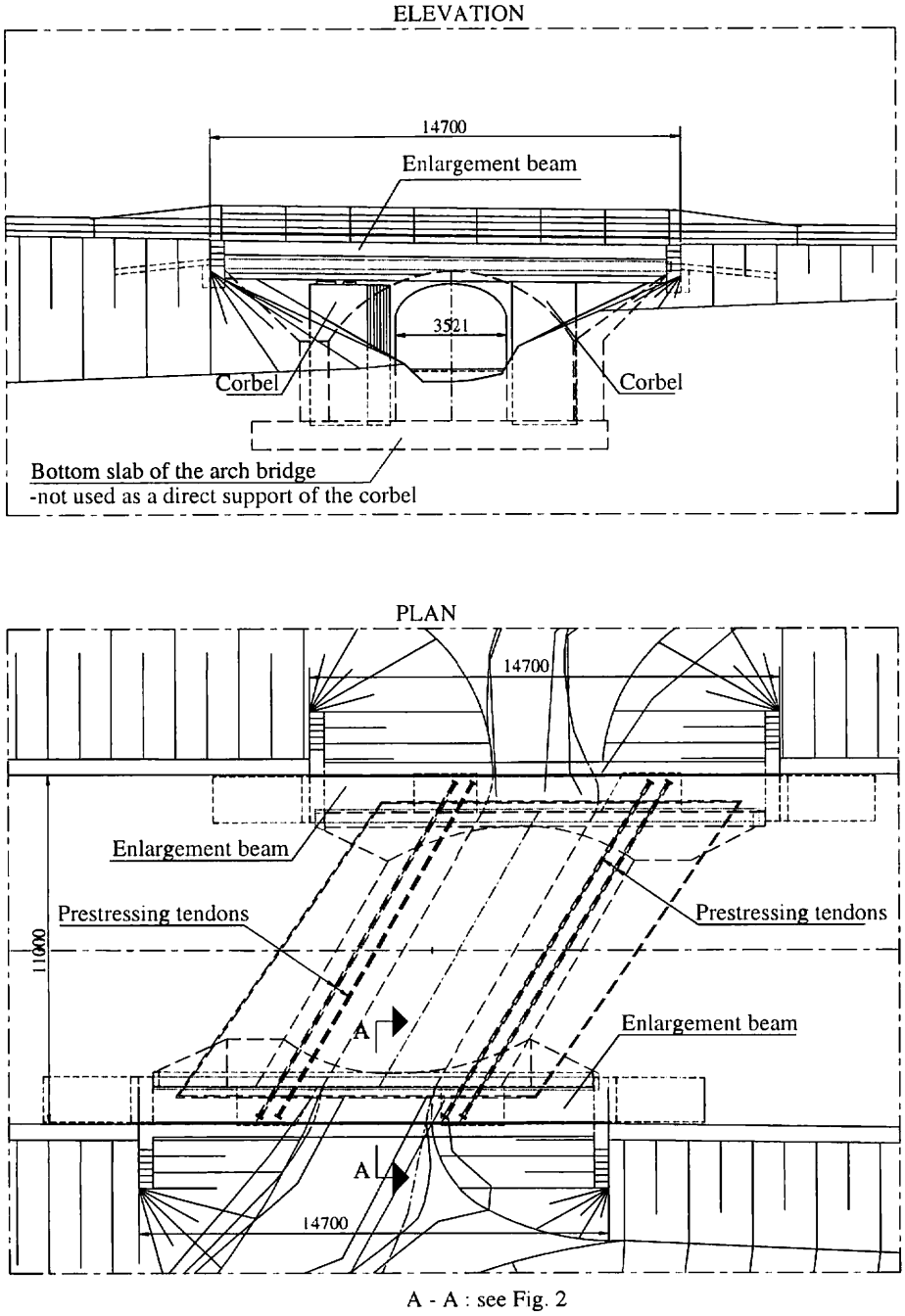

Fig. 1: The arch bridge and it's enlargement structures

The enlargement structure consists of two reinforced concrete cantilever beams, one an each side of the bridge. Both beams are supported by two supports. The spans of the beams are (3.60) + 5.84 + (3.26) m and the total length is 14.70 m. The increase of the effective width of the deck is 2 x 1.50 m being totally 11.00 m after the construction works.

The supports of the enlargement beams are sort of reinforced concrete corbels. They were cast against the faces of the old arch and anchored to it by prestressing tendons and reinforcing bars. Prestressing tendons were placed in holes (ø100 mm) which were drilled through the walls of the arch from one side of the road to the other, about 10 m distance. The surface of the old structure was roughened before casting the corbels.

In this example the transfer of the loads from an enlargement beam into one of the corbels and across the construction (shear) joint into the old structure is studied. A strut and tie model is developed to illustrate the path of the forces.

This problem of anchoring a new concrete member to the old one is one of the most often encountered in the reparation and strengthening works of the old concrete structures.

2 Design information

2.1 Intended use of structure

A member of an enlargement structure of an old arch bridge.

2.2 Materials and their design parameters

Concrete: - Arch bridge C20
(FIP Recommendations (Rec.) 2.1) $f_{ck} = 20$ MPa
$f_{ctm} = 2.2$ MPa
$f_{1cd} = f_{ctk}/\gamma_c = 0.85 \times 20 / 1.50 = 11.3$ MPa

- Corbel C30
$f_{ck} = 30$ MPa
$f_{ctm} = 2.9$ MPa
$f_{1cd} = 0.85 \times 30 / 1.50 = 17.0$ MPa

Reinforcing steel: S500
(Rec. 2.2) $f_{yk} = 500$ MPa
$f_{yd} = f_{yk}/\gamma_s = 500 / 1.15 = 435$ MPa

Prestressing steel: St 1570/1770
(Rec. 2.3) $f_{ptk} = 1770$ MPa
$f_{ptd} = 0.90 \times f_{ptk}/\gamma_s = 0.90 \times 1770/1.15 = 1385$ MPa

2.3 Main Loads

Permanent actions:	- an enlargement beam and a corbel, surfacing, prestress
Variable actions:	- vertical traffic load, breaking of the vehicles, uneven temperature

3 The ULS and SLS verifications in the interface

3.1 The structure and the loads

The size of the rectangular corbel is 4.30 x 2.00 x 1.00 m^3 and the area of the construction joint, the interface is 3.50 x 2.00 m^2 (Fig. 2)

The main loads from the enlargement beam are the vertical load V and the bending moment M that acts in the parallel plane with the construction joint. These loads result primarily shear in the interface.

The line of prestressing tendons form an angle of 60° with the plane of the joint. Therefore the prestressing load P has two components, perpendicular to and parallel with the plane of the construction joint.

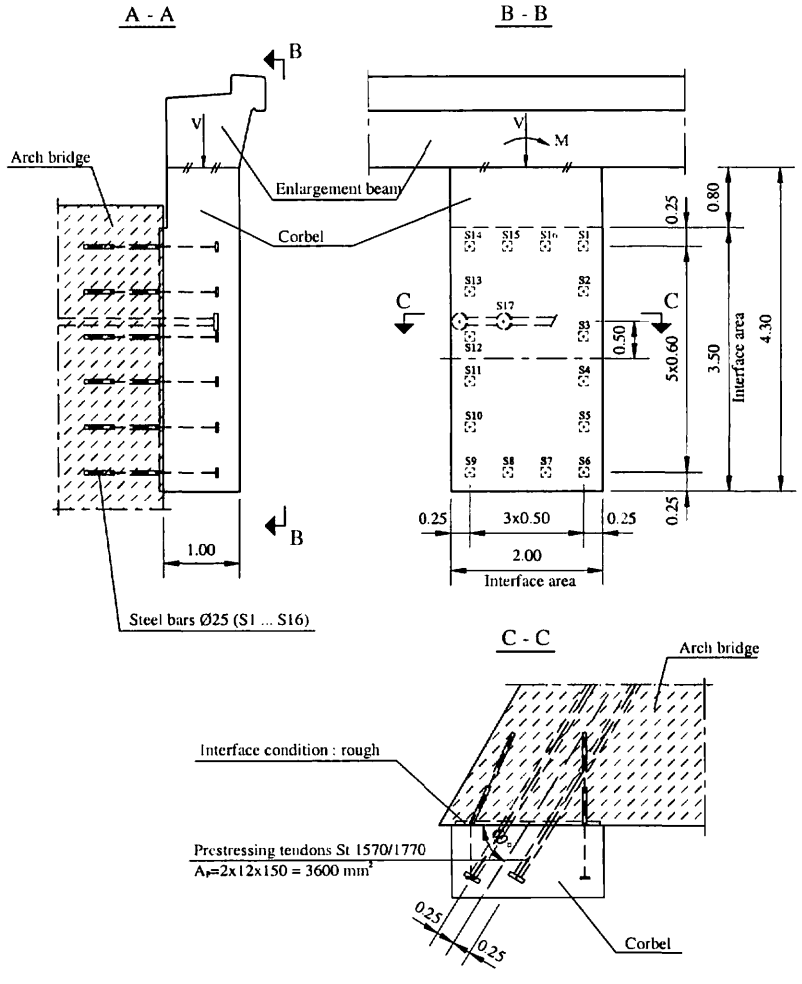

Fig. 2: The concrete corbel

3.2 Check of the maximum shear stress (ULS)

The maximum shear stress to be transferred across the interface is
$\tau_{fd} = 0.25 \times f_{1cd} = 0.25 \times 11.3 = 2.8$ MPa (Equ 5.17 in Rec.)

The distribution of the effects of the torsion and the shear force to the interface is done according to the model given in the CEB/FIP Model Code 1990 (sect 6.3.5.2).

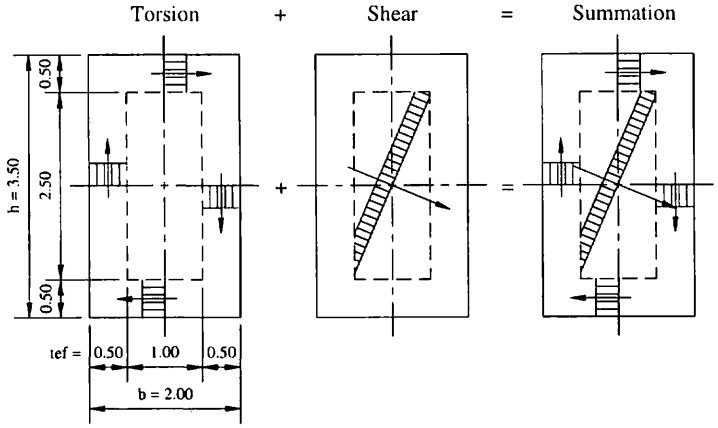

Fig. 3: Summation of torsion and shear

The design values (ULS) of the resultant actions including the prestressing are
$V_d = 2.21$ MN
$T_d = 5.39$ MNm

Shear stress due to the torsion T_d is
$\tau_{Td} = T_d/2xA_{ef}xt_{ef} = 5.39/2x1.50x3.00x0.50 = 1.20$ MPa $< \tau_{fd}$ (Equ 6.23 in Rec.)

Shear stress due to the shear force V_d is
$\tau_{vd} = V_d/A_c = 2.21/1.00x2.50 = 0.88$ MPa $< \tau_{fd}$

3.3 Check of the serviceability limit state (SLS)

To quarantee an efficient transfer of the forces across the construction joint the corbel was compressed against the face of the old arch.
The order of magnitude of the compression stress in the joint is

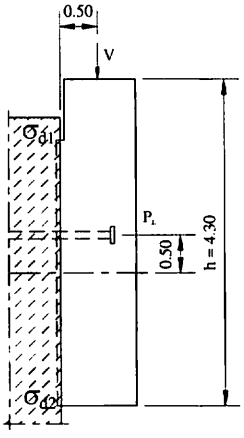

$\sigma_{d1,2} = P\perp/A \pm M/W$; A $= 3.50x2.00 = 7.00$ m^2
W $= 3.50^2x2.00/6 = 4.08$ m^3
P⊥ $= P \sin \alpha$
$= 4.08 \times \sin 60° = 3.53$ MN
$V_{max} = 0.88$ MN
M $= 3.53x0.50 - 0.88x0.50 = 1.33$ MNm

$\sigma_{d1,2} = -3.53 / 7.00 \pm 1.33 / 4.08 = -0.83...-0.18$ MPa
$< \sigma_{lim} = 0$ MPa

Fig 4: Compression in the interface

4 Design of the reinforcement

4.1 Modelling the flow of forces

The anchorage of the corbel is provided by transverse steelbars (S1...S16) which are distributed evenly in the peripheral zone of the interface and two prestressing tendons (S17) in the central part of the construction joint.

The shearforce in the construction joint is transferred across the interface by means of inclined concrete struts which together with the ties - steelbars (S1...S16) and prestressing tendons (S17) - form the supports („small corbels") of the corbel.

The loads V and M are taken into the corbel by resultant forces F_c and F_s derived by ULS design at the top of the corbel. (Fig. 5). The resultant of the tension steel is placed at the distance of 0.25 m from the edge of the corbel - it is in the same vertical line with the supports S9...S14.

The model is developed keeping in mind that the ties should be arranged with consideration of practicality of the reinforcement layout (parallel to the corbel edges).

It is then assumed that the path of the vertical resultant force F_c - having now the magnitude C1 because of the slight inclination - leads first to the support S1. The reaction force of the support S1 equals to its load - bearing capacity. As the support S1 deforms, part of the rest of the load F_c is transferred into the next supports (S2...S5) in the vertical line. It is considered that the structure is ductile enough to make this redistribution possible.

The magnitude of the force in the strut C2 is defined by the united capacity of supports S2...S5. The remaining part of the load F_c is then led to the support S17 in the middle of the construction joint by the strut C6.

The vertical resultant force F_s is taken into the corbel by reinforcing steel. Supports S9...S13 act like supports S1...S5 but in opposite direction.

Changes in the direction of forces in some nodes result in horizontal forces which are resisted by the supports S6...S8, S14...S16 and S17.

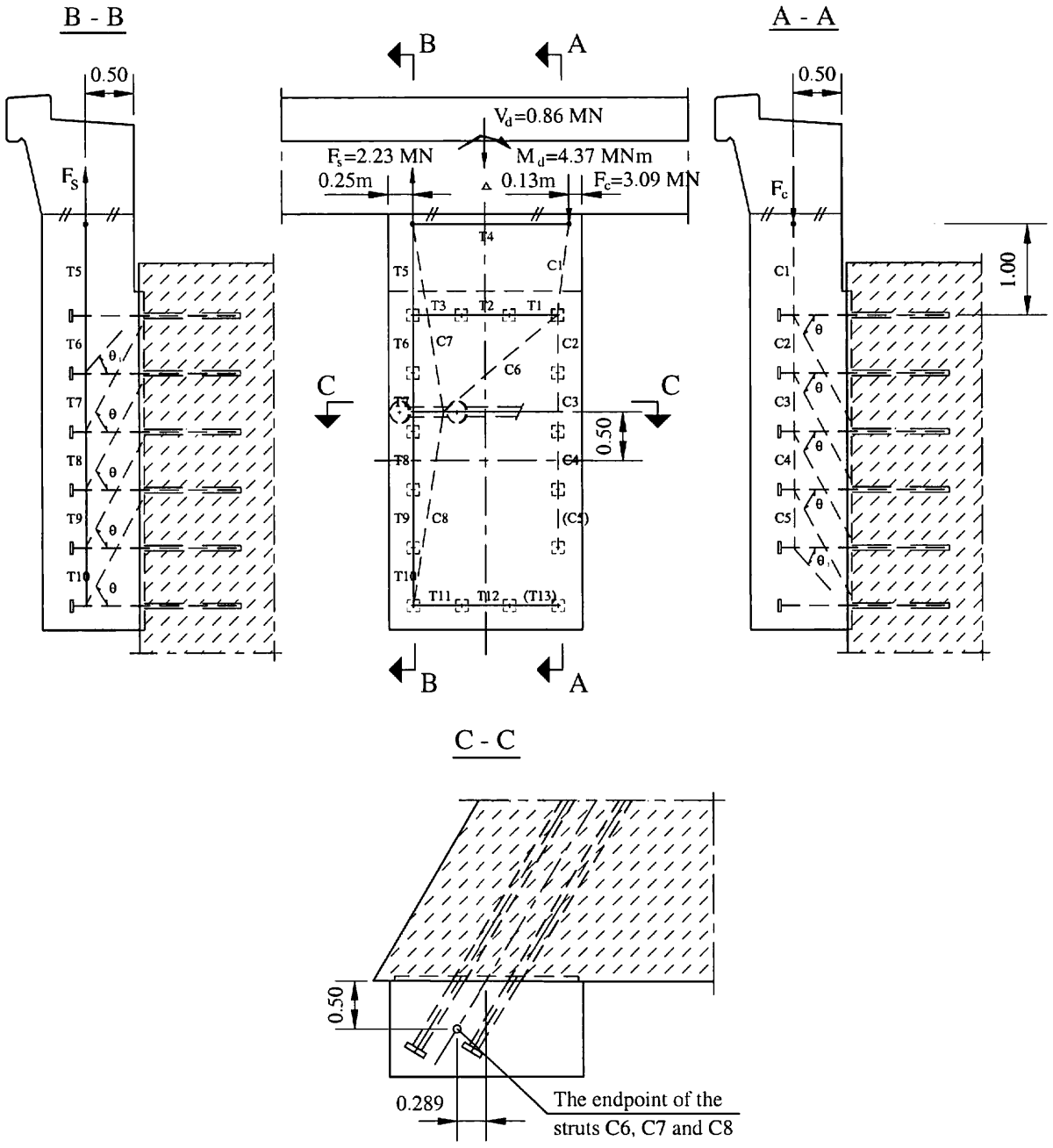

Fig. 5: The strut-and-tie model of the corbel

4.2 Determining the forces in the struts and ties

The capacities of the individual supports (S1...S16) are determined first to make it possible to calculate the forces in the struts (C1...C8) and ties (T1...T13) of the model.

The rules given in Rec. 6.5.2.3 „Concentrated load near a support and corbels" are applied in calculating the load-bearig capacities of the individual supports.

The capacities of the invidual supports S1...S16

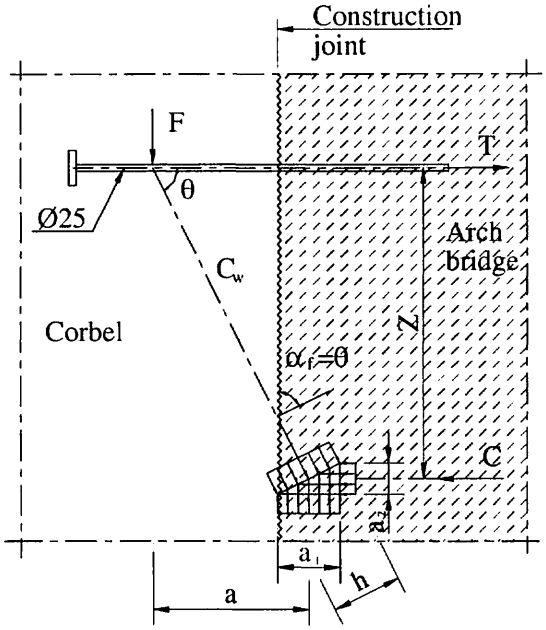

Table 5.1 / Rec. 5.5
β = 0.4 (Interface condition rough)
μ = 0.9

Fig. 6: Model for the individual supports S1...S16

Let us suppose, that the capacity of the corbel is defined by the capacity of the tie

$T_{Rd} = A_s \times f_{yd} = 491 \times 435 \times 10^{-6} = 0.214$ MN

Let us choose $\tan \theta = z/a = 2 \Rightarrow \theta = 63.4°$ (Limitation for θ in the strut-and-tie model in Fig 6.15/Rec. 6.5.2.3)

The load carrying capacity of the corbel is

$F_{Rd} = T_{Rd} \times \tan \theta = 0.214 \times 2 = 0.427$ MN

The force in the strut is

$C_w = T_{Rd}/\cos \theta = 0.214/0.447 = 0.478$ MN

The capacity of the strut is defined by the capacity for the transfer of compressive forces across an interface by means of concrete to concrete friction (Rec. 5.5)

$f_{cd,\,eff} = \nu_3 \times f_{1cd}$

$\nu_3 = \beta \times f_{ctm} \div f_{1cd} \times (1 + \tan^2\alpha_f) \div (\tan\alpha_f - \mu) = 0.4 \times 2.2 \div 11.3 \times (1 + \tan^2 63.4°) \div (\tan 63.4° - 0.9) = 0.35$

$f_{cd,\,eff} = 0.35 \times 11.3 = 3.96$ MPa

The dimensions of the strut in the old concrete are

$a_1 = F \div (f_{cd,\,eff} \times b) = 0.427 \div (3.96 \times 0.50) = 0.216$ m

$h = a_1/\sin\theta = 0.242$ m

$h \times b = 0.242 \times 0.500$ m^2 (These dimensions are realistical)

The capacity of the supports S1...S4, S6, S7, S9...S12, S14, S15 is $F_{Rd} = 0.427$ MN.

In the supports S5, S8, S13 and S16 the angle between the inclined strut and a tie $\theta_1 < \theta$ because of the location of the support near the transverse edge of this corbel. From that follows that the capacity of the support is less than calculated F_{rd}.

4.3 Forces in the struts C1...C8 and ties T1...T13

Forces in the struts C1...C8 and ties T1...T13 in the table below are calculated in order of appearance.

Strut/Tie	C1	C5 [1]	C4	C3	C2	C6	T1	T2 [2]	T3	T4	C7
$F_{act,\,d}$ [MN]	-3.11	0	0.43	-0.86	-1.29	-1.98	1.06	0.79	0.36	0.37	-1.65
Strut/Tie	T5	T6	T7 [1]	T8	T9	T10	C8	T11	T12	T13	
$F_{act,\,d}$ [MN]	3.83	3.83	3.83	3.40	2.97	2.54	-2.17	0.49	0.22	0	

1) It is supposed that support S5 (S13) does not carry any load because $\theta_1 < \theta$. This assumption is clearly on the safe side.

2) Support S16 has smaller capacity ($F_{rd} = 0.27$ MN) because $\theta_1 < \theta$.

4.4 The check of the capacity of the support S17

Vertical and horizontal force resultants V_{sd} and H_{sd} in support S17 are:

$V_{sd} = 0.86$ MN

$H_{sd} = 0.57$ MN

Tension force in the tendons:

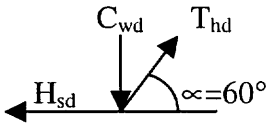

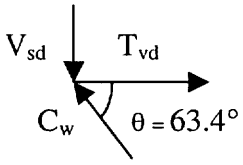

$T_{sd} = H_{sd}/\cos \propto + V_{sd}/\tan\theta = 0.57/0.50 + 0.86/2.00 = 1.57$ MN

$< T_{Rd} = A_{pt} \times f_{ptd} = 0.003600 \times 1385 = 4.99$ MN

4.5 Reinforcement layout of the corbel

In order to transfer the tension forces of the ties the reinforcement must have the dimension A_s so that

$T_{sd} \leq A_s \times f_{yd}$ ($f_{yd} = 435$ MPa) and be anchored properly in the nodes.

Reinforcement is symmetrical, because the bending moment may also be applied to the opposite direction.

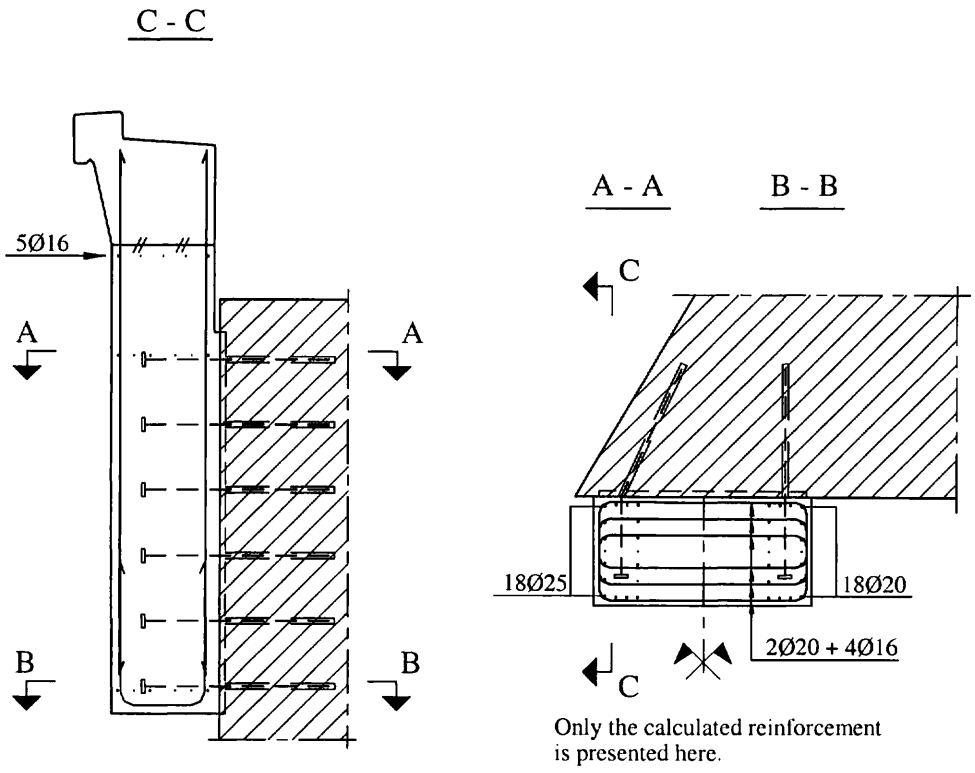

Fig. 7: Reinforcement layout in the corbel

Background paper 10

Shear design in a consistent design concept for structural concrete based on strut-and-tie models

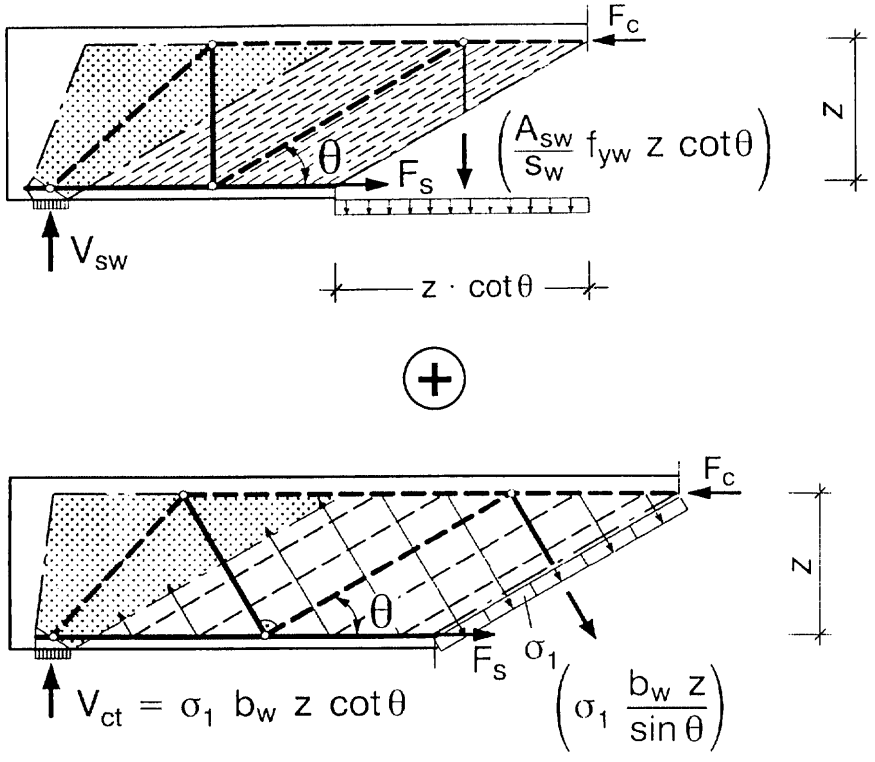

Karl - Heinz Reineck

Universität Stuttgart, Institut für Leichtbau Entwerfen und Konstruieren
(University of Stuttgart, Institute for Lightweight Structures Conceptual and Structural Design)
Stuttgart, Germany

A draft of this article was presented at the Session 2: Practical Design of Structural Concrete *fib* Symposium 1999 Prague "Structural Concrete - The Bridge between People"

1 Introduction

The shear design of structural concrete members, i.e. reinforced and prestressed concrete members, has been a fascinating and heavily disputed topic from the beginning of reinforced concrete. Even nowadays, the codes all over the world still reflect the controversial views or researchers and code makers. In the following some contributions to the state-of-the-art are made, which supplement the surveys given by ASCE-ACI Committees 426 (1973) and 445 (1998), in the CEB 223 (1995) and also by Marti (1991, 1999).

The oldest and mainly empirically derived approach is to add a "concrete term" V_c to a "steel term" like e.g. in the old codes DIN 1045 and SIA as well as traditionally in the ACI 318, and more recently in the EC2, part 1 as the so called "standard method". Thereby the steel term is for the capacity of a truss with parallel chords, in which the web is formed by ties, representing the transverse reinforcement and inclined struts, which are assumed to be inclined at an angle of 45°. The concrete term has been derived empirically, although several explanations by means of models were given, e.g. by Leonhardt (1965, 1977).

The alternative approach "variable strut angle method" is based on the theory of plasticity, as e.g. developed by Thürlimann et al. (1975, 1983) or Nielsen (1984) and Nielsen/ Braestrup (1976). It is assumed that the inclination of the struts in the web of the truss may be freely selected, and only lower bounds for it as well as for the strength of the struts are given. However, the proposals for these lower bounds vary in a wide range: like e.g. for θ from 18° ($\cot\theta = 3$), like in the CEB-FIP Model Code 1990, up to 30° ($\cot\theta = 1{,}75$), like in Germany for the application of EC 2, part 1.

In view of two available methods the questions arises: "has the addition of a concrete term V_c any physical meaning ?", and is really a controversy necessary "V_c-term" versus "variable strut angle method"? Furthermore, the question is, how these methods for shear design comply with the main development of the last two decades, which is to develop a consistent design concept based on strut-and-tie models covering as well the B-regions as also the D-regions. In the following it is shown, that the state-of-the-art on the shear design now allows to give a practical solution, which likewise complies with the need for clear models so that designers can cope with problems when designing structures. It is hopefully shown that the practical shear design method of the FIP Recommendations 1996 "Practical Design of Structural Concrete" solves or makes futile the above cited controversy.

2 Theoretical background for the different approaches

The failure of members or structures is mostly determined by the formation of cracks, from which one opens widely due to the strains of the reinforcements crossing the crack, and this eventually leads to crushing of the compression zone over the crack tip. There are critical cases of unreinforced members, where cracking leads to non-ductile behaviour and yielding of the reinforcement is not reached at failure of the member. It is therefore understandable, that designers first looked for the weakest sections along the cracks and determined the required reinforcement there, and this has been done for the flexural design since the beginning of reinforced concrete.

For the shear design, the thorough observation of cracking and failure of beams led Mörsch (1909,1922) to regard the concrete between the inclined cracks as struts of a truss (Fig. 1). This demonstrates that Mörsch looked at the equilibrium along the failure surface in the B-region, initially by means of graphical statics. The same approach was later used by Lessig (1959), who proposed skew, spatial failure surfaces for reinforced concrete beams subjected to torsion, respectively to torsion combined with shear forces and bending moments.

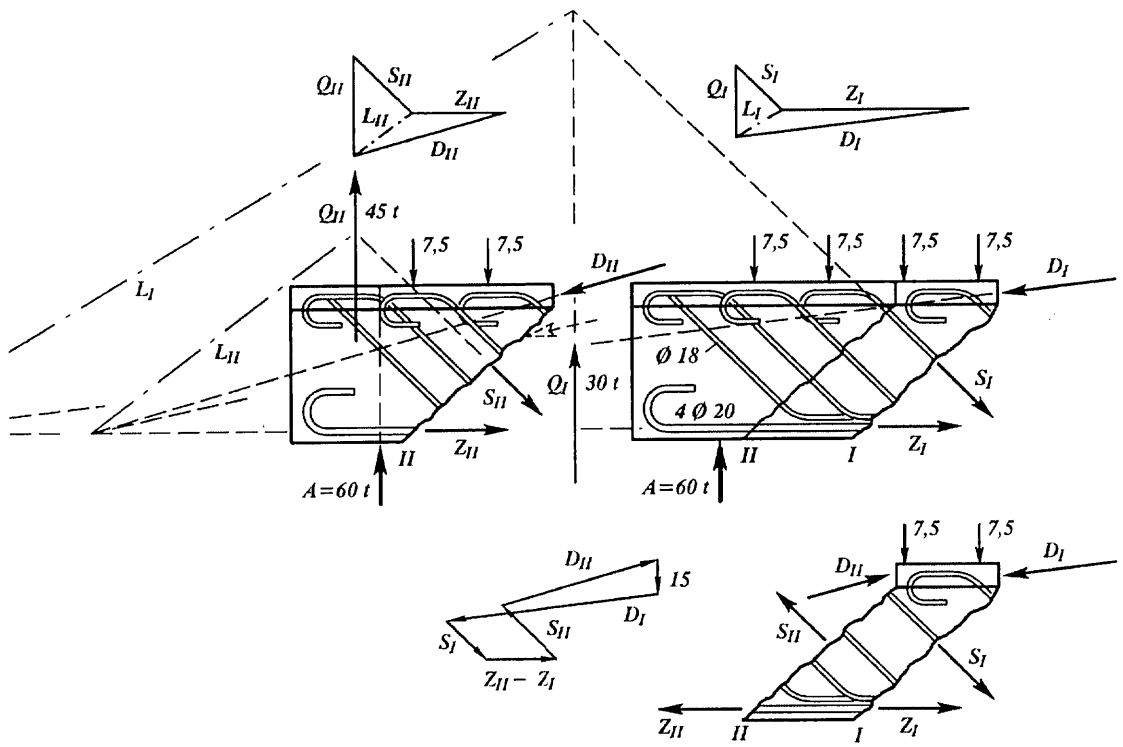

Fig. 1: The approach by Mörsch (1909,1922) for the shear design

The ASCE-ACI Committee 426 in their State-of-the-Art Report on Shear from 1973 also was guided by the idea of looking at failure mechanisms, and they extensively reviewed the shear failure modes and the possible mechanisms for the shear transfer at cracks. The research of the last 20 years has enabled an even deeper insight into the shear behaviour and into the shear transfer mechanisms. Especially the transfer of forces across cracks has been identified as a main shear transfer mechanism and its behaviour been clarified to a large extent.

Generally, the "failure mechanism approaches" are not restricted to the kinematic method of the theory of plasticity, but are approaches characterised by the modelling of the actual failure surface in a member or the critical crack and the localised crushing in the concrete compression zone. This approach has been followed for members without transverse reinforcement by Kani (1964), Fenwick and Paulay(1968), Taylor(1974), Hamadi (1976) and Reineck (1990, 1991 b, 1991 e), and for members with transverse reinforcement by the researchers given with the later explained "truss model with crack friction". In this sense, the failure mechanism approaches have a common feature with fracture mechanics approaches, where the localisation of the failure zone either in tension or compression plays the major role.

The assumption for the failure surface, for the shear transfer mechanisms as well as those for the material properties influence of course the failure load. With respect to shear, it is important to note that rarely all the shear transfer mechanisms were modelled in the theories presented in the past. Despite the fact that a failure mechanism approach is used, it may well be that a lower bound estimate of the failure load is attained, like for any other non-linear analysis, if safe assumptions for the material characteristics and shear transfer mechanisms are made.

The "truss model with crack friction" for members with transverse reinforcement is such a failure mechanism approach and a "discrete" approach with respect to cracking. It is based on the works by dei Poli et al (1987, 1990), Gambarova (1979), Kirmair (1985/87), Kupfer and his coworkers Mang, Bulicek, Moosecker and Karavesyrouglou (1979, 1983, 1991), Bulicek (1993) and Reineck (1990, 1991 a, 1995). The shape and the geometry (inclination) of the crack is modelled and also the spacing. Therefore, this approach is in principle different from the following smeared approaches.

In the "smeared approaches" the compression fields are modelled independently from the crack pattern, like in the cases of the shear-compression field theory by Collins (1978) or Collins and Mitchell (1980) and the rotating-angle softened truss model by Hsu(1993). These works are based on earlier works by Kupfer (1964), Baumann (1972), Potucek (1977). Only Hardjasaputra (1987) differs from that by considering the cracks in a smeared approach. The smeared approaches are extensively discussed in the ASCE-ACI Committee 445 State-of-the-Art Report (1998), so that only the main difference of these approaches is pointed out here, and that is the relationship between the crack angle β_r and the angle θ of the compression field. These angles are clearly identified and are different in the above described approach of the "truss model with crack friction" as well as in the „fixed-angle softened truss model" by Hsu (1993). This is not the case for any of the smeared approaches.

Therefore, Reineck (1995) classified the different approaches accordingly as shown in Fig. 2. If the assumption is made that both angles are equal, i.e. $\beta_r = \theta$, like in all smeared approaches, then this also means that no slip occurs and thus the friction cannot be checked directly. Furthermore, the angle of the principal strains complies with that of the principal compressive stresses, i.e. the strut angle. Despite of all these relations, Vecchio and Collins (1986) attempted in the modified compression field theory a check of the friction, even though the assumption was remained that the angles β_r and θ are equal. This is of course a gross simplification or a mistake, since it is not really possible that friction forces can be transferred at cracks which are assumed parallel to the compression field. In the discrete approaches of the truss model with crack friction no kinematic assumptions are made and constitutive laws for friction have to be formulated.

The emphasis of the truss-analogy or generally of strut-and-tie models is to describe the load transfer in the member, whereas a failure mechanism approach aims directly at determining the failure load or at designing the reinforcement for given ultimate loads. Probably the best known application of this approach is the "truss model with crack friction", because it explains the traditional concrete contribution V_c in the shear design, The advantage is, that the essential dimensions for the reinforcement and for the concrete are directly determined, and so this very practical design method was selected for the FIP Recommendations 1996.

	Smeared truss model, compression field theories		Truss model with crack friction	
Analytical procedure	Kinematic condition $\tan^2\theta = \frac{\varepsilon_x + \varepsilon_2}{\varepsilon_z + \varepsilon_2}$		crack opening $w \perp \theta$	Discrete cracks – friction law – cracks: β_{cr}; s_{cr}
Slip Δs θ **of** σ_2 φ_2 **of** ε_2 ε_{cw} **in strut**	$\Delta s = 0$ $\theta = \beta_{cr}$ $\varphi_2 = \theta$ $\varepsilon_{cw} = \varepsilon_2$		$\Delta s \neq 0$ $\theta < \beta_{cr}$ $\varphi_2 \neq \theta$ $\varepsilon_{cw} \neq \varepsilon_2$	slip considered
Strength criteria	empirical effect. strength $f_{cwu} = \nu\ f_{1c}$ ("softening of concrete")			– solid concrete: $f_{cwu} = 0.80\ f_{1c}$ – friction often limits shear capacity
Authors	Mörsch (1922); Thürlimann (1975, 1983); Kupfer (1964); Baumann (1972); Potucek (1977); Collins (1978); Collins, Mitchell (1980, 1987, 1991); Vecchio, Collins (1986); Hsu (1993);	Hardjasaputra (1987)		Kupfer, Mang, Karavesyrouglou (1983); Kupfer, Kirmair (1983); Kirmair, Mang (1987); Bulicek (1991); Gambarova (1979); dei Poli, Gambarova, Karakoc (1987); Reineck (1990,1991)

Fig. 2: Comparison of smeared and discrete approaches in shear design

3 The truss model with crack friction in the FIP Recommendations 1996

3.1 Equilibrium

The shear design method "truss model with crack friction" was implemented as shear design in the FIP Recommendations 1996 "Practical Design of Structural Concrete", and the background for this method has already been explained by Reineck (1995) as well as in ASCE-ACI 445 (1998), This approach starts from the fundamental free-body diagram in Fig. 3, which is obtained by separating the member along an inclined crack in the B-region of a structural concrete member with transverse reinforcement, like it was done by Mörsch (see Fig. 1). The forces acting on the free body are the forces at the end support, the chord forces, the forces in the stirrups and the friction forces along the crack, which are given in Fig. 3 b.

In Fig. 3 the dowel force of the longitudinal reinforcement is neglected, which plays a role in members without transverse reinforcement. Furthermore for simplicity of Fig. 3 , the chords are assumed to be parallel to the axis of the member, so that there are no vertical components of an inclined compression chord or an inclined tension chord of the truss.

The basic requirement for the shear design is:

$$V_{Rd} \geq V_{Sd} \qquad (1)$$

where: V_{Sd} = shear force at about a distance ($z \cot\theta$) from the face of the support.

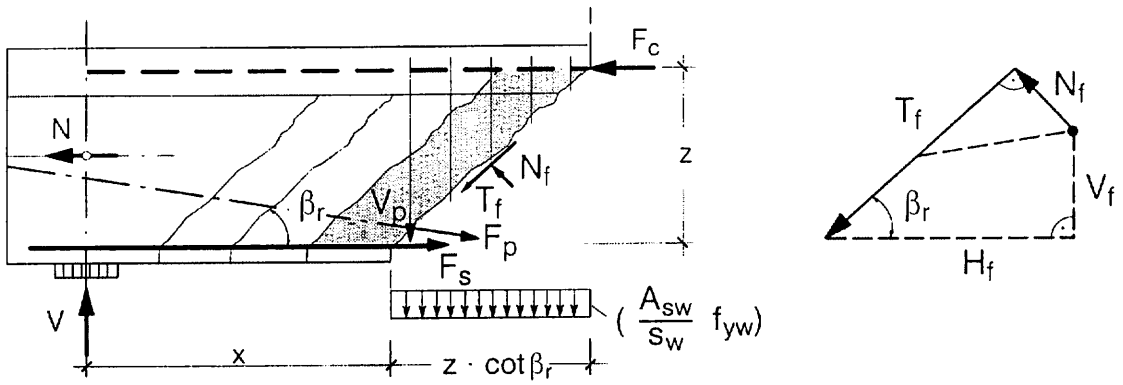

a) free-body with forces acting on it *b) forces due to friction*

Fig. 3: Free-body of an end support of a beam with applied forces

The basic equation for the shear resistance follows directly from the vertical equilibrium:

$$V_{Rd} = V_{swd} + V_{fd} + V_{pd} + V_{ccd} \quad (2)$$

where: V_{swd} = shear force carried by the stirrups across the crack

V_{fd} = vertical component of friction forces at crack (Fig. 3 b)

V_{pd} = vertical component of force in prestressing tendon

V_{ccd} = vertical component of the force in an inclined compression chord.

From the equations (1) and (2) a design shear force for the web of a structural concrete member may be defined:

$$V_{Sd,web} = V_{Sd} - V_{pd} - V_{ccd} \quad (3)$$

Therefore, the web must provide the following resisting shear force:

$$V_{Rd,web} = V_{swd} + V_{fd} \geq V_{Sd,web} \quad (4)$$

The shear force component V_{swd} carried by vertical stirrups across the inclined crack is at ULS:

$$V_{swd} = (A_{sw} / s_w) f_{ywd} z \cot\beta_r \quad (5)$$

where: A_{sw} = area of transverse reinforcement

s_w = stirrup spacing in the longitudinal direction

f_{ywd} = design yield strength of transverse reinforcement

z = inner lever arm

β_r = crack angle

The shear force component V_{sw} is known at any load level (not only at ULS) if the shear force component V_f due to friction is known, as well as of course the amount of transverse reinforcement and the crack angle. The force V_f is the vertical component of the combined friction forces T_f and N_f across the inclined crack in the web, as shown in Fig. 3 b. It should be noted, that normally only a part of the force T_f combines with N_f to an inclined compressive force, but additionally a component without axial stresses on the crack surface exists. The shear force component V_f due to friction represents the "concrete contribution" appearing in many codes such as ACI 318, as later explained in Section 4.1.

3.2 Inclination and spacing of inclined cracks

The crack inclination as well as the crack spacing must be assumed or be determined by a non-linear analysis. It may be noted, that relatively little attention has been given to these important parameters in previous research.

The angle of the inclined cracks is normally assumed at 45° for a reinforced concrete member. Only Kupfer /Moosecker (1979) pointed out, that it could be up to 5° flatter, due to a reduced modulus of elasticity caused by micro-cracking. Flatter angles will appear for prestressed concrete members or for members with axial compression, and steeper angles occur for members with axial tension. For such members, commonly the angle of the principal compressive stress at the neutral axis of the uncracked state is assumed as the crack angle.

The spacing of the inclined cracks is mainly determined by the amount of reinforcement and relevant formulae have been proposed by Gambarova et al. (1979, 1991), dei Poli et al. (1987, 1990) and Kirmair (1985/87) amongst others.

3.3 Constitutive laws for crack friction

Any approach like the "truss model with crack friction", relies on constitutive laws for the transfer of forces over cracks by friction or interface shear. This shear transfer mechanism was clearly defined by the works of Fenwick/ Paulay (1968) or Taylor (1972, 1974) and others, but only few tests and no theories were available for formulating reliable constitutive laws. This has considerably changed through the research in the last 20 years including works by Hamadi (1976), Walraven (1980), Walraven/ Reinhardt (1981), Gambarova (1979), Daschner (1980), Nissen (1987), Tassios/Vintzeleou (1987). An extensive state-of-the-art report on interface shear was presented by Gambarova and di Prisco (1991). The constitutive law proposed by Walraven (1980) has been used very often by others because it completely describes not only the shear stress - slip relation for different crack widths but also the associated normal stresses.

3.4 Shear force component V_f due to crack friction

The shear force component V_f in Eq. (1) or (2) transferred by friction across the cracks depends on the available slip and crack width, so that these displacements have to be calculated, and this requires to determine the strains in the chords and in the web. In return, the displacements and the strains must be compatible with the forces in the model according to the constitutive laws for the shear force components. The force V_f is plotted in Fig. 4 and it depends on the magnitude of the shear, on the strain conditions in the member, on the longitudinal strain ε_x in the middle of the web, and on the crack spacing. However, for simplicity a constant value V_f may be assumed for code purposes, as indicated in Fig. 4 a.

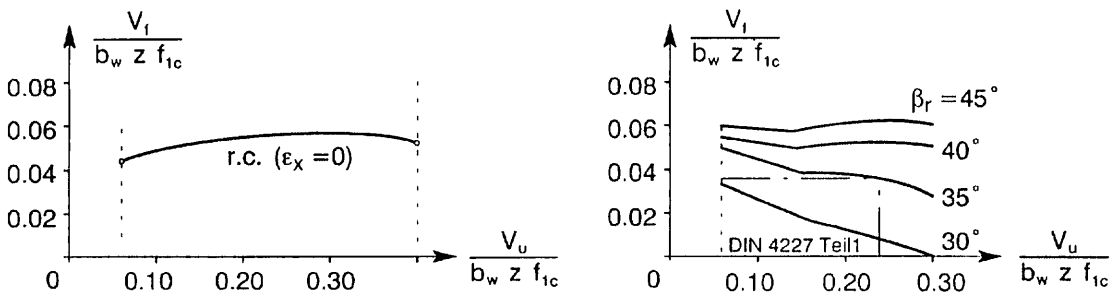

a) reinforced concrete members *b) prestressed concrete members*

Fig. 4: Results of parameter studies for the shear force component V_f [Kirmair (1985/87)]

The practical result for the shear design is a constant value for the shear force component V_f, and in the FIP Recommendations 1996 the following value was defined along with the crack angle for r.c. members without axial forces:

$$V_{fd} = 0.070\,(b_w\, z\, f_{cwd}) \qquad (6\,a)$$

$$\cot\beta_r = 1.20 \qquad \text{i.e. } \beta_r \approx 40° \qquad (6\,b)$$

The result of the Eq. (4), (5) and (6) is plotted in the simple, dimensionfree design diagram in Fig. 5, which is well known and used in many codes. The friction in the cracks governs the design for low and medium shear, and only for a small range of very high shear, the strength of the compression struts f_{cwd} is reached, which is characterised by the quarter circle in Fig. 5.

For low shear or reinforcing ratios ρ_w the diagram is limited by the minimum reinforcement ratios $\rho_{w,min}$ specified in codes, and the corresponding values $\omega_{w,min}$ therefore represent the lower limit for applying Eq. (6). For members without transverse reinforcement the capacity V_{Rd} is far lower than the value for V_f. For members with lower amounts of transverse reinforcement than $\omega_{w,min}$ no shear design is available, and the scatter of the tests in this range does not support the idea, that it is possible to develop one.

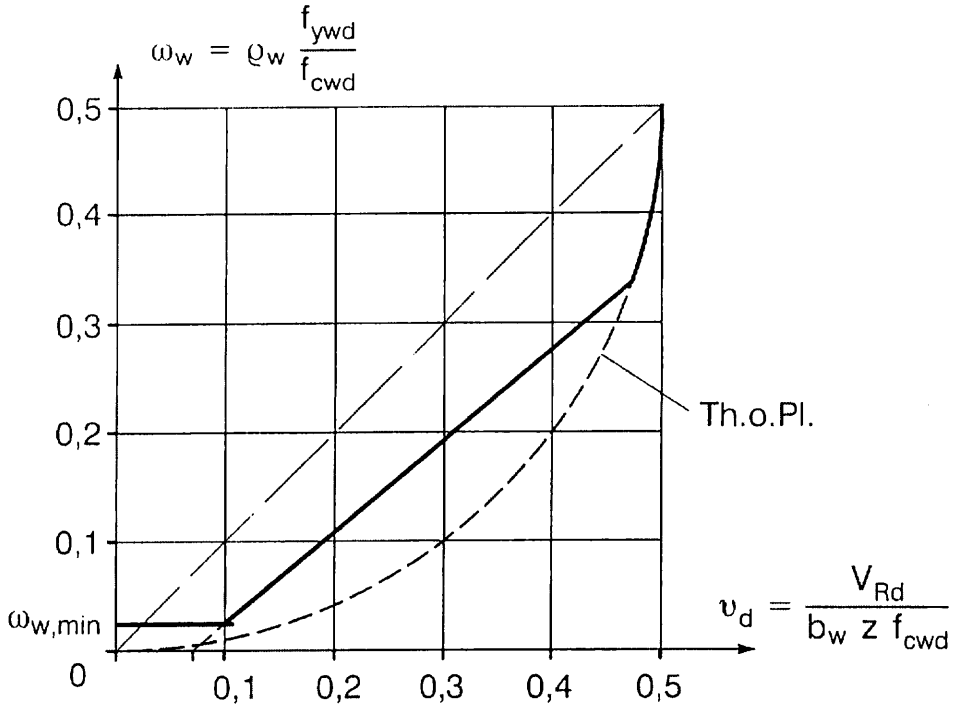

Fig. 5: Dimensioning diagram for the design of vertical stirrups for r. c. members without axial forces

The approach "truss model with crack friction" considers the influence of axial forces as well as prestress, because flatter cracks appear and V_f may be reduced as consequence of the negative longitudinal strain ε_x. The influence of the crack inclination is very pronounced as Fig. 3b and Fig. 4 b show, and for cracks flatter than about 30° the shear force component V_f plays no role any longer and the struts are parallel to the cracks. In the FIP Recommendations 1996 the following relationships are proposed for members with axial compression or prestress, and the practical results are shown in the dimensioning diagram in Fig. 6.

$$\cot\beta_r = 1.20 - 0.2\,\sigma_{xd} / f_{ctm} \qquad (7\text{ a})$$

$$V_{fd} = 0.10\,(1 - \cot\beta_r/4)\,(b_w\ z\ f_{cwd}) \geq 0 \qquad (7\text{ b})$$

where: $\sigma_{xd} = N_{Sd}/A_c$ = axial stress [(-) in compression]

$f_{cwd} = 0.80\,f_{1cd}$ = compressive strength of inclined struts

In the case of axial tension the cracks may be steeper than 45° and the strain ε_x is positive. In the FIP Recommendations the following relations were given for members with axial tension:

$$\cot\beta_r = 1.20 - 0.9\,\sigma_{xd}/f_{ctm} \qquad \geq 0 \qquad (8\text{ a})$$

$$V_{fd} = 0.10\,(1 - 0.36/\cot\beta_r)\,(b_w\ z\ f_{cwd}) \qquad \geq 0 \qquad (8\text{ b})$$

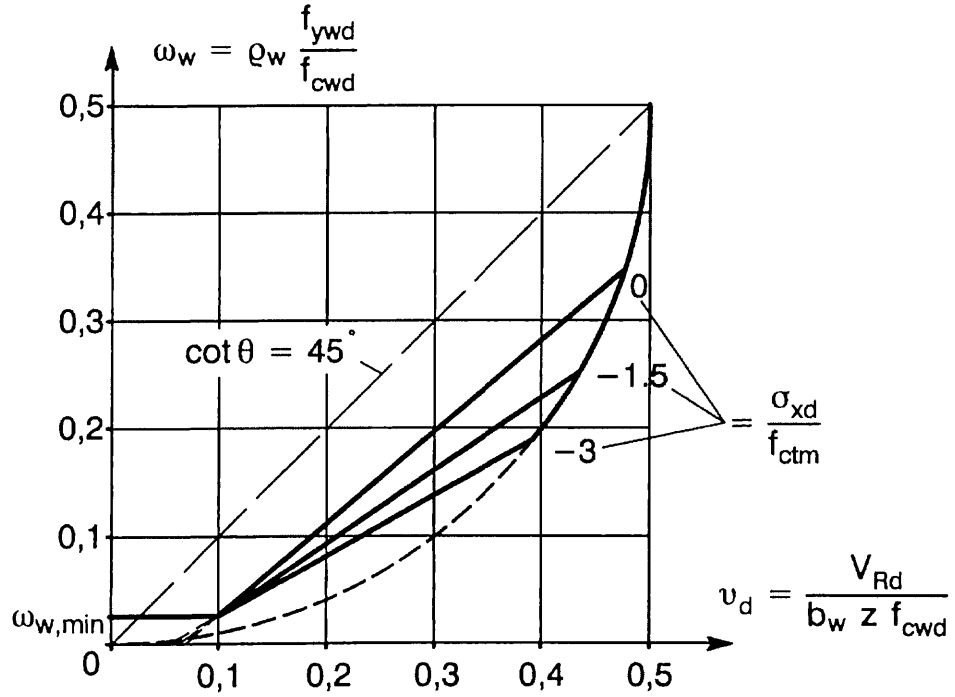

Fig. 6: Dimensioning diagram for vertical stirrups for prestressed concrete members and members with axial compression

The influence of axial tension is quite noticeable, because the $V_{fd} = 0$ is already attained for a valued of $\sigma_{xd} = 0.933\ f_{ctm}$ with a crack angle of about 70°, corresponding to a value $\cot\beta_r = 0.36$. This leads to high amounts of stirrups. It must be pointed out that this proposal may be on the safe side, because the crack angle is evaluated on basis of the uncracked state. Unfortunately there are too few tests to compare with and to propose a better relationship.

3.5 The truss - model

When the shear force component V_f is known, all the forces are defined at the crack or failure surface, so that the state of stress in the struts between the cracks is also known. The obvious action of the solid concrete between the cracks is, that it represents the struts of a truss formed together with the stirrups (Fig. 7 a). This was the action, which Mörsch only utilised in his truss analogy (see Fig. 1). The additionally friction forces acting result in a biaxial state of stress as shown in the Fig. 7 b. Therefore, the combined state of stress is biaxial with a principal compression field at a flatter inclination than that of the cracks, and a tension field perpendicual to it.

However, it should be noted, that for high shear forces the minor principal stress turns into compression, because the normal stresses due to friction prevail. However, these compressive stresses are so small, that they are usually neglected, so that only the truss of Fig. 8 a remains with a uniaxial compression field, which is the usual model of the theory of plasticity.

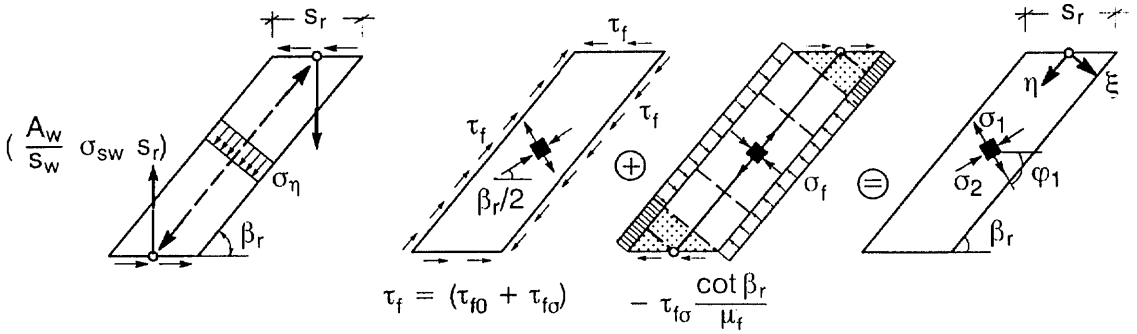

a) truss action *b) biaxial stresses due to friction*

Fig. 7: Forces and stresses in the discrete concrete struts between the inclined cracks

The minor principal stress is tension for small shear forces, so that the state of stress may be visualised by the two trusses shown in Fig. 8. The usual truss - model with uniaxial compression inclined at the angle θ in Fig. 8 a is superimposed by a truss with the same direction of compression struts and concrete ties perpendicular to the struts (Fig. 8 b). So there are two load paths for the shear transfer, as defined by Schlaich/ Schäfer/ Jennewein (1987), and as also earlier shown by Reineck (1982) and with different explanations by Lipski (1971/72) and Vecchio and Collins (1986) in their "modified compression field theory". The model in the Fig. 8 b is the same as that proposed by Reineck (1990, 1991 b and e) for members without transverse reinforcement, so that the transition from members with to members without transverse reinforcement is consistently covered.

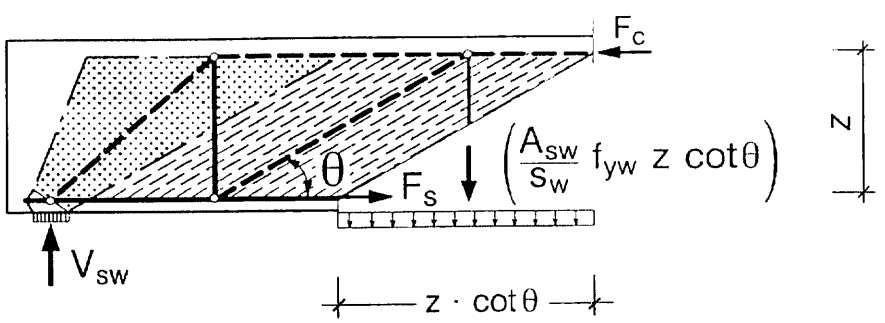

a) truss model with uniaxial compression field in B-region

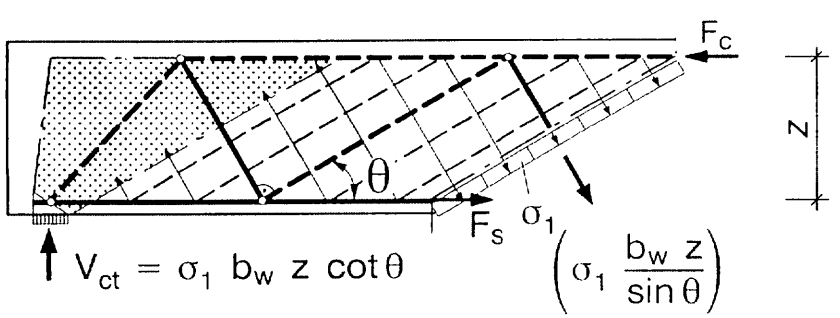

b) biaxial tension-compression field in concrete for low shear

Fig. 8: Models for B-regions with shear force

For simplicity mostly only the truss with a uniaxial compression field is taken as model, since it applies well for the medium and high range of shear forces $\upsilon_d = \tau_{Rd} / f_{cwd}$. With the shear force components V_{sw} and V_f defined by the eqations given above, the angle θ of the inclined struts in the web may be derived as follows:

$$\cot\theta = \frac{\cot\beta_r}{\left(1 - \frac{V_{fd}}{V_{Sd,web}}\right)} \tag{9 a}$$

or

$$\cot\theta = \frac{V_{Sd,web}}{\left(\frac{A_{Sw,web}}{s_w}\right) f_{ywd}\, z} \tag{9 b}$$

with $V_{Rd,web} = V_{swd} + V_{fd} \geq V_{Sd,web}$

This means that the angle θ varies with the magnitude of the applied shear force, i.e the angle θ increases with increasing $V_{Sd,web}$.

The upper limit of the resistant shear force may then be derived as follows:

$$V_{Rd,web,max} = b_w\ z\ f_{cwd}\ \sin\theta\ \cos\theta \quad = b_w\ z\ f_{cwd} / (\cot\theta + \tan\theta) \tag{10 a}$$

For $\theta = 45°$ and $f_{cwd} = 0.80\ f_{1cd}$ ($\nu = 0.80$) the highest value is reached with

$$V_{Rd,web,max} = 0.5\ b_w\ z\ f_{cwd} = 0.4\ b_w\ z\ f_{1cd} \tag{10 b}$$

However, this check is rarely required, because it is only relevant in a small range of very high shear forces, as it can be seen from Fig. 5 and Fig. 6 and Figures 9 to 11. For example, for r.c beams the web compression failure only occurs for values $\upsilon_d > 0.472$.

3.6 Strength of concrete between cracks

The concrete between the cracks is uncracked and forms the strut. However, apart from the compressive stresses due to the truss action there are also transverse tension in the struts, due to the friction stresses and due to the forces induced by the bonded stirrups. This leads to a strength reduction in comparison to the uniaxial compressive strength allowed in compression chords. Further reasons for such a reduction are also the smaller effective width of the strut (rough crack surfaces) and the disturbances by the crossing stirrups. Altogether it was found by Schlaich/ Schäfer (1983), Schäfer/ Schelling/ Kuchler (1990), Eibl/ Neuroth (1988) and Kollegger/ Mehlhorn (1990) that the following value may be assumed for the concrete strength of the struts:

$$f_{cwu} = 0.80\ f_{1c} \tag{11}$$

with f_{1c} = uniaxial compressive strength of concrete (strength of slender prism)

This is a relatively high value compared to lower values proposed elsewhere as so-called "effective strengths" of e.g. $\nu\ f_{1c} = 0.60\ f_c$ or $0.50\ f_c$ used in the theory of plasticity. This illustrates that these lower effective strengths are meant also to cover the insufficient transfer of forces across the cracks by friction. The practical outcome of the above higher value for the compressive strength is, that for high ratios of transverse

reinforcement the capacities are far higher compared to the variable truss angle method in the EC 2 respectively the theory of plasticity, as pointed out by Reineck (1991 a) and demonstrated in the following (see Fig. 10).

4 Comparison of shear design methods for members with vertical stirrups

4.1 The concrete term V_c in shear design of codes

The so-called "concrete contribution" in codes is added to the resistance of the truss-model with 45° - struts, and so the resistance is for members with vertical stirrups (perpendicular to member axis):

$$V_{Rd} = V_{swd} + V_{cd} = (A_{sw}/s_w)\, f_{ywd}\, z + V_{cd} \qquad (12)$$

This is the basic equation of the "standard method" of the EC 2, respectively it is sometimes referred to as „modified truss model" approach, as e.g. by Ramirez/ Breen (1991). This concrete contribution V_c was controversially discussed in the past and has mostly been taken as either the shear force at cracking or the ultimate shear force of the relevant member without transverse reinforcement. Therefore detailed expressions have been given for V_c in terms of the same parameters as are relevant for the capacity of these member. The current ACI 318 design procedures give the most detailed expressions for V_c of all codes by considering most of the possible parameters such as the influence of axial compression, axial tension and of prestress. All such values for the concrete contribution have mainly been justified empirically.

However, it must clearly be stated, that none of these two explanations for the concrete contribution V_c is valid, as has often been pointed by Leonhardt (1965, 1977). The physical explanation for the V_c-term is obvious when comparing Eq. (4) and (5) with Eq. (10): both have a "concrete term" added to the shear force carried by the shear reinforcement crossing the crack or failure surface. In the case of 45° for the crack inclination, i.e. $\cot\beta_r = 1$ in Eq. (5), the two equations (4) and (10) are identical, so that the V_c really is the shear force component V_f transferred by friction across the cracks. Therefore, it can be stated that the approach "truss model with crack friction" offers a clear physical explanation for the concrete contribution and for the addition principle of steel term plus concrete term in the shear design.

4.2 Comparisons of the shear design methods of FIP Recommendations with EC2

In the following the design method for shear "truss model with crack friction" of the FIP Recommendations 1996 is compared for members with transverse stirrups with the different proposals of the EC 2, part 1, which are just discussed for the future revision. The results are plotted in the well known dimensionfree ω_w - υ_d - diagrams of the required amount of transverse reinforcement versus the dimensionfree shear force, which are defined as follows:

$\omega_w = \rho_w\, f_{ywd} / f_{cwd}$ = mechanical reinforcement ratio

with: $\rho_w = A_{sw} / (b_w s_w)$ = geometrical ratio for vertical stirrups

$\upsilon_d = V_{Rd} / (b_w z f_{cwd})$ = design valued of dimensionfree shear force

$f_{cwd} = 0.80 f_{1cd}$ = strength of struts

$f_{1cd} = 0.85 f_{ck} / \gamma_c$ = uniaxial compr. strength with $\gamma_c = 1.50$ normally

In these diagrams the relationship for the 45° truss of Mörsch appears as the diagonal, and the theory of plasticity as quarter circles depending on the given value for the strength of the struts $\nu = f_{cwd} / f_{1cd}$.

The first comparison of the shear design of the FIP Recommendations 1996 is carried out with the standard method of the EC 2, p. 1, and this is in principle also relevant for ACI 318. The results in Fig. 9 for reinforced concrete members without axial forces shows that the FIP Recommendation is far more economical over the whole range of the dimensionfree shear force. It is especially noteworthy that far higher values are possible for the maximum shear force due to the high value for the allowable strut strength of $\nu = 0.80$ as compared to a value of about $\nu = 0.50$ in the EC2.

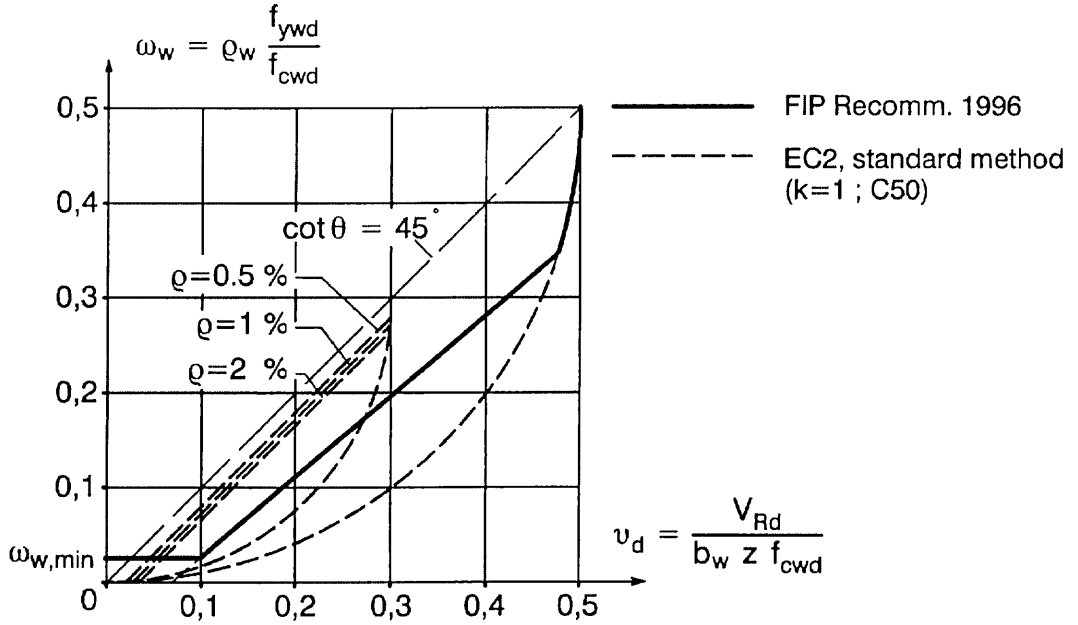

Fig. 9: Comparison of the required transverse reinforcement between the FIP Recommendation 1996 and the "standard method" of the EC 2 for r.c.-members with vertical stirrups for the concrete class C50

The comparison of the shear design of the FIP Recommendation with the "variable strut angle method" of EC 2 is carried out in Fig. 10 for reinforced concrete members. It shows that the FIP Recommendations are considerably more economical in the low shear range up to values for the dimensionfree shear force of about $\upsilon_d = 0.18$. This is relevant and important for beams in buildings as well as for and slabs with transverse reinforcement like for foundations and soil covered structures like e.g. subway tunnels.

In the medium shear range around $\upsilon_d = 0.25$ the EC 2 requires slightly less stirrups, but this range is very small, because the maximum shear force is reached due to the low value for the strength of the struts. The latter values are plotted in Fig. 10 for the concrete classes C20 and C50, and slightly higher values are attained for the lower

concrete class. However, the FIP Recommendations allow far higher values for the maximum shear force, and this is relevant for prefabricated beams.

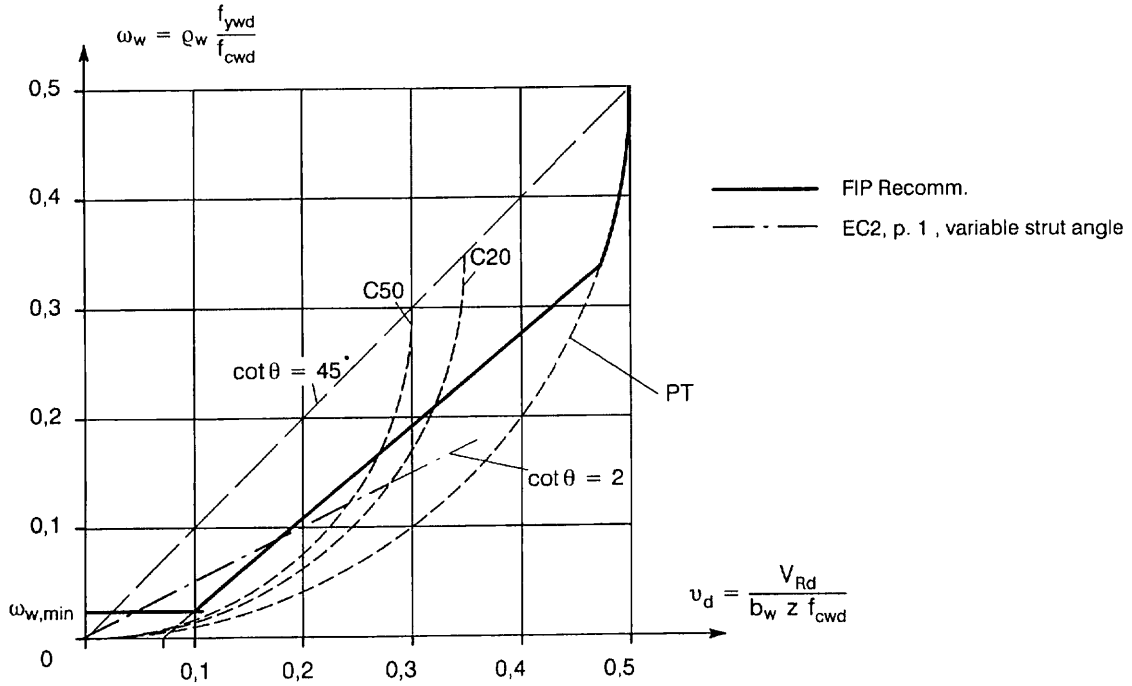

Fig. 10: Comparison of the required transverse reinforcement between the FIP Recommendation 1996 and the "variable strut angle method" of the EC 2 for r.c.-members with vertical stirrups and without axial forces

For prestressed concrete members and members with axial compression the comparison is shown in Fig. 11, and generally the same conclusions as above can be drawn. The "variable strut angle method" does not consider the influence of axial compression, and it is therefore uneconomical in the whole shear range, until again the low value for the maximum shear force is reached. This also applies to the "standard method", unless for the high value for the compression shown in Fig. 11, which may yield lower values for the transverse reinforcement for a small range around $\upsilon_d = 0.12$. Thereby it must be mentioned, that the influence of the prestress or axial compressive force was considered by an increase of V_{Rd1} by the value ($0.12\ \sigma_{cd}\ b_w\ d$), which is slightly less than that in the EC2 (1991).

Again the fact should be pointed out that the FIP Recommendations 1996 allow far higher values for the maximum shear force, because this is especially relevant for prestressed concrete members like prefabricated beams or bridge girders. This means practically for example that free cantilevering bridges may be built with thin webs up to high shear forces, whereby of course high amounts are required for the transverse stirrups depending on the amount of prestress, as Fig. 11 shows.

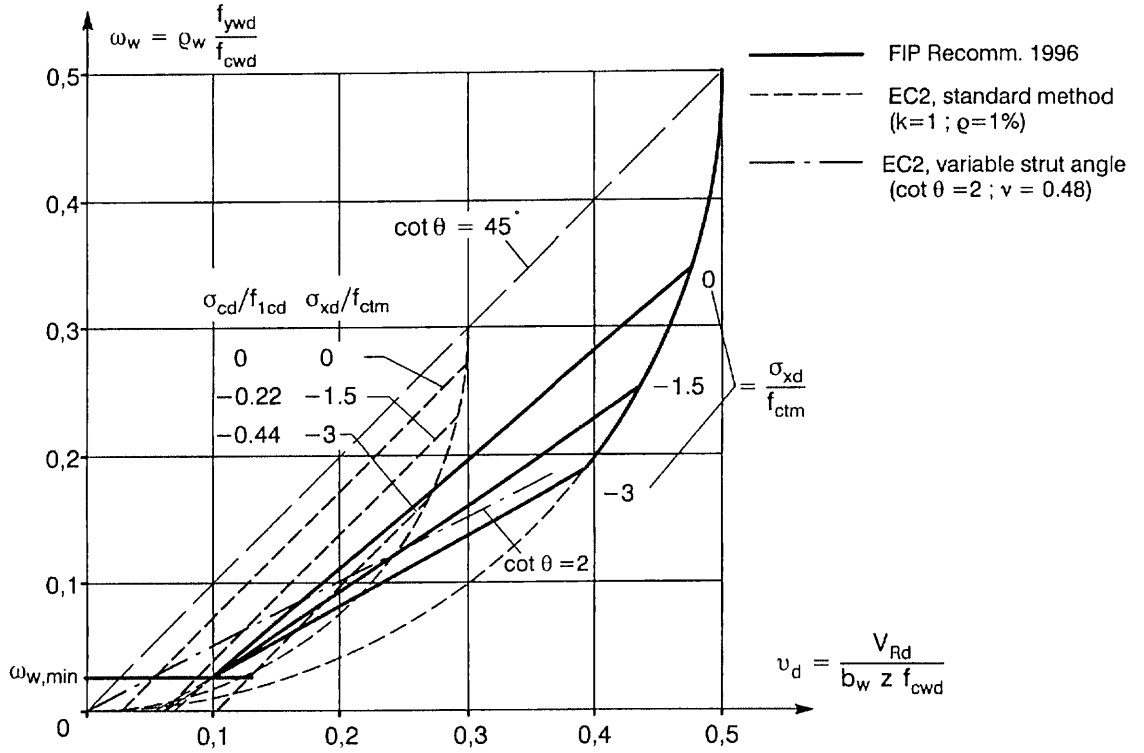

Fig. 11: Comparison of the required transverse reinforcement between the FIP Recommendation 1996 and the "variable strut angle method" for p.c.-members and members with axial compression with vertical stirrups

4.3 Comparisons of the shear design methods of FIP Recommendations 1996 with the CEB-FIP Model Code 1990

The comparison of the shear design methods of the FIP Recommendations 1996 with that of the CEB-FIP Model Code 1990 may be briefly done, because the design rules of MC 90 are almost the same as that of the previously compared "variable strut inclination method" of the EC 2, p.1.

The first important difference between the FIP Rec. and MC 90 lies in the limiting value for the strength of the struts in the web:

- FIP Rec.: $f_{cwd} = 0.80\ f_{1cd}$
- MC 90: $f_{cwd} = 0.60\ (1 - f_{ck}/250)\ f_{cd}$

Referring both to the uniaxial design strength of $f_{1cd} = 0.85\ f_{cd} = f_{ck}/1.50$ of the FIP Rec., which complies with MC 90, gives the relationships shown in Fig. 12 plotted versus the concrete class. The strength value of the FIP Rec. is independent of f_{ck} and is far higher than that in MC 90, especially for high strength concrete. The reason for this is, that the friction is explicitly checked in the FIP Rec. and this leads to the limitation of the angle θ, as described before.

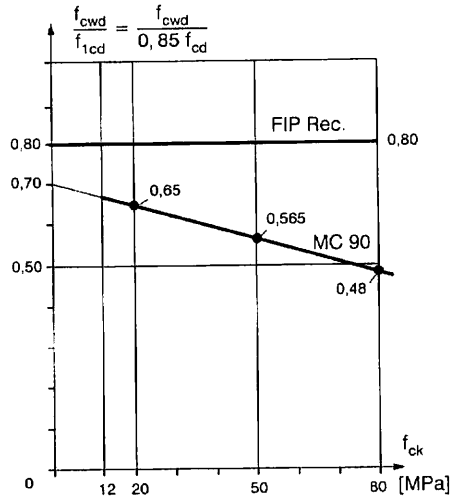

Fig. 12: Comparison of the allowable values for the strength of the struts between the FIP Recommendations 1996 and the CEB-FIP Model Code 1990

The obvious result of this fact is that the maximum allowable shear force is far higher, as demonstrated in Fig. 13, where for reinforced concrete members the amount of required transverse reinforcement is plotted versus the shear force in a dimensionfree format. The quarter circles of MC 90 for the different concrete classes mean that according to MC 90 the strength of the struts determines the ultimate capacity, until the lower limit of $\theta = 18{,}4°$ or $\cot\theta = 3{,}0$ is reached. In the medium range of the dimensionfree shear force υ_d between about $\upsilon_d = 0.12$ and $\upsilon_d = 0.20$ (for C80), respec-

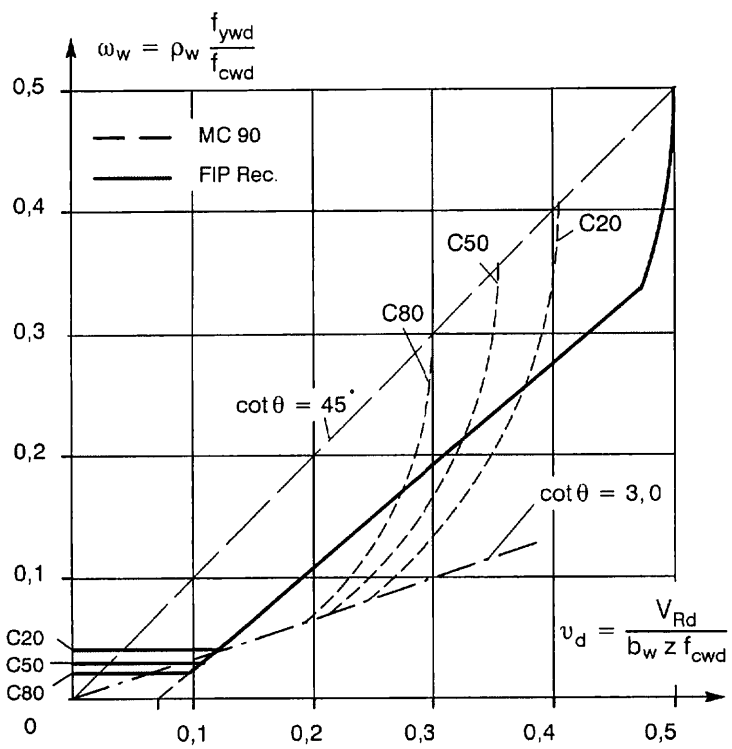

Fig. 13: Comparison of the required transverse reinforcement between the FIP Recommendations 1996 and the CEB-FIP Model Code 1990 for r.c.-members with vertical stirrups

tively $\upsilon_d = 0.25$ (for C20), the MC 90 requires less transverse reinforcement than the FIP Rec. However, it can be shown that this is unsafe, i.e. there are tests points over the design curves of MC 90; this cannot be further dealt with here.

A similar comparison for prestressed concrete members is beyond the scope of this paper, because it would require too much space due to the fact that rules in MC 90 are so complicated. It takes 9 pages in MC 90 to explain the design rules for p.c.-members, whereas in the FIP Rec. the effect of axial compression is taken into account in 2 design equations which are anyway required for r.c.-members.

4.4 Conclusions of the comparisons

Summarizing the following conclusions may be drawn.

The shear design according to the "truss model with crack friction" as defined in the FIP Recommendations 1996 is economical in a wide range for r.c.- and p.c.-members. The values for the maximum shear forces are considerably higher than in present codes like in MC 90 or in the EC 2, p.1, which is important for prefabricated members and for wide span structures, like free cantilevering bridges.

The main feature of the shear design in the FIP Recommendations 1996 is that axial compressive forces are considered, and this makes the method far more versatile than the presently in Europe favoured "variable strut angle method". In the latter method lower limits for θ and low values for ν have to be linked to secure a safe design, because a lower limit of e.g. $\cot\theta = 2$ is unsafe for values of about $\upsilon_d > 0.30$ to 0.35. This is the range which is opened by the FIP Recommendations 1996 due to limiting the angle θ depending on the design shear force υ_d.

It should be mentioned that the FIP Recommendations 1996 did not deal with lightweight aggregate concrete because of its rare use. In principle, the concept of the "truss model with crack friction" is still valid, but the contribution of the crack friction and thus that of V_{fd} may be lower in comparison to the equations given above.

5 Members without transverse reinforcement

The design model for members without transverse reinforcement. i.e. mainly slabs, has been presented with Fig. 8 b, as also explained in the keynote lecture for the *fib* Symposium in Prague 1999 [Reineck (1999)]. However, the capacity of this model is not determined by the concrete ties attaining the axial tensile strength, but by the failure of the friction forces and dowel forces at the cracks. The cracks are roughly inclined at 60° in r.c.-members, i.e. members without axial forces. There are some proposals for theoretical models as e.g. summarised in the recent state-of-the-art report in CEB Bulletin 237 (1997), but the issue is still controversial. Therefore, the empirical formula of the CEB-FIP MC 90 was taken in a slightly revised form:

$$V_{Rd} = [0.10\,\kappa\,(\rho_l\, f_{ck})^{1/3} - 0.12\,\sigma_{cd}]\; b_w\, d \qquad (13)$$

where: $\kappa = 1 + \sqrt{(200/d)} \le 2$ = factor for size effect

d [mm] = effective depth

f_{ck} [MPa] = characteristic cylinder strength

ρ_l [-] = A_s / b d = longitudinal reinforcement ratio

σ_{cd} [MPa] = N / b d = axial stress (- for compression)

The factor of 0.10 in the above equation is based on a recent evaluation of 282 reliable tests out of more than 600 tests on r.c.-members without axial forces, which showed that the factor 0.12 of the CEB-FIP MC 90 was unsafe. The characteristic value for this factor was only about 0.13, so that in comparison to the above value of 0.10 only a resistance (material) safety factor of $\gamma_c = 1.30$ is given. Thereby, this safety factor γ_c is applied to the resistance V_{Rd} of the whole member, but this is disputable and König (1999) showed with more refined safety considerations that the above value of 0.10 may be justified.

6 Typical D-regions associated with shear

The basic concept of the "truss model with crack-friction" may not only be regarded as a refined design method valid only for B-regions, but similar procedures may also be used for the design of the D-regions. In D-regions and especially in those with geometrical discontinuities the formation of a single crack initiating a failure surface is very likely, so that investigating the equilibrium of the free-bodies formed by such a crack is a safe procedure and almost an indispensable requirement. Windisch (1988) applied this approach to a dapped end of a prefabricated girder. The pedagogical value of such a procedure is the same as for any failure mechanism approach: it leads the designer to think of likely cracks and to avoid models with overoptimistic redistribution capacities after cracking.

Typical examples for D-regions are presented, which are presently dealt with as shear design problems, such as indirectly supported members or point loads near supports. A very critical case is the dapped beam-end, especially in case of slabs or slab bridges without transverse reinforcement. Such problems have been dealt with on basis of the FIP Recommendations 1996 "Practical Design of Structural Concrete", which are fully based on the concept of designing concrete structures with strut-and-tie models, and some examples are given by Reineck (1999).

7 Concluding remarks

The "truss-model with crack friction" is a failure mechanism approach, where the expected failure cracks are considered discretely. The possible transfer of forces over the crack due to friction or interface shear is explicitly modelled. The approach gives directly the possible shear capacity respectively the required transverse reinforcement. The contribution of the friction across the cracks gives the physical explanation of the "concrete term V_c" as being the vertical component V_f of the forces transferred across the crack. For practical design it may be assumed as a good approximation that this shear force component V_f is independent from the applied shear force V_u. This yields for a reinforced concrete beam the dimensioning diagram in Fig. 5, which is similar to the well proposals (standard method) by Leonhardt (1965, 1977), the EC 2 and the ACI 318. Similar diagrams (Fig. 6) may be derived for members subjected to shear and axial compressive forces or prestress, the influence of which is covered consistently.

The state of stress is defined at the crack, and from this definition the principal stresses between the cracks may be evaluated. The resulting biaxial stress field is

represented by the superposition of the two trusses in Fig 8. These trusses are statically admissible stress-fields for the web in the B-region of a beam, so that the "truss model with crack friction" fulfils the requirements of a lower-bound method, if safe strength limits are defined in the constitutive laws for the shear transfer mechanisms at the crack.

These models demonstrate that both approaches, i.e. the discrete and smeared ones, result in the same design models, and only the failure criteria are different. In discrete approaches the shear transfer mechanisms like the friction are explicitly checked, whereas the smeared approaches give empirically derived limits for the strut angle or the strength of struts. Important is to state, that with respect of the design models a common view is gained in the shear design, so that the controversy over "standard method" versus "variable strut angle" is futile and unproductive. More important is whether the behaviour and the test results are realistically and economically covered, and this is the case with the design method presented in the FIP Recommendations 1996 "Practical Design of Structural Concrete".

References

Abbreviations:		
	ACI	= American Concrete Institute
	ASCE	= American Society of Civil Engineering
	BuStb	= Beton- und Stahlbetonbau
	CEB	= Comité Eurointernational du Beton (until 1998)
	DAfStb	= Deutscher Ausschuß für Stahlbeton
	fib	= Fédération Internationale du Béton (since 1998, joint CEB and FIP)
	FIP	= Fédération Internationale du Précontrainte (until 1998)
	IABSE	= International Association for Bridge and Structural Engineering
	PCI	= Prestressed Concrete Institute
	SIA	= Schweizer Ingenieur und Architekt

ACI 318 (1989): Building Code Requirements for reinforced concrete (ACI 318-89) and Commentary ACI 318 R-89, ACI, Detroit 1989, 352pp

ASCE-ACI Task Committee 426, J.G. Mac Gregor (Chairman) (1973): The shear strength of reinforced concrete members. ASCE-Journ. of Struct. Div.99 (1973), June, 1091-1187

ASCE-ACI 445 (1998): Recent approaches to shear design of structural concrete. State-of-the-Art-Report by ASCE-ACI Committee 445 on Shear and Torsion. ASCE-Journ. of Structural Engineering 124 (1998), No. 12, 1375 - 1417

Baumann, Th. (1972): Zur Frage der Netzbewehrung von Flächentragwerken (On the Problem of Net Reinforcement of Surface Structures). Bauingenieur 47 (1972) H.10, 367-377

Bulicek, H. (1993): Zur Berechnung des ebenen Spannungs- und Verzerrungszustandes von schubbewehrten Stegen profilierter Stahlbeton- und Spannbetonträger im Grenzzustand der Tragfähigkeit. Diss. am Lehrstuhl für Massivbau, TU München, 1993

CEB-FIP MC 90: CEB-FIP Model-Code 1990, Design Code. Thomas Telford, 1993

Collins, M.P. (1978): Towards a Rational Theory for Reinforced Concrete Members in Shear. ASCE-Proc. V 104, No.ST4 (1978), 649-666

Collins, M.P.; Mitchell, D. (1980): Shear and torsion design of prestressed and non-prestressed concrete beams. PCI-Journ. V.25 (1980), No. 5, 32-100, Discussion in: V.26, (1981), No.6, 96-118

Daschner, F. (1980): Shear-transfer in cracks of normal- and lightweight concrete (in German). Report of Institute für Massivbau, TU München, March 1980, 1-93

Dei Poli, S.; Gambarova, P.G.; Karakoc, C. (1987): Aggregate interlock role in r.c. thin-webbed beams in shear. ASCE-Journ.of Struct.Div.113 (1987), No.1, 1-19

Dei Poli, S.; Di Prisco, M.D.; Gambarova, P.G. (1990): Stress Field in Web of RC Thin-Webbed Beams Failing in Shear. ASCE-Journ. of Struct. Div., V.116 (1990) No.9, 2496-2515

DIN 1045 (1988): Beton und Stahlbeton, Bemessung und Ausführung. DIN 1045, Juli 1988

EC 2, T.1 (1991): DIN V 18 932, T1, Eurocode 2, Planung von Stahlbeton- und Spannbetontragwerken, T1: Grundlagen und Anwendungsregeln für den Hochbau. Beuth Verlag Berlin, Okt. 1991

Eibl, J.; Neuroth, U. (1988): Untersuchungen zur Druckfestigkeit von bewehrtem Beton bei gleichzeitig wirkendem Querzug. Inst. für Massivbau u. Baustofftechnologie, Univ. Karlsruhe, 1988
Fenwick, R.C.; Paulay, Th. (1968): Mechanisms of shear resistance of concrete beams. ASCE-Journ. V.94, (1968), ST 10, Oct., 2325-2350
FIP-Recommendations (1996): Practical Design of Structural Concrete. FIP-Commission 3 "Practical Design". SETO, London, 1999 (distributed by *fib*, Lausanne)
Gambarova, P.S. (1979): Aggregate interlock role in r.c. thin-webbed beams in shear. ASCE-Journ. of Struct.Div.113 (1979), No.1, 1-19
Gambarova, P.G.; di Prisco, M. (1991): Interface Behaviour. Chapter 5 in Behavior and Analysis of Reinforced Concrete Structures under Alternate Actions Inducing Inelastic Response, Vol.1: General Models.CEB-Bull. 210, Lausanne, July 1991
Hamadi, Y.D. (1976): Force transfer across cracks in concrete structures. PhD-thesis, Polytechnic of Central London, 1976
Hardjasaputra, H. (1987): Consideration of the state of strain in the shear design of r.c.- and p.c.-girders. Dr.-thesis, Univ. Stuttgart, 1987
Hsu, T.T.C. (1993): Unified Theory of Reinforced Concrete. CRC Press, Inc., Florida
Kani, G.N.J. (1964): The riddle of shear failure and its solution. ACI-Journ. V.61 (1964), No.4, April, 441-467, Disc. in December 1964, 1587-1636
Kirmair, H.; Kupfer, H. (1983): Versuche zur Schubbewehrung von Bauteilen aus Stahlleichtbeton. BuStb 78 (1983), H. 5, 125-132
Kirmair, M. (1985/87): Das Schubtragverhalten schlanker Stahlbetonbalken - theoretische und experimentelle Untersuchungen für Leicht- und Normalbeton. Diss., TU München, 1985, sowie: DAfStb H.385, Berlin, 1987
König, G. (1999): Vergleichsrechnung Schubtragfähigkeit ohne Schubbewehrung für Platten des üblichen Hochbaus. Unpubl. Febr. 1999
Kollegger, J.: Mehlhorn, G. (1990): Experimentelle Untersuchungen zur Bestimmung der Druckfestigkeit des gerissenen Stahlbetons bei einer Querzugbeanspruchung. DAfStb H.413, Beuth Verlag, Berlin, 1990
Kupfer, H. (1964): Generalization of Mörsch's Truss Analogy Using the Principle of Minimum Strain Energy. CEB-Bull. No.40 (1964), 44-57
Kupfer, H.; Moosecker, W. (1979): Beanspruchung und Verformung der Schubzone des schlanken profilierten Stahlbetonbalkens. In: Forschungsbeiträge für die Baupraxis, 225-236, W. Ernst und Sohn, Berlin, 1979
Kupfer, H.; Mang, R.; Karavesyrouglou, M. (1983): Bruchzustand der Schubzone von Stahlbeton- und Spannbetonträgern. - Eine Analyse unter Berücksichtigung der Rißverzahnung. Bauingenieur 58 (1983), 143-149
Kupfer, H.; Bulicek, H. (1991): Comparison of fixed and rotating crack models in shear design of slender concrete beams. In: Progress in Structural Engineering., 129-138. Hrsg.: Grierson, D.E. et.al., Brescia (Italia). Kluwer Acad. Publ.
Leonhardt, F. (1965): Reducing the shear reinforcement in reinforced concrete beams and slabs. Magazine of Concrete Research 17 (1965), No. 53, December, 187-198
Leonhardt, F. (1977): Schub bei Stahlbeton und Spannbeton. Grundlagen der neueren Schubbemessung. BuStb 72 (1977), H.11, 270-277 u. H.12, 295-302
Lessig, N.N. (1959): Determination of the load bearing capacity of reinforced concrete elements with rectangular cross-section subjected to flexure with torsion. Foreign literature study No. 371, Portland Cement Ass., Skokie, Ill. 1959
Lipski, A. (1971/72): Poutres a âme mince en béton armé ou précontraint. Ann. d. Travaux Publ. d. Belgique No.1-2, 1971/72
Marti, P. (1991): Dimensioning and detailing. IABSE Rep. V.62 (1991 a), 411-443
Marti, P. (1999): How to treat shear in structural concrete. ACI-Struct. Journ. V.96 (1999), No.3, May-June, 408-414
Mörsch, E. (1909): Concrete Steel Construction. McGraw-Hill, New York, (1909), 368 (English translation of "Der Eisenbetonbau", 1902)
Mörsch, E. (1922): Der Eisenbetonbau - Seine Theorie und Anwendung (Reinforced concrete Construction - Theory and Application). 5th Edition, Vol.1, Part 2, K. Wittwer, Stuttgart, 1922
Nielsen, M.P. (1984): Limit State Analysis and Concrete Plasticity. Prentice-Hall, Englewood Cliffs, New Jersey, 1984, 420
Nielsen, M.P.; Bræstrup, M.W. (1976): Plastic shear strength of reinforced concrete beams. University of Denmark, Rapport Nr. R 73, 1976

Nissen, I. (1987): Rißverzahnung des Betons - gegenseitige Rißuferverschiebungen und übertragbare Kräfte. Diss., TU München, 1987
Potucek, W. (1977): Die Beanspruchung der Stege von Stahlbetonplattenbalken durch Querkraft und Biegung. Zement u. Beton 22 (1977), H.3, 88-98
Ramirez, J.A.; Breen, J.E. (1991): Evaluation of a modified truss-model approach for beams in shear. ACI-Struct. Journ. V.88 (1991), No.5, Sept.-Oct., 562-571
Reineck, K.-H. (1982 a): Models for the design of reinforced and prestressed concrete members. CEB-Bull.146, 43-96, Paris, Jan. 1982
Reineck, K.-H. (1990): Mechanical model for the behaviour of reinforced concrete members in shear. Dr.-thesis, Univ. Stuttgart, Febr. 1990, 1-273
Reineck, K.-H. (1991): Modelling of members with transverse reinforcement. IABSE Rep. V.62 (1991 a), 481-488
Reineck, K.-H. (1991 b): Model for Structural Concrete Members without Transverse Reinforcement. IABSE Rep. V.62 (1991 a), 643-648
Reineck, K.-H. (1991 e): Ultimate shear force of structural concrete members without transverse reinforcement derived from a mechanical model. ACI Struct.-Journ. V.88 (1991), No.5, Sept./Oct., 592-602
Reineck, K.-H. (1995): Shear design based on truss models with crack-friction. 137-157, in: Ultimate Limit State Models - A state-of-the-art report by CEB Task Group 2.3, CEB-Bull. 223, June 1995, Lausanne
Reineck, K.-H. (1997 a): Modelling the Shear Behaviour and Size Effect of Structural Concrete Members without Transverse Reinforcement. CEB-Bull.237 'Concrete Tension and Size Effect', 185-198, April 1997, Lausanne
Reineck, K.-H. (1997 b): Concrete tension and Size Effect – Summary and Discussion. CEB-Bull.237 'Concrete Tension and Size Effect', 247-253, April 1997, Lausanne
Reineck, K.-H. (1999 a): Towards a Modern Design Concept for Structural Concrete. Keynote Address for Session 2 "Practical Design of Structural Concrete". Appendix a - o (after p. 343) in: Proc. Vol. 1: "Structural Concrete - The Bridge between People", *fib* Symposium 1999 Prague, 12-15 October 1999. *fib*, Lausanne 1999
Schäfer, K.; Schelling, G.; Kuchler, T. (1990): Druck- und Querzug in bewehrten Betonelementen. DAfStb H. 408, Beuth Verlag, Berlin, 1990
Schlaich, J.; Schäfer, K; Jennewein, M. (1987): Toward a consistent design for structural concrete. PCI-Journ. V.32 (1987), No.3, 75-150
Schlaich, J.; Schäfer, K. (1983): Zur Druck-Querzug-Festigkeit des Stahlbetons. BuStb 78 (1983), H.3, 73-78
Schäfer, K.; Schlaich, J.; Jennewein, M. (1991): Strut-and-tie modelling of structural concrete. IABSE Rep. V.62 (1991 a), 235-240
Tassios, T.P.; Vintzeleou, E.N. (1987): Concrete-to-Concrete Friction. ASCE-Journ. of Struct. Eng., V.113, No.4, April 1987, 832-849
Taylor, H.P.J. (1972): Shear strength of large beams. ASCE-Journ.of Struct.Div., V.98 (1972), ST11, 2473-2490
Taylor, H.P.J. (1974): The fundamental behaviour of reinforced concrete beams in bending and shear. In: ACI SP 42, 43-77, Detroit 1974
Thürlimann, B.; Grob, J.; Lüchinger, P. (1975): Torsion, Biegung und Schub in Stahlbetonträgern. Fortbildungskurs für Bauingenieure, April 1975 Institut für Baustatik und Konstruktion, ETH Zürich
Thürlimann, B.; Marti, P.; Pralong, J.; Ritz, P.; Zimmerli, B. (1983): Anwendung der Plastizitätstheorie auf Stahlbeton. Fortbildungskurs für Bauingenieure, Institut für Baustatik und Konstruktion, ETH Zürich, April 1983
Vecchio, F.J.; Collins, M.P. (1986): The Modified Compression Field Theory for Reinforced Concrete Elements Subjected to Shear. ACI-Journ. V 83 (1986), No.2, 219-231
Walraven, J.C. (1980): Aggregate interlock: a theoretical and experimental analysis. Dr.-thesis, Delft Univ. Press, 1980, 1-197
Walraven, J.C.; Reinhardt, H.W. (1981): Concrete mechanics port A – theory and experiment on the mechanical behaviour of cracks in plain and reinforced concrete subjected to shear loading. TU Delft, Heron, V.26, No.1A, 1981
Windisch, A. (1988): Das Modell der charakteristischen Bruchquerschnitte. Ein Beitrag zur Bemessung der Sonderbereiche von Stahlbetontragwerken. BuStb 83 (1988), H.9, S.251-255 and H.10, S.271-274

Background paper 11

Shear design of a bridge girder

Manfred Miehlbradt
MCS – DGC
EPFL
Lausanne, Schweiz

Shear design of a bridge girder

The following completes the example B included in the FIP Handbook on practical design (Telford, London, 1990): Bridge near Yverdon (CH) composed by single-span beams for multispan continuous road bridge.

The figures B1 to B5 are taken from the Handbook as well as the other design information, especially the material strengths, i.e. concrete C40 and welded wire fabric S 500.

Shear design summary

1. Design shear forces (per girder)

$V_{Sd,max} = \frac{27}{2}(1{,}35 \cdot 44 + 1{,}5 \cdot 27{,}6) + 1{,}5 \cdot 300$

$= 1\,811$ kN

$P_{mO} = 1\,777$ kN (48Ø6 tendon)

$\tan\alpha_p \approx \frac{2 \cdot 1{,}15}{15{,}5} = 0{,}15$

$V_{pd,max} = 1\,777 \cdot 0{,}15 = 267$ kN

$V_{Sd,web,max} = 1\,811 - 267 = 1\,544$ kN [6.5]

2. Basic data for shear design

$f_{cwd} = 0{,}8 \cdot f_{1cd} = 0{,}8 \cdot \frac{0{,}85}{1{,}5} \cdot 40$ [5.5], [2.1]

$= 18{,}1$ MPa

$\sigma_{xd} = \sum \frac{P_{m\infty}}{A_c} \approx -7$ MPa (from SLS results)

$\cot\beta_r = 1{,}2 - 0{,}2\,\frac{(-7)}{3{,}5} = 1{,}6$ [6.9b], table 2.1

$\tan\beta_r = 0{,}63$

$V_{fd} = 0{,}1\,(1 - \frac{1{,}6}{4}) \cdot 0{,}18 \cdot 1{,}66 \cdot 18100$ [6.10b]

$= 325$ kN

3. Design of stirrups

$$\frac{A_{sw}}{s_w} = \frac{1544 - 325}{1{,}66 \cdot \frac{0{,}5}{1{,}15}} \cdot 0{,}63 = 1064\ \frac{mm^2}{m}$$ [6.6], [6.8]

chosen : stirrups Ø10 s150 (2 legs) section 6.4.3.1

$s_w < 0{,}2 \cdot 1660 = 332$ mm

$s_w < 200$ mm

4. Check of struts

$$\cot\theta = \frac{1{,}6}{1-\frac{325}{1544}} = 2{,}03 \qquad [6.11a]$$

$\theta = 26°$; $\sin\theta = 0{,}44$; $\cos\theta = 0{,}90$

($z \cdot \cot\theta = 2{,}03 \cdot 1{,}66 = 3{,}37$ m > 2,57;safe side)

$V_{Rd,web,max}$ = 0,18 1,66 18100 0,44 0,90 [6.13]
= 2 140 kN > 1 544 kN [6.3]

5. Check of tension chord

F_t = 0,5 1 811 2,03 = 1 838 kN (at point M=0) [6.15]
8strands + 8∅22

F_{Rd} $= \frac{1}{1{,}15}$ (744 0,9 1,820 + 3040 0,400) [2.10], [2.7]
= 2 117 kN > 1 838 kN

6. Concluding remark

The above results (sections 3 and 4) fit rather well with those of the original design of the bridge built 20 years ago.

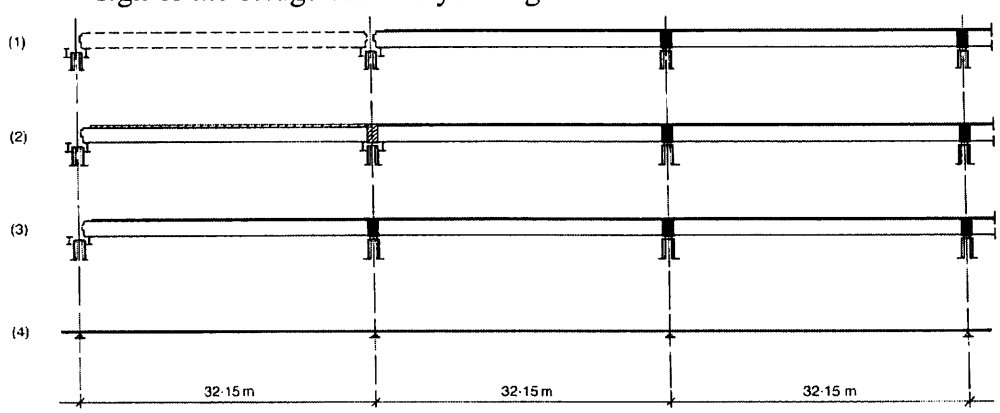

B 1 Longitudinal section illustrating the span by span erection of the bridge

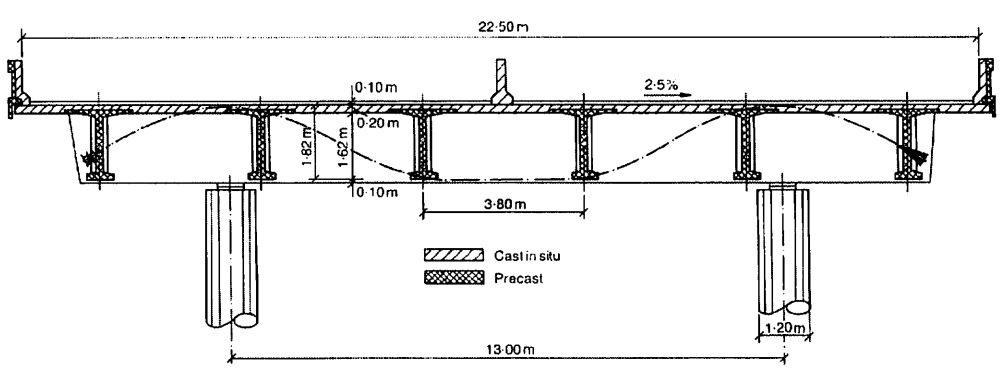

B 2 Cross section with precast girders completed by in situ concrete

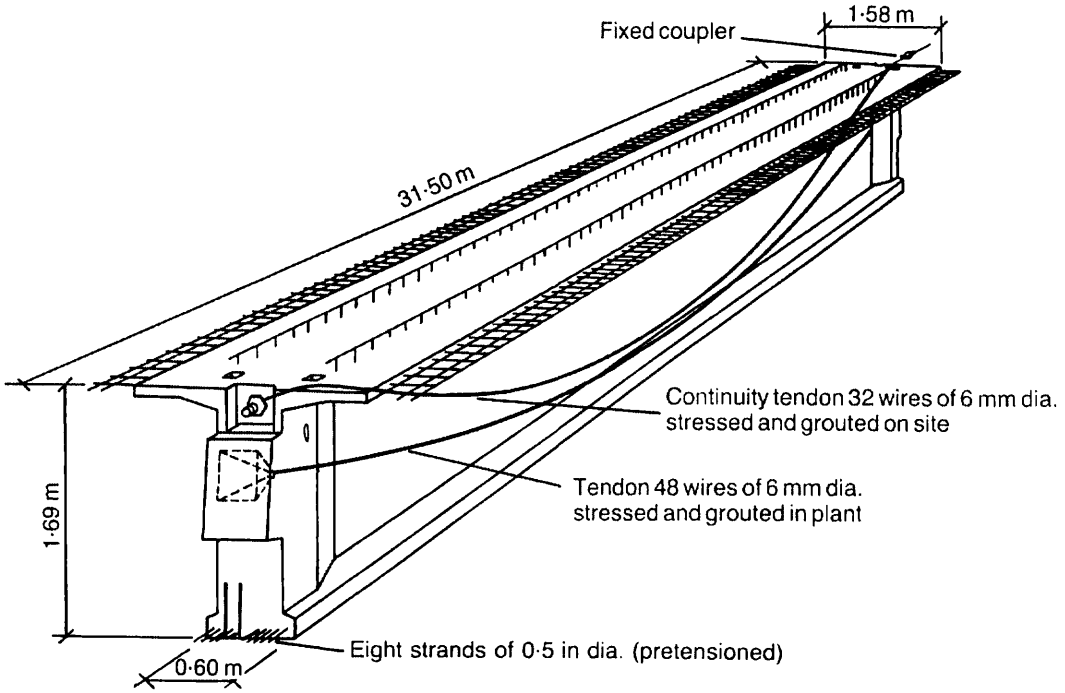

B 3 Precast girder with tendons and continuity reinforcement

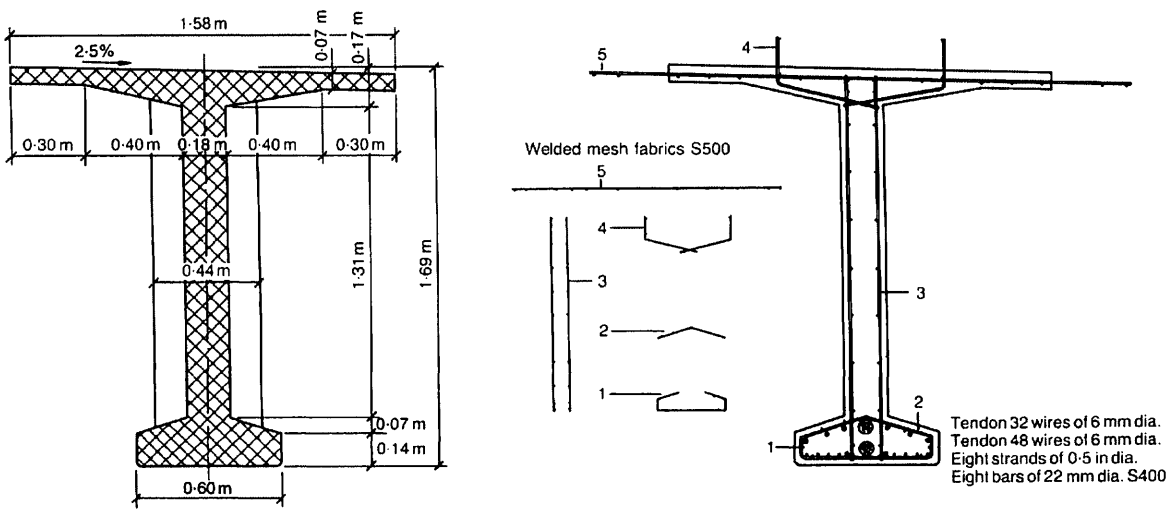

B 4 Precast girder cross section and reinforcement

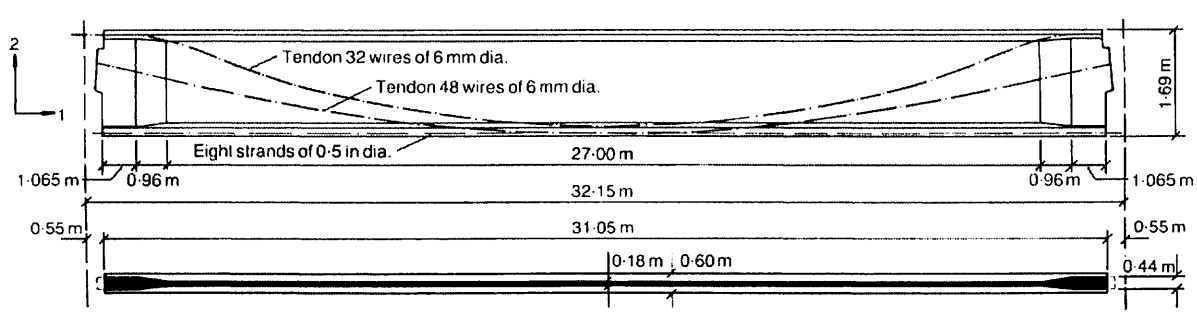

B 5 Elevation of the girder and horizontal section

Summary and conclusions

Karl - Heinz Reineck, Joåo F. Almeida, Manfred Miehlbradt

The primary aim of this Bulletin was to present examples where the application of the design with strut-and-tie models is demonstrated as presented in the chapter 6.5 of the FIP Recommendations 1996 "Practical Design of Structural Concrete". These FIP Recommendations 1996 are a revision of the edition from 1984, and are based on the CEB-FIP Model Code 1990. However, some further developments were made, and this especially refers to the full implementation of the design with strut-and-tie models into the code structure.

The six examples in this Bulletin deal with structures taken from the practice of the members of the Working Group, and they cover critical details of several bridges, of two prestressed beams and even a concrete offshore platform. This Bulletin hopefully convinces practising engineers from consultants, contractors and authorities to use of a consistent design and detailing tool like the strut-and-tie-models.

In Example 1 the design of an anchor block of an externally prestressed bridge is shown using strut-and-tie models three-dimensionally. This problem is still discussed by researchers up to now, but using strut-and-tie models a satisfactory solution was found by the designers for this critical and highly stressed D-region. Even furthermore, the models triggered discussions on how this detail could possibly be improved in future cases.

For example 2 two basic and common structural elements, i..e. D-regions, were chosen from the Viaduct over the Ribeira de Grandola in the South Motorway A2 in Portugal. They illustrate the use of the Recommendations for the design of a pier column head and of a pylon cap. The beam-slab superstructure with two beams is supported by pier cap in form a double corbel where prestressing tendons were placed near the upper face of the corbel. For the pier column head the strut-and-tie models were presented for the design for service loads and for the construction phase, where only prestressing is applied. For the pile cap a 3-dimesnional strut-and-tie model was developed. For checking the elements of the models, especially the struts and nodes, simple assumptions were used. Although further considerations are still needed this example especially demonstrates the potential of the strut-and-tie method proposed by FIP Recommendations to design very complex D-regions.

The example 3 deals with the design of D-regions of a very complex concrete structure, the Vallhall Monotower Concrete Offshore Platform. The global FE analysis served as the main basis for the design of the platform and provided the required input for the design of the selected D-Regions, like the connection between the minicell and the dome. It showed the need of carefully detailing the reinforcement, so that strength of struts, nodes and anchorage of the reinforcing bars are guaranteed.

Example 4 had the objective to compare the design models for a precast, pretensioned beam in combined action with in situ concrete using FIP-Recommendations and other codes, such as Eurocode and Swedish code. The beam is a part of a floor of a tennis hall in Stockholm. The design was performed for both SLS and ULS from load definition, check for bending and shear to checking reinforcement anchorage. This example demonstrated that the FIP Recommendations could be applied to such a complicated detail.

Example 5 described the design of a precast post-tensioned concrete I-beam of 40 m span for the Sungai Terengganu bridge in Malaysia. Strut-and-tie models were developed to design and detail for different load cases the end support regions of the beams, where the prestressing tendons are anchored .

Example 6 dealt with the design of concrete piers supporting a Viaduct over the Alberche river in Spain: The piers with a hollow cross section are up to 44.5 m high and very slender. The example focuses on the buckling design of the pier using the FIP Recommendations in comparison to a non-linear analysis taking into account both material and geometric non-linearity. It showed that the method proposed by FIP Recommendations is appropriate and thus practical for design of slender concrete columns subjected to skew bending. It provides results on the safe side and is much simpler than the more precise, but complicated non-linear method.

The further chapters 7 to 11 mainly deal with topics where FIP Recommendations differ technically from the rules of MC 90 and give justifications for these changes and present the background. This refers to the design of columns or the buckling design dealt with in the chapters 7 and 8 and the shear design dealt with in chapters 10 and 11, and the reasons for these changes and justifications have already been explained in the introduction. The chapter 9 presents an example which is commonly also regarded as shear design, which is the design of an interface between old and new concrete due to the widening of an old arch bridge in southern Finland.

In concluding, the examples fully demonstrated that the modern concepts of the FIP Recommendations 1996 "Practical Design of Structural Concrete" enabled practising engineers to solve quite complicated problems by using strut-and-tie models.

Appendix

Corrections for the:
FIP Recommendations "Practical Design of Structural Concrete"

SETO, London, 1999 (distributed by *fib*, Lausanne)

p. 51, Table 6.1, line 3: read: γ_q = **1.50** (instead of 1.35)

p. 57, Eq. (6.15): read subscripts "**S**" for M and N (instead of "s")

p. 57, section 6.4.3.4 (1): add after Eq.(6.12) the following:

with: ν_2 **see section 6.4.3.1 (1) and (2)**

b_w = **web width, or** b_{red} **acc. to section 5.3.5**